

# Sheffield Hallam University

*Transfer lubrication techniques in a stick slip situation.*

COCKERHAM, G.

Available from the Sheffield Hallam University Research Archive (SHURA) at:

<http://shura.shu.ac.uk/19485/>

## A Sheffield Hallam University thesis

This thesis is protected by copyright which belongs to the author.

The content must not be changed in any way or sold commercially in any format or medium without the formal permission of the author.

When referring to this work, full bibliographic details including the author, title, awarding institution and date of the thesis must be given.

Please visit <http://shura.shu.ac.uk/19485/> and <http://shura.shu.ac.uk/information.html> for further details about copyright and re-use permissions.

TRANSFER LUBRICATION TECHNIQUES IN A STICK SLIP SITUATION

by

G Cockerham BTech(Hons) CEng MIMechE

being a thesis submitted for the CNAAB degree of

MASTER OF PHILOSOPHY

Department of Mechanical &  
Production Engineering  
Sheffield City Polytechnic

May 1976

ProQuest Number: 10694366

All rights reserved

INFORMATION TO ALL USERS

The quality of this reproduction is dependent upon the quality of the copy submitted.

In the unlikely event that the author did not send a complete manuscript and there are missing pages, these will be noted. Also, if material had to be removed, a note will indicate the deletion.



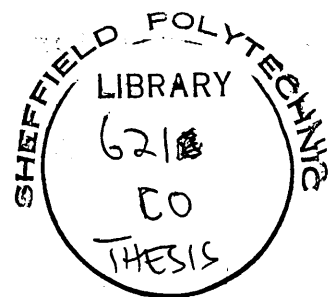
ProQuest 10694366

Published by ProQuest LLC (2017). Copyright of the Dissertation is held by the Author.

All rights reserved.

This work is protected against unauthorized copying under Title 17, United States Code  
Microform Edition © ProQuest LLC.

ProQuest LLC.  
789 East Eisenhower Parkway  
P.O. Box 1346  
Ann Arbor, MI 48106 – 1346



76-20908 01

## SYNOPSIS

The thesis describes a theoretical and experimental investigation into the transfer lubrication technique as a means of eliminating stick slip vibratory motion.

The experimental apparatus consisted of a replaceable disc fastened to a rotor supported in air journal bearings. The disc was driven rotationally via an elastic member and radially loaded by two diametrically opposed pistons pneumatically pressed against the disc circumference. A metal piston pressed against the metal disc induced the stick slip motion whilst the other piston consisted of a dry lubricant compact providing for the transfer of solid lubricant to the metal junction. Instrumentation was incorporated in order to measure appropriate stick slip properties and the major parameters of the system were varied.

Unlubricated stick slip experimental results have been compared with analyses based upon upper and lower bound linearised dynamic friction models. Corresponding theoretical stability relationships have been developed for transfer lubricated conditions and experimental comparison also made. In addition detailed circumstances whereby stick slip motion is successfully eliminated by transfer lubrication have been defined including limiting load ratio and oil contamination conditions.

## ACKNOWLEDGEMENTS

The author would like to record his thanks to G R Symmons BSc, PhD, MIMechE, CEng, for the initiation of the program of research and the guidance and supervision offered in its execution. Also Mr A E De Barr BSc, FInstP, Director of Research, MTIRA, Macclesfield, is thanked for the helpful suggestions made in his role as external supervisor. In addition thanks are due to Mr O Bardsley MA, MSc, FRAeS, CEng, Head of Department of Mechanical and Production Engineering, Sheffield Polytechnic, for the provision of the facilities which enabled the research to be undertaken. Gratitude is expressed to the technician staff of the above department for the assistance supplied in the construction and instrumentation of the experimental equipment, particularly Mr R Wilkinson and Mr D McKay.

# LIST OF CONTENTS

	<u>Page No.</u>
Synopsis	(i)
Acknowledgements	(ii)
List of Contents	(iii)
List of Figures	(v)
Notation	(xi)
Chapter 1 INTRODUCTION	1
1.1 Stick Slip Motion and Transfer Lubrication	
1.2 Review of Previous Work	
1.2.1 Stick Slip Motion	
1.2.2 Transfer Lubrication	
1.3 Objectives of Investigation	
Chapter 2 THEORETICAL ANALYSES	11
2.1 Introduction	
2.2 Blok Dynamic Friction Model Analysis	
2.3 Negative Damping Dynamic Friction Model Analysis	
2.4 Theoretical Comparisons of Stick Slip Analyses	
2.5 Theoretical Analysis of Dry Lubricant Friction Effects	
Chapter 3 EXPERIMENTAL APPARATUS	41
3.1 Introduction	
3.2 Stick Slip Machine	
3.3 Instrumentation	
3.4 Calibration and Specimen Preparation	
3.5 Tolerances in Experimental Measurements	
3.6 Experimental Procedure	
Chapter 4 EXPERIMENTAL RESULTS AND COMPARISON WITH THEORIES FOR UNLUBRICATED STICK SLIP	68
4.1 Dynamic Friction Characteristics	
4.2 Comparison of Experimental Results with Linearised Theories	
4.3 Variation of Dynamic Gradient with System Parameters	
Chapter 5 EXPERIMENTAL RESULTS AND COMPARISON WITH THEORIES FOR TRANSFER LUBRICATED STICK SLIP	103
5.1 Introduction	
5.2 Dynamic Friction Characteristics	

5.3	Friction Components of Transfer Lubricants	
5.3.1	Introduction	
5.3.2	Variation of Transfer Lubrication Friction Components with System Parameters	
5.4	Comparison of Experimental Results with Stability Theories	
5.4.1	Introduction	
5.4.2	Stability Comparisons	
5.5	Stick Slip Elimination Distances and Transfer Lubricant Wear Rates	
Chapter 6	CONTAMINANT EFFECTS	157
6.1	Introduction	
6.2	Graphite on Cast Iron Results	
6.3	PTFE on Steel Results	
6.4	Vespel on Steel Results	
Chapter 7	GENERAL DISCUSSION	168
7.1	Unlubricated Stick Slip	
7.2	Transfer Lubricated Stick Slip	
	CONCLUSIONS	178
	List of References	180
APPENDIX I	- Tabular Results for Unlubricated Stick Slip	A1
APPENDIX II	- Tabular Results for Transfer Lubricant Characteristics	A31
APPENDIX III	- Tabular Results for Transfer Lubricated Stick Slip	A66
APPENDIX IV	- Record of Specialist Courses Attended	A87

## LIST OF FIGURES

- 1.1 Rotational Stick-Slip configuration
- 1.2 Translational stick-slip configuration
  
- 2.1 Static Instantaneous Constant Kinetic Friction Torque characteristic
- 2.2 Negative damping friction torque characteristic
- 2.3  $\psi$  vs.  $w_1 t_1$  for various values of  $c_2$
- 2.4  $\psi$  vs.  $\frac{w_s}{w_1}$  for various values of  $c_2$
- 2.5 Stability condition for Blok friction model theory
- 2.6  $\psi$  vs.  $w_1 t_2$  for various values of  $c_2$
- 2.7  $\frac{\dot{\theta}_{\max}}{\dot{\phi}}$  vs.  $\psi$  for various values of  $c_2$
- 2.8  $c_1$  vs.  $w_1 t_2$  for various values of  $c_2$
- 2.9  $\frac{\dot{\theta}_{\max}}{\dot{\phi}}$  vs.  $c_1$  for various values of  $c_2$
- 2.10  $c_1$  vs.  $w_1 t_3$  for various values of  $c_2$
- 2.11  $c_1$  vs.  $\frac{w_s}{w_1}$  for various values of  $c_2$
- 2.12 Stability condition for negative damping friction model
- 2.13  $(\phi - \theta)$  and  $\frac{\dot{\theta}_{\max}}{\dot{\phi}}$  for Blok friction model
- 2.14  $(\phi - \theta)$  and  $\frac{\dot{\theta}_{\max}}{\dot{\phi}}$  for negative damping friction model
- 2.15 Variation of stick slip amplitude with  $\dot{\phi}$ , J and k for  $(T_s - T_k) = 0.055\text{Nm}$
- 2.16 Variation of stick slip amplitude with  $\dot{\phi}$ , J and k for  $c_1 = 0.4$
- 2.17 Variation of stick slip amplitude with  $(T_s - T_k)$  and  $c_1$
  
- 3.1 Rotor and disc in journals
- 3.2 Mercury bath with copper finned tufrol insulated rotor

- 3.3 Complete stick slip apparatus
- 3.4 Torsional spring and strain gauges
- 3.5 Friction force filter
- 3.6 Amplitude response of friction force filter to various inputs
- 3.7 Stick slip instrumentation
- 3.8 Angular displacement of torsional spring vs. u.v. recorder displacement
- 3.9 Spring stiffness graph
- 3.10 Free vibrations of disc and spring
- 3.11 Friction force calibration
- 3.12 'Kopp' setting vs. drive velocity
- 3.13 Angular velocity vs. u.v. recorder displacement
- 3.14 Taylor-Hobson Talysurf
- 3.15 Typical surface profiles for disc
  
- 4.1 Typical friction force slip velocity traces
- 4.2 Amplitude of vibrations compared to both theories
- 4.3 Typical stick slip properties
- 4.4 Comparison of experimental acceleration time period with Blok model theory, steel on steel
- 4.5 Comparison of experimental acceleration time period with negative damping theory, steel on steel
- 4.6 Comparison of experimental deceleration time period with Blok model theory, steel on steel
- 4.7 Comparison of experimental deceleration time period with negative damping theory, steel on steel
- 4.8 Comparison of experimental slip frequency with Blok

- model theory, steel on steel
- 4.9 Comparison of experimental slip frequency with negative damping theory, steel on steel
  - 4.10 Comparison of experimental  $\dot{\theta}_{\max}/\dot{\phi}$  with Blok model theory, steel on steel
  - 4.11 Comparison of experimental  $\dot{\theta}_{\max}/\dot{\phi}$  with negative damping model theory, steel on steel
  - 4.12 Comparison of experimental acceleration time period with Blok model theory, cast iron
  - 4.13 Comparison of experimental acceleration time period with negative damping theory, cast iron
  - 4.14 Comparison of experimental deceleration time period with Blok model theory, cast iron
  - 4.15 Comparison of experimental deceleration time period with negative damping theory, cast iron
  - 4.16 Comparison of experimental slip frequency with Blok model theory, cast iron
  - 4.17 Comparison of experimental slip frequency with negative damping theory, cast iron
  - 4.18 Comparison of experimental  $\dot{\theta}_{\max}/\dot{\phi}$  with Blok model theory, cast iron
  - 4.19 Comparison of experimental  $\dot{\theta}_{\max}/\dot{\phi}$  with negative damping theory, cast iron
  - 4.20 Dynamic gradient as a function of system parameters, cast iron on cast iron
  - 4.21 Dynamic gradient as a function of system parameters, steel on steel
  - 4.22 Log ( dynamic gradient) vs. log (drive velocity in

- mm/s), cast iron
- 4.23 Log (dynamic gradient) vs. log (drive velocity in mm/s), steel on steel
  - 4.24 Log (drive speed exponent) vs. log (normal load(N)), cast iron on cast iron
  - 4.25 Log (kJ) vs. log ( $C_F$ ) cast iron on cast iron
  - 4.26 Log (normal load (N)) vs. log ( $C_F$ ) cast iron on cast iron
  - 4.27 Variation of negative damping coefficient ( $c_1$ ) with system frequency - cast iron
  - 4.28 Variation of negative damping coefficient ( $c_1$ ) with system frequency - mild steel
- 
- 5.1 Reduction of stick-slip amplitude due to transfer lubrication, ptfe on steel
  - 5.2 Transfer lubricated tabular results graphite on cast iron
  - 5.3 Transfer lubricated tabular results ptfe on steel
  - 5.4 Transfer lubricated tabular results ptfe on cast iron and graphite on steel
  - 5.5 Dynamic friction characteristics - transfer lubricated metal junction
  - 5.6 Amplitude response trace for graphite on cast iron
  - 5.7 Amplitude response trace for ptfe on steel
  - 5.8 Typical amplitude response curves for transfer lubricant friction components
  - 5.9 Typical calculations for transfer lubricant components of friction
  - 5.10 Components of friction graphite on cast iron 6.6Hz

- 5.11 Components of friction graphite on cast iron 10Hz
- 5.12 Components of friction graphite on cast iron 13.7Hz
- 5.13 Components of friction ptfе on steel 6.6Hz
- 5.14 Components of friction ptfе on steel 10Hz
- 5.15 Components of friction ptfе on steel 13.7Hz
- 5.16 Components of friction graphite on mild steel all frequencies
- 5.17 Components of friction ptfе on cast iron all frequencies
- 5.18 Variation of coefficient of dynamic friction with normal pressure at zero velocity - ptfе
- 5.19 Variation of coefficient of dynamic friction with sliding velocity for  $0.8\text{MN/m}^2$  pressure ptfе
- 5.20 Variation of coefficient of dynamic friction with normal pressure at zero velocity - cast iron
- 5.21 Variation of coefficient of dynamic friction with sliding speed for  $0.8\text{ MN/m}^2$  pressure graphite
- 5.22 Stability relationships cast iron 6.6Hz (Blok model)
- 5.23 Stability relationships cast iron 6.6Hz (Negative damping model)
- 5.24 Stability relationships cast iron 10Hz (Blok model)
- 5.25 Stability relationships cast iron 10Hz (Negative damping model)
- 5.26 Stability relationships cast iron 13.7Hz (Blok model)
- 5.27 Stability relationships cast iron 13.7Hz (Negative damping model)
- 5.28 Stability relationships mild steel 6.6Hz (Blok model)
- 5.29 Stability relationships mild steel 6.6Hz (Negative damping model)

- 5.30 Stability relationships mild steel 10Hz (Blok model)
- 5.31 Stability relationships mild steel 10Hz (Negative damping model)
- 5.32 Stability relationships mild steel 13.7Hz (Blok model)
- 5.33 Stability relationships mild steel 13.7Hz (Negative damping model)
- 5.34 Stick-slip elimination point as a function of normal load - graphite on cast iron
- 5.35 Stick slip elimination point as a function of normal load - ptfе on steel
- 5.36 Volumetric wear graphite on cast iron, 6.6Hz
- 5.37 Volumetric wear ptfе on steel, 6.6Hz
- 5.38 Stick-slip elimination point vs. load ratio graphite on cast iron, 6.6Hz
- 5.39 Stick slip elimination point vs. load ratio ptfе on steel, 6.6Hz
  
- 6.1 Amplitude vs. time for graphite on cast iron, oil contaminated
- 6.2 Amplitude vs. time for ptfе on mild steel, oil contaminated
- 6.3 Transfer lubricant components of friction oil contaminated ptfе on steel, 6.6Hz
- 6.4 Stability relationship, ptfе on steel, oil contaminated
- 6.5 Volumetric wear of ptfе on steel, oil contaminated
- 6.6 Components of friction, 'Vespel' on steel, oil contaminated
- 6.7 Stability relationship, 'Vespel' on steel, oil contaminated
- 6.8 Amplitude of vibrations vs. time for 'Vespel' on steel, oil contaminated

## NOTATION

- $\theta$  = angular displacement of driven disc
- $\phi$  = angular displacement of driver
- $\psi$  = Blok parameter =  $\frac{\dot{\phi} \sqrt{KJ}}{(T_s - T_k)}$
- $C$  = viscous damping torque proportional to slip velocity
- $C_F$  = Dynamic friction model gradient =  $(T_s - T_k) / \dot{\theta}_{\max}$
- $C_1$  = Negative damping coefficient =  $C_F / 2\sqrt{KJ}$
- $C_2$  = viscous damping coefficient =  $C / 2\sqrt{KJ}$
- $J$  = inertia of disc and rotor
- $K$  = torsional spring stiffness
- $t$  = slip time
- $t_1$  = slip time period
- $t_2$  = acceleration slip time period
- $t_3$  = deceleration slip time period
- $T_S$  = friction torque at zero slip velocity (static friction)
- $T_K$  = friction torque at maximum slip velocity (kinetic friction)
- $w$  = damped natural frequency of system subjected to viscous damping  $(\sqrt{K/J - (C/2J)^2})$
- $w_1$  = natural frequency of system  $(\sqrt{KJ})$
- $w_2$  = damped natural frequency of system subjected to viscous and dynamic friction model damping  $(\sqrt{K/J - ((C-C_F)/2J)^2})$ .
- $w_s$  = slip frequency =  $2\pi/t_1$

1.1 Stick Slip Motion and Transfer Lubrication

Stick-Slip vibratory motion is a phenomenon occurring between slow moving bodies in dry frictional contact when one of the bodies is driven through an elastic member, and can be present in the rotational or translational situation, as shown in figures 1.1 and 1.2.

Self generated vibrations are brought about in such systems by the variation of friction force between the contacting bodies, the friction force depending upon the relative velocity of the bodies. When the frictional contact is between stationary bodies there exists a resistance to motion due to friction which we shall call "static friction". If a force, and hence motion, is applied to the free end of the driving elastic member, the member compresses and stores energy continuously until sufficient force is available to overcome the static friction force, at which point the driven body is caused to move. As this motion proceeds the frictional resisting force in the static situation ("static friction") falls to a lower level of frictional resistance ("kinetic friction") in the moving situation. This drop in friction force effectively increases the energy available from the compressed elastic member and induces an acceleration in the moving body, thus causing it to move forward sharply, and the elastic member to lose some of its stored energy. Acceleration of the driven body continues until the decreasing force available from the

elastic member falls below the resisting kinetic friction force level so causing a deceleration of the body until the point where motion ceases ("stick"). When the driven body comes to rest the friction force is once again that due to static friction. The process is repeated and continuous self-generated vibrations occur. Since most drives in general engineering are transmitted via elastic members (e.g. leadscrews, hydraulic oil, etc.) then the vibratory motion of stick-slip can be seen to be a phenomenon which can produce difficulties in situations where accurate motion or positional control is required. In addition to the well-known undesirable existence of stick slip vibrations in machine tool tables and drives (1), other observations of the phenomenon in practice are common. Catling has described the torsional vibration problems associated with stick slip motion between threads and textile drafting rollers (2). It has also been observed between steel wires and dip rollers in the galvanising process (3) and Thompson (4) has recorded its presence in hydrostatic extrusion devices.

Dry lubricant materials have been used as load carrying members hitherto for their low friction and anti-stick-slip properties. A recent development, however in the lubrication of friction junctions rigidly driven relative to each other has been lubrication by transferred films of solid lubricant. The solid lubricant is located away from the friction junction and pressed on to the moving member of that junction. Wear of the lubricant causes transfer to the friction junction and consequent beneficial modification of the friction characteristics.

## 1.2 Review of Previous Work

### 1.2.1 Stick-Slip Motion

The basic cause of stick slip as the fluctuation in friction force at low relative sliding speeds was first observed by Thomas (5) in experiments on friction forces at low velocities of sliding.

Bowden and Leben (6) also conducted experiments on friction force fluctuation at low sliding speeds, paying particular attention to the variation in static friction force due to normal load and friction junction material variations.

Further experimental information was provided by Morgan et al (7) who measured kinetic friction force against sliding velocity. The method of measurement appeared to be rather unsophisticated, involving conversion of slip displacements to slip velocities by the taking of gradients. The results demonstrated a drop from static to kinetic friction force for all materials tested, with a long transition period for steel on steel.

The time dependent nature of static friction force has figured largely in experimental and theoretical work to date; Rabinowicz (8) and Kragelski (9) have shown experimentally that the static friction force is dependant upon the time of metallic contact. Rabinowicz demonstrated a reduction in stick slip amplitudes with increase in drive speed as a consequence of lack of junction growth i.e. reduction of time of metallic contact and

hence static friction force.

An analysis of stick slip motion was performed by Blok (10) in which the dynamic friction model was one of a constant kinetic friction force during slip following an instantaneous drop from a constant static level. By considering an additional viscous damping element in the system he determined a limiting condition for the persistence of stick-slip after which smooth sliding of the driven member occurred. Derjaguin et al (11) developed this approach further, to the extent of demonstrating the dependence of this stability condition on two dimensionless groups - viscous damping coefficient and  $\frac{\dot{\phi} \sqrt{KJ}}{(T_s - T_k)}$ . In addition they also attempted to consider the variations in friction force due to junction growth. A further dynamic friction model involving an instantaneous drop in static friction force followed by a negative damping relationship continuous for the slip period, was also considered but cannot be considered practically realistic. No experimental evidence was presented.

Brockley et al (12) investigated theoretically the existence of a critical velocity to bring about stability, for a time dependent parameter situation including viscous damping, using the Blok dynamic friction model. Reasonable confirmation with experimental results was achieved although some scatter is evident and the number of results taken were quite small.

Banerjee (13) proposed a purely kinetic friction concept, modelling the dynamic friction characteristic with a continuous 2nd

order polynomial based on steady state experimental results. His analysis showed the existence of a critical drive velocity and demonstrated the way in which the velocity of sliding returned to the impressed velocity under such conditions. No experimental confirmation of the analysis was included however. By careful measurement of stick slip amplitude and comparison with predictions from a non-linear analysis Symmons (14) showed the drop from static to kinetic friction force during slip to be proportional to the (slip velocity)<sup>0.5</sup> for a steel on steel junction. Bell and Burdekin (15) have produced a theoretical analysis by considering two linearised dynamic friction models, both based on a negative viscous damping concept for the accelerating part of the slip. A negative damping gradient is defined as  $\left(\frac{T_s - T_k}{\dot{\theta}_{\max}}\right)$  and a negative damping coefficient as  $\frac{(T_s - T_k)}{\dot{\theta}_{\max} 2\sqrt{KJ}}$ . The first analysis considered the negative damping effect to be continuous throughout slip; whilst the second, a discontinuous model, considered a constant value of kinetic friction force to be present for the decelerating part of the slip period. For both models, relationships between maximum slip velocity and negative damping coefficient and stick-slip frequency were developed. Comparisons with experimental results for a cast machine tool table were given. The stick slip frequency graph failed to provide an adequate comparison between theory and experimental results however, since it represented the time interval between the commencement of successive vibrations. A large proportion of this time period must be made up of 'stick time' and therefore it is difficult to assess the merit of the analysis from this method of presentation. For the former graph (maximum slip velocities) for values of negative

damping coefficient up to about 0.5, there was close agreement between theory and experimental results. Experimental results showing dynamic gradient as a function of impressed velocity were negative for all natural frequencies examined (metal to metal sliding). By the introduction of polar lubricant the friction dynamic gradient was modified and became zero at very low velocities. This point of zero gradient was suggested by Burdekin and Bell as being the condition at which stability would occur in any system. Further analysis by the author of the negative damping friction characteristic (see section 2.3) by the inclusion of a positive damping term into the system will show that stability can in fact be induced when the friction dynamic gradient is still negative. Earlier work by Burdekin and Bell (16) had shown the presence of a dynamic friction characteristic with positive gradient at low sliding velocities for cast iron surfaces lubricated by polar lubricants; a system in which stick-slip vibration was not observed.

### 1.2.2 Transfer Lubrication Techniques

Recently Hemingray, Cowley and Burdekin (17, 18) have discussed the use of plastics as part of a slideway joint to eliminate vibrations due to stick slip and also reduce the friction forces. When used in this manner however several undesirable features can be produced. These include low wear resistance, as indicated in results obtained by Lapidus (19) and consequent high frequency of overhauls and dimensional instability. Filling of the plastics can increase the strength and reduce the wear rates but problems of separation can arise due to differential coefficients of thermal expansion.

The use of plastics as a lubricating medium by transferred films of solid lubricants avoids some of these problems. Devine, Lamson and Bowen (20) quote many examples of the transfer lubrication technique being used in rigidly driven situations with success. The dry lubricant is introduced between two mating surfaces under load, usually by pressure contact with one of the surfaces. Using a lubricant composed of molybdenum disulphide, graphite and sodium silicate located in reservoir pockets of a rolling element bearing the above authors demonstrated an extension of life over unlubricated running of up to 20 times. This transfer lubrication technique is relatively simple to use and avoids the costly surface preparation and treatment hitherto found necessary for dry film lubrication as indicated by A C Wood (21). Similarly the strength requirement for a bearing material acting as a load carrying member is not necessary, since a relatively weak material can wear at a sufficient rate to maintain replenishment of the lubricant. J K Lancaster (22, 23, 24) has provided extensive information on lubrication by transferred films of solid lubricants, experiments being conducted mostly on a pin and disc, rigidly driven apparatus with the load applied vertically through the pin. Transfer took place from a lubricant compact located diametrically opposite the friction interface and provided for continuous replenishment of the lubricant at friction junction. Using predominantly graphite, p.t.f.e. and molybdenum disulphide he demonstrated the validity of the lubrication by examining the surfaces, declaring the lubricant

to have failed when scuffing of the surfaces occurred. Maximum scuffing loads were found, indicating molybdenum disulphide, p.t.f.e. and graphite, in that order, as supporting the highest loads. The speed of sliding of the junction was 60 cm/s and surface finish  $30\mu\text{in}$  ( $0.75\mu\text{m}$ ) C.L.A. for steel on steel. With the same speed, surface finish and material, evidence was also produced to show that although continuous replenishment of the lubricant extends the life of the bearing surface it is still a finite rather than infinite process.

Using this technique in a stick slip situation involves the action of two dynamic friction characteristics on the driven member, that of the metal to metal interface and that of the transfer lubricant to metal interface. The metal to metal interface characteristic is modified by the lubricant transferred to the junction until a coherent film of lubricant is formed and the lubricant to metal characteristic governs the motion of the driven member. For a suitable lubricant this will cause the elimination of stick slip. However any positive viscous damping effect from the dynamic characteristic of the transfer lubricant itself acting upon the driven member can assist in eliminating the stick slip under minimal lubricant film conditions at the friction junction. Dynamic friction characteristics of the dry lubricants to be used in the experimental programme are not available, but steady state measurements by Hemingray (17) and Lewis (25) showed an increase in friction force for increasing sliding velocity for p.t.f.e. and graphite rubbing on steel. This encourages the author to propose a dynamic friction model for the transfer

lubricants based upon a constant Coulomb resistance together with a positive viscous damping resistance. Thus it seems possible that transfer lubrication of solid lubricant films can provide a simple solution to the problems of stick-slip vibratory motion and present itself as a viable alternative to the use of plastics as a structural material such as happens in slideways.

### 1.3 Objectives of Investigation

From the foregoing it was proposed to examine experimentally the circumstances in which transfer lubrication could be successful in eliminating stick slip vibrations and theoretically explain the method of elimination in terms of stability relationships brought about by the dynamic viscous damping action of the dry lubricant. This necessitated comparison of the upper and lower bound linearised dynamic friction model theories under unlubricated conditions, measurement of the dynamic viscous action of the dry lubricant under transfer lubricated conditions and comparison of experimental transfer lubricated results with theoretical stability relationships developed using the above stick slip dynamic friction models.

Fig 1.1 Rotational Stick Slip Configuration

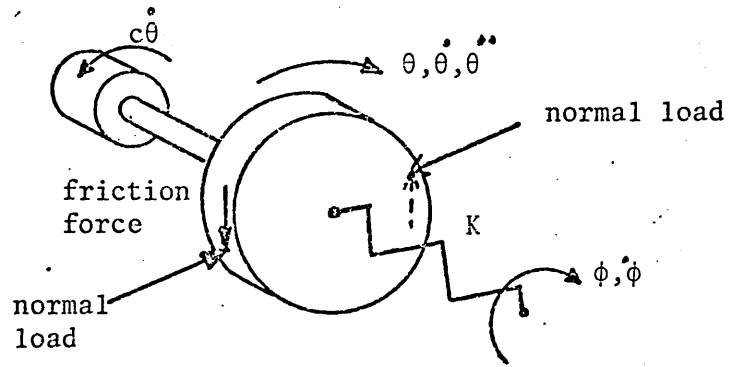
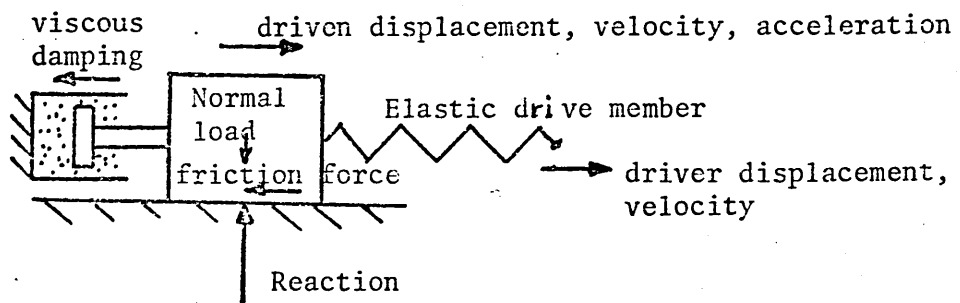


Fig 1.2 Translational Stick Slip Configuration



## 2.1 Introduction

Two linearised dynamic friction models are used in sections 2.2 and 2.3 in providing an analysis of stick-slip motion in a rotating system. The constant static, instantaneous constant kinetic friction torque model shown in fig. 2.1 was first suggested by Blok. Utilising this model, the analysis of section 2.2 examines various stick-slip properties in terms of the dimensionless parameter  $\frac{\dot{\phi} \sqrt{KJ}}{(T_s - T_k)}$ . A stability relationship is also determined for the system subjected to viscous damping which demonstrates that value of viscous damping which will eliminate vibrations for any particular value of the dimensionless parameter.

The second dynamic friction model considered is shown in fig. 2.2 where the drop from a static friction torque to a kinetic friction torque is linear for the acceleration period and the kinetic friction torque is considered constant for the deceleration period. This model will be called a negative damping model. Stick-slip properties are again determined and a stability condition demonstrated, depending upon applied viscous damping. As previously mentioned Symmons demonstrated the drop from static friction force to friction force at maximum slip velocity to be proportional to (slip velocity)<sup>0.5</sup>. However the method he used, of comparing measured amplitudes to theoretical amplitudes based on non-linear analysis, indicated stick slip amplitude to be insensitive to variations in the shape of the dynamic friction model. Confirmation of this was

provided by Cockerham and Cole (26), in an analogue simulation of unlubricated stick slip for a selection of non-linear friction characteristics. They showed amplitude of vibrations to be almost directly proportional to  $(T_s - T_k)$  for a variety of friction characteristics. Amplitude of vibrations is therefore considered an unsuitable basis for comparison of the accuracy of the above linearised model theories and will not be used extensively for comparison purposes.

Stability conditions for both theories rely upon the incorporation of a viscous damping element into the system and measurements by previous workers suggest dry lubricants exhibit such damping properties. It is therefore necessary in the experimental programme to determine a value of viscous damping for each lubricant. A dynamic friction model for the dry lubricant consisting of coulomb plus linear viscous damping is suggested and an expression is developed in section 2.5 from which the components of dry lubricant friction can be evaluated. This is achieved from an amplitude response curve obtained by applying an initial displacement to a mass-spring system subjected to dry lubricant damping.

## 2.2 Stick-Slip Analysis for Blok Dynamic Friction Model

Consider the friction force velocity characteristic as shown in Fig. 2.1 with a constant static value of friction torque  $T_s$  instantaneously falling to a constant kinetic friction torque value  $T_k$ . Considering the forces acting on the disc as shown in Fig. 1.1, the equation of motion is given by:

$J\ddot{\theta} + C\dot{\theta} + K\theta = K\phi - (\pm T_K)$  the direction of  $T_K$  depends upon the direction of velocity  $\dot{\theta}$

$$\ddot{\theta} + \frac{C}{J}\dot{\theta} + \frac{K}{J}\theta = \frac{K}{J}\phi - \left(\pm \frac{T_K}{J}\right)$$

Solving for  $\theta$

$$\theta = \phi - \frac{T_K}{K} - \frac{C\dot{\phi}}{K} + e^{\frac{-ct}{2J}} (A \cos wt + B \sin wt)$$

Boundary conditions:-

$$\text{At } t = 0, \theta = 0, \dot{\theta} = 0 \text{ and } \phi = T_S/K$$

Resulting in the following values for A and B:

$$A = \frac{-1}{K}(T_S - T_K - C\dot{\phi})$$

$$B = \frac{-C}{2JKW}(T_S - T_K - C\dot{\phi}) - \frac{\dot{\phi}}{W}$$

Giving the complete solution as follows:-

$$\theta = \phi - \frac{T_K}{K} - \frac{C\dot{\phi}}{K} - e^{\frac{-ct}{2J}} \left( \frac{(T_S - T_K - C\dot{\phi})}{K} \cos wt + \left( \frac{C}{2JKW} (T_S - T_K - C\dot{\phi}) + \frac{\dot{\phi}}{W} \right) \sin wt \right) \dots \dots \dots (1)$$

∴ the difference between the drive and driven displacement is given by

$$\phi - \theta = \frac{T_K}{K} + \frac{C\dot{\phi}}{K} + e^{\frac{-ct}{2J}} \left( \frac{(T_S - T_K - C\dot{\phi})}{K} \cos wt + \left( \frac{C}{2JKW} (T_S - T_K - C\dot{\phi}) + \frac{\dot{\phi}}{W} \right) \sin wt \right) \dots \dots \dots (2)$$

In order to determine the value of  $\phi - \theta$  it is necessary to find the value of  $wt$  for the occurrence of stick-slip.

Stick-slip period

Stick will re-occur when  $\dot{\theta} = 0$ .

From equation (1) therefore, differentiating and letting

$$c/2J = \mu$$

$$\dot{\theta} = \dot{\phi} + (-\mu e^{-\mu t} (A \cos wt + B \sin wt) + w e^{-\mu t} (-A \sin wt + B \cos wt)$$

where  $A = \frac{-1}{K}(T_S - T_K - C\dot{\phi})$        $B = \frac{-\mu}{KW}(T_S - T_K - C\dot{\phi}) - \frac{\dot{\phi}}{W}$

$$\therefore \dot{\theta} = \dot{\phi} - e^{-\mu t} \cos wt (\mu A - wB) - e^{-\mu t} \sin wt (\mu B + wA)$$

$$\dot{\theta} = \dot{\phi} - e^{-\mu t} (\cos wt (-\frac{\mu}{K} (T_S - T_K - C\dot{\phi}) + \frac{\mu}{K} (T_S - T_K - C\dot{\phi}) + \dot{\phi}) + \sin wt (\frac{-\mu^2}{KW} (T_S - T_K - C\dot{\phi}) - \frac{\mu\dot{\phi}}{W} - \frac{W}{K} (T_S - T_K - C\dot{\phi})))$$

letting  $1/\psi = \frac{(T_S - T_K)}{\dot{\phi} \sqrt{KJ}}$  and  $C_2 = \frac{\mu}{W_1}$

$$\dot{\theta} = \dot{\phi} \cdot (1 - e^{\frac{-C_2}{\sqrt{1-C_2^2}} wt} \cos wt - e^{\frac{-C_2}{\sqrt{1-C_2^2}} wt} \sin wt \cdot (\frac{C_2}{\sqrt{1-C_2^2}} - \frac{1}{\psi \sqrt{1-C_2^2}}) \dots \dots \dots (3)$$

equating  $\dot{\theta}$  to zero gives

$$1 - e^{\frac{-C_2}{\sqrt{1-C_2^2}} wt_1} \cos wt_1 = \sin wt_1 (\frac{C_2}{\sqrt{1-C_2^2}} - \frac{1}{\psi \sqrt{1-C_2^2}}) - e^{\frac{-C_2}{\sqrt{1-C_2^2}} wt_1} \dots \dots \dots (4)$$

Solving for  $wt_1$  and  $\psi$  for selected values of  $C_2$  gives the graph of fig. 2.3. Using these values of  $wt_1$  in equation (2) gives the relative displacement of driver to driven ( $\phi-\theta$ ), for any situation.

The values of  $wt_1$  are converted to non-dimensional form as

follows:-

$$\text{slip frequency, } \omega_S = \frac{2\pi}{t_1} = \frac{2\pi W}{\omega t_1} = \frac{2\pi W_1 \sqrt{1 - c_2^2}}{\omega t_1}$$

$$\therefore \frac{\omega_S}{\omega_1} = \frac{2\pi \sqrt{1 - c_2^2}}{\omega t_1} \quad (\text{see fig. 2.4})$$

It can be seen from figs. 2.3 and 2.4 that each curve tends towards a maximum i.e. a point where the condition for stick-slip is no longer valid, from which a condition for stability (i.e. no stick slip vibrations) can be determined.

From equation (4)

$$1 - e^{-F\omega t_1} \cos \omega t_1 = \sin \omega t_1 Fe^{-F\omega t_1} - \frac{G}{\psi} \sin \omega t_1 e^{-A\omega t_1}$$

$$\text{where } F = \frac{c_2}{\sqrt{1 - c_2^2}}$$

$$G = \frac{c_2}{\sqrt{1 - c_2^2}}$$

Re-arranging for  $\psi$  gives

$$\psi = \frac{G \sin \omega t_1 e^{-F\omega t_1}}{-1 + e^{-F\omega t_1} \cos \omega t_1 + \sin \omega t_1 Fe^{-F\omega t_1}}$$

$$\begin{aligned} \therefore \frac{d\psi}{d(\omega t_1)} &= (-1 + e^{-F\omega t_1} \cos \omega t_1 + \sin \omega t_1 Fe^{-F\omega t_1}) \\ &\quad (-G \sin \omega t_1 Fe^{-F\omega t_1} + G \cos \omega t_1 e^{-F\omega t_1}) \\ &\quad - (G \sin \omega t_1 e^{-F\omega t_1}) (-e^{-A\omega t_1} \sin \omega t_1 - Fe^{-F\omega t_1} \cos \omega t_1 - \\ &\quad F^2 \sin \omega t_1 e^{-F\omega t_1} + F \cos \omega t_1 e^{-F\omega t_1}) \end{aligned}$$

Equating to zero and re-arranging gives

$$e^{-F\omega t_1} + \sin \omega t_1 (F-1) (1 + e^{-F\omega t_1} \cos \omega t_1) = 0,$$

which for discrete values of  $c_2$  gives the value of  $\omega t_1$  corresponding to  $\psi_{\max}$  and hence the stability condition

indicated in fig. 2.5.

### Acceleration time period

From equation (3)

$$\dot{\theta} = (1 - e^{-Fwt} \cos wt - e^{-Fwt} \sin wt (F - \frac{G}{\psi}))\dot{\phi} \dots\dots (5)$$

The maximum velocity occurs when  $\frac{d\dot{\theta}}{dt} = 0$

$$\text{i.e. } 0 = we^{-Fwt} \sin wt + Fwe^{-Fwt} \cos wt - (F - \frac{G}{\psi})$$

$$(we^{-Fwt} \cos wt - Fwe^{-Fwt} \sin wt)$$

Re-arranging gives

$$\tan wt_2 = \frac{\sqrt{1-C_2^2}}{C_2 - \psi} \quad \text{where } t_2 \text{ represents the acceleration time period}$$

This relationship is shown in fig. 2.6 with  $wt_2$  converted to  $w_1 t_2$ .

### Maximum slip velocity

Utilising information from fig. 2.6 in equation (5) gives maximum slip velocity as a function of drive velocity -

$$\frac{\dot{\theta}_{\max}}{\dot{\phi}} = 1 - e^{-Fwt_2} \cos wt_2 - e^{-Fwt_2} \sin wt_2 (F - \frac{G}{\psi})$$

which is shown in fig. 2.7 for selected values of  $c_2$ .

## 2.3 Stick Slip Analysis for Negative Damping Dynamic Friction

### Model

Since the friction-velocity characteristic is discontinuous (see fig. 2.2) the motion must be considered in two parts - acceleration and deceleration.

Consider the acceleration phase of the friction characteristic shown in fig. 2.2.

Where  $C_F = \frac{T_S - T_K}{\dot{\theta}_{max}}$ , negative friction damping; C = positive applied viscous damping.

For the rotational system of fig. 1.1 the equation of motion is given by:

$$J\ddot{\theta} + (C - C_F)\dot{\theta} + K\theta = K\phi - (\pm T_S) \quad (\text{sign according to } \dot{\theta})$$

Solving for  $\theta$  gives

$$\theta = \phi - \frac{T_S}{K} - \frac{(C - C_F)\dot{\phi}}{K} + e^{\frac{-(C - C_F)t}{2J}} (D \cos w_2 t + E \sin w_2 t)$$

Boundary conditions

$$\text{at } t = 0, \theta = 0, \dot{\theta} = 0 \text{ and } \phi = \frac{T_S}{K}$$

$$\text{resulting in } D = \frac{(C - C_F)\dot{\phi}}{K}$$

$$E = \frac{\dot{\phi}}{w_2} \left( \frac{(C - C_F)^2}{2JK} - 1 \right)$$

$$\therefore \theta = \phi - \frac{T_S}{K} - \frac{2C_T\dot{\phi}}{w_1} + e^{\frac{-C_T}{\sqrt{1-C_T^2}}w_2 t} \frac{\dot{\phi}}{w_1} (2C_T \cos w_2 t + \left( \frac{2C_T^2 - 1}{1 - C_T^2} \right) \sin w_2 t) \dots \dots \dots (6)$$

where  $C_T = (C_2 - C_1)$

Acceleration time period

$$\dot{\theta} = \frac{d\theta}{dt} = \dot{\phi} - \dot{\phi} e^{\frac{-C_T w_2 t}{\sqrt{1-C_T^2}}} (\cos w_2 t + \frac{C_T}{\sqrt{1-C_T^2}} \sin w_2 t) \dots \dots \dots (7)$$

$$\ddot{\theta} = \dot{\phi} e^{\frac{-C_T w_2 t}{\sqrt{1-C_T^2}}} \sin w_2 t \left( \frac{w_1}{\sqrt{1-C_T^2}} \right)$$

Equating  $\ddot{\theta}$  to zero gives the value of  $w_2 t$  for maximum slip velocity i.e.  $0 = \sin w_2 t_2$

$$w_2 t_2 = 0, \pi \text{ etc.}$$

The value of  $w_2 t_2$  is converted to  $w_1 t_2$  and shown in fig. 2.8.

Substituting  $w_2 t = \pi$  in equation (7) gives the maximum slip velocity -

$$\dot{\theta}_{\max} = \dot{\phi} \left( 1 + e^{\frac{-C_T}{\sqrt{1-C_T^2}} \pi} \right) \dots \dots \dots (8)$$

The ratio of maximum slip velocity to drive velocity is shown in fig. 2.9 as a function of  $C_1$ , for various values of  $C_2$ .

Deceleration period

The equation of motion for the deceleration phase contains a constant kinetic friction force  $T_K$  and a positive applied viscous damping term  $C$  (see fig. 2.2).

$$\therefore J\ddot{\theta} + C\dot{\theta} + K\theta = K\phi - (\pm T_K)$$

Solving for  $\theta$  gives

$$\theta = \phi - \frac{T_K}{K} - \frac{C}{K}\dot{\phi} + e^{\frac{-ct}{2J}} (\text{A} \cos wt + \text{B} \sin wt) \dots \dots \dots (9)$$

Boundary conditions:-

$$\text{at } t = 0, \dot{\theta} = \dot{\theta}_{\max} = \dot{\phi} \left( 1 + e^{\frac{-C_T}{\sqrt{1-C_T^2}} \pi} \right), \theta = 0$$

Resulting in

$$A1 = -\frac{2C_2}{w_1} e^{\frac{-C_T \pi}{\sqrt{1-C_T^2}}} \dot{\phi} \quad B1 = \frac{(1-2C_2^2)}{w_1 \sqrt{1-C_2^2}} e^{\frac{-C_T}{\sqrt{1-C_T^2}} \pi} \dot{\phi}$$

$$\dot{\theta} = \dot{\phi} + e^{\frac{-C_T \pi}{\sqrt{1-C_T^2}}} \dot{\phi} e^{\frac{-C_2}{\sqrt{1-C_2^2}} wt} (\cos wt + \frac{C_2}{\sqrt{1-C_2^2}} \sin wt)$$

Stick will re-occur when  $\dot{\theta} = 0$

$$\therefore -1 = e^{\frac{-C_2 wt_3}{\sqrt{1-C_2^2}}} \cdot e^{\frac{-C_T \pi}{\sqrt{1-C_T^2}}} \cdot (\cos wt_3 + \frac{C_2}{\sqrt{1-C_2^2}} \sin wt_3) \dots \dots \dots (10)$$

is the condition for stick slip to occur.

This enables a plot of  $C_1$  against  $wt_3$  to be made for a selection of values of  $C_2$  (since  $C_1 = C_2 - C_T$ ) where  $t_3 =$  deceleration period. (see fig. 2.10). The values of  $wt_3$  are converted to  $w_1 t_3$  by dividing by  $\sqrt{1 - C_2^2}$ .

### Frequency of stick slip vibrations

Total slip time period is the sum of acceleration and deceleration time periods

$$\therefore w_1 t_1 = w_1 t_2 + w_1 t_3$$

Hence slip frequency

$$w_s = \frac{2\pi}{t_1} \quad \text{i.e.} \quad \frac{w_s}{w_1} = \frac{2\pi}{w_1 t_1}$$

The ratio of slip frequency to natural frequency is shown in fig. 2.11 plotted against  $C_1$  - negative damping friction coefficient, for selected values of  $C_2$  - applied viscous damping coefficient.

### Limiting conditions for stability

From fig. 2.10 it can be seen that the curves tend to a minimum, giving rise to a situation where stick does not re-occur, i.e. stability is achieved. Differentiating equation (10) with respect to  $wt_3$  where  $C_2$  is a constant gives the following:

$$\begin{aligned} 0 = & -e^{\frac{-C_T \pi}{\sqrt{1-C_T^2}}} (\cos wt_3 + \frac{C_2}{\sqrt{1-C_2^2}} \sin wt_3) \frac{C_2}{\sqrt{1-C_2^2}} e^{\frac{-C_2 wt_3}{\sqrt{1-C_2^2}}} \\ & + e^{\frac{-C_2}{\sqrt{1-C_2^2}} wt_3} (e^{\frac{-C_T \pi}{\sqrt{1-C_T^2}}} (-\sin wt_3 + \frac{C_2}{\sqrt{1-C_2^2}} \cos wt_3) \\ & + (\cos wt_3 + \frac{C_2}{\sqrt{1-C_2^2}} \sin wt_3) \frac{dC_T}{dw_1 t_3} e^{\frac{-C_T \pi}{\sqrt{1-C_T^2}}} \left( \frac{(1-C_T^2)^{\frac{1}{2}} - (1-C_T^2)^{-\frac{1}{2}}}{(1-C_T^2)} \right) \end{aligned}$$

From which

$$\frac{dC_T}{dwt_3} = 0 = \left( \frac{C_2^2}{1-C_2^2} \right) \sin wt_3, \text{ gives } wt_3 = \pi$$

Substituting  $wt_3 = \pi$  into equation (10) gives

$$-1 = -e^{\frac{-C_2 \pi}{\sqrt{1-C_2^2}}} \cdot e^{\frac{-C_T \pi}{\sqrt{1-C_T^2}}} \text{ as the stability condition.}$$

Since  $C_T$  is negative this condition is satisfied when

$$C_2 = -C_T \text{ which is shown in fig. 2.12 as } C_1 = 2C_2.$$

## 2.4 Comparisons between the two dynamic friction model theories

### 2.4.1 Comparison of relative displacements and slip velocities

Theoretical relative displacements and relative slip velocities are presented in figs. 2.13 and 2.14 as an indication of the variation of stick slip properties with dynamic friction model, together with the effect of viscous damping on the system. The assumed system parameters for the calculations are as follows; spring stiffness  $K = 5.5\text{Nm/rad}$ , system inertia  $J = 3.5 \times 10^{-3}\text{Kgm}^2$ , static friction torque  $T_S = 0.25\text{Nm}$ , drive velocity  $\dot{\phi} = 0.1 \text{ rad/s}$ .

For the negative damping coefficient friction model a value of 0.4 for  $C_1$  is assumed giving the relative displacement and slip velocity distributions shown in fig. 2.13. Progressive inclusion of a positive viscous damping coefficient  $C_2$  reduces the maximum slip velocity and re-stick relative displacement and increases the slip time period. When the value of  $C_2$  reaches the critical value of half the negative damping coefficient  $C_1$  then the slip velocity becomes continuous and decays to the drive speed  $\dot{\phi}$ , and the relative displacement also becomes continuous.

Taking a value of 0.055Nm for  $(T_S - T_K)$  gives a Blok parameter of  $\psi = 0.25$  for use in the appropriate equations. Theoretical values of slip velocity and relative displacements are calculated and shown in fig. 2.14 for no damping. Increasing the viscous damping coefficient gives a similar effect as for the negative damping model. A value of  $C_2 = 0.68$  obtained from the stability relationship of fig. 2.5 produces continuous slip velocity and relative displacement, i.e. stability.

#### 2.4.2 Stick-Slip Amplitude and its variation with System Parameters

The theoretical amplitude of vibrations is given by the difference between the maximum relative displacement and the minimum relative displacement. The latter is available using the relative displacement equations and values of  $\omega t_1$  from figs. 2.3 and 2.11. Maximum relative displacements, however do not occur at the initial point of slip. This maximum will occur when  $\frac{d}{dt}(\phi - \theta) = 0$ .

For Blok friction model differentiating equation (3) with respect to time and equating to zero gives

$$0 = \cos \omega t + \sin \omega t \frac{\psi C_2 - 1}{\psi \sqrt{1 - C_2^2}}$$

$$\text{giving } \tan \omega t_4 = \frac{-\psi \sqrt{1 - C_2^2}}{\psi C_2 - 1} \dots \dots \dots (11)$$

where  $t_4$  = time period of maximum displacement.

For negative damping coefficient model differentiating equation (6) with respect to time and equating to zero gives

$$0 = e^{\frac{-C_T \omega_2 t}{\sqrt{1 - C_T^2}}} (\cos \omega_2 t + \frac{C_T}{\sqrt{1 - C_T^2}} \sin \omega_2 t)$$

$$\text{giving } \tan \omega_2 t_4 = \frac{\sqrt{1 - C_T^2}}{C_T} \dots\dots\dots (12)$$

Using the condition represented by equation (11) in equation (2) and the condition represented by equation (12) in equation (6) thus enables maximum relative displacements and hence stick slip amplitudes to be obtained.

As an indication of the effect of varying system parameters on the theoretical amplitude of stick slip, graphs of amplitude are presented in figs. 2.15 and 16 for variations in spring stiffness, system inertia, drive velocity and dynamic friction values. Using a nominal value of  $C_1 = 0.4$  for the negative damping coefficient theory gives fig. 2.16 and a value of  $(T_S - T_K) = 0.055\text{Nm}$  for the Blok model theory gives fig. 2.15. It can be seen from these graphs that increasing spring stiffness values causes a reduction in stick slip amplitudes for both theories, the rate of amplitude reduction being almost identical. Comparing the effects of variation of  $\dot{\phi}$  and J shows considerable difference between the two theories. For the Blok model theory the amplitude of vibrations is practically independent of  $\dot{\phi}$  and J, showing slight decreases for increasing drive speed and system inertia. However for the negative damping coefficient model theory considerable reduction in amplitude occurs for decreasing values of drive velocity and system inertia.

Variations in stick slip amplitude with dynamic friction model are shown in fig. 2.17. Amplitude of vibrations is seen to be directly proportional to  $(T_S - T_K)$  levels, but increases

exponentially with  $C_1$  values. Above negative damping coefficient values of 0.4 large increases in vibration amplitude are evident.

## 2.5 Theoretical Analysis of Dry Lubricant Friction Effects

As suggested in Chapter 1, the dynamic friction model for the transfer lubricant acting on the disc is considered to consist of a coulomb friction resistance, together with a positive viscous damping resistance. If this model is accurate then difficulty will be experienced in quantifying the friction components by direct measurement. In order to separate and evaluate the coulomb and viscous friction components of the dry lubricants, a method proposed by Kennedy (27) is utilised, necessitating the modification of initial displacement amplitude response curves as follows.

Consider a characteristic made up of coulomb damping (T) plus positive viscous damping (C), then the equation of motion for a freely vibrating torsional mass-spring system subjected to such damping is

$$J\ddot{\theta} + c\dot{\theta} + K\theta = \pm T$$

For 1st half cycle T is positive

$$\therefore \theta = \frac{T}{K} + Me^{-\mu t} \cos (wt - \alpha) \text{ where } M \text{ is a constant,}$$

$\alpha$  a constant phase angle

for an initial displacement of  $\theta = \theta_0$  at  $t = 0$ ,

$$M = \frac{\theta_0 - T/K}{\cos (-\alpha)}$$

First peak occurs at  $wt = \pi$

$$\therefore -\theta_1 = \frac{T}{K} + \frac{\theta_0 - \frac{T}{K}}{\cos(-\alpha)} e^{-\frac{\mu\pi}{w}} \cos(\pi - \alpha)$$

$$\theta_1 = \frac{-T}{K} + (\theta_0 - \frac{T}{K}) e^{-\frac{\mu\pi}{w}}$$

For next half cycle T is negative

$$\therefore \theta_2 = \frac{-T}{K} + (\theta_1 - \frac{T}{K}) e^{-\frac{\mu\pi}{w}}$$

In terms of  $\theta_0$  gives

$$\theta_2 = \frac{-T}{K} - \frac{2T}{K} e^{-\frac{\mu\pi}{w}} + (\theta_0 - \frac{T}{K}) e^{-\frac{2\mu\pi}{w}}$$

$$\theta_3 = \frac{-T}{K} - \frac{2T}{K} e^{-\frac{\mu\pi}{w}} - \frac{2T}{K} e^{-\frac{2\mu\pi}{w}} + (\theta_0 - \frac{T}{K}) e^{-\frac{3\mu\pi}{w}}$$

In general terms for 'n' peaks

$$\begin{aligned} \theta_n &= \frac{-T}{K} + (\theta_0 - \frac{T}{K}) e^{-\frac{n\mu\pi}{w}} - \frac{2T}{K} (e^{-\frac{\mu\pi}{w}} + e^{-\frac{2\mu\pi}{w}} \dots e^{-\frac{(n-1)\mu\pi}{w}}) \\ &= \frac{-T}{K} + (\theta_0 - \frac{T}{K}) e^{-\frac{n\mu\pi}{w}} - \frac{2T}{K} (e^{-\frac{\mu\pi}{w}} (1 + e^{-\frac{\mu\pi}{w}} \dots e^{-\frac{(n-2)\mu\pi}{w}})) \end{aligned}$$

$$\theta_n = (\theta_0 - \frac{T}{K}) e^{-\frac{n\mu\pi}{w}} - \frac{T}{K} \left\{ \frac{1 + e^{-\frac{\mu\pi}{w}}}{1 - e^{-\frac{\mu\pi}{w}}} \right\} \dots \dots \dots (13)$$

Therefore a plot of the successive peak amplitudes of such a system subjected to initial displacement can be modified by adding the constant value  $\frac{T}{K} \left\{ \frac{1 + e^{-\frac{\mu\pi}{w}}}{1 - e^{-\frac{\mu\pi}{w}}} \right\}$  until an exponential relationship is obtained.

The ratio of amplitudes of the modified values is used in finding the viscous component of damping (c), and the constant value added is used to determine the coulomb component of damping (T).

Fig. 2.1 'Static Instantaneous Constant Kinetic Friction Torque' characteristic

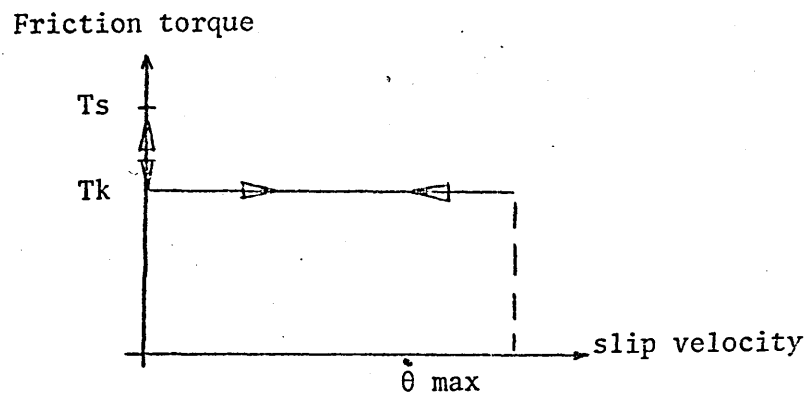


Fig. 2.2 'Negative Damping Friction Torque' characteristics

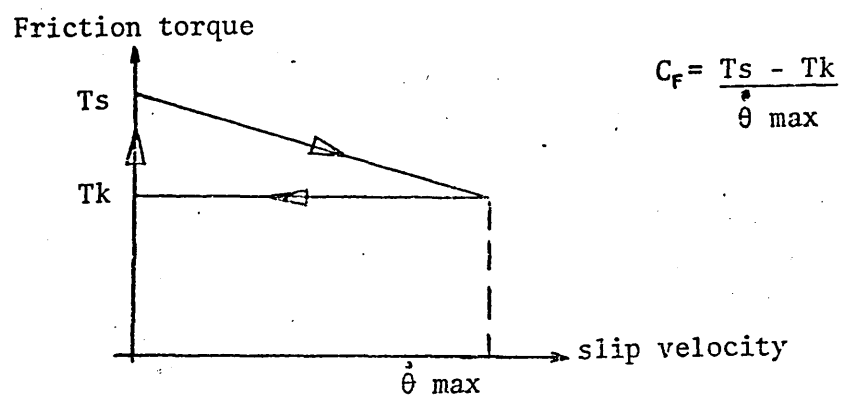


Fig 2.3

$\psi$  vs  $\omega t_1$ , for various values of  $c_2$  applied damping

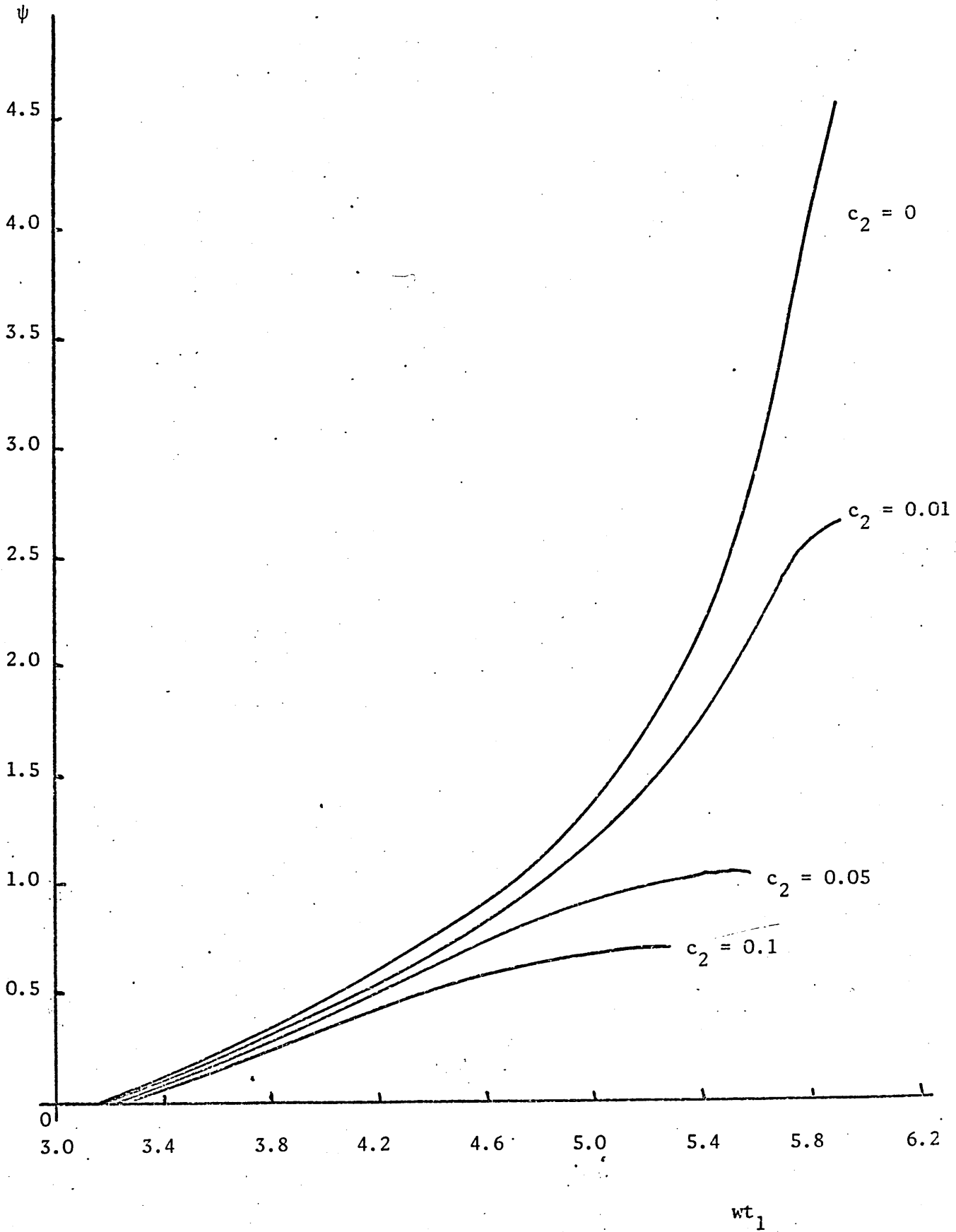


Fig 2.4  
 $\psi$  vs  $\frac{w_s}{w_1}$  for various values of  $c_2$  - applied damping

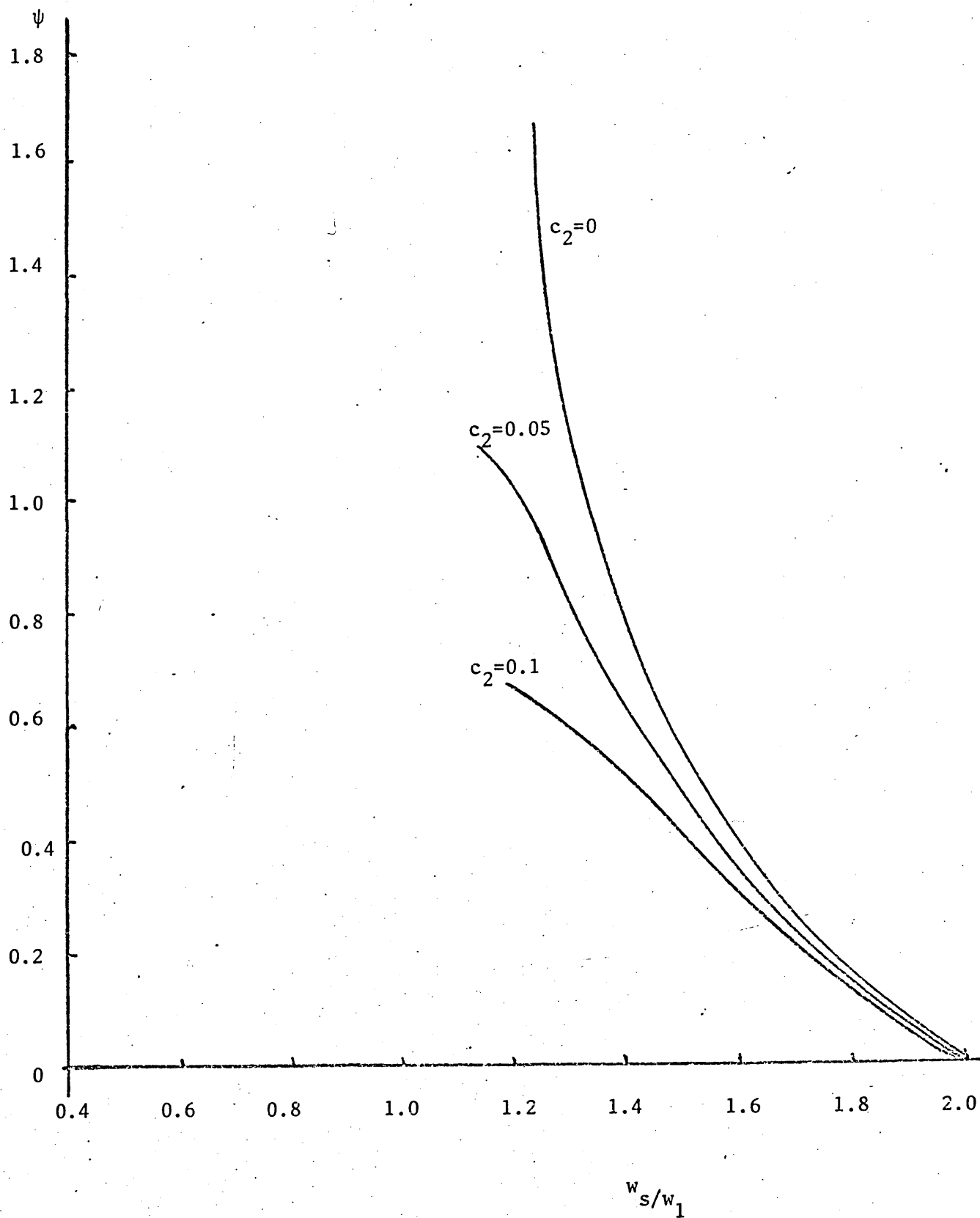


Fig 2.5

$\psi$  vs.  $c_2$  (applied damping) showing  
stability condition (Blok model)

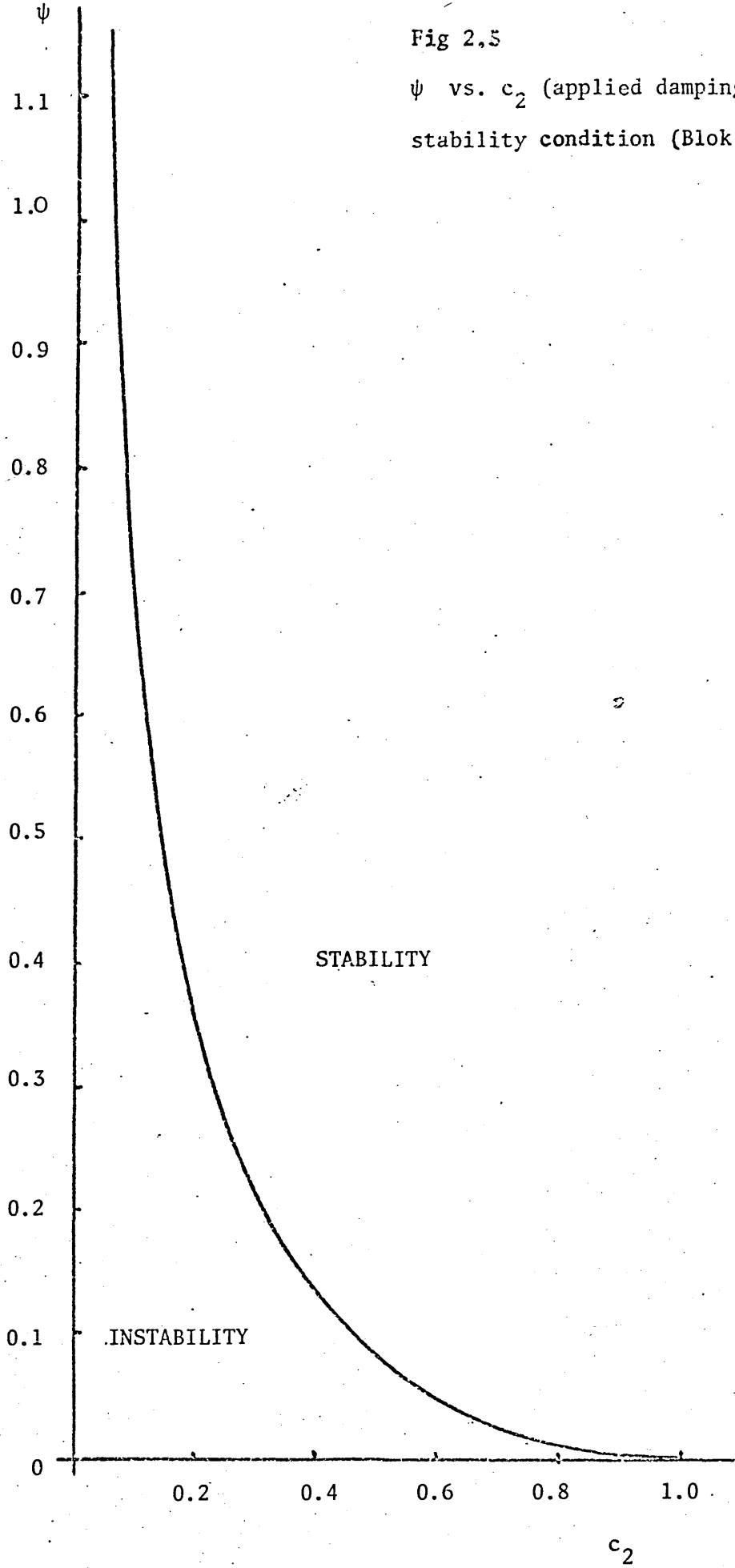


Fig 2.6

$\psi$  vs.  $w_1 t_2$  (acceleration period) for selected values of  $c_2$  - applied damping coefficient.

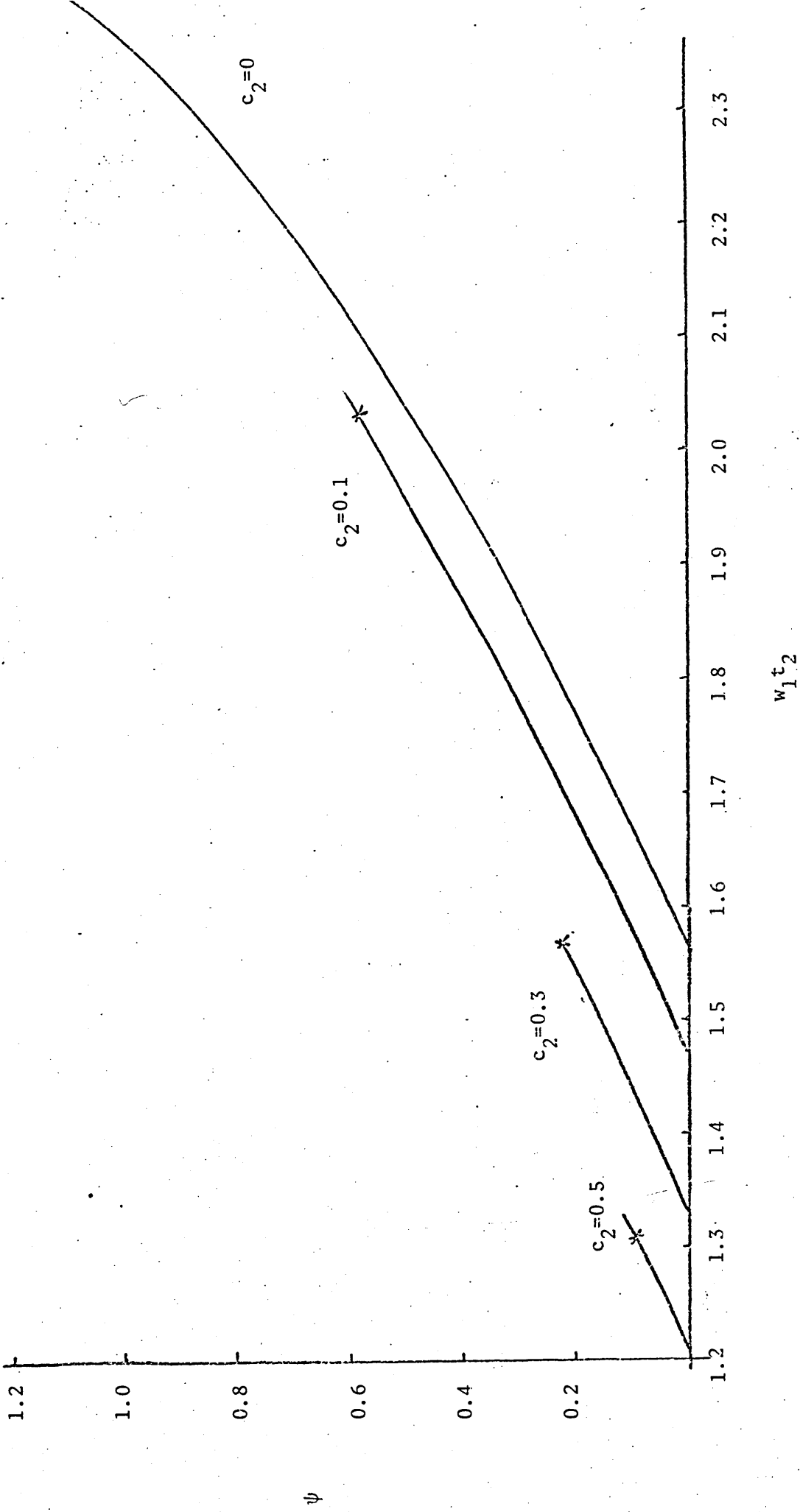


Fig 2.7

$\frac{\dot{\theta}_{max}}{\phi}$  vs  $\psi$  for selected values of  $c_2$  - applied damping coefficient

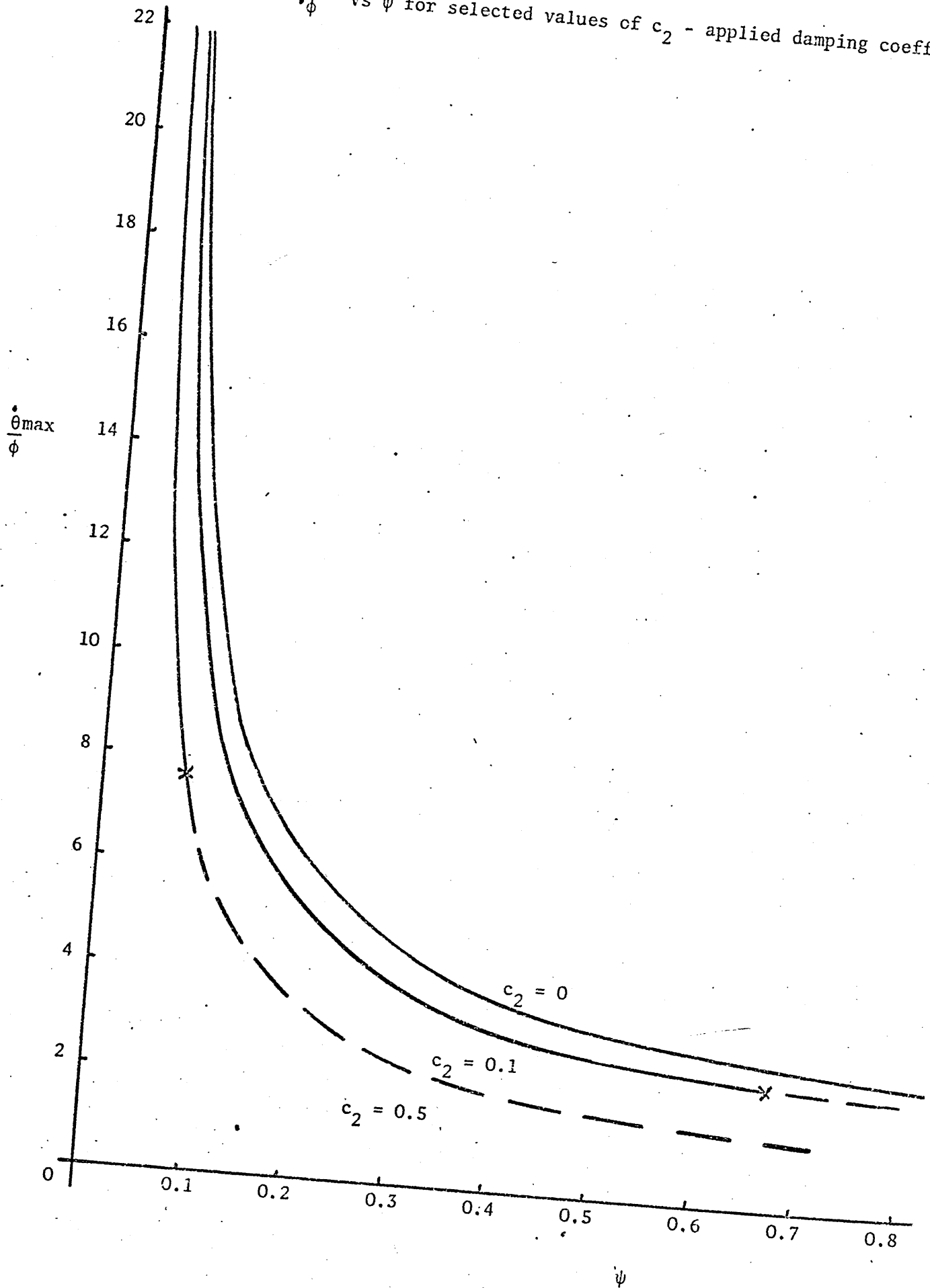


Fig 2.8

$c_1$  (negative damping coefficient) vs  $w_1 t_2$  (acceleration period) for various values of  $c_2$  - applied damping.

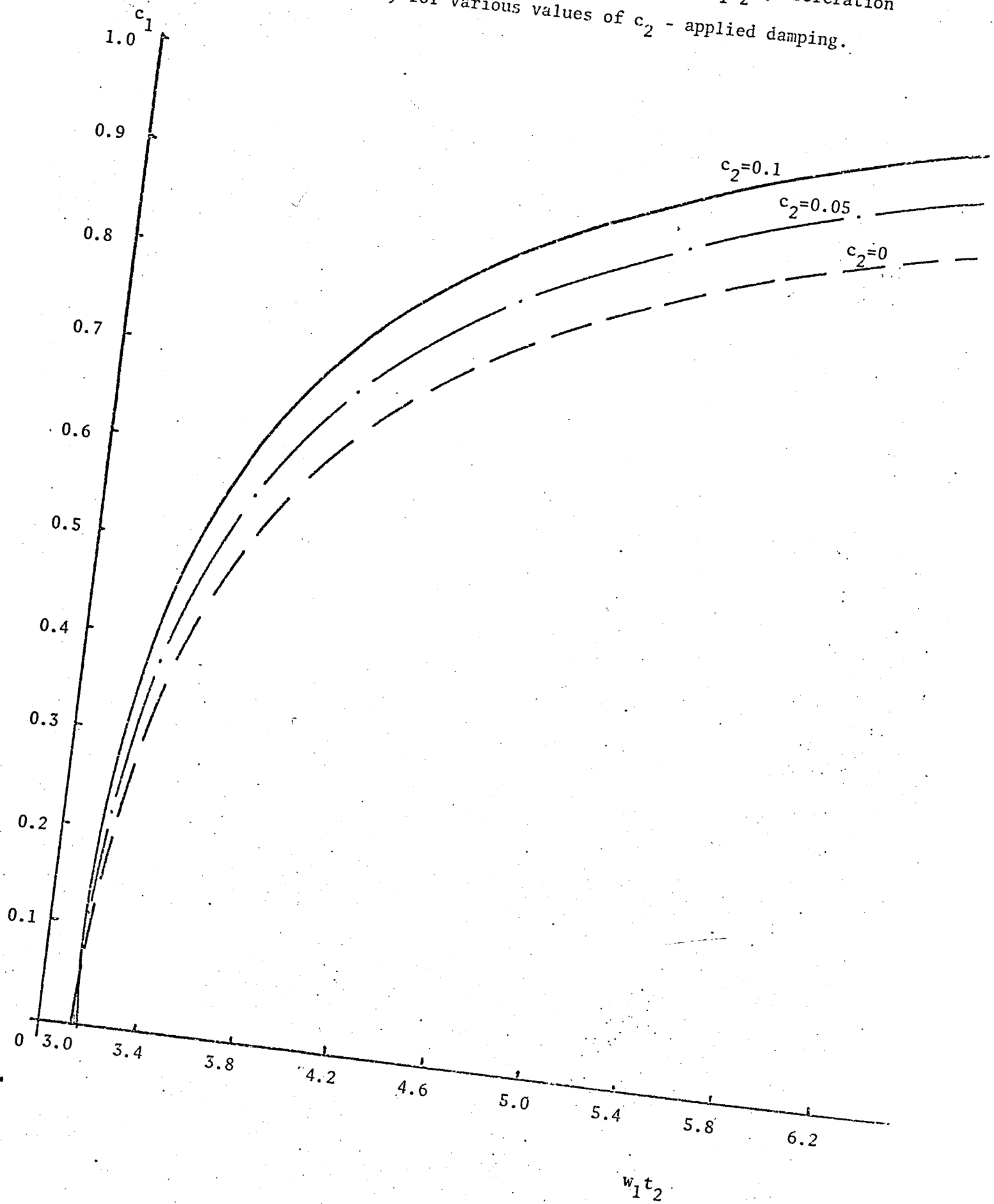


Fig 2.9

$\frac{\theta_{max}}{\phi}$  vs  $c_1$  for various values of  $c_2$

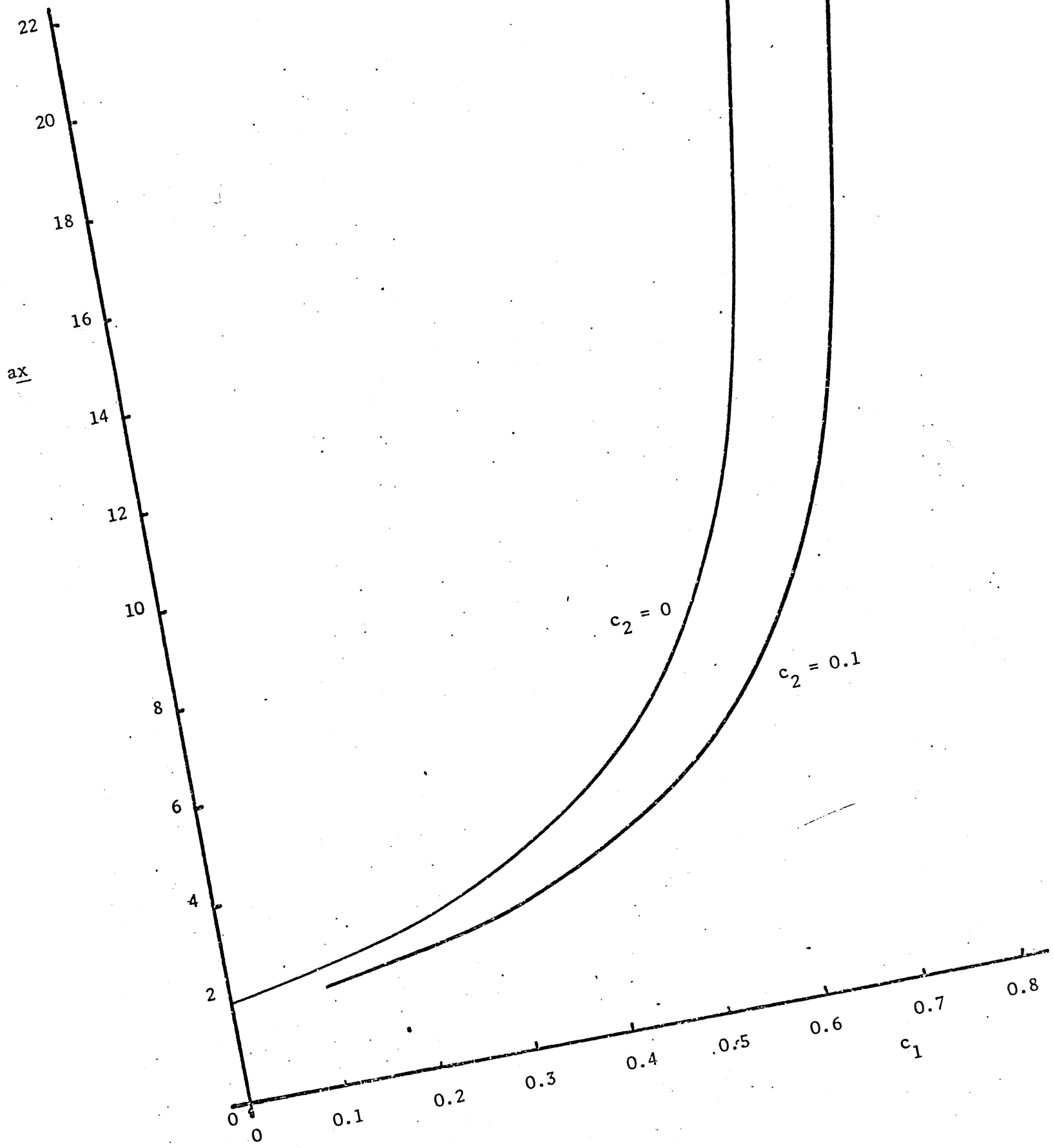


Fig 2.10

$c_1$  vs  $w_1 t_3$  (deceleration period) for various values of  $c_2$

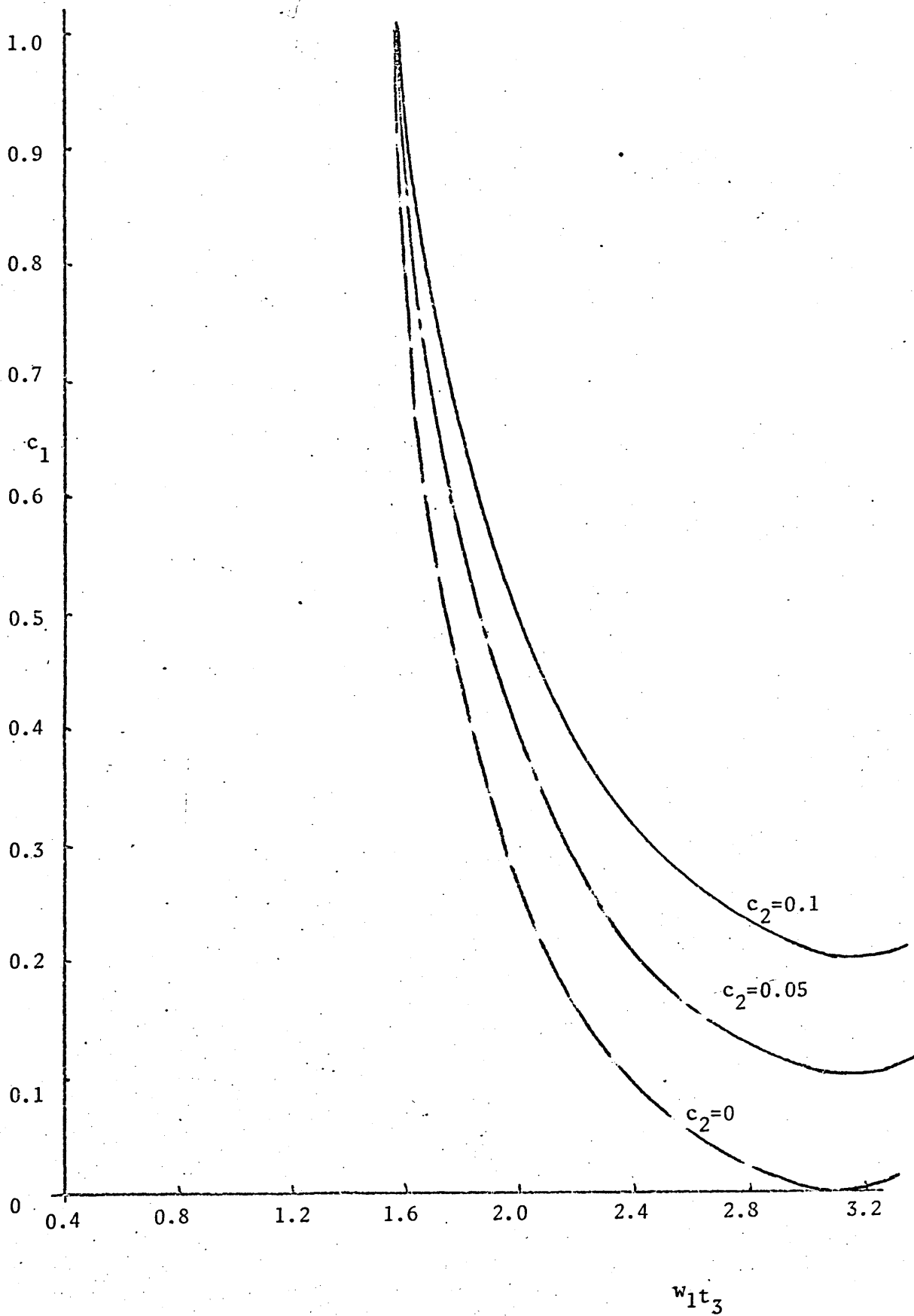


Fig 2.11

$c_1$  vs  $w_s/w_1$  for various values of  $c_2$

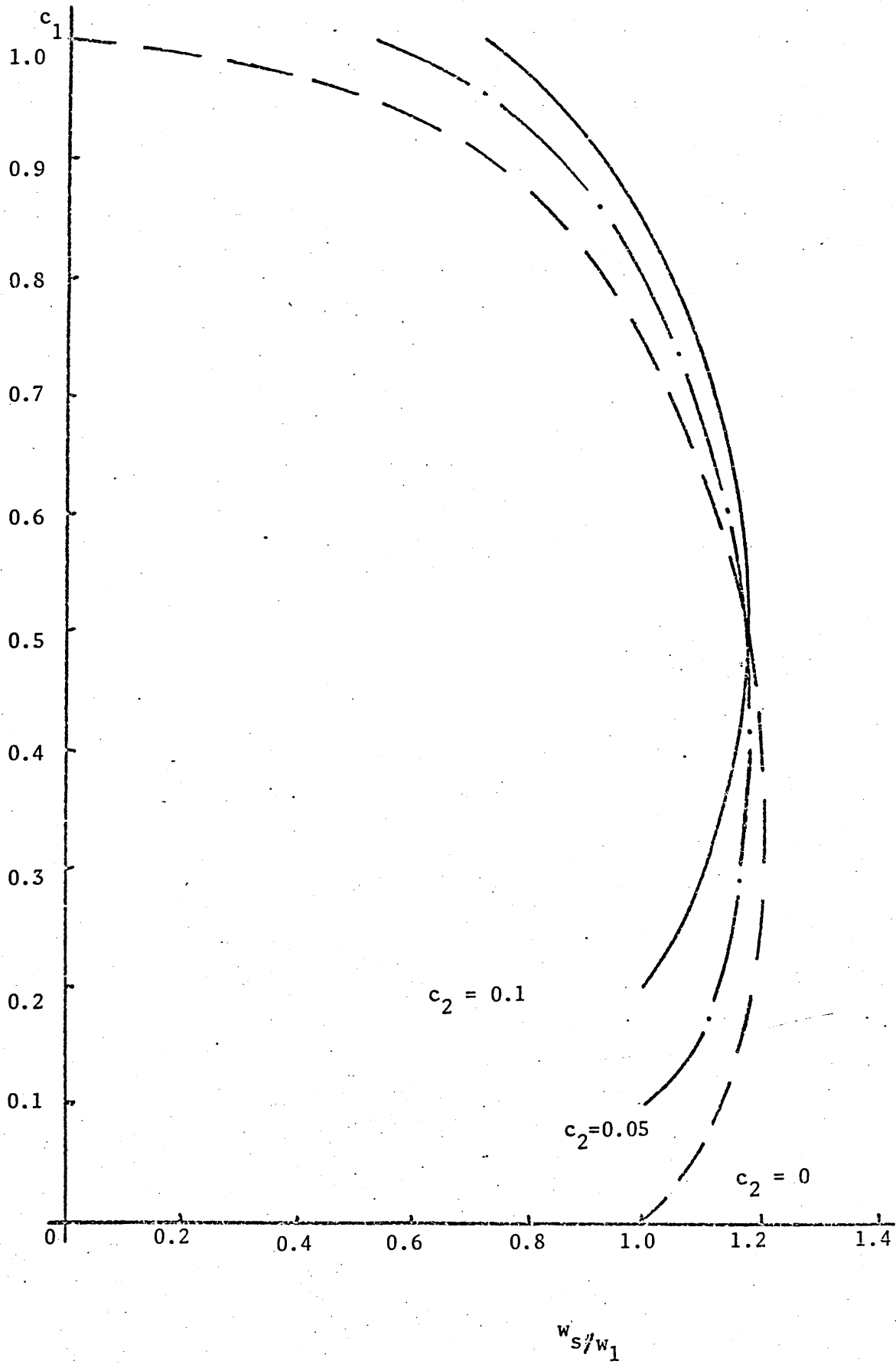
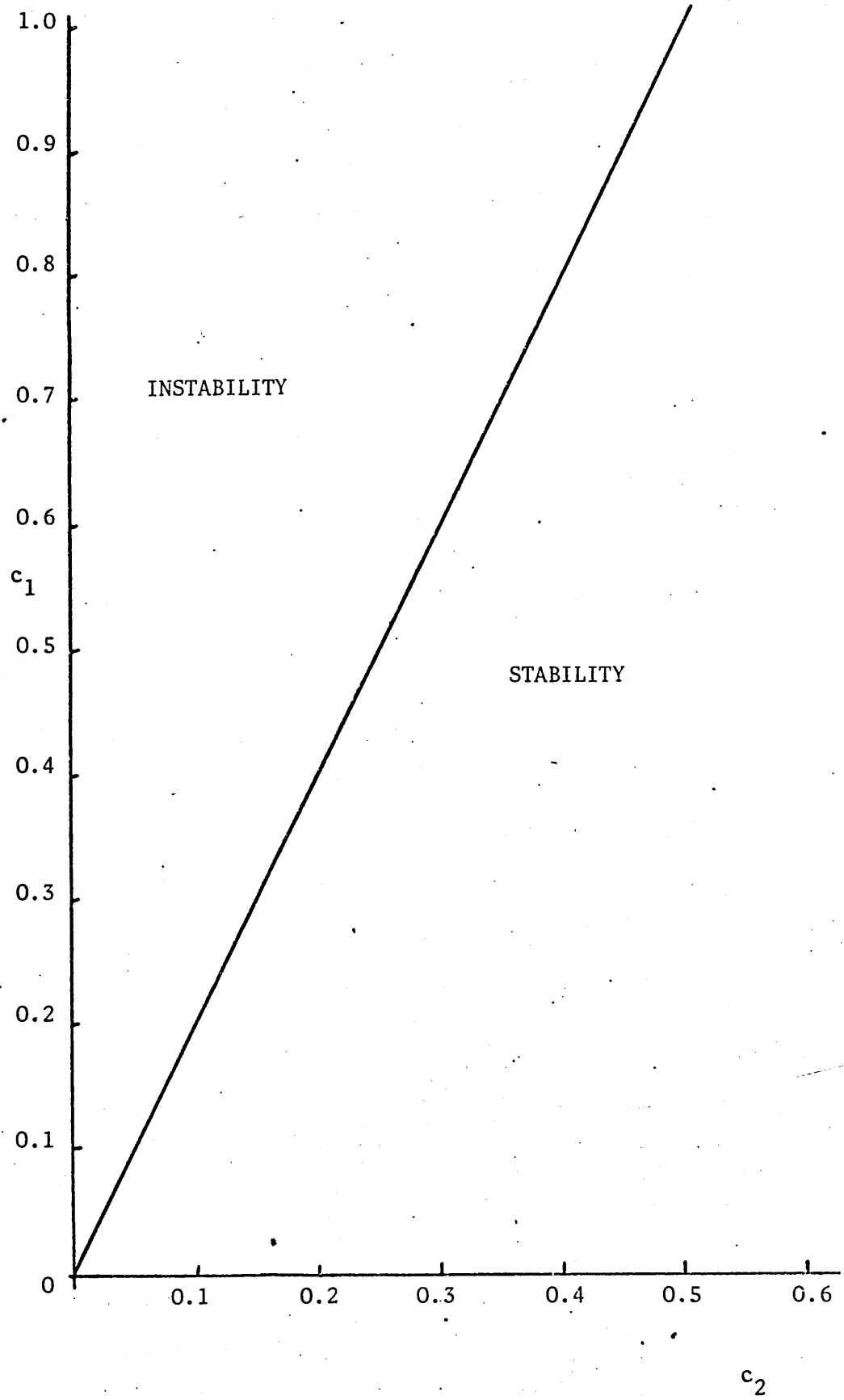


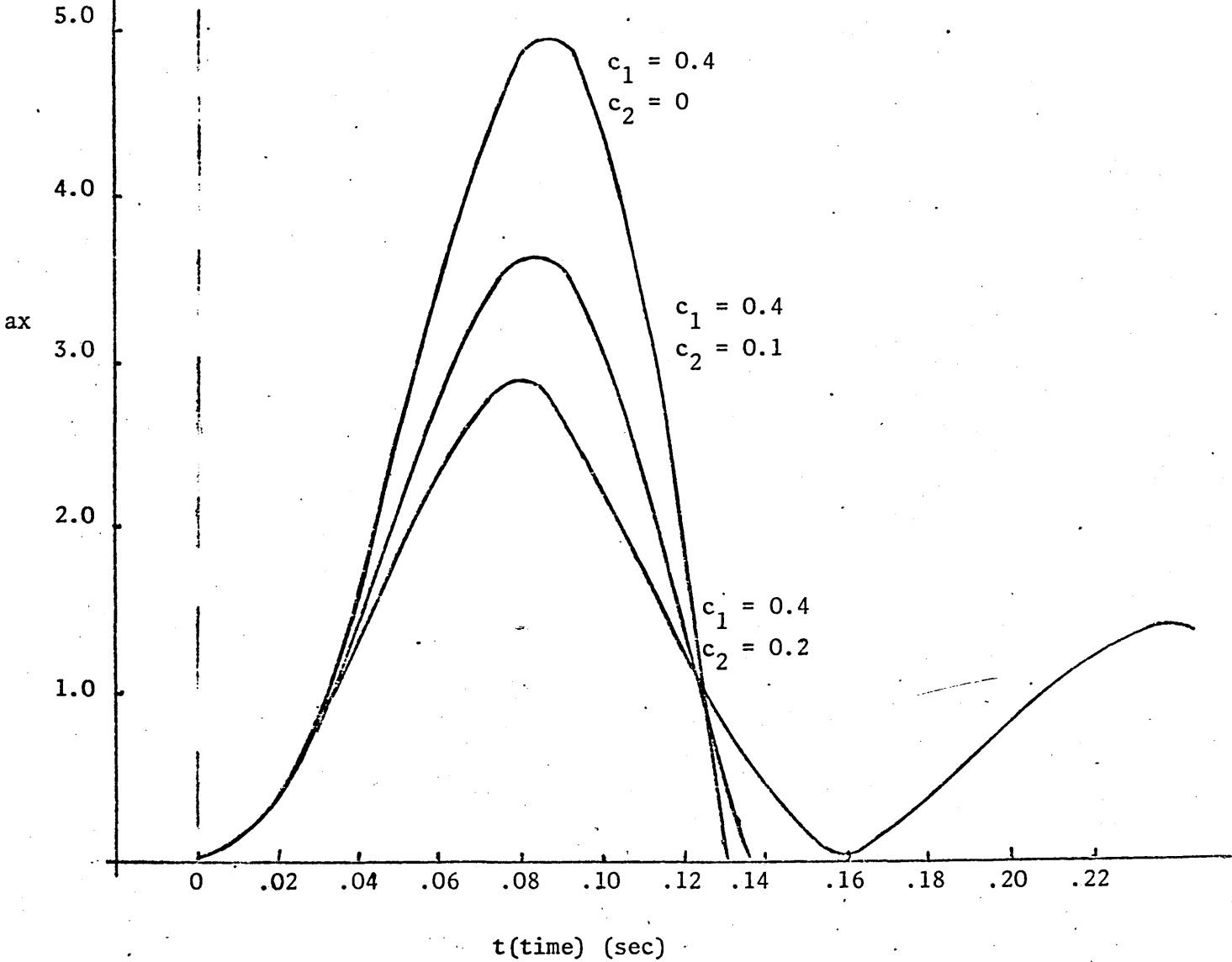
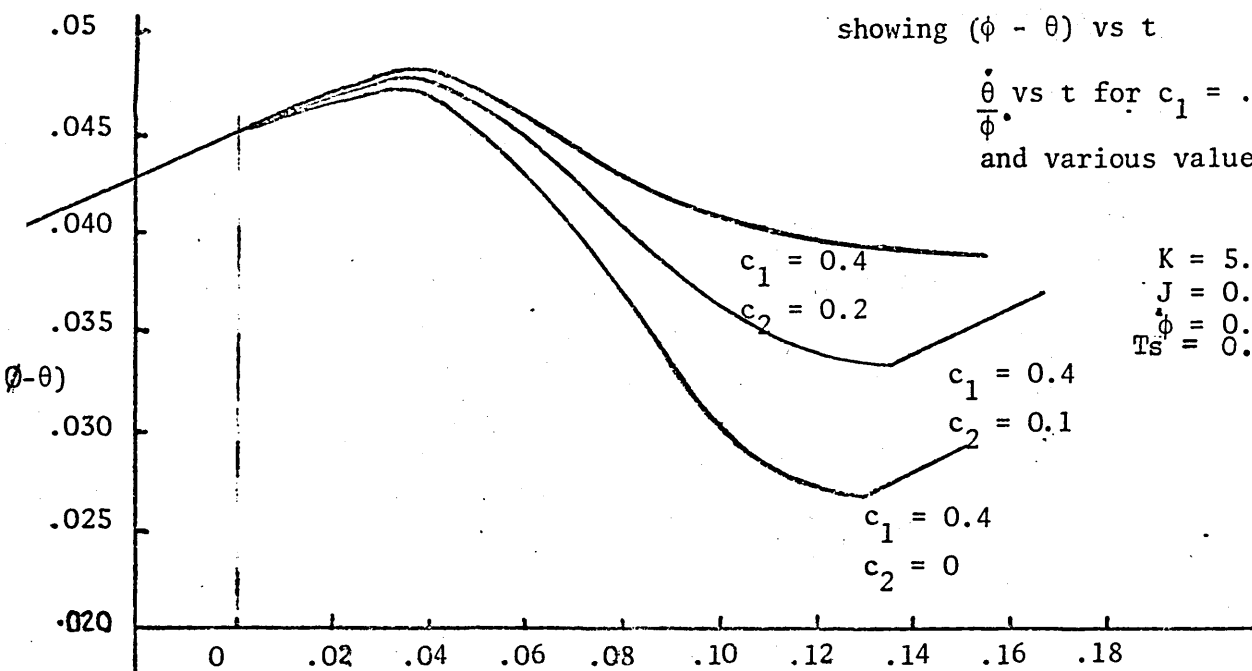
Fig 2.12

$c_1$  vs  $c_2$  showing stability condition for negative damping model theory



showing  $(\phi - \theta)$  vs  $t$

$\dot{\theta}$  vs  $t$  for  $c_1 = .4$   
and various values of  $c_2$



$\frac{\dot{\theta}}{\dot{\phi}}$  vs t  
 for  $\psi = .25$  and various values of  $c_2$

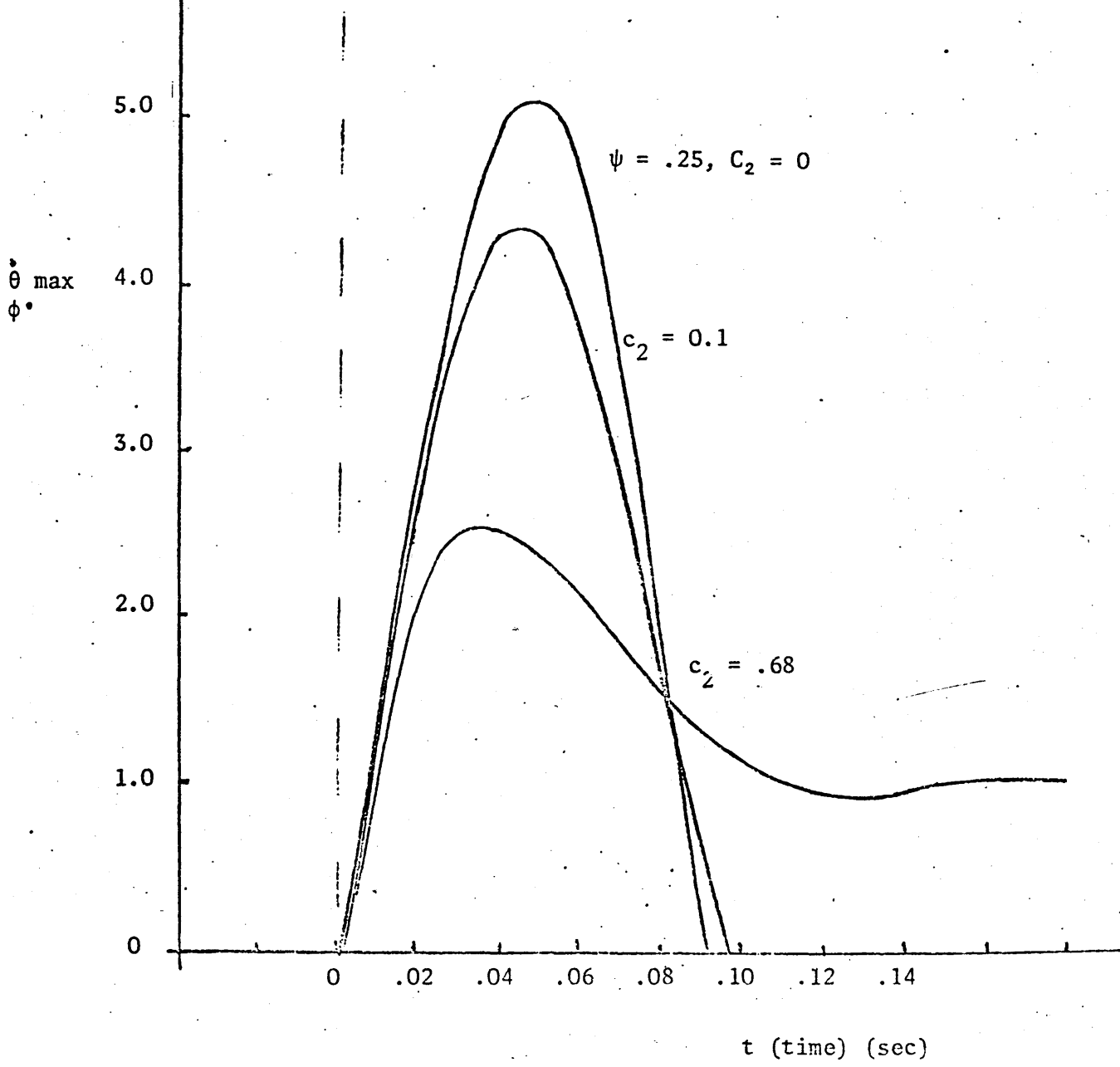
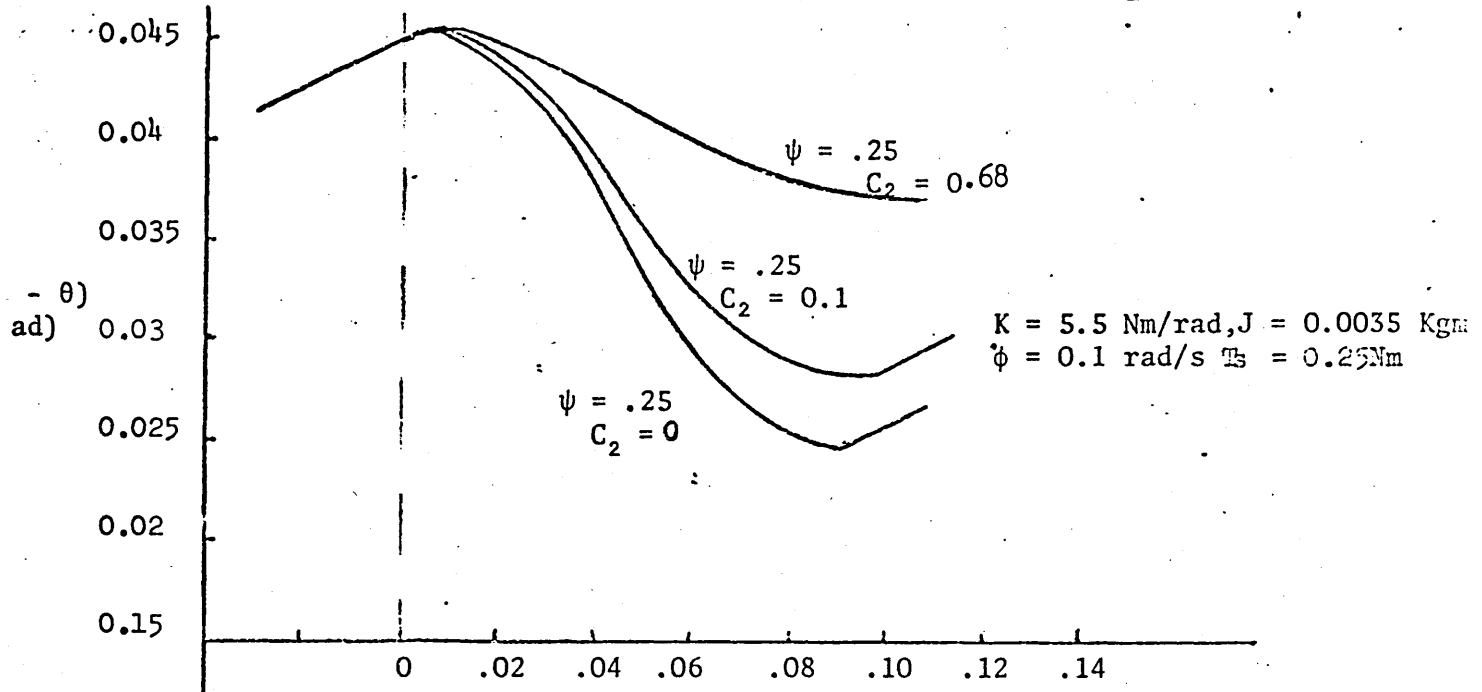


Fig 2.15 Variation of stick-slip amplitude with  $\dot{\phi}$ , J & K for (Ts - Tk) = 0.055 Nm  
 Blok model, Ts = 0.25Nm

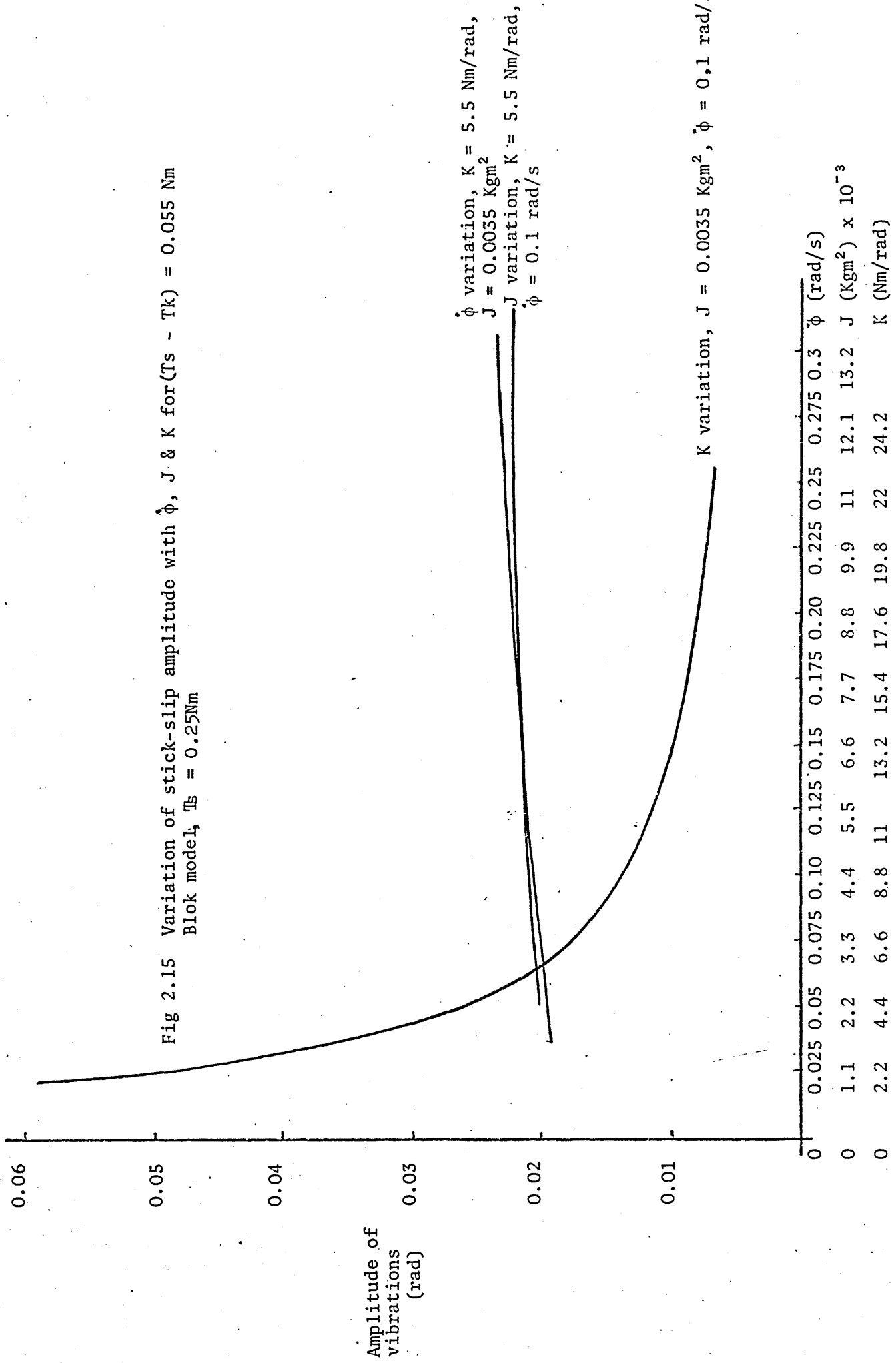


Fig 2.16 Variation of stick-slip amplitude with  $\dot{\phi}$ , J & K for  $C_1 = 0.4$   
negative damping model,  $T_s = 0.25\text{Nm}$

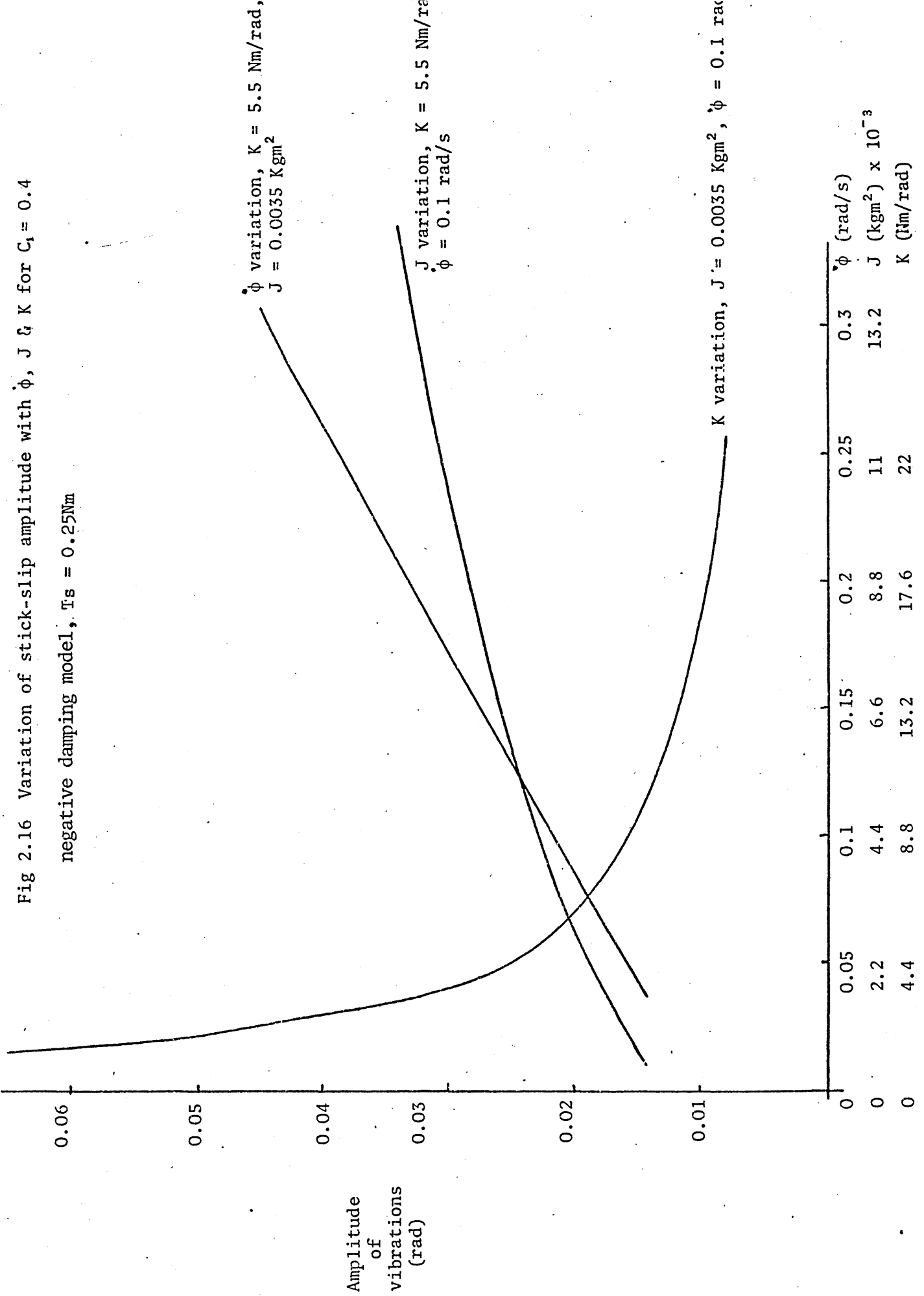
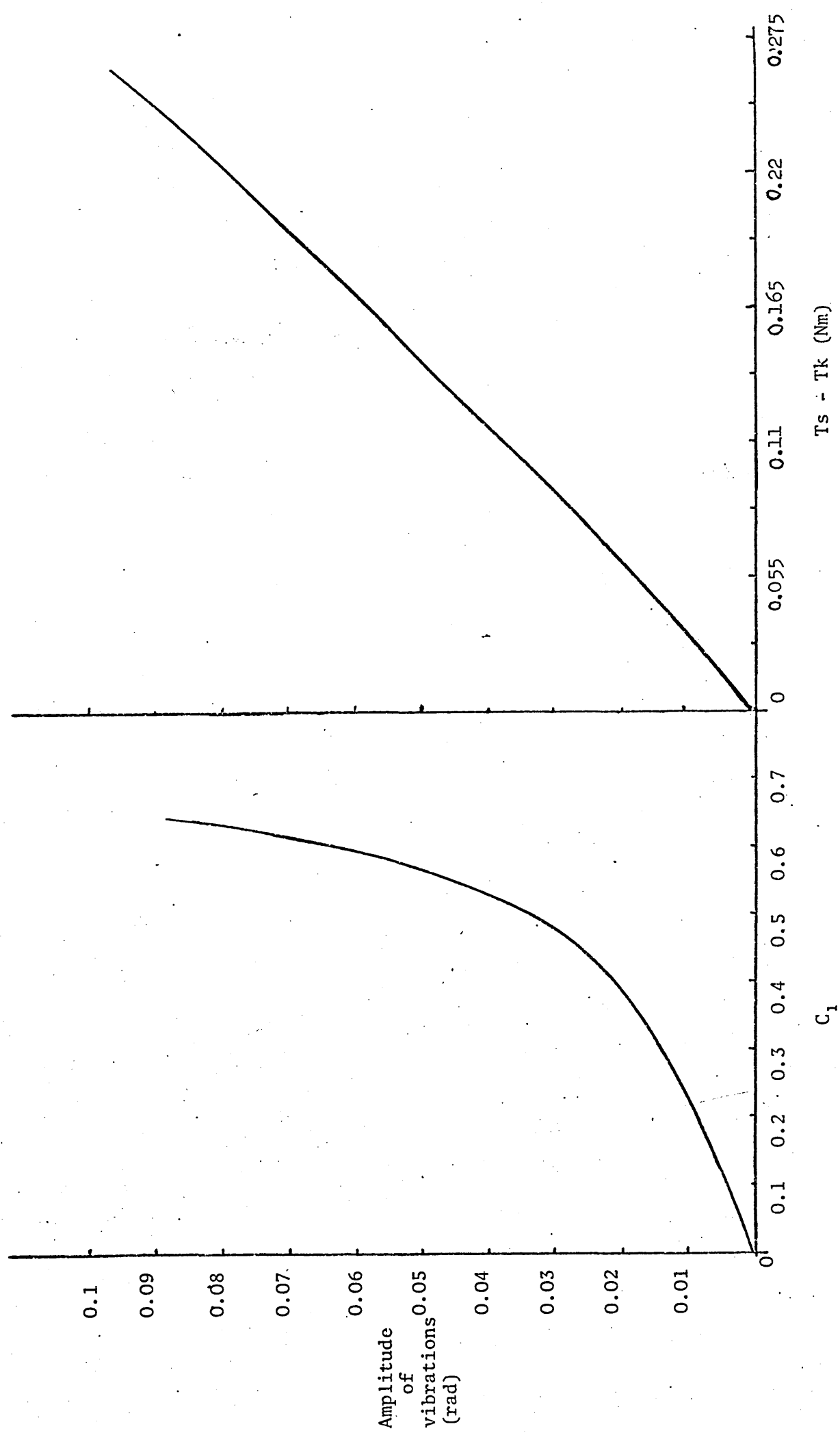


Fig 2.17 Variation of stick slip amplitude with  $(T_s - T_k)$  and  $C_1$ ,  $K = 5.5 \text{ Nm/rad}$ ,  $J = 0.0035 \text{ kgm}^2$ ,  $\phi = 0.1 \text{ rad/s}$ ,  $T_s = 0.25 \text{ Nm}$



### 3.1 Introduction

The basic requirement of the apparatus designed, was one of providing a means of examining stick slip motion for the variation of a selection of system parameters. These parameters were as follows; applied normal load, drive speed, drive stiffness, junction surface finish, junction material and driven disc. The stick slip properties to be measured were stick slip amplitude, slip velocity, slip frequency and dynamic friction forces.

### 3.2 Stick-slip machine

Several items were available from an apparatus originally designed by G R Symmons (14) to investigate stick slip motion. This was a rotational system enabling continuous generation and measurement of the stick slip oscillations. The items available were as follows:-

- (1) Pair of hydrostatic journal bearings to support a rotor.
- (2) Rotor to carry interchangeable discs, and
- (3) Mercury bath to transmit displacement signals.

Items (1) and (2) are shown in fig. 3.1 and item (3) is shown in fig. 3.2.

The first requirement of a continuously driven mass supported with minimal frictional resistance was thus satisfied by items (1) and (2) above. A second element was required to operate as the friction junction rigid member with facility

for normal load application and variation on to the moving disc. At this stage there was a choice of loading action, either radial on to the disc edge or axial on to a disc face. The former provides an arc area of contact with constant velocity at the friction junction, the latter system achieving a flat contact area but giving a variable junction velocity across the friction interface. The system selected was one involving two diametrically opposed pneumatically loaded pistons acting on the circumference of the disc.

Fig. 3.1 shows details of the loading arrangement, with the piston located in a cylinder having compressed air supplied to it from the compressor via a gauge and filter. A Key and Keyway in the piston prevented rotation and a replaceable element was located within the piston with a grubscrew which provided for interchangeability of the friction junction materials. The hydrostatic bearing journals were mounted in vee blocks with removable clamps to enable quick release. In this way the friction interface between piston and disc could be varied to provide a selection of junction surface finishes and materials. A hacksaw blade was incorporated as the elastic drive member necessary to bring about stick slip vibrations in the system. The drive to the system was required to provide low but variable speeds, and was achieved utilising a "Kopp" unit from Allspeeds of Accrington, type MSR3. This consisted of a 0.375 kW, 960 rev/min motor driving a ball and disc, handwheel controlled, variable speed unit which in turn drives a 30:1 fixed reduction gear box. An output speed range of 10 - 90 rev/min obtained from this unit was then further reduced by a 2:1 vee belt drive and type "22" 10:1 worm and wheel fixed reduction gearbox manufactured by Crofts of Bradford. This brought about a final system ro-

tational speed range of 0.05 to 0.5 rad/s. Changing the vee belt pulleys to bring about a 5:1 reduction ratio further reduced the minimum drive speed to 0.02 rad/s. The complete stick-slip machine is shown in fig. 3.3.

### 3.3 Instrumentation

It was necessary to instrument the apparatus to provide facilities for measuring the following properties of stick-slip vibrations; amplitude and frequency of vibrations, friction forces, and instantaneous slip velocity. Strain gauges were located at  $45^{\circ}$  to the longitudinal axis, on opposite sides of the torsional spring (hacksaw blade) and incorporated into a wheatstone bridge with two dummy gauges for temperature compensation. This provided a measure of the relative displacement between driving and driven member, the arrangement being shown in fig. 3.4.

Since the strain gauges were located on a rotating member it was necessary to transfer the signal to a fixed set of terminals for conditioning and display. The device used was the copper finned Tufnol insulated rotor connected to the torsional spring and rotating in a fixed 4-section mercury bath, mentioned earlier. Signals from the gauges pass to fixed terminals via the rotor fins and mercury baths. (see fig. 3.2).

The friction forces at the piston and disc interface were measured directly from the piston itself. By creating a reduced spindle diameter on the cylinder and allowing a small extension from it's base bracket, a simple cantilever system

was produced which deflected slightly under the transverse loading brought about by frictional contact at the piston and disc interface. Locating strain gauges on the top and bottom surface of this reduced portion of the piston, enabled a measure of the friction force to be obtained. As the friction force varies rapidly with time it was necessary to have a high natural frequency for the arrangement to obtain a faithful reproduction of the friction force. In addition, high transverse stiffness minimised the deflection of the piston thus maintaining a close approximation to the ideal situation of rigidity in the piston. This high cantilever stiffness reduced the available signal from the strain gauges and the final design was a compromise resulting in a maximum piston displacement of  $25\mu\text{m}$  and a natural frequency of approximately  $210\text{Hz}$ . The signal obtained from this device was amplified by a factor of 50 for display purposes. This resulted in a noise problem of  $50\text{Hz}$  frequency. It was considered acceptable to filter the friction force signal and in order to minimise amplitude attenuation at critical frequencies an inductance-capacitance low pass filter with a cut off frequency of  $40\text{Hz}$  was designed and is shown in fig. 3.5. Fig. 3.6 shows details of the frequency-amplitude response obtained from this filter by feeding a variety of waveform signals with constant amplitude from an oscillator into the filter and monitoring the output from it. It can be seen that acceptable attenuation of the signal is produced for frequencies relevant to the investigation.

For the measurement of the slip velocity of the disc it was

decided to use a tachogenerator located on a spring loaded swinging arm. A rubber rimmed pulley was fastened on to the generator spindle and motion imparted to it from the disc by a rubber ring fastened to the extended rotor on which the disc was located. The generator provided 7 volts output per 1000 rev/min spindle speed. All three signals were fed via amplifiers to a u.v. recorder using galvanometers with natural frequencies of 1000Hz. Fig. 3.7 illustrates the instrumentation used on the stick slip machine.

#### 3.4 Calibration and Specimen Preparation

External calibration was performed for the measurement of torsional spring displacement, friction force and slip velocity as follows.

In order to calibrate the torsional spring it was disconnected from the main rotor and then supported in a flat horizontal position by the use of a screw-jack. A torque arm of 0.4m length was then clamped at the end of the spring in the same position as the connection to the rotor had been. By applying loads to one end of the torque arm and measuring its deflection a calibration curve of angular displacement of torsional spring vs u.v. recorder reading (fig. 3.8) was obtained. Fig. 3.9 shows the spring displacement plotted against applied loads on the torque arm from which a value for torsional spring stiffness was obtained. This procedure was repeated for three different springs giving stiffness values of 7.3, 16.3 and 31Nm/rad respectively. By subjecting the disc and torsional spring system to free vibrations following an initial displacement the system frequency and hence disc and rotor inertia were obtained (fig. 3.10). Using each of the springs in turn system

frequencies of 6.6, 10 and 13.7Hz were measured giving an average disc inertia value of  $4 \times 10^{-3} \text{Kgm}^2$ .

In order to calibrate the friction force transducer the bracket holding the piston cantilever was clamped in a position away from the rotor arrangement. The piston itself was located a fixed distance from the bracket boss and weights suspended from the end of the piston using thin wire. Calibration graph fig. 3.11, showing piston transverse load against u.v. recorder displacement was thus produced.

To effect angular speed calibration the main rotor was run and

the speed checked manually with a stop watch. By adjusting the speed box, graphs of speed setting vs. angular velocity vs u.v. recorder displacements (figs. 3.12 and 3.13).

Conditions used for the test were restricted to lubricants. Discs of mild steel EN1B and 17 (BS1452) were made, together with pistons 1 and also carbon graphite and ptfе pistons. was used to produce an appropriate surface circumference. Three values of surface finish at of the profile in the direction of ved using the radial arm attachment on the rf Model 3 (fig. 3.14). Several ken at various positions around the disc, ted provided each of the surface finish

measurements was within a tolerance band of  $\pm 10\%$  of the norm value. Typical surface profile traces and measurements are

1. DECERA ROOF SYSTEMS (UK). LTD  
2. CRAMPTON WAY, MANOR ROYAL,  
CEAULLEY RHIO 10QR.  
3. DECERA ROOFING SYSTEM  
TECHNICAL INFORMATION.  
4.  
5. DECERA.  
6. (47)

shown in fig. 3.15 for 0.03in (0.75mm) cut off wavelength, stroke setting K. Surface finishes of 20, 30 and 45  $\mu$ ins (0.5, 0.75 and 1.1 $\mu$ m) CLA were utilised. These are identified as SFI, SFII and SFIII respectively throughout the remainder of the thesis.

### 3.5 Tolerances in Experimental Measurements

An estimation has been made of the % tolerances (or % uncertainty) in the system parameters and experimental results due to the random errors associated with calibration and primary measurements. These errors have been considered to be due to equipment error and observation error. Where derived results have been produced from combinations of other results the following procedure has been adopted.

For a result P as a function of independent variables a, b, c etc.

$$P = f(a, b, c)$$

If  $x_p$ ,  $x_a$ ,  $x_b$ ,  $x_c$  are the errors associated with P, a, b, c then

$$x_p^2 = \left(\frac{\partial P}{\partial a} x_a\right)^2 + \left(\frac{\partial P}{\partial b} x_b\right)^2 + \dots$$

#### System Parameters

Assuming a tolerance of  $\pm 1\%$  in the weights used for calculating the spring stiffness together with an observation tolerance of  $\pm 1\%$  in the measurement of the torque arm radius and spring angular deflection then spring stiffness (s) = weight (w) x radius arm (l)/vertical deflection of radius arm ( $\delta$ )/radius arm (l).

$$\text{i.e. } s = \frac{wl^2}{\delta}$$

$$x_S^2 = \left(\frac{\partial s}{\partial w} x_w\right)^2 + \left(\frac{\partial s}{\partial l} x_l\right)^2 + \left(\frac{\partial s}{\partial \delta} x_\delta\right)^2$$

$$x_S^2 = \left(\frac{wl^2}{\delta} \frac{x_w}{w}\right)^2 + \left(\frac{2wl^2}{\delta} \frac{x_l}{l}\right)^2 + \left(-\frac{wl^2 x_\delta}{\delta^2}\right)^2$$

$$\text{i.e. } (\% \text{ error in } s)^2 = (\% \text{ error in } w)^2 + (2 \times \% \text{ error in } l)^2 + (\% \text{ error in } \delta)^2$$

$$\therefore \% \text{ error in spring stiffness} = \pm\sqrt{6}\%$$

The natural frequency of the system was evaluated from u.v. recordings having an estimated timing accuracy of  $\pm 2\%$  together with an observation tolerance of  $\pm 1\%$ , giving  $\pm\sqrt{5}\%$  as the tolerance for system frequency measurements.

System frequency was used together with spring stiffness to calculate the system inertia. Since inertia is a direct function of spring stiffness and dependent upon  $1/(\text{frequency})^2$  then the % error associated with the inertia results is  $\pm\sqrt{20 + 6} = \pm\sqrt{26}\%$ . For the system drive speed an estimated  $\pm 2\%$  setting error in the 'Kopp Box',  $\pm 1\%$  error in the tachogenerator,  $\pm 1\%$  error in the stop watch and  $\pm 1\%$  observation error in the timing and recording produced a total drive speed tolerance of  $\pm\sqrt{8}\%$ .

### Stick-Slip Results

The friction torque measurements were considered subject to an estimated equipment tolerance of  $\pm\sqrt{2}\%$  ( $\pm 1\%$  strain gauge tolerance and  $\pm 1\%$  calibration weight tolerance), and an

observation tolerance on the u.v. recordings of  $\pm 1\%$ .

Additionally the location of the friction torque measuring device provided a further source of error. Estimating this at  $\pm 2\%$  provided a total uncertainty in the friction torque results of  $\pm\sqrt{7}\%$ .

Relative displacement errors made up of observation error in the calibration process of  $\pm\sqrt{2}\%$ , strain gauge tolerance of  $\pm 1\%$  and u.v. recording observation errors of  $\pm 1\%$  produced a total tolerance on this measurement of  $\pm 2\%$ .

For the measurement of slip velocities the component measurements are those associated with drive speed with the exception of 'Kopp Box' setting. Consequently a  $\pm 2\%$  tolerance on slip velocities resulted. Viscous damping results were calculated from vibration amplitude ratios and system parameters. From equation (13)

$$\frac{\theta_1}{\theta_n} = e^{(n-1)\frac{\mu\pi}{w}}$$

$$c = \frac{-\log_e(R)2Jw}{(n-1)\pi} \quad \text{where } R = \theta_1/\theta_n$$

Giving viscous damping coefficient as

$$c_2 = \frac{\log_e(R)w}{(n-1)\pi w_1}$$

$$\therefore x_{c_2}^2 = \left\{ \frac{w}{(R)(n-1)\pi w_1} \cdot x_R \right\}^2 + \left\{ \frac{\log_e(R)}{(n-1)\pi w_1} x_w \right\}^2 + \left\{ \frac{-\log_e(R)w}{(n-1)\pi} \cdot x_{w_1} \right\}^2$$

$$\therefore (\% \text{ error in } c_2)^2 = \left\{ \frac{\% \text{ error in } (R)}{\log_e(R)} \right\}^2 + \{ \% \text{ error in } w \}^2$$

$$+ \{ - \% \text{ error in } w_1 \}^2$$

The amplitude ratio measurements contribute significantly to the total error in the viscous damping coefficient especially for low R values. Assuming a tolerance of  $\pm 5\%$  in producing the amplitude ratio values, a minimum  $\log_e R$  factor of 0.4, and  $\pm 2\%$  for both frequency measurements produced a total tolerance for  $c_2$  of  $\pm 13\%$ .

Tolerance on Blok parameter due to individual tolerances becomes  $\pm\sqrt{8+8+7}\% = \pm\sqrt{23}\%$ .

Similarly negative damping coefficient results are subject to a tolerance of  $\pm\sqrt{7+8+4}\% = \pm\sqrt{19}\%$ .

The system parameters with estimated tolerances, and measured results estimated tolerances are given below.

<u>Parameter</u>	<u>Measured Value</u>	<u>Estimated Tolerance (%)</u>
Spring Stiffness	7.3,16.3,31.0Nm/rad	$\pm 2.4$
Inertia	0.004Kgm <sup>2</sup>	$\pm 5.1$
Natural frequency	6.6,10.0,13.7Hz	$\pm 2.2$

<u>Measured Result</u>	<u>Estimated Tolerance (%)</u>
Friction torque	$\pm 2.6$
Relative displacement	$\pm 2.0$
Slip frequency	$\pm 2.2$
Slip velocity	$\pm 2.0$
Drive speed	$\pm 2.8$
Viscous damping coefficient	$\pm 13.0$
Blok parameter	$\pm 4.8$
Negative damping coefficient	$\pm 4.4$

### 3.6 Experimental Procedure

The first requirement of the experimental programme was to examine the dynamic friction characteristics of the cast iron

and steel combinations for qualitative comparison with the linearised dynamic friction models. This was achieved by feeding the friction force and slip velocity signals respectively to the vertical and horizontal axes of an oscilloscope. Polaroid photographs of the dynamic friction characteristics were then obtained and used as a qualitative guide to the accuracy of the linearised models. As the system parameters were varied, occasional photographic traces were taken as a check on the shape of the friction characteristic. Quantitative results were obtained from u.v. recordings of friction torque, slip velocity and relative displacement between driver and driven disc. Slow paper speed was set on the recorder so as to enable slip time and hence slip frequency to be measured accurately. From these readings the governing parameters  $\psi$  and  $C_1$  for each theory were evaluated and comparison made between theory and experimental results.

Tests conducted to examine the effect of transfer lubricant on stick slip motion necessitated the replacement of one metal piston by a dry bearing compact enabling transfer of the dry lubricant to the metal junction. The effect of variations in normal load, surface finish, system frequency and metal and lubricant combinations were monitored. Since both theories suggest the elimination to be brought about by transferred lubricant modifying the negative metal to metal dynamic friction characteristic together with a viscous damping action from the transfer lubricant, then these two characteristics required examination. At regular intervals throughout the

selected tests, the stick-slip machine was stopped. The dry lubricant piston was removed from contact with the disc and readings taken with the metal piston only in contact.

Running the machine briefly gave results from which the modified dynamic friction characteristics of the stick slip junction were obtained. The dry lubricant piston was then brought back into contact with the disc and the metal piston removed. With the drive end of the machine stationary, the disc was subjected to an initial displacement and allowed to vibrate under the influence of the dry lubricant. Measurement of successive disc amplitudes enabled the theory of section 2.4 to be used in determining the individual coulomb and viscous components of damping.

Prior to the commencement of all tests the friction junctions were chemically cleaned with carbon tetrachloride.

Fig 3.1 Rotor and disc in journals with piston acting radially on disc

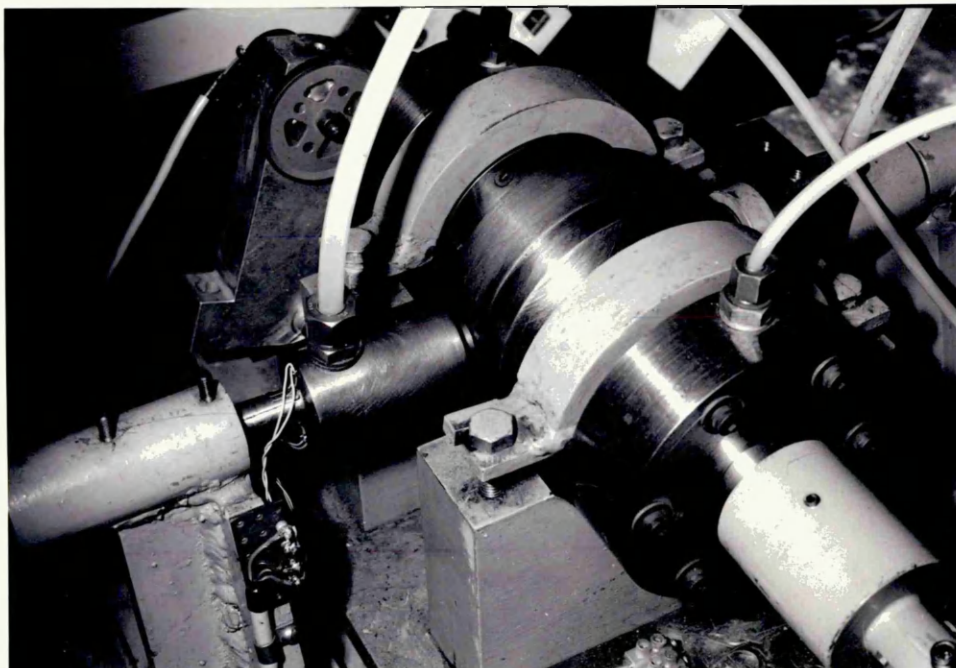


Fig 3.2 Mercury bath with copper finned tufnol insulated rotor

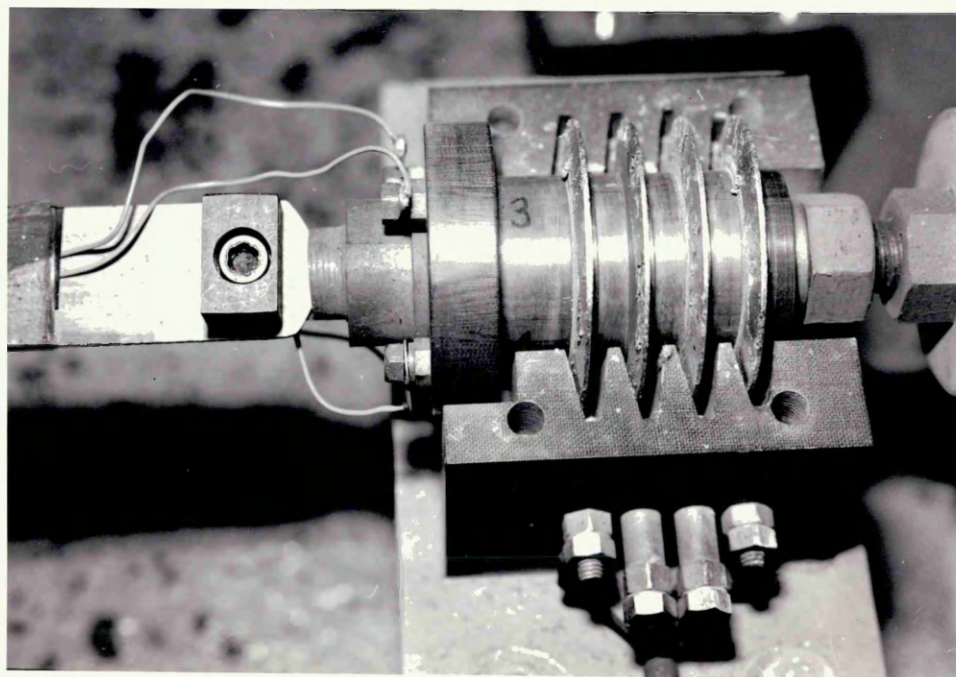


Fig 3.3 Complete stick slip apparatus

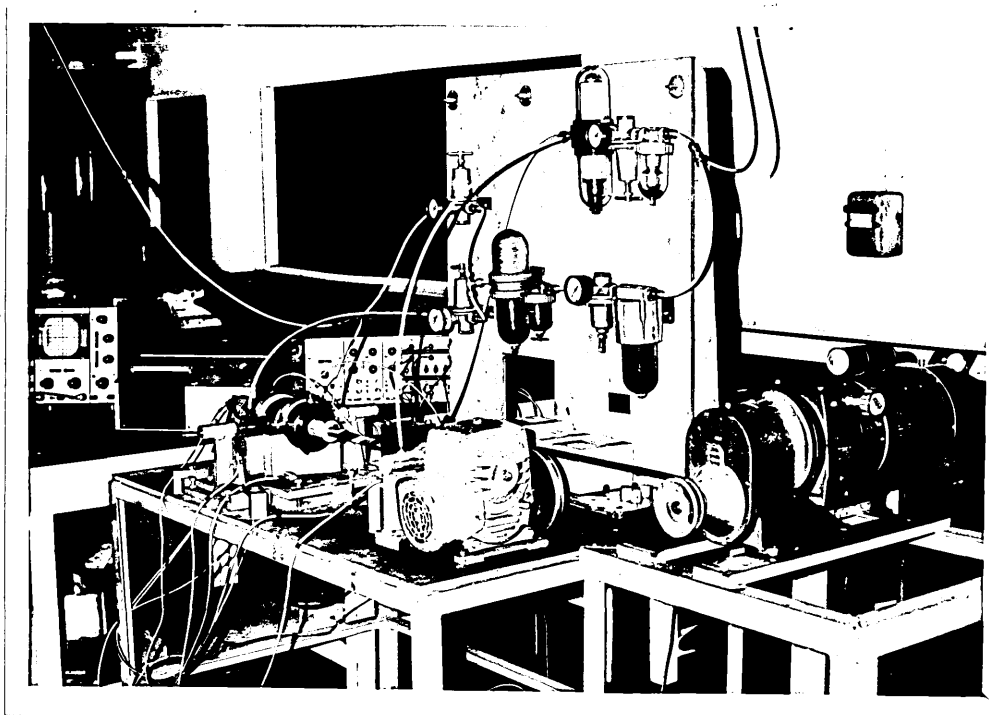


Fig 3.4 Torsional spring and strain gauges

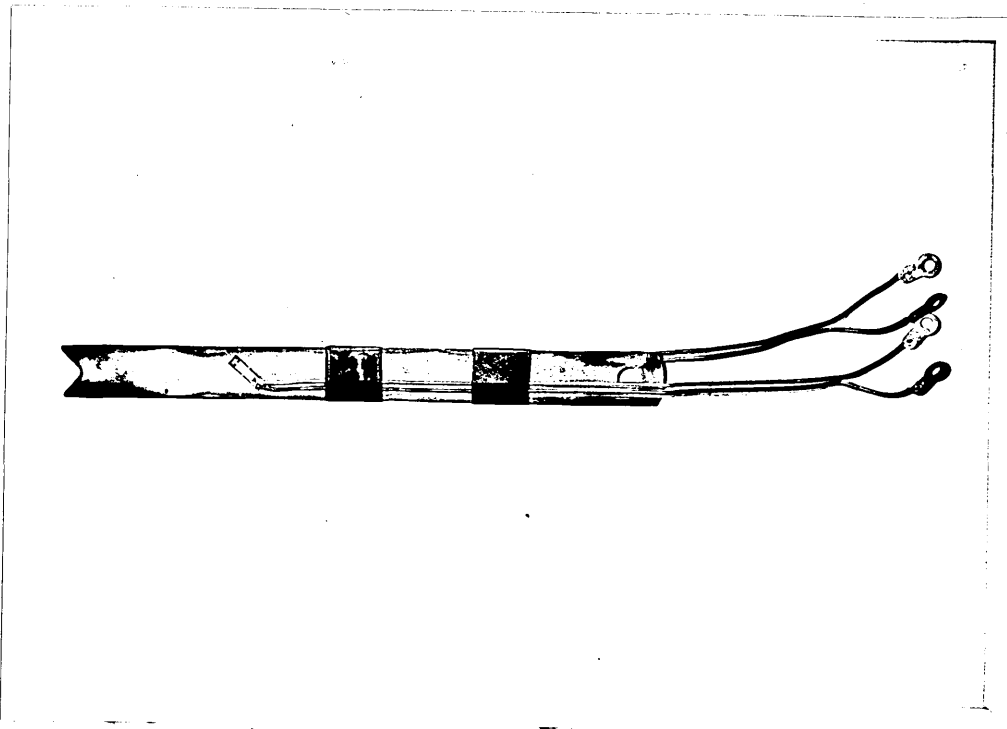
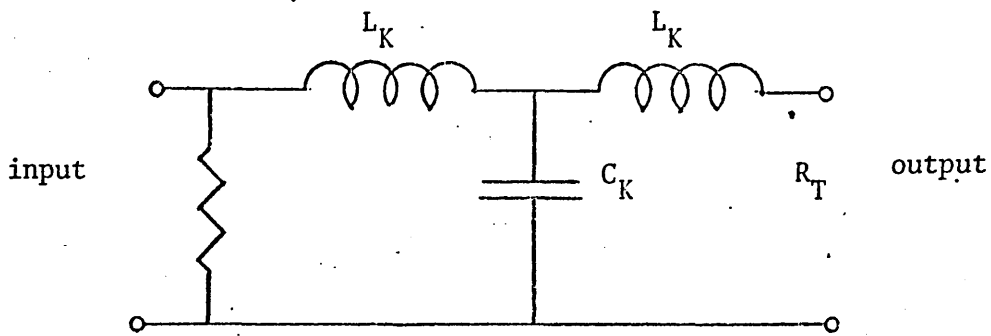


Fig 3.5 Friction force filter circuit



$L_K = \text{inductance} = 150 \text{ mH}$

$C_K = \text{capitance} = 200 \text{ } \mu\text{F}$

$R_T = \text{additional resistance across galvanometer}$

$f_c = \text{cut-off frequency} = 40 \text{ Hz}$

$$2L_K = \frac{R}{\pi f_c} \quad R = \pi \times 40 \times 300 \times 10^{-3}$$

$$R = \underline{\underline{40\Omega}}$$

also

$$C_K = \frac{1}{\pi f_c R} \quad \therefore R = \frac{10^6}{200 \times \pi \times 40}$$

$$R = \underline{\underline{40\Omega}}$$

If  $R_G = \text{galvanometer resistance} = 115\Omega$

then  $\frac{1}{R} = \frac{1}{R_T} + \frac{1}{R_G}$

$$\frac{1}{R_T} = \frac{1}{R} - \frac{1}{R_G} = \frac{1}{40} - \frac{1}{115} = \frac{1}{65}$$

$$\underline{\underline{R_T = 65\Omega}}$$

i.e.  $L_K = 150 \text{ mH}$  )

$C_K = 200 \text{ } \mu\text{F}$  )

$R_T = 65\Omega$  )

for cut-off frequency of 40 Hz

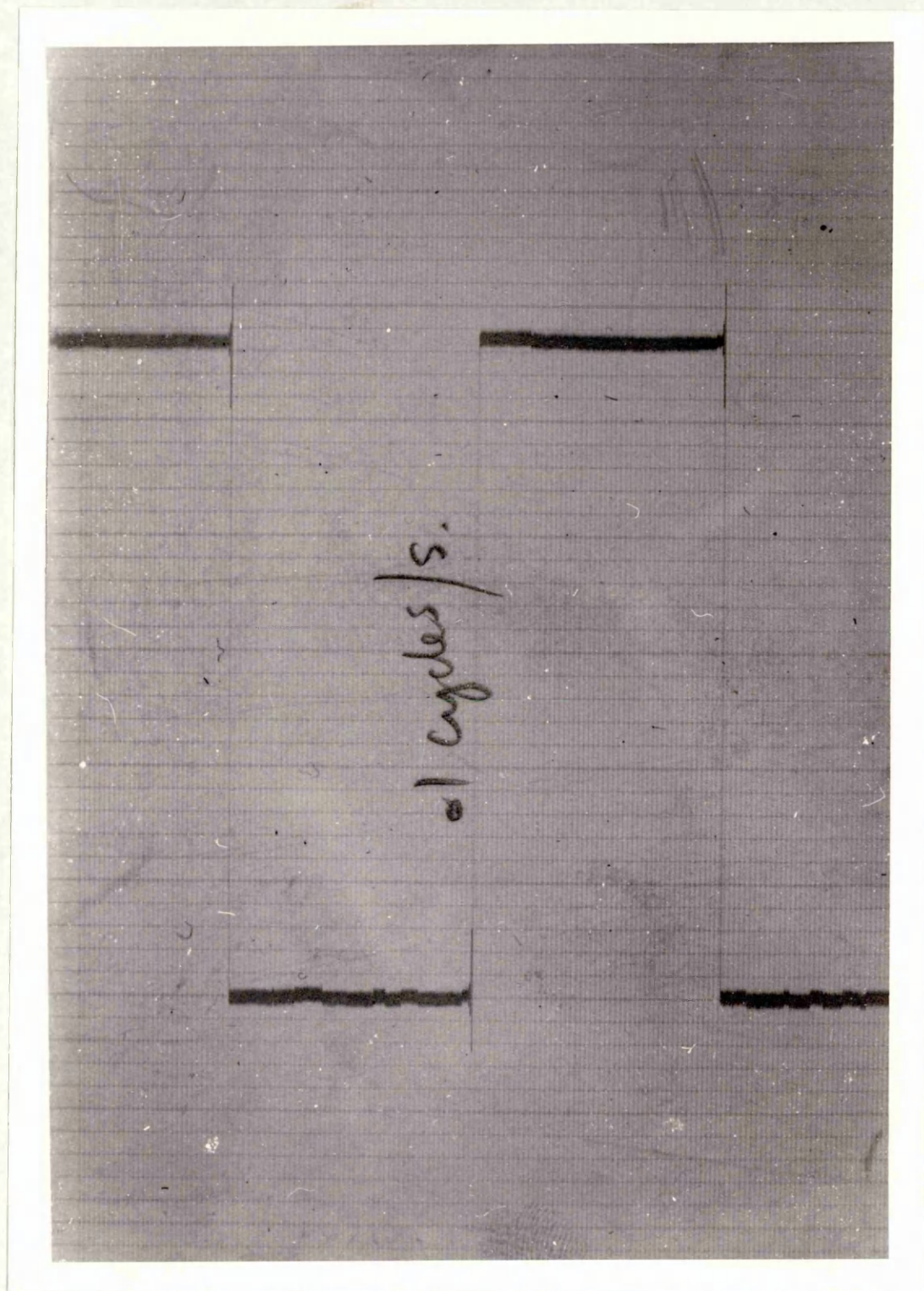


Fig 3.6(a) Friction force filter output for 0.1/Hz square wave input

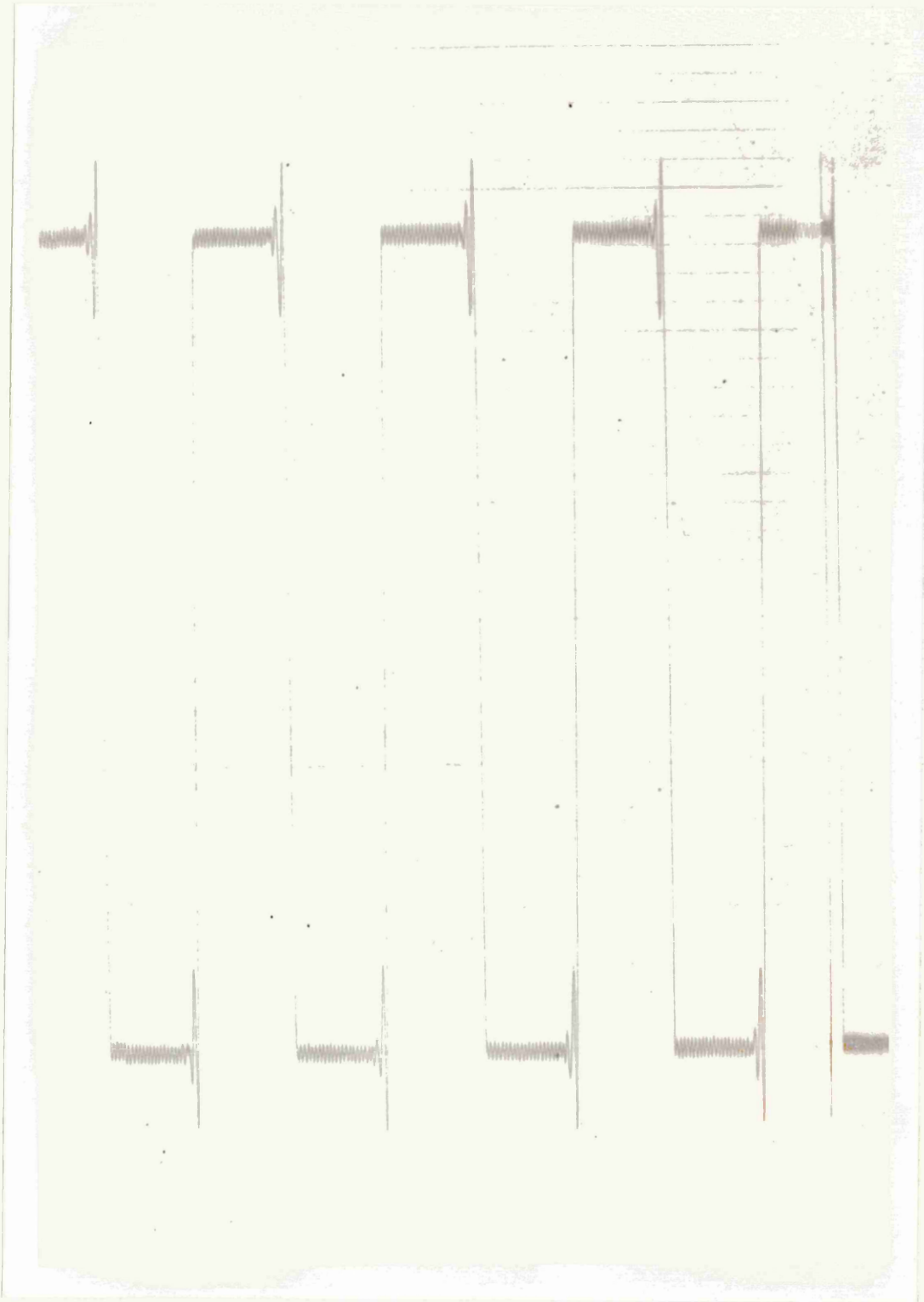


Fig 3.6(b) Friction force filter output for 3Hz square wave input

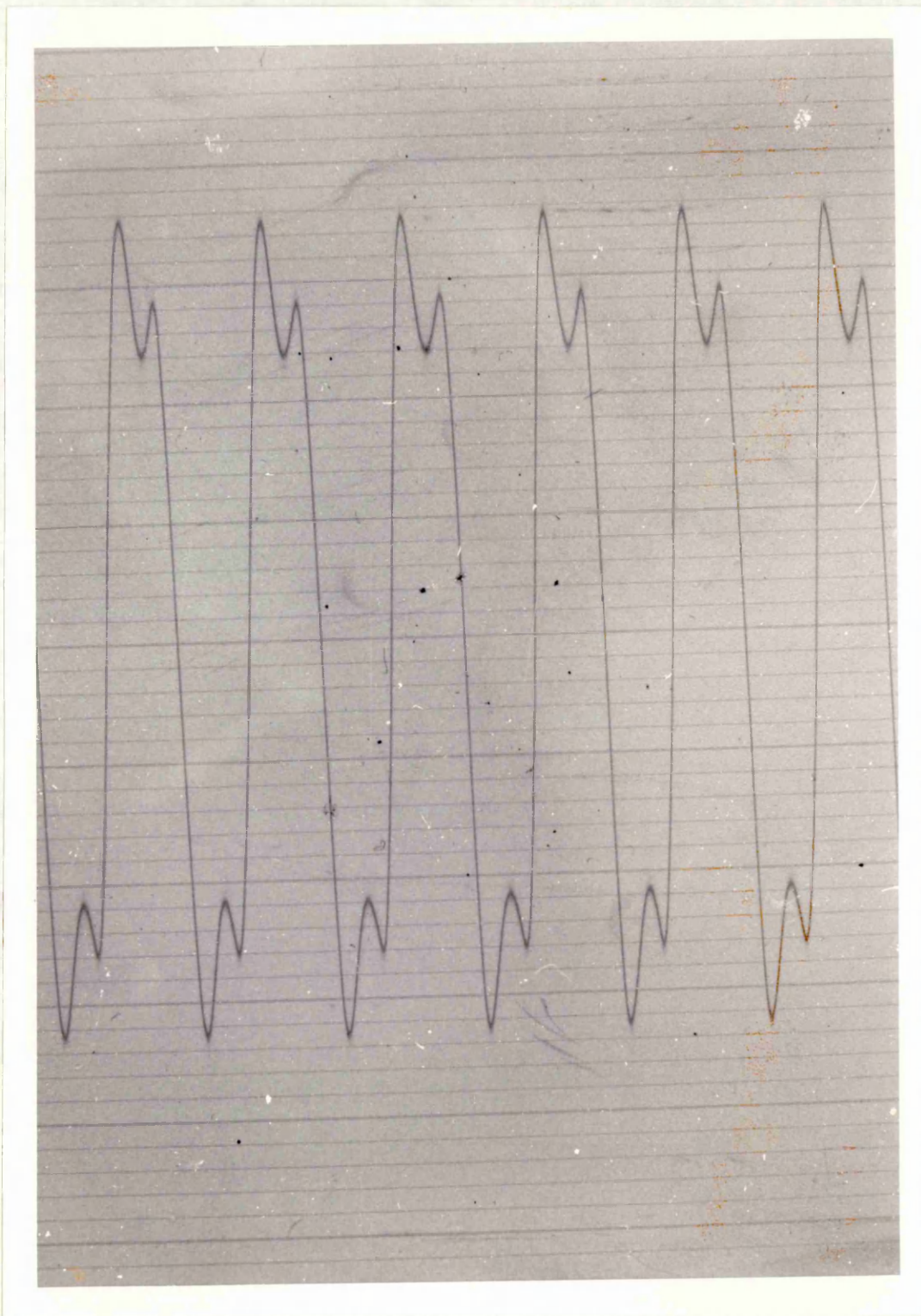
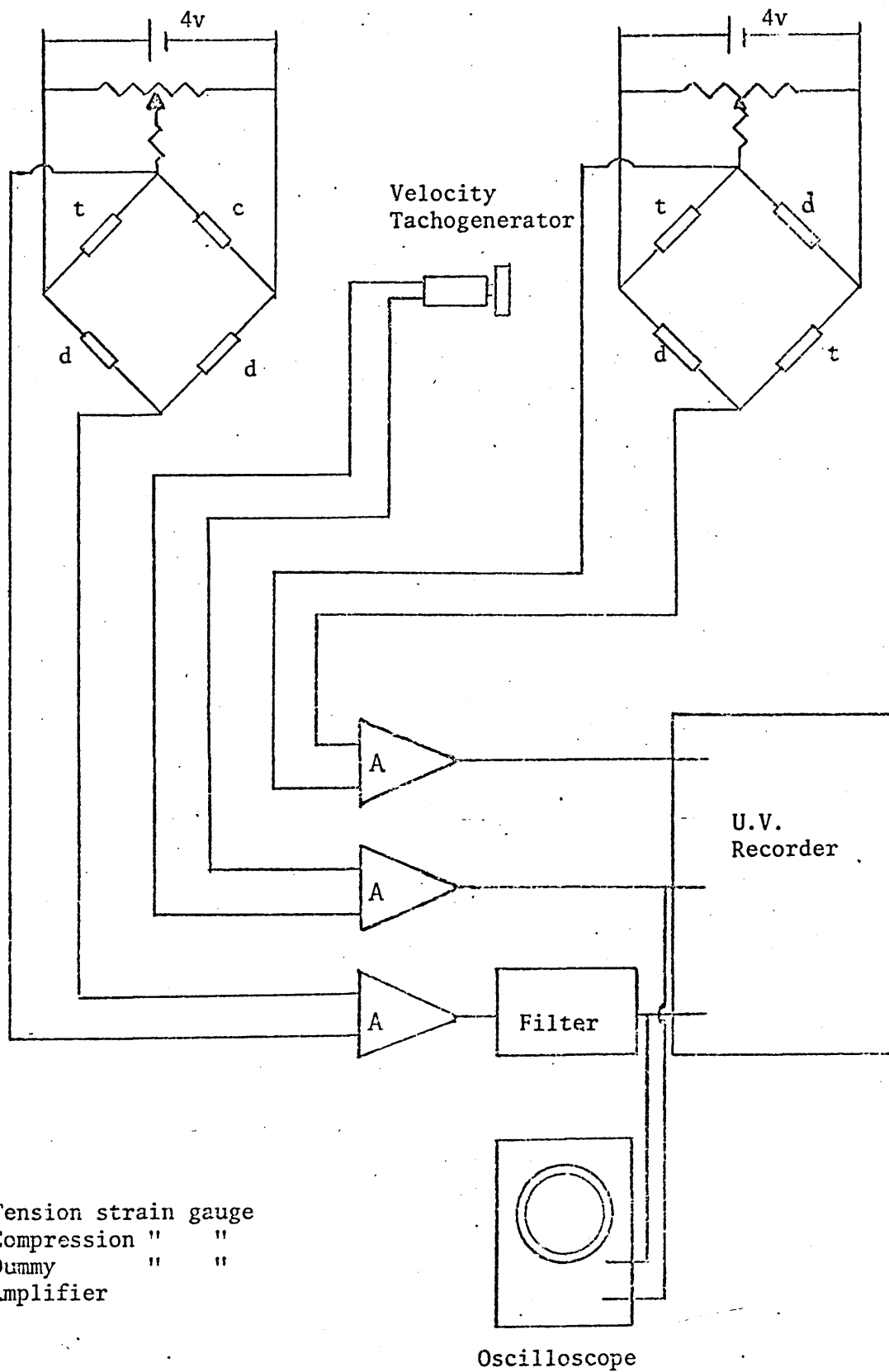


Fig 3.6(c) Friction force filter output for 20Hz truncated saw tooth input



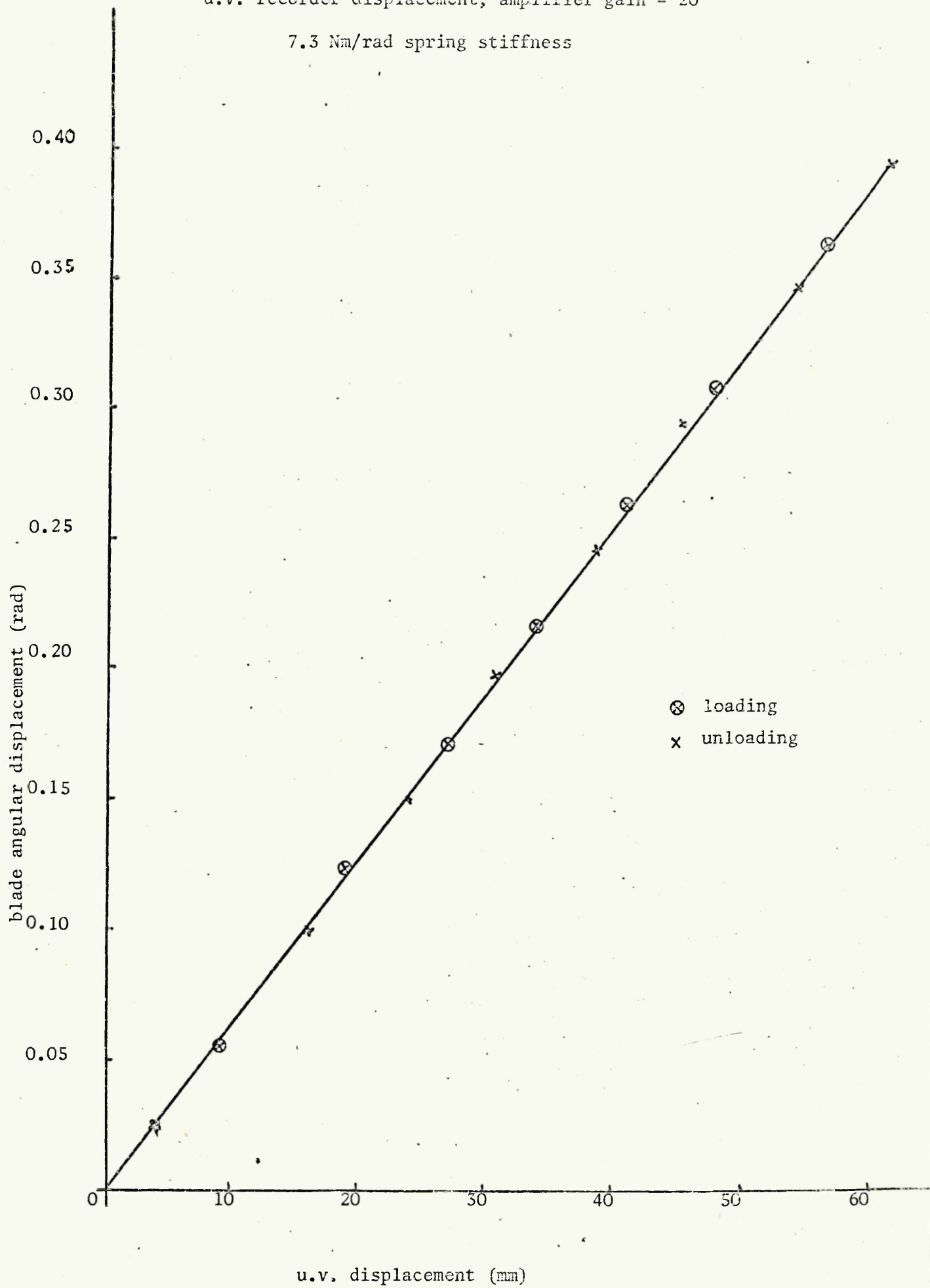
t = Tension strain gauge  
 c = Compression " "  
 d = Dummy " "  
 A = Amplifier

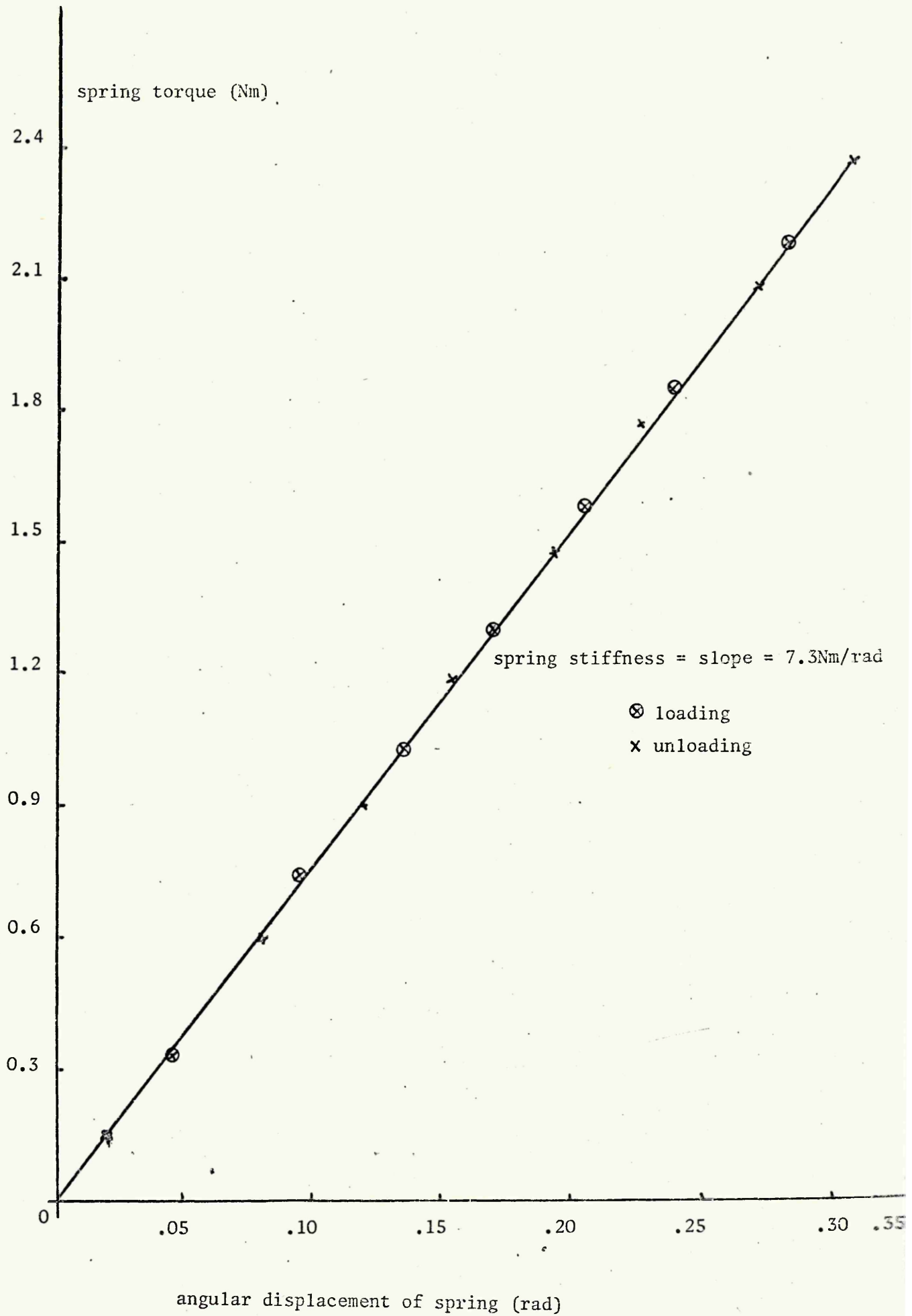
Oscilloscope

Fig. 3.7 Stick Slip instrumentation

u.v. recorder displacement; amplifier gain = 20

7.3 Nm/rad spring stiffness





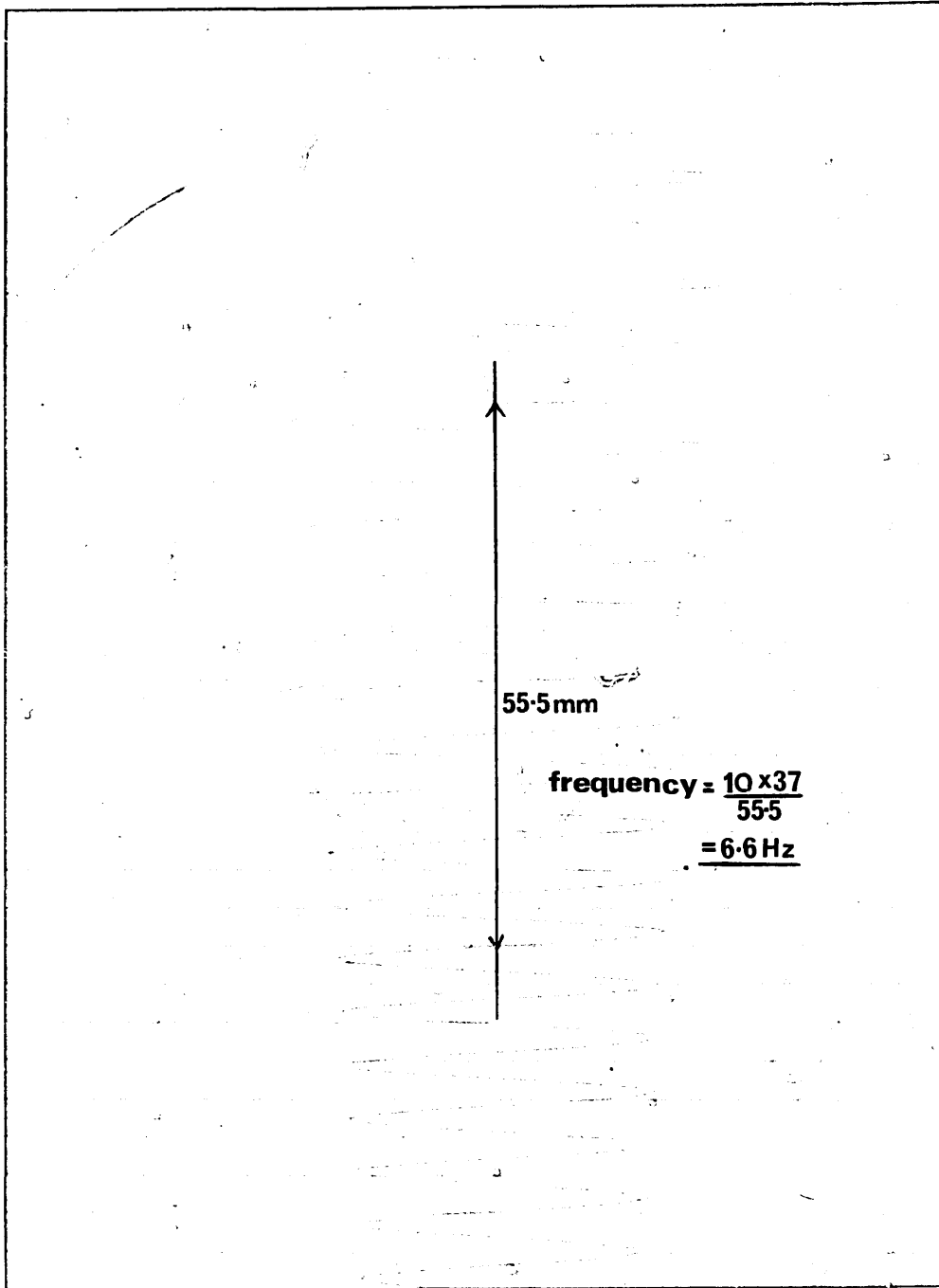
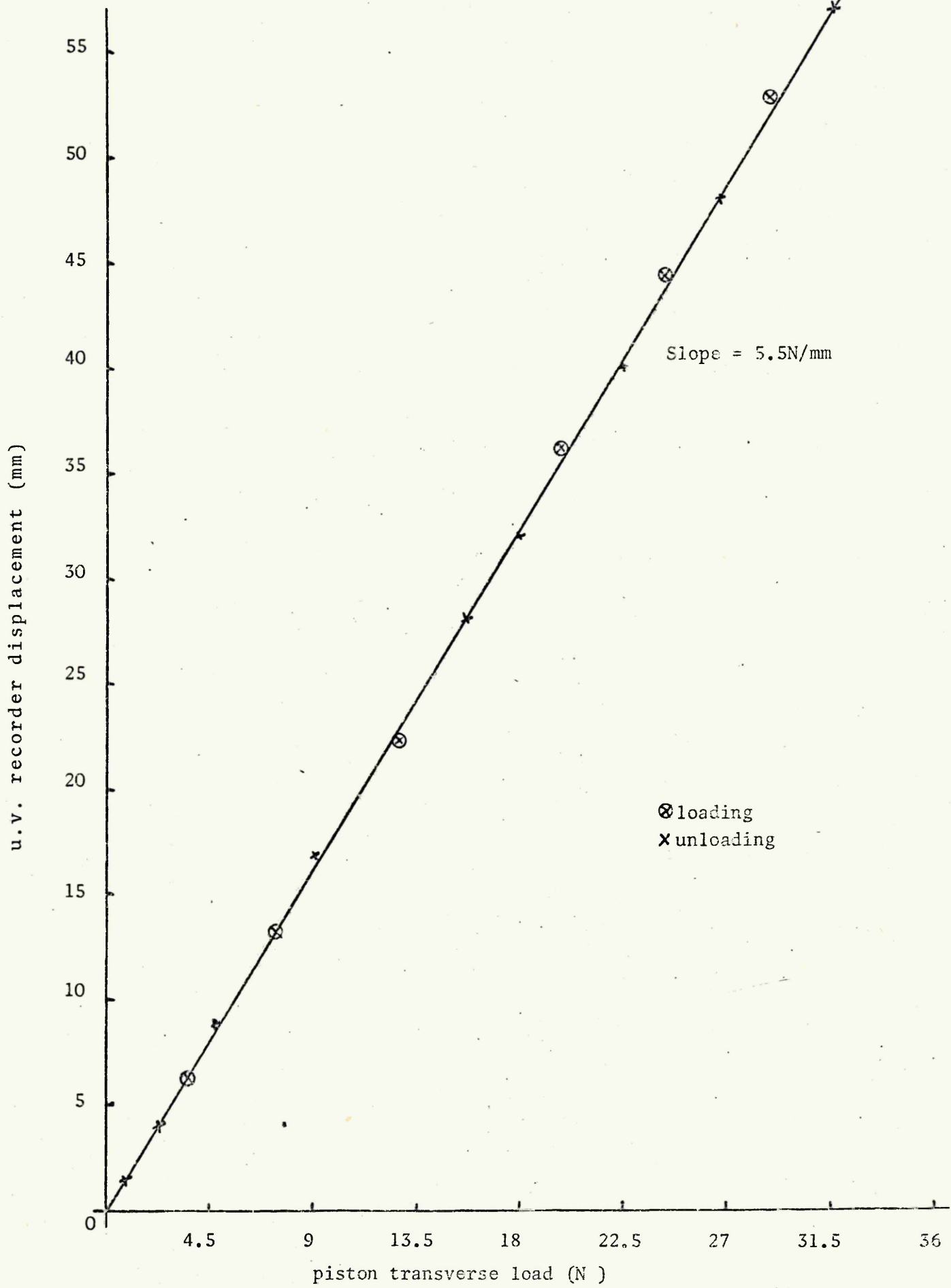
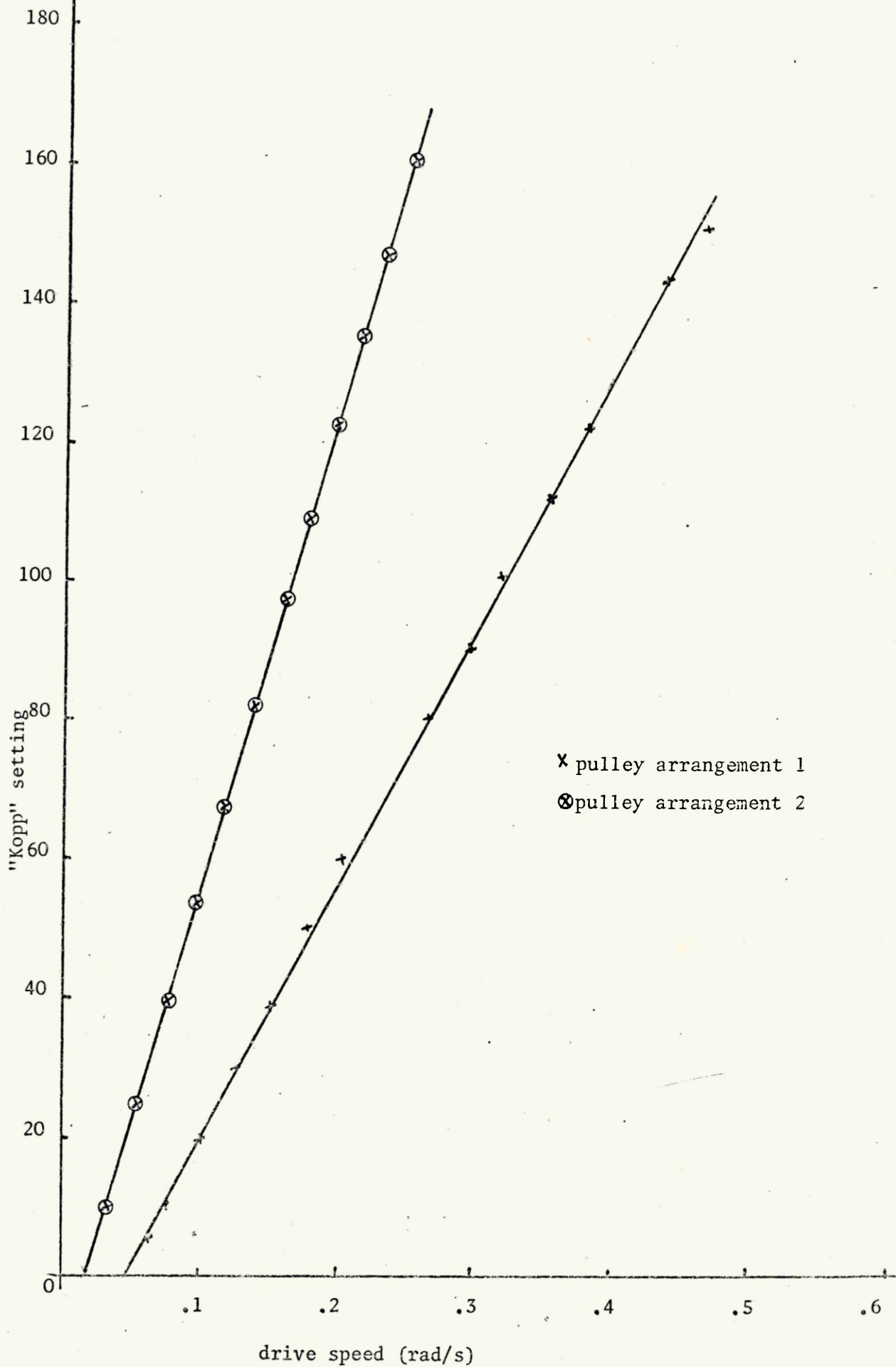


Fig 3.10 Free vibrations of disc and spring (7.3Nm/rad stiffness)

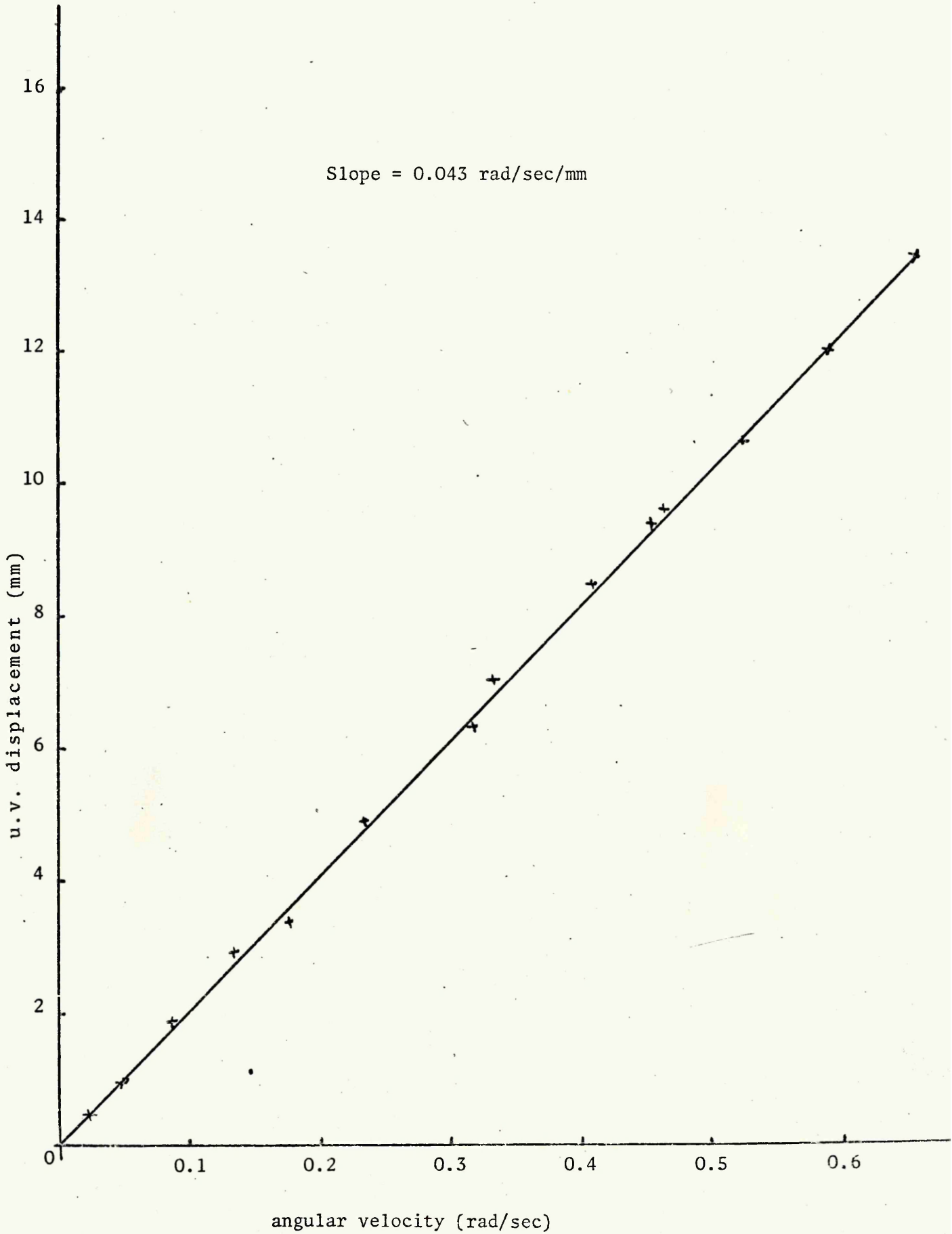
amplifier gain = 500





amplifier gain = 50/100

Slope = 0.043 rad/sec/mm



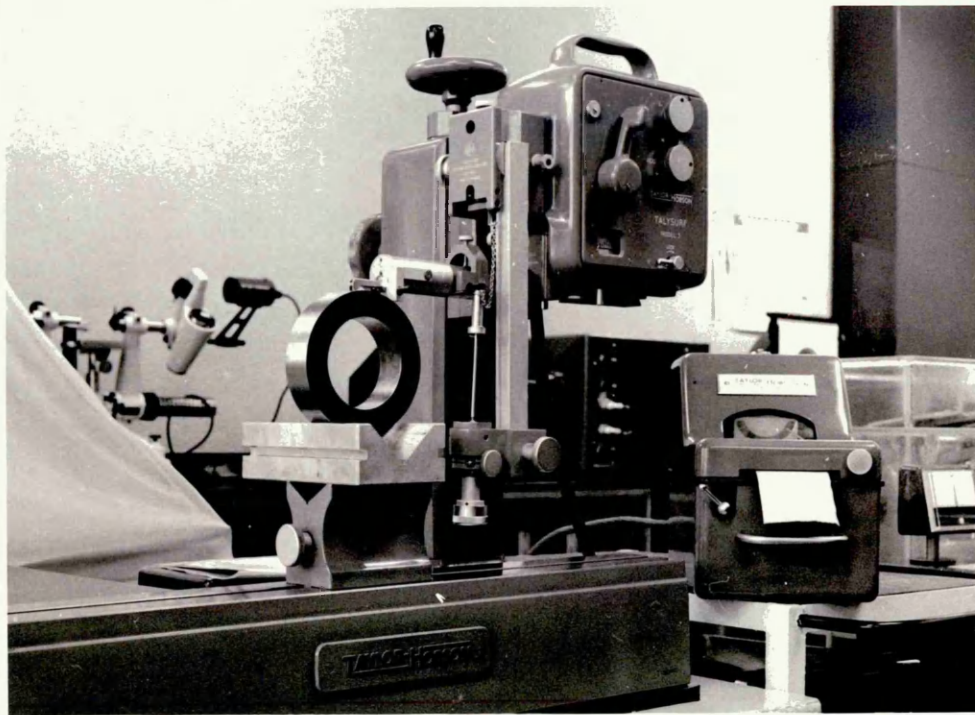
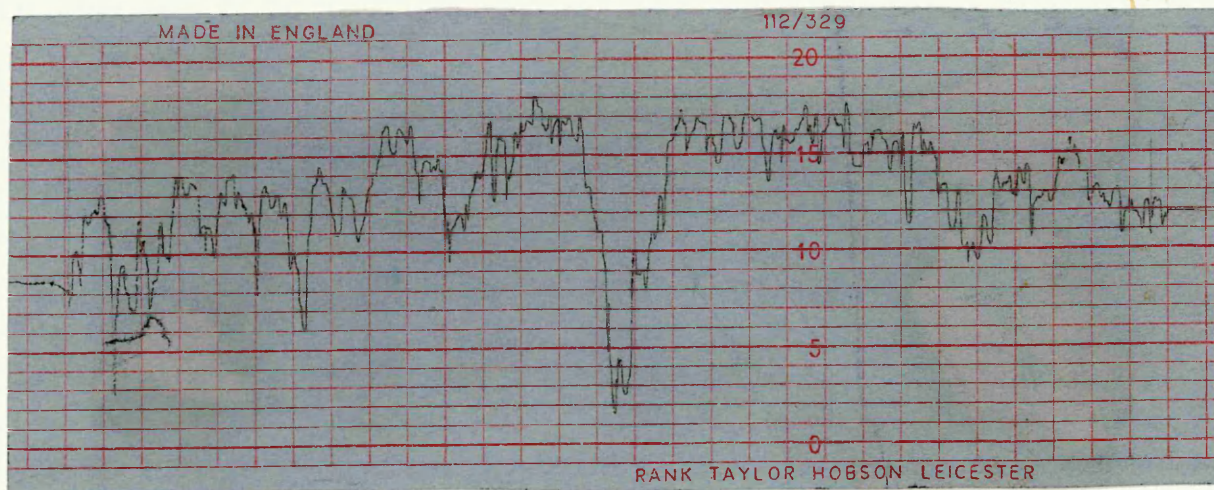
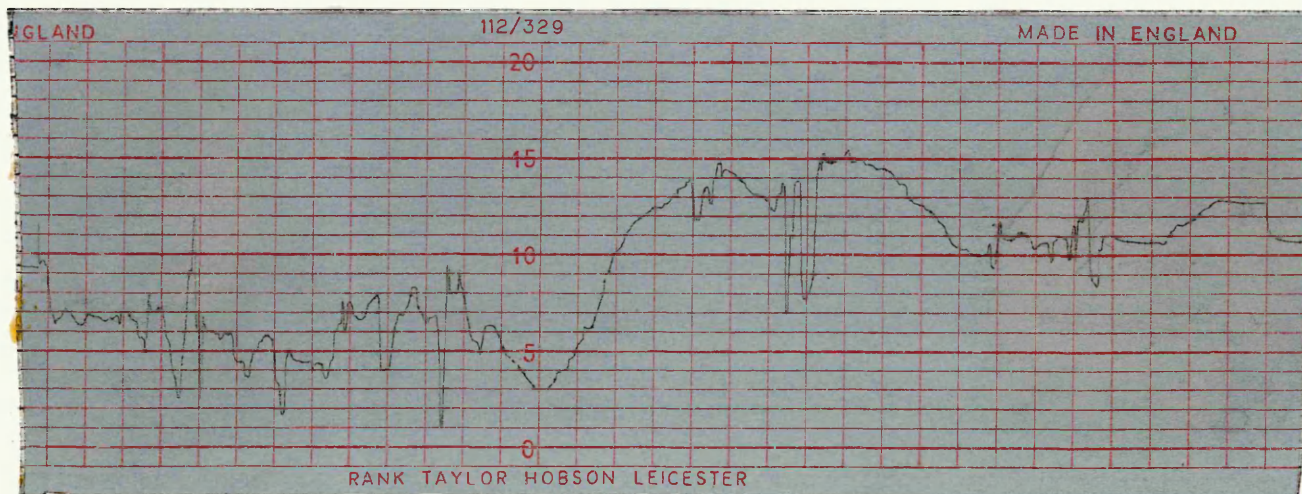


Fig 3.14 Taylor-Hobson Talysurf set up to measure along disc circumference

Fig 3.15 Typical disc surface profiles taken along circumference



a) horizontal magnification = 20 vertical magnification = 10,000  
surface finish = 14 CLA  $\mu$ ins (0.35 $\mu$ m)



b) horizontal magnification = 20 vertical magnification = 5000  
surface finish = 28 CLA  $\mu$ ins (0.7 $\mu$ m)

#### 4.1 Dynamic friction characteristics

Fig. 4.1 shows oscilloscope photographs of friction force-slip velocity characteristics for steel and cast iron friction junctions respectively. The traces were obtained for variations in system frequency, drive speed and surface finish.

The friction level at zero velocity reduces with increase in velocity, the shape of the drop not being easily definable although it always appears to be of concave form i.e. inside a negative damping model. For the deceleration phase the friction level is generally constant although some increase is noticeable and very occasionally some decrease in friction force occurs.

It can be seen therefore that the actual friction characteristics fall between the upper and lower linearised models suggested in Chapter 2.

#### 4.2 Comparison of Experimental Results with Linearised Theories

As stated in Chapter 2, amplitude of vibrations appears not to be a suitable criterion for the assessment of the accuracy of any dynamic friction model. This is confirmed by fig. 4.2 which shows the comparison between actual and theoretically predicted values of vibration amplitude for a particular set of system parameters. It can be seen that both theories predict

vibration amplitudes close to the experimental values. This parameter therefore has not been used in comparing the linearised theories with experimental results. It can also be seen from fig. 4.2 that a running in period was evident and this was noticed on all unlubricated stick slip results. (Tabular results are included in Appendix I )

The vibrations occurring at the steel on steel and cast iron on cast iron interface were examined using the measurements of u.v. recorder traces typically shown in fig. 4.3. The system frequency was varied by using different springs, stiffness values of 7.3, 16.3 and 31 Nm/rad being used providing system frequencies of 6.6, 10 and 13.7Hz. The normal loads applied to the friction junction were 10, 20, 60 and 120N, and the drive speeds were 0.02, 0.08, 0.2, 0.35 and 0.5 rad/s. In all cases the pistons were run-in on a dummy disc prior to the tests in order to produce nominally the same area of contact of approximately  $35 \times 10^{-6} \text{m}^2$  between piston and disc. Measurements were taken of static friction torque, friction torque at maximum slip velocity, maximum slip velocity itself and time period of acceleration and deceleration (fig. 4.3). From these results the non-dimensional parameters  $\psi$  and  $C_1$  (governing parameters of linearised theories) were obtained and the graphs shown in figs. 4.4 to 4.11 plotted for the steel on steel interface. Similar results were obtained for cast iron on cast iron contact and are shown in figs. 4.12 to 4.19.

It can be seen that for those graphs involving comparisons

of slip time period of acceleration and deceleration the negative damping coefficient friction model offers closer correlation than the Blok model for both materials (see Figs. 4.4-7 and 4.12-15). Since the linearised models are generally disposed either side of the observed dynamic friction characteristics the time period for the acceleration phase would be expected to follow suit. This is confirmed by graphs 4.4, 4.5, 4.12 and 4.13 with the negative damping model theory offering closer correlation with experimental values. For both materials the predicted slip time period of deceleration is accurate to a high degree for the negative damping model theory. This is not so for the Blok model theory, which shows deviation from experimental results. Consequently the total slip period results of figs. 4.8, 4.9, 4.16 and 4.17 show the negative damping model theory to be the more accurate of the two suggested.

The correlation between theories and experimental results is similar for both steel and cast iron materials i.e. negative damping friction model is more accurate for both materials. The results indicating relationships between friction governing parameters and maximum slip velocity (figs. 4.10, 11, 18 and 19) show the Blok model to be reasonably accurate in predicting maximum velocity of vibrations with predicted values generally higher than those measured. Results have been taken for a large range of Blok parameter values and approximate correlation exists over the whole range for both materials. For the negative damping model theory, correlation exists for low values of  $C_1$  but some deviation from predictions does occur at

higher values. These experimental values are generally higher than theoretical predictions with little evidence of variation between cast iron and steel junctions.

#### 4.3 Variation of dynamic gradient with system parameters

Since the comparison between linearised models indicates the negative damping concept to be the more accurate in representing the friction characteristic of the materials used then an appreciation of the variation and values of that parameter for a range of system parameters is most useful.

Figs. 4.20 and 21 show the dynamic gradient  $C_F = \frac{T_S - T_K}{\dot{\theta}_{\max}}$  expressed as a function of normal load, system frequency, and drive speed. For both cast iron and steel junctions,  $C_F$  is seen to increase with increasing system frequency and increase with increasing normal load. Surface finish of the disc appears to have no influence on dynamic gradient values. Dynamic gradient increases slightly with reducing drive speed to approximately 0.1rad/s ( $5 \times 10^{-3}$  m/s surface speed), but for lower drive speeds a sharp increase in dynamic gradient is evident. This is true for both cast iron and steel junctions, with the absolute values of dynamic gradient generally lower for cast iron than steel.

In an attempt to produce an empirical formula representing the relationship between dynamic gradient and normal load, system stiffness and drive speed, the results are presented in log-log form in fig. 4.22 and 23. For cast iron, fig. 4.22 indicates the dynamic gradient to be a function of drive speed for each

normal load condition independent of system frequency. As the normal load increases, the slope of the log (C<sub>F</sub>) against log (drive speed) relationship reduces. This suggests the drive speed exponent itself to be an inverse function of normal load. This relationship is obtained as shown in fig. 4.23 plotting log (drive speed exponent) against log normal load from which the drive speed exponent relationship is obtained. Since dynamic gradient is dependent on system frequency then the exponent of (KJ) is found by plotting log (KJ) against log dynamic gradient for any values of drive speed and all values of normal load (fig. 4.24). Repeating the process for the relationship between dynamic gradient and normal load at 1 mm/s drive speed provides the load exponent (fig. 4.25). Bringing all the system parameters together and considering a particular value of dynamic gradient, provides a constant which completes the following empirical relationship

$$C_F = \frac{0.12 L^{0.25} (KJ)^{0.4}}{\dot{\phi}^{0.45} / L^{0.2}}$$

The units are:- L(N), K(Nm/rad) , J(Kgm<sup>2</sup>),  $\dot{\phi}$ (rad/s).

Converting the dynamic gradient values into negative damping coefficients ( $\div 2\sqrt{KJ}$ ) gives the graph shown in fig. 4.27 and the empirical relationship is modified to

$$C_1 = \frac{0.06 L^{0.25}}{\dot{\phi}^{0.45} / L^{0.2} \cdot (KJ)^{0.1}} \quad \text{i.e. negative}$$

damping coefficient reduces for increasing system (KJ) values.

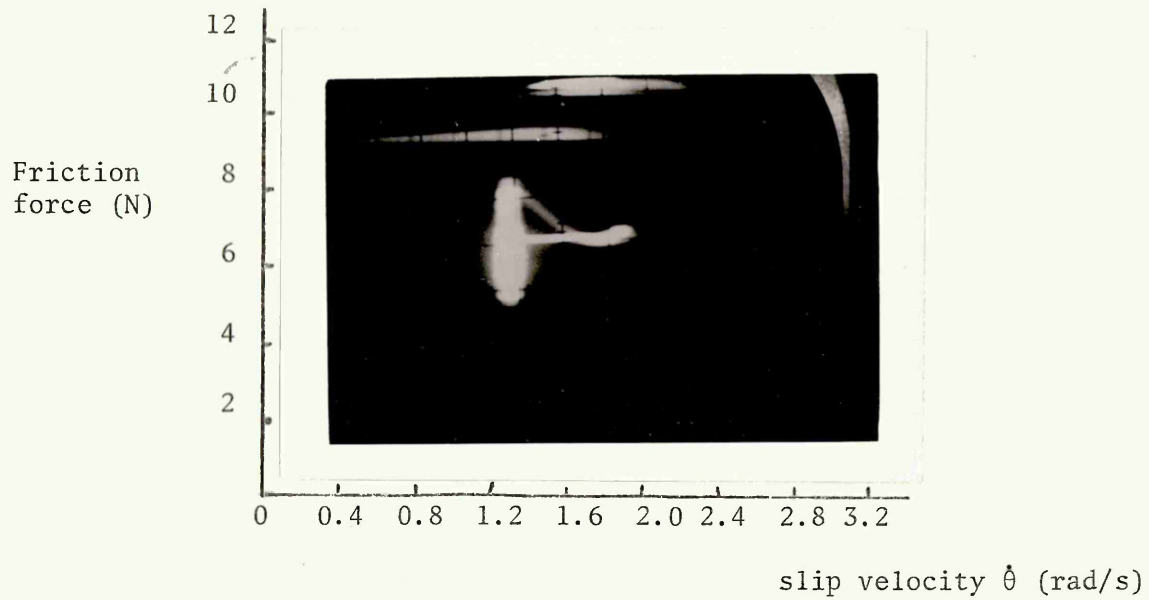
For the steel junction, dynamic gradients from fig. 4.21 presented in log-log form in fig. 4.23 are less easy to define than those for steel. Dynamic gradient is approximately a

constant function of drive speed for all normal load conditions although there is some evidence of deviation from this in fig. 4.23. Using the same basic form and approach as for steel junction results gives the following

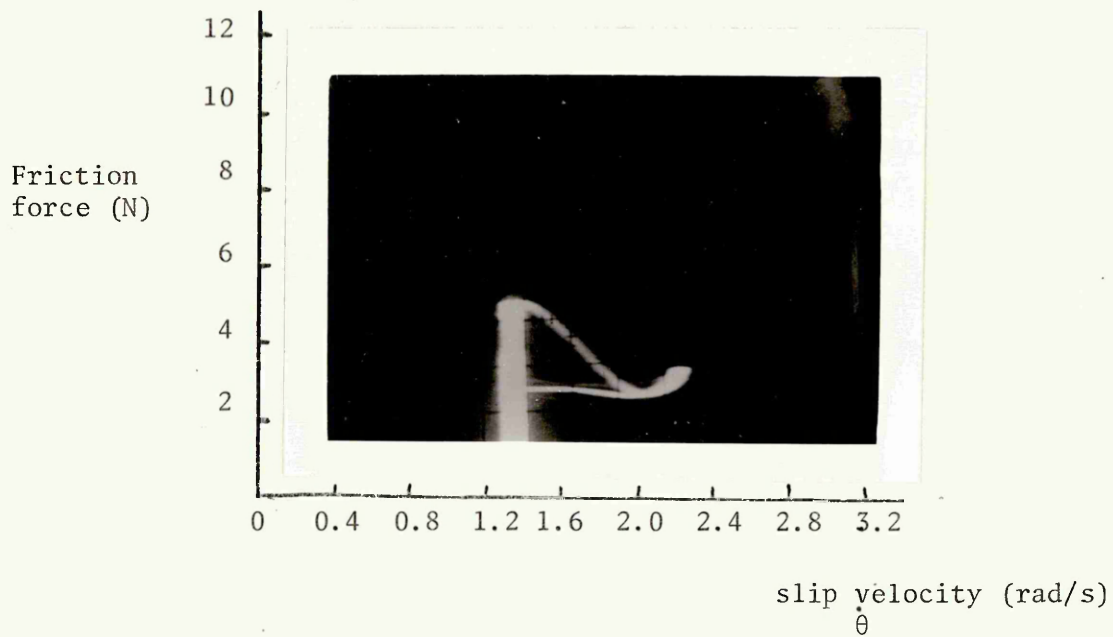
$$C_F = \frac{0.19 L^{0.2} (KJ)^{0.4}}{\dot{\phi}^{0.35} / L^{0.16}}$$

Converting the dynamic gradient results to negative damping coefficients (fig. 4.28) also indicates a decrease in negative damping coefficient for increase in system frequency.

Fig 4.1 (a) Typical friction force-slip velocity oscilloscope photographs.

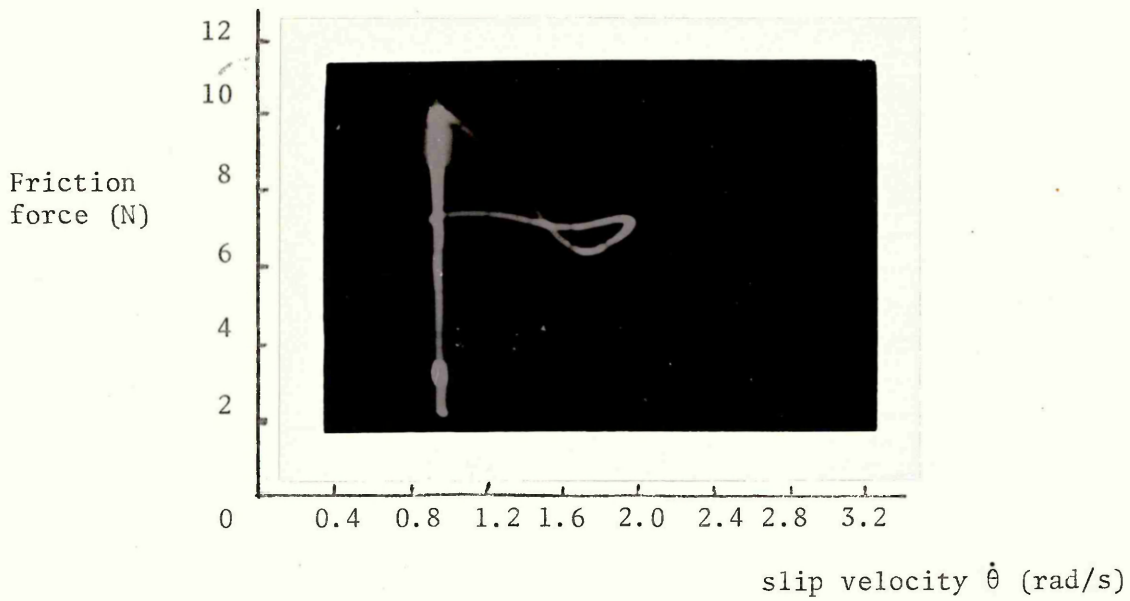


(i) Cast iron, 60N normal load, 6.6 Hz frequency, 0.02 rad/s drive speed, SF III.

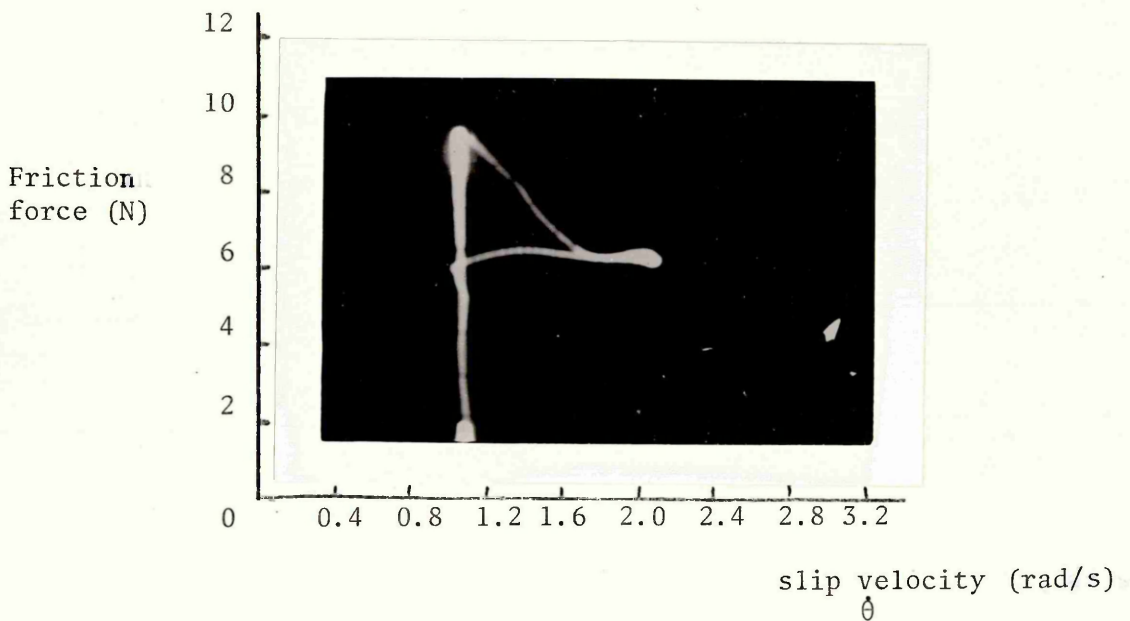


(ii) Cast iron, 60N normal load, 13.7 Hz frequency, 0.08 rad/s drive speed, SF II.

Fig 4.1 (b) Typical friction force-slip velocity oscilloscope photographs.

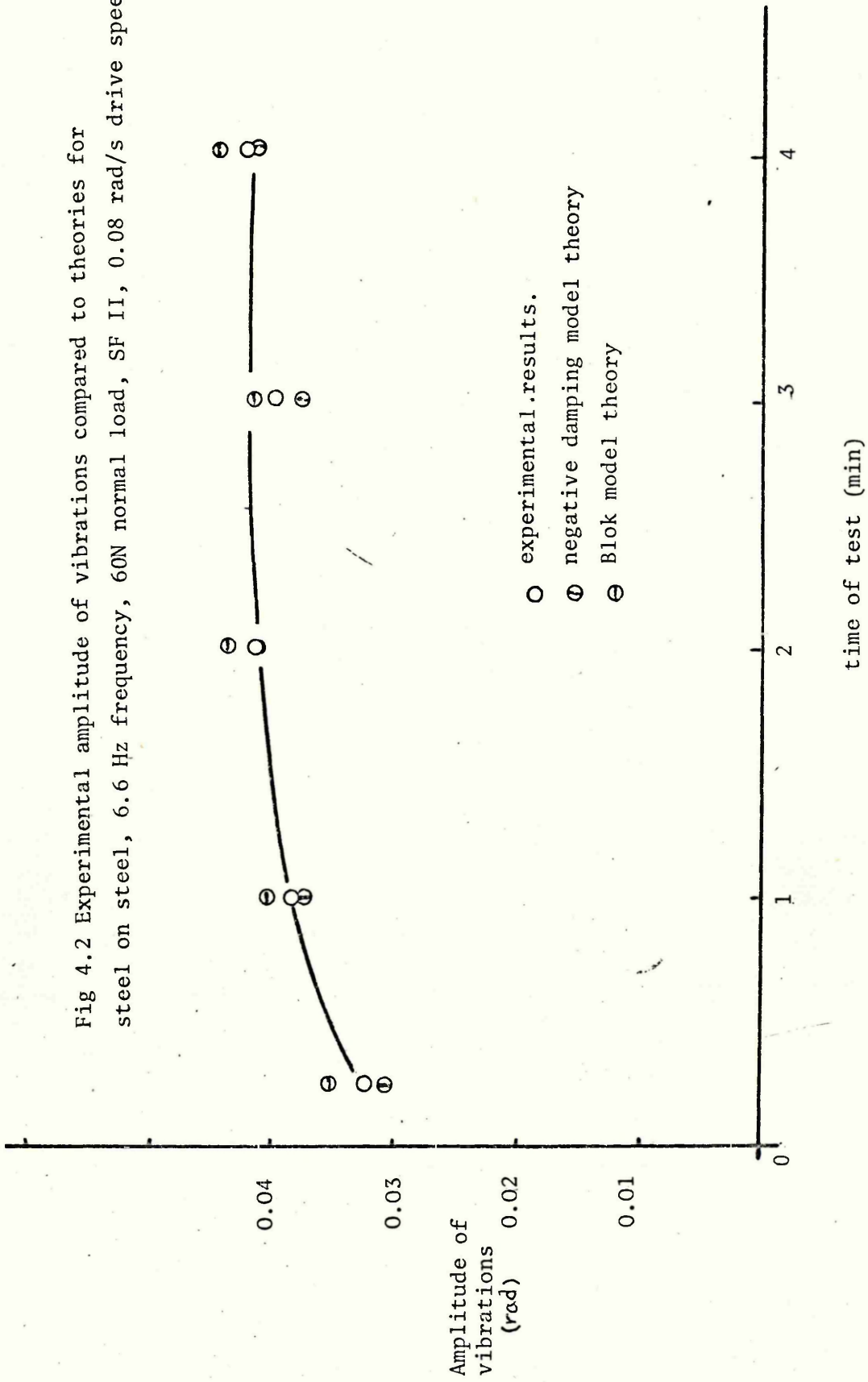


(i) Steel, 60N normal load, 10 Hz frequency, 0.08 rad/s drive speed, SF I.



(ii) Steel, 60N normal load, 13.7 Hz frequency, 0.08 rad/s drive speed SF II.

Fig 4.2 Experimental amplitude of vibrations compared to theories for steel on steel, 6.6 Hz frequency, 60N normal load, SF II, 0.08 rad/s drive speed



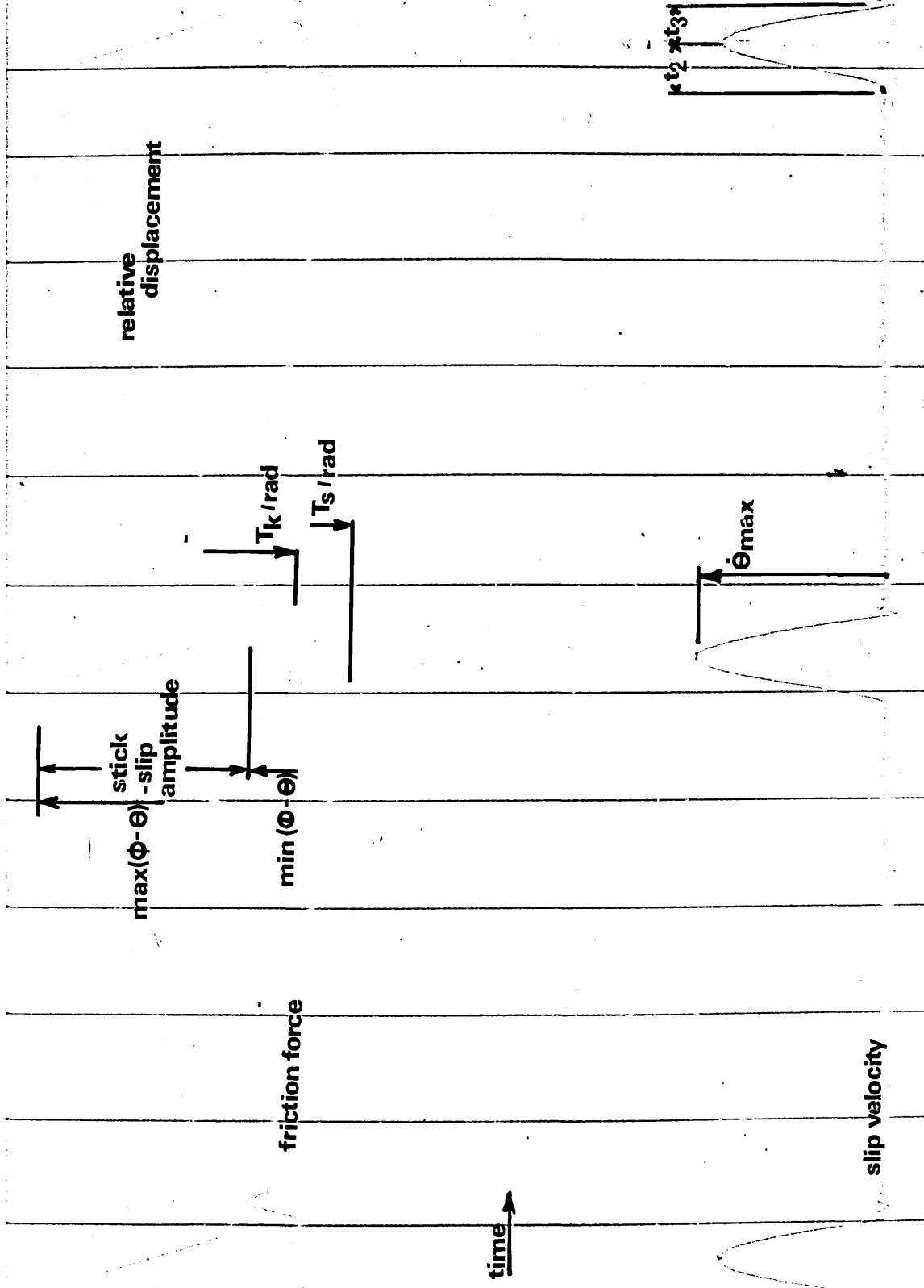


Fig 4.3 Typical stick slip u.v. recorder traces

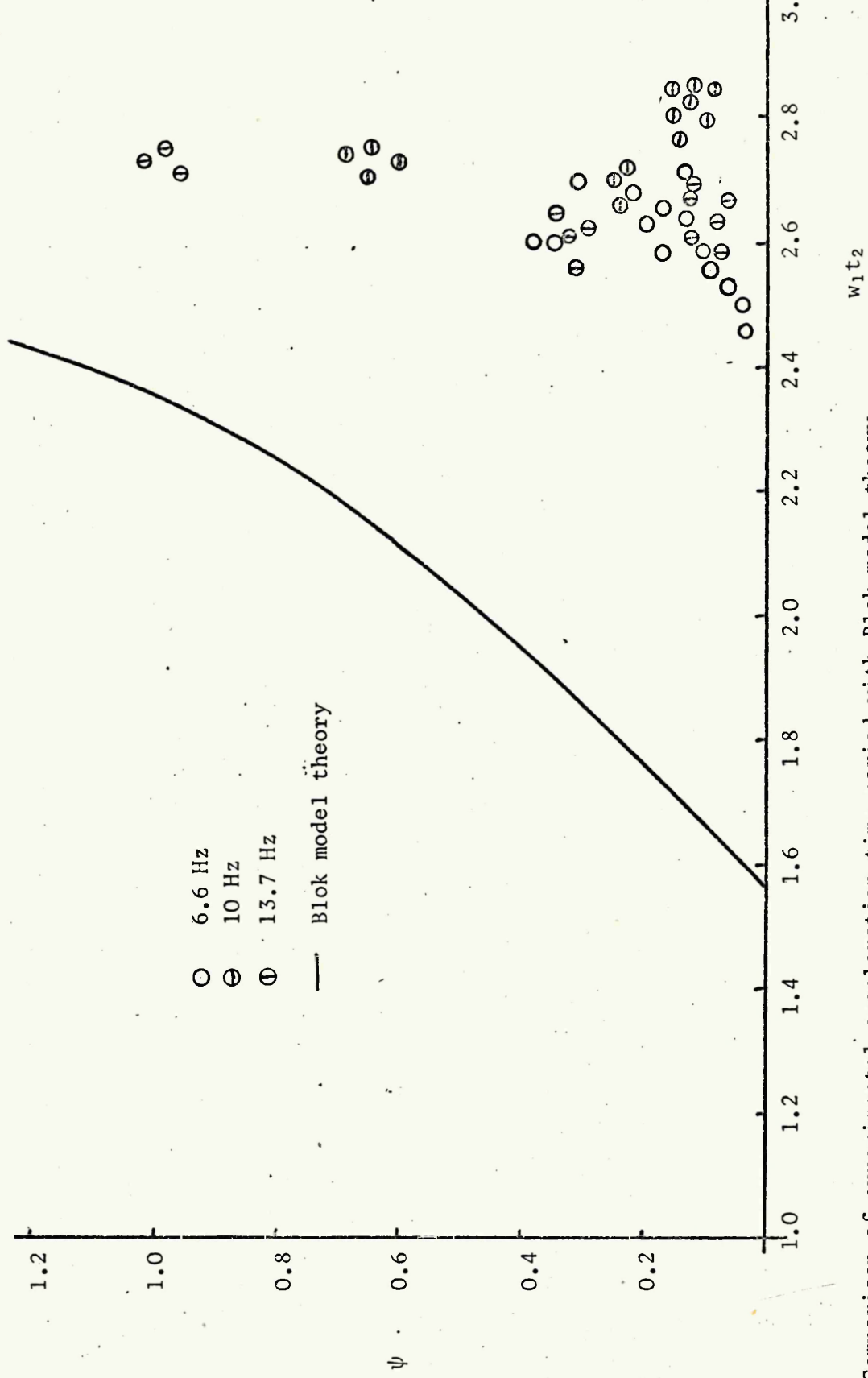


Fig. 4.4 Comparison of experimental acceleration time period with Blok model theory for variations in drive speed, normal load, surface finish and system frequency, steel on steel

Fig. 4.5 Comparison of experimental acceleration time period with negative damping model theory for variations in normal load, drive speed, surface finish and system frequency, steel on steel

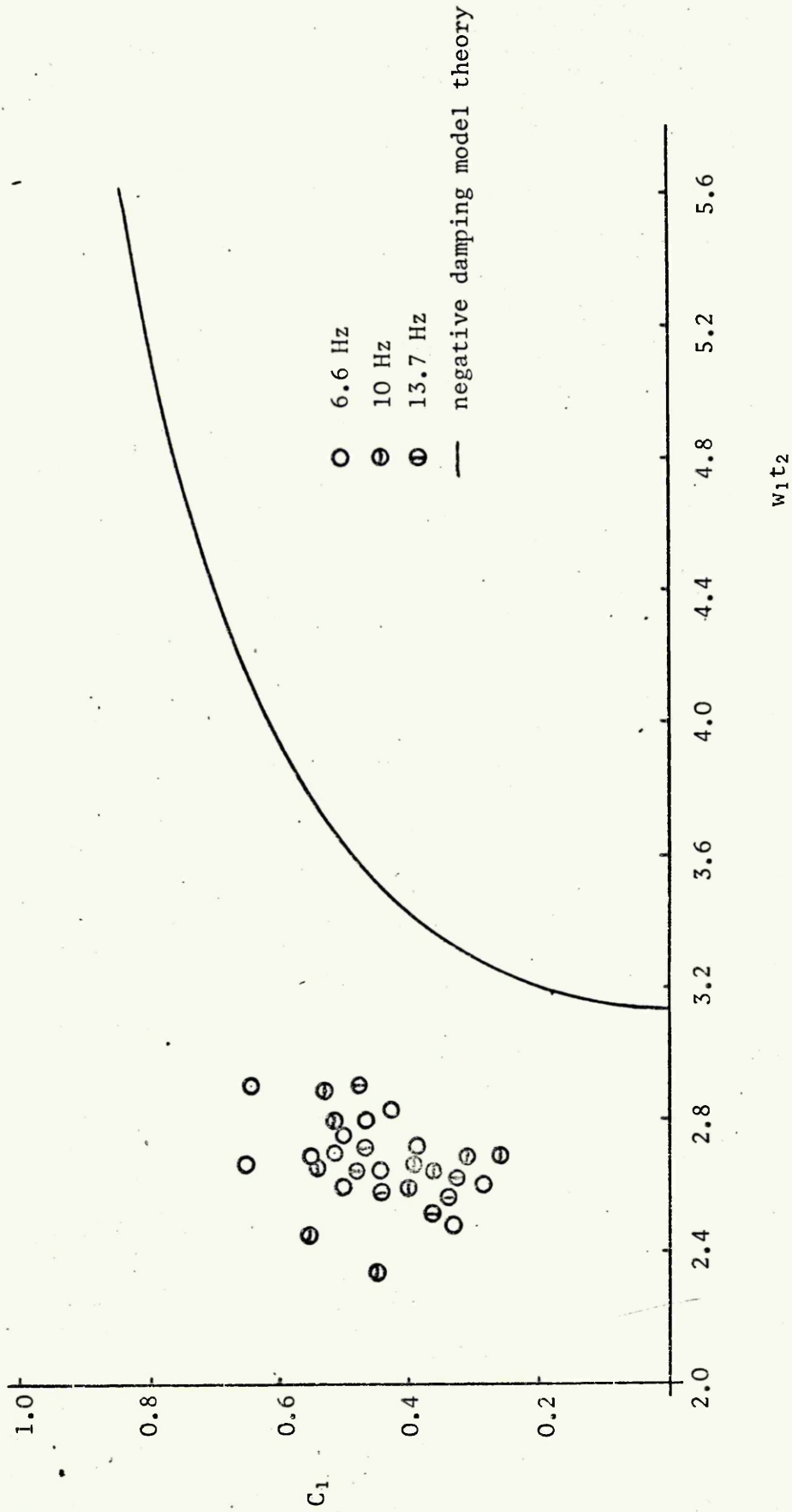


Fig 4.6 Comparison of experimental deceleration time period with Blok model theory, steel on steel

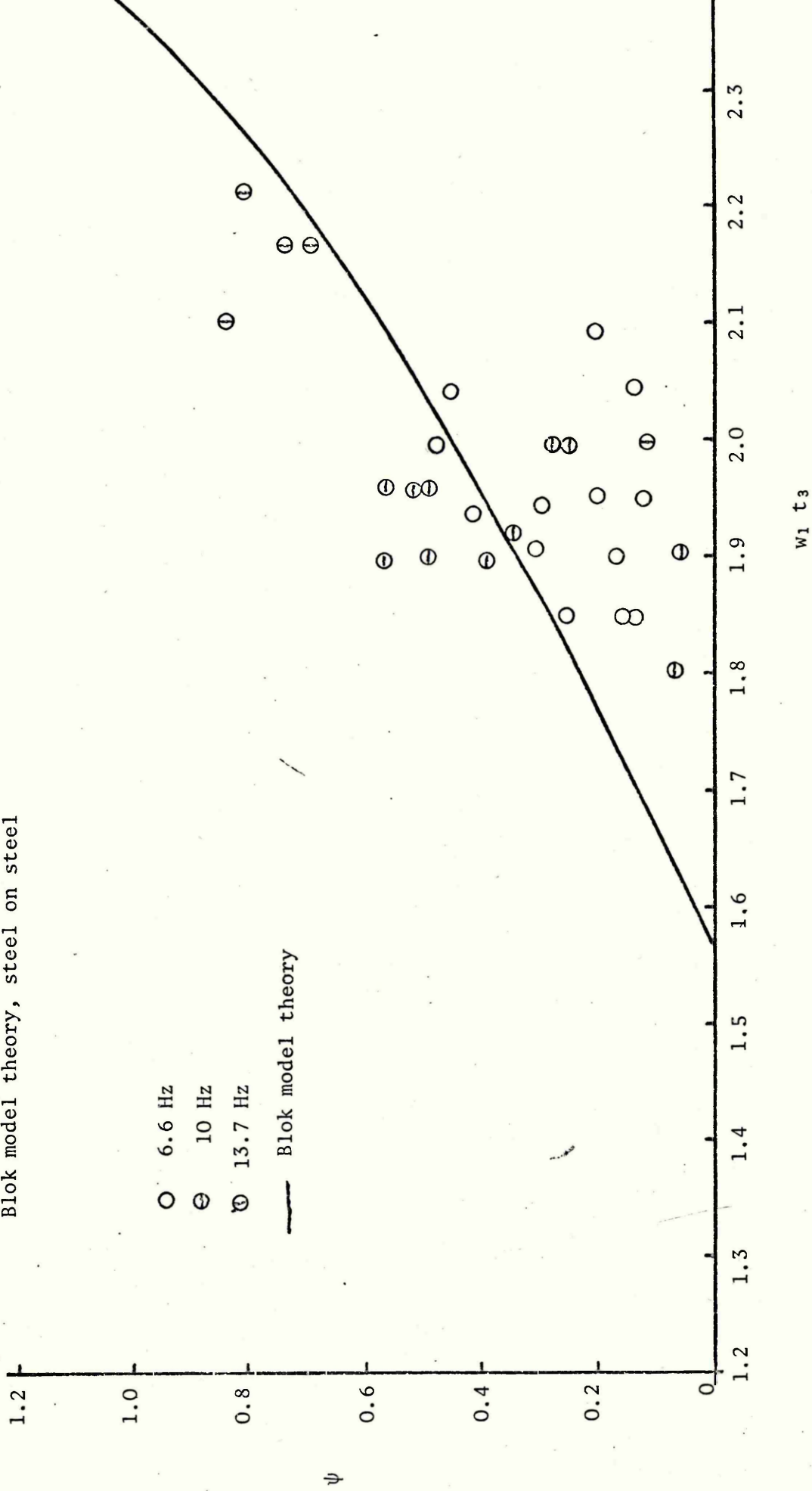


Fig. 4.7 Comparison of experimental deceleration time period with negative damping theory variations in normal load, drive speed, surface finish and system frequency, steel

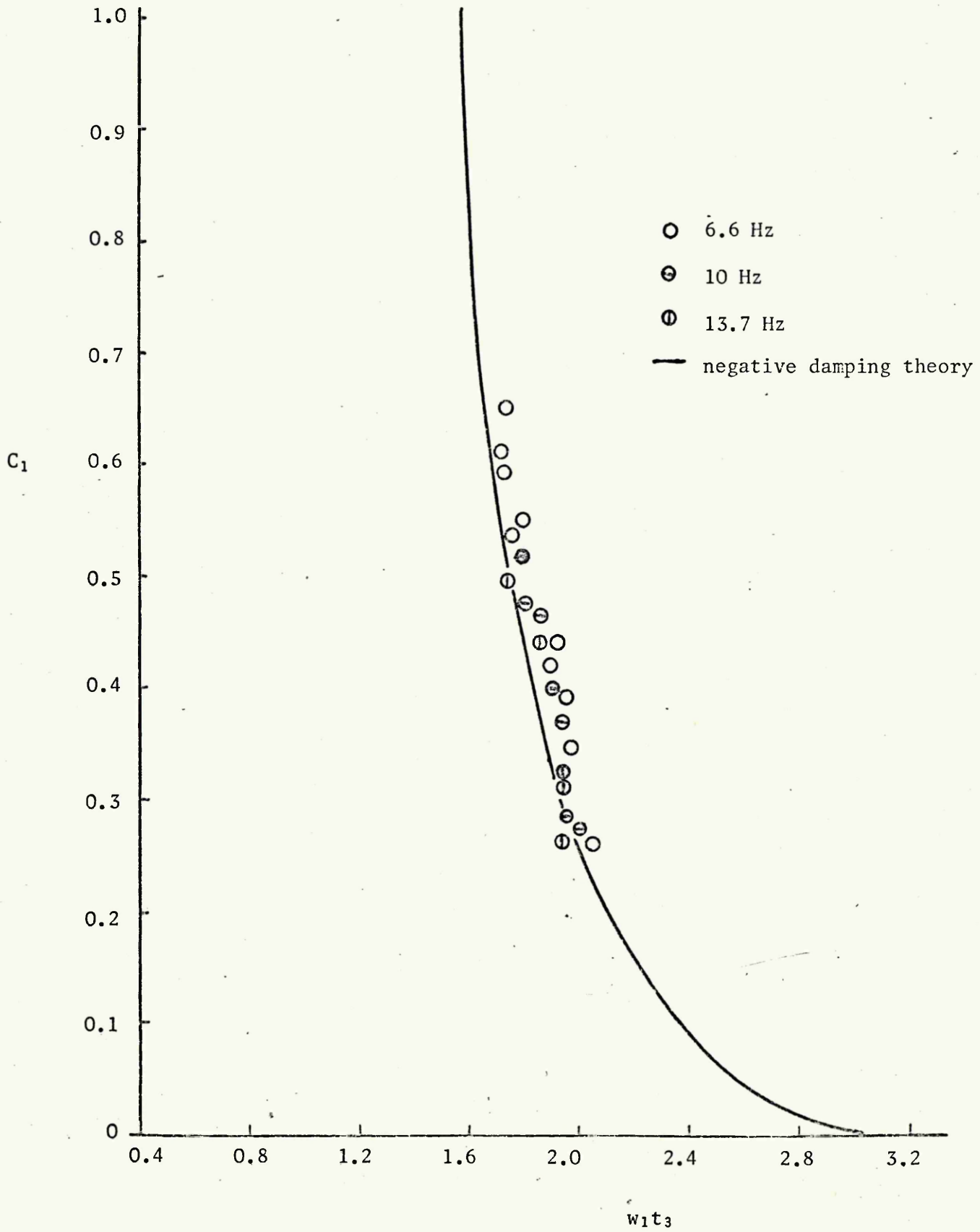


Fig. 4.8

Comparison of experimental slip frequency with Blok model theory for variations in surface finish, load, drive speed, system frequency, steel on steel

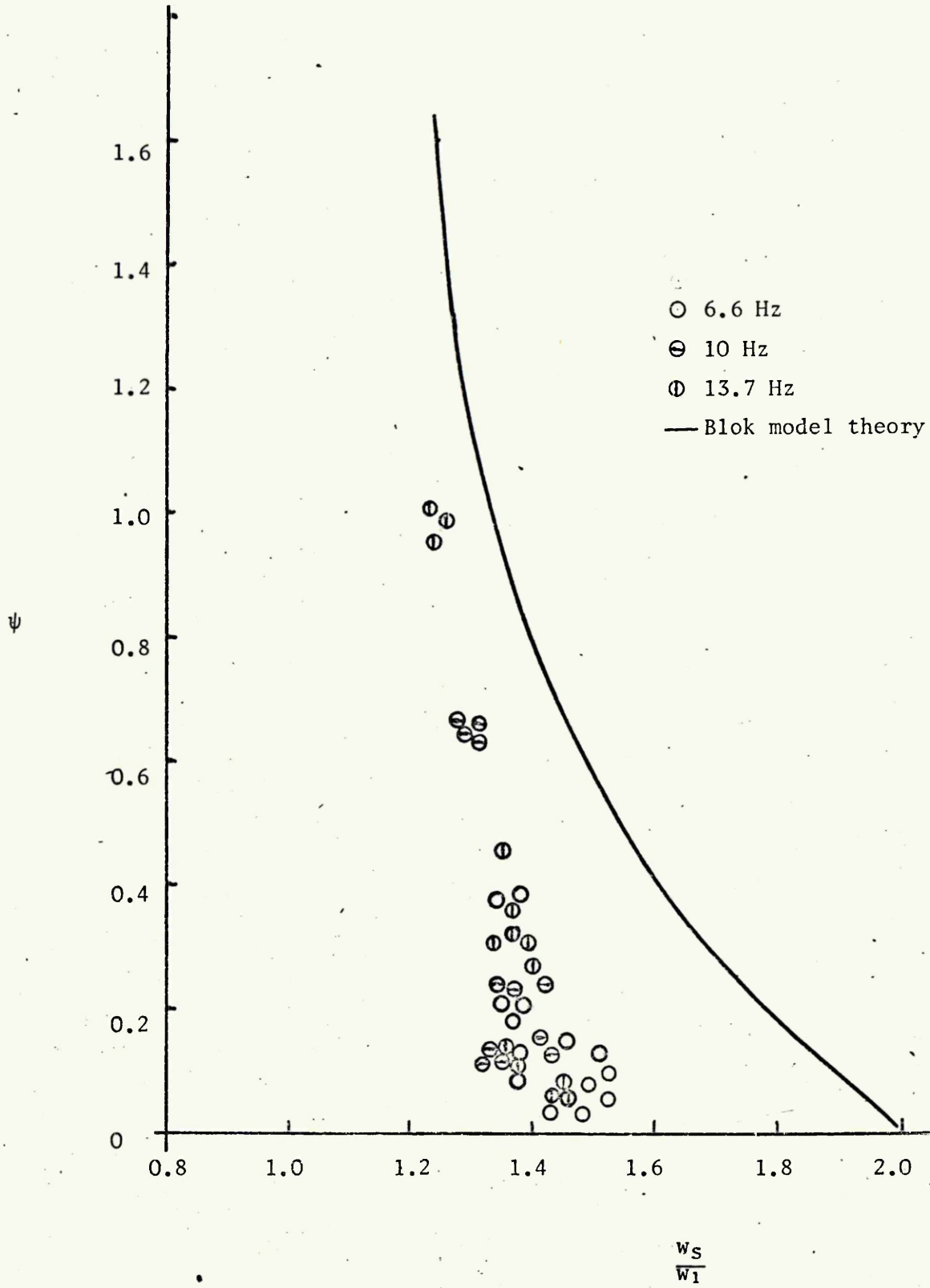
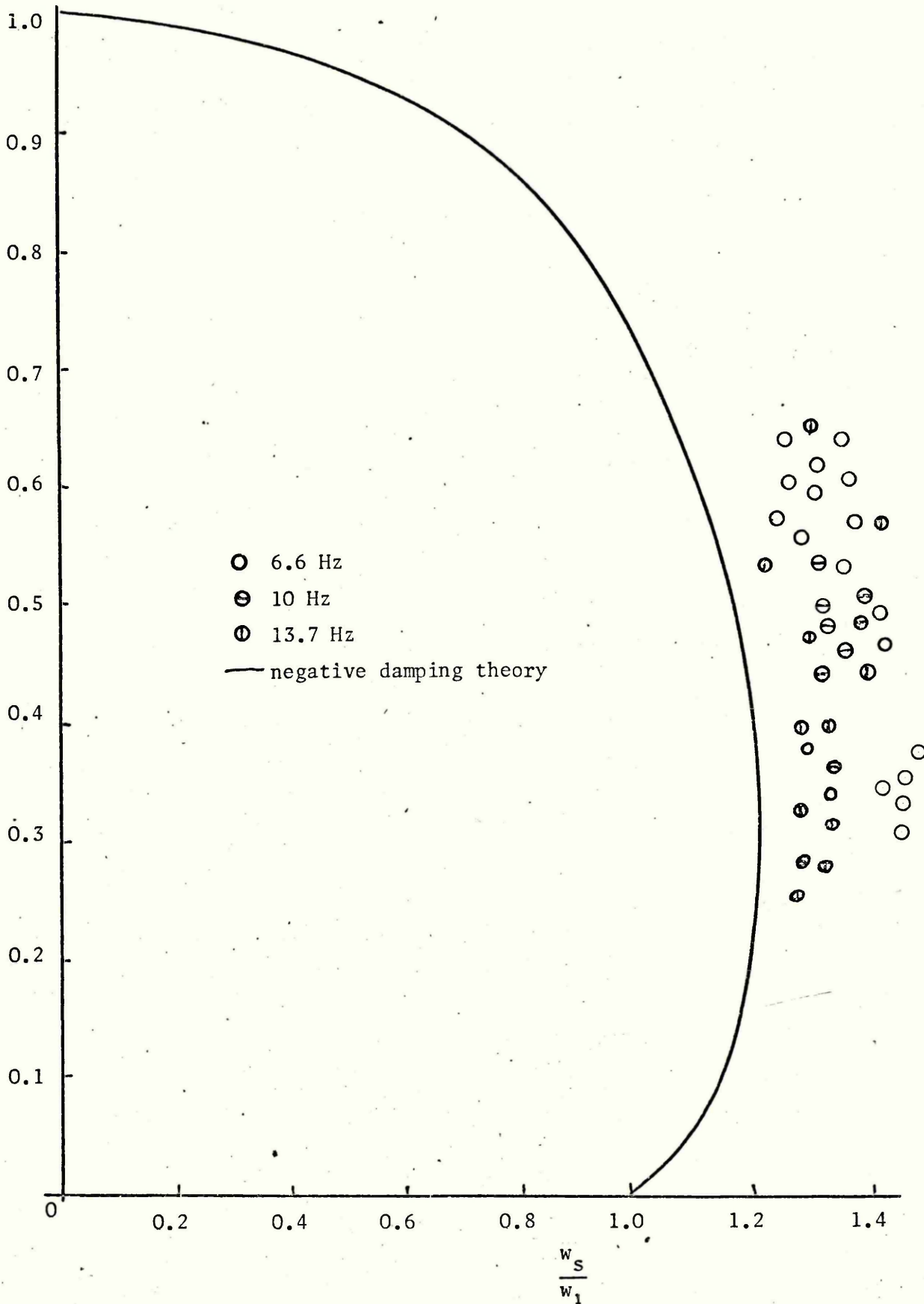
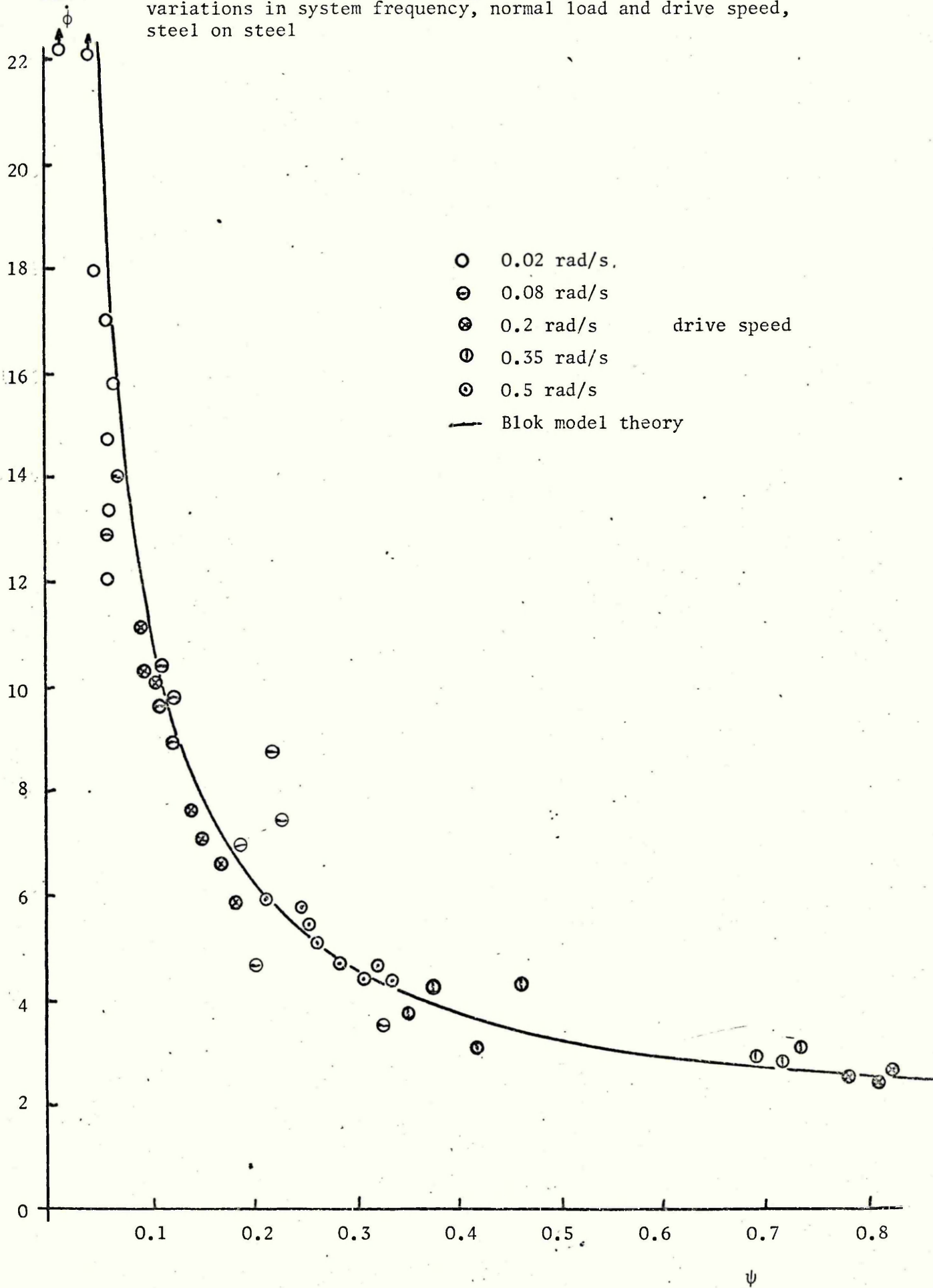


Fig. 4.9 Comparison of experimental slip frequency with negative damping theory for variations in normal load, drive speed, surface finish and system frequency (negative damping model), steel on steel



$\frac{\theta_{max}}{\phi}$

Comparison of experimental  $\frac{\theta_{max}}{\phi}$  with Blok model theory for variations in system frequency, normal load and drive speed, steel on steel



negative damping model theory, steel on

steel

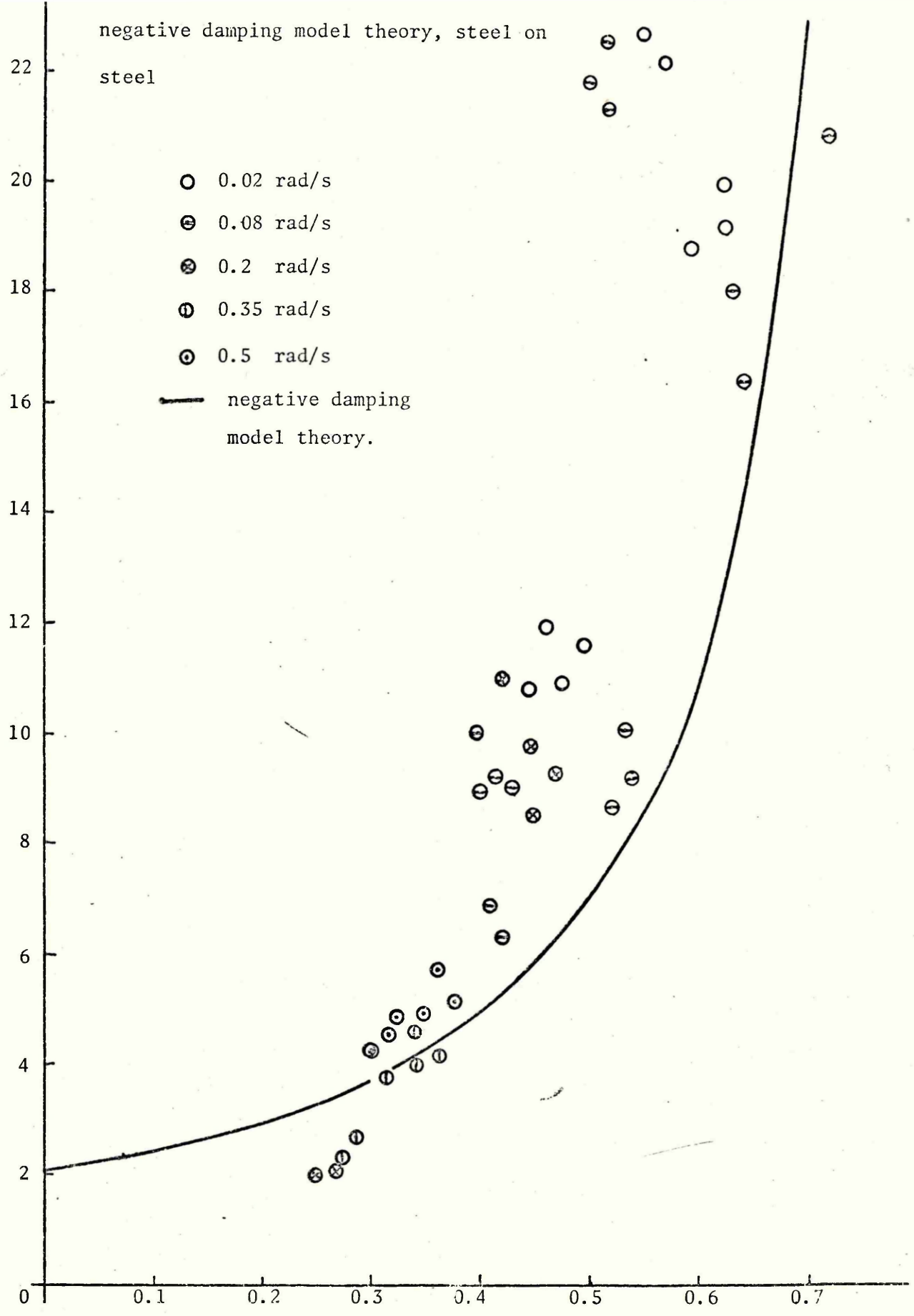
max  
 $\dot{\phi}$

22  
20  
18  
16  
14  
12  
10  
8  
6  
4  
2  
0

- 0.02 rad/s
- ⊖ 0.08 rad/s
- ⊗ 0.2 rad/s
- ⊕ 0.35 rad/s
- ⊙ 0.5 rad/s

— negative damping  
model theory.

$C_1$



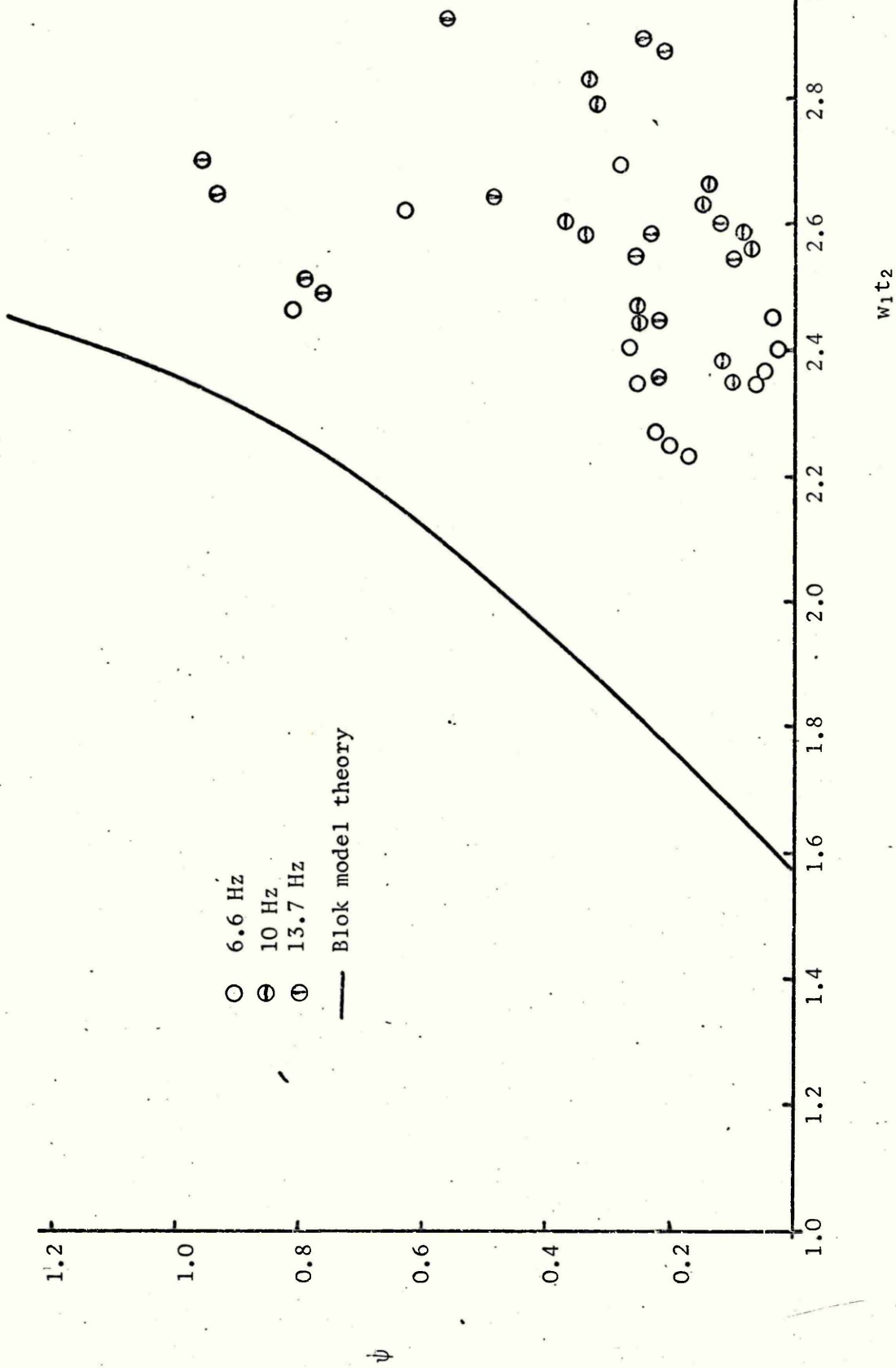


Fig. 4.12 Comparison of experimental acceleration time period with Blok model theory for variations in drive speed, normal load, surface finish and system frequency, cast iron

Fig. 4.13 Comparison of experimental acceleration time period with negative damping theory for variations in normal load, drive speed, surface finish and system frequency, cast iron

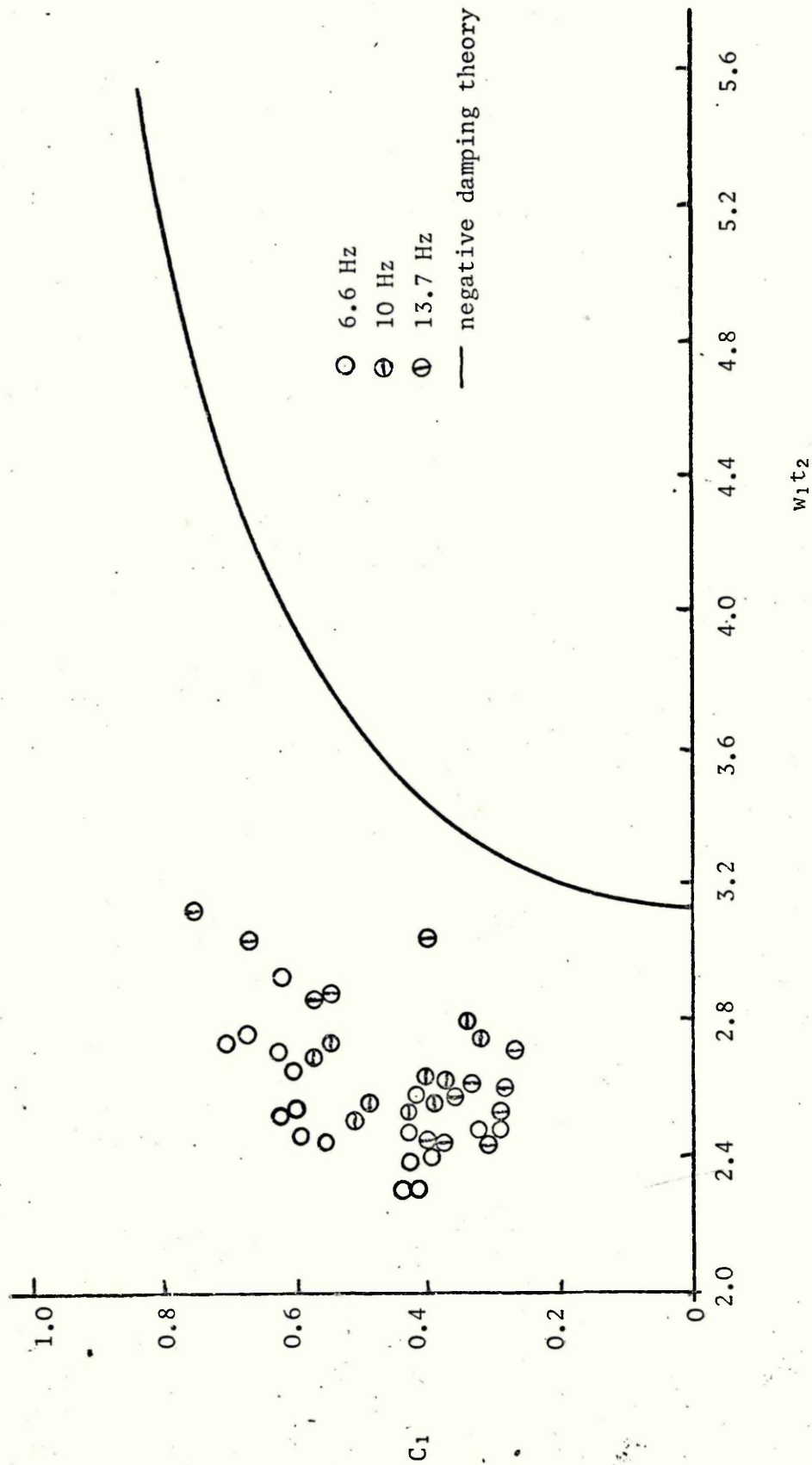


Fig 4.14 Comparison of experimental deceleration time period with Blok Model theory, cast iron

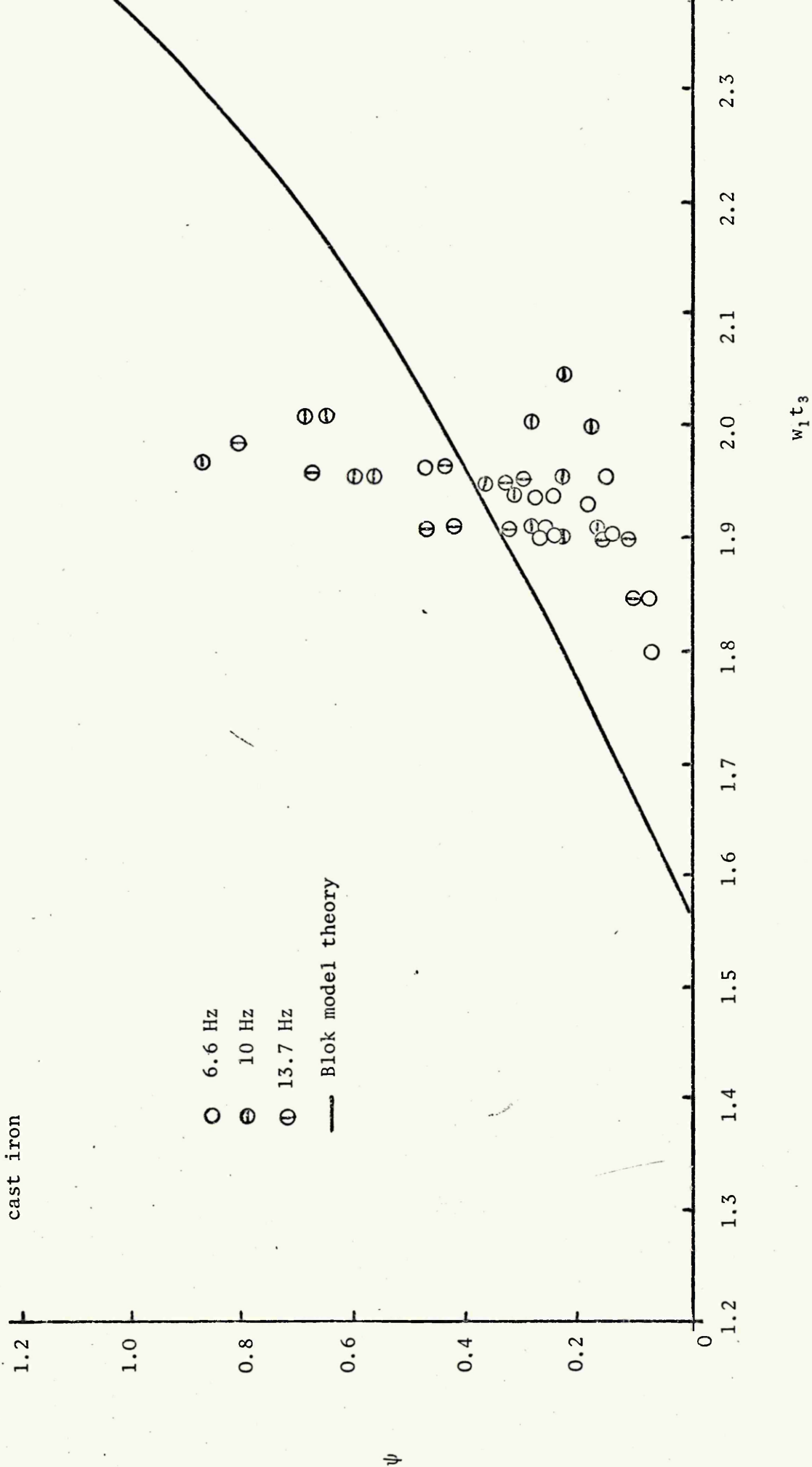


Fig. 4.15

Comparison of experimental deceleration time period with negative damping theory for variations in normal load drive speed, surface finish and system frequency, cast iron

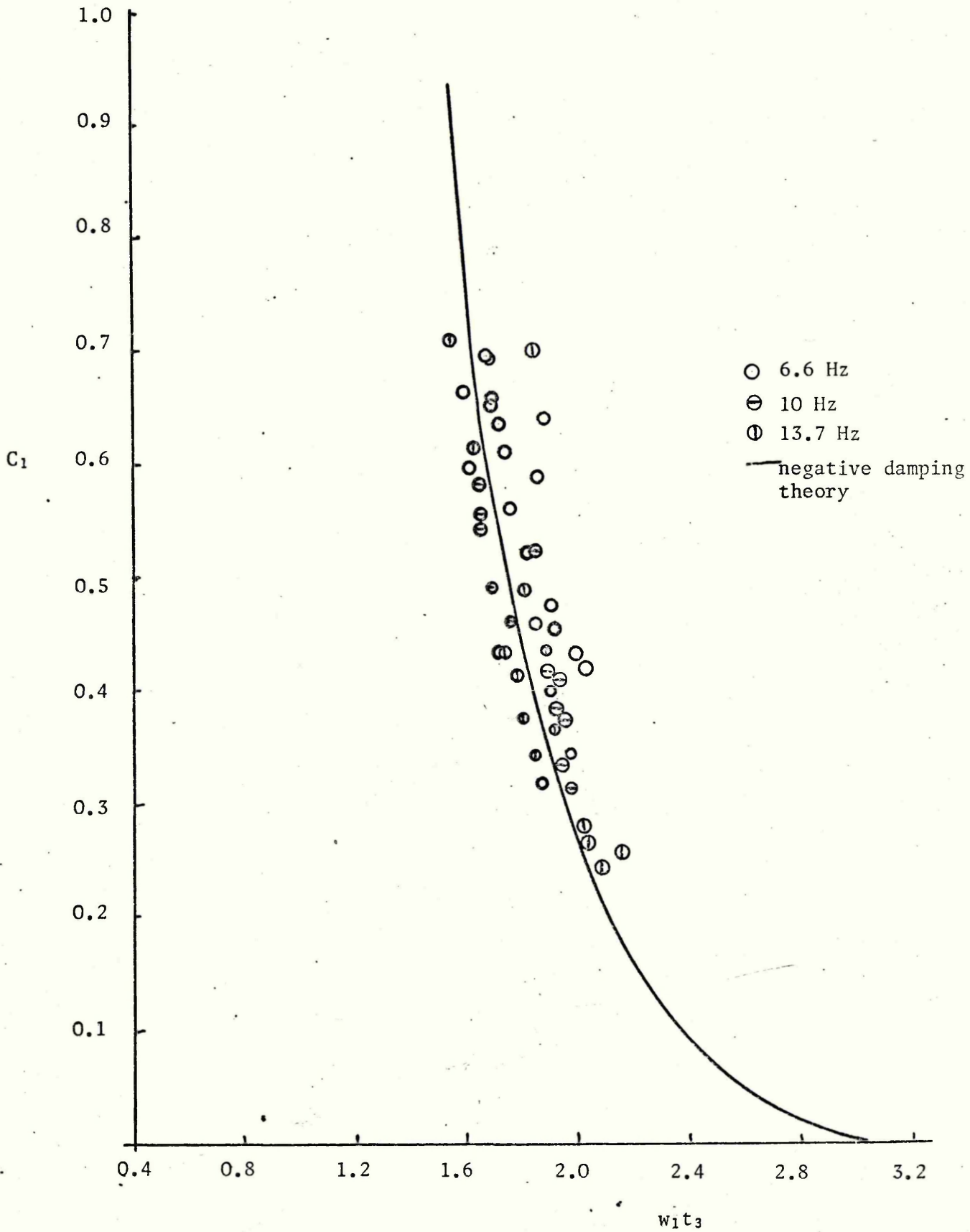




Fig. 4.17 Comparison of experimental slip frequency with negative damping theory for variations in normal load, drive speed, surface finish and system frequency, cast iron

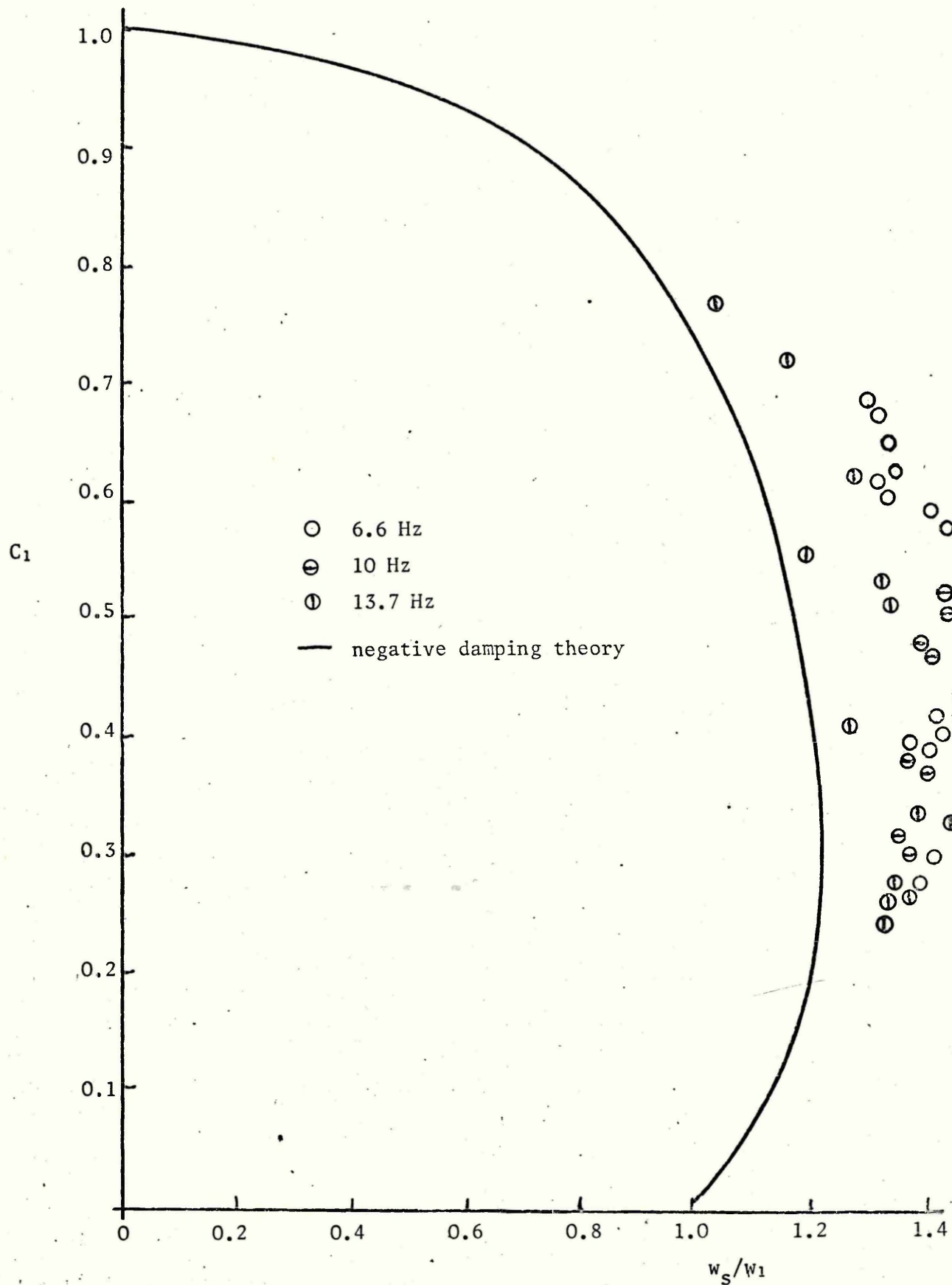
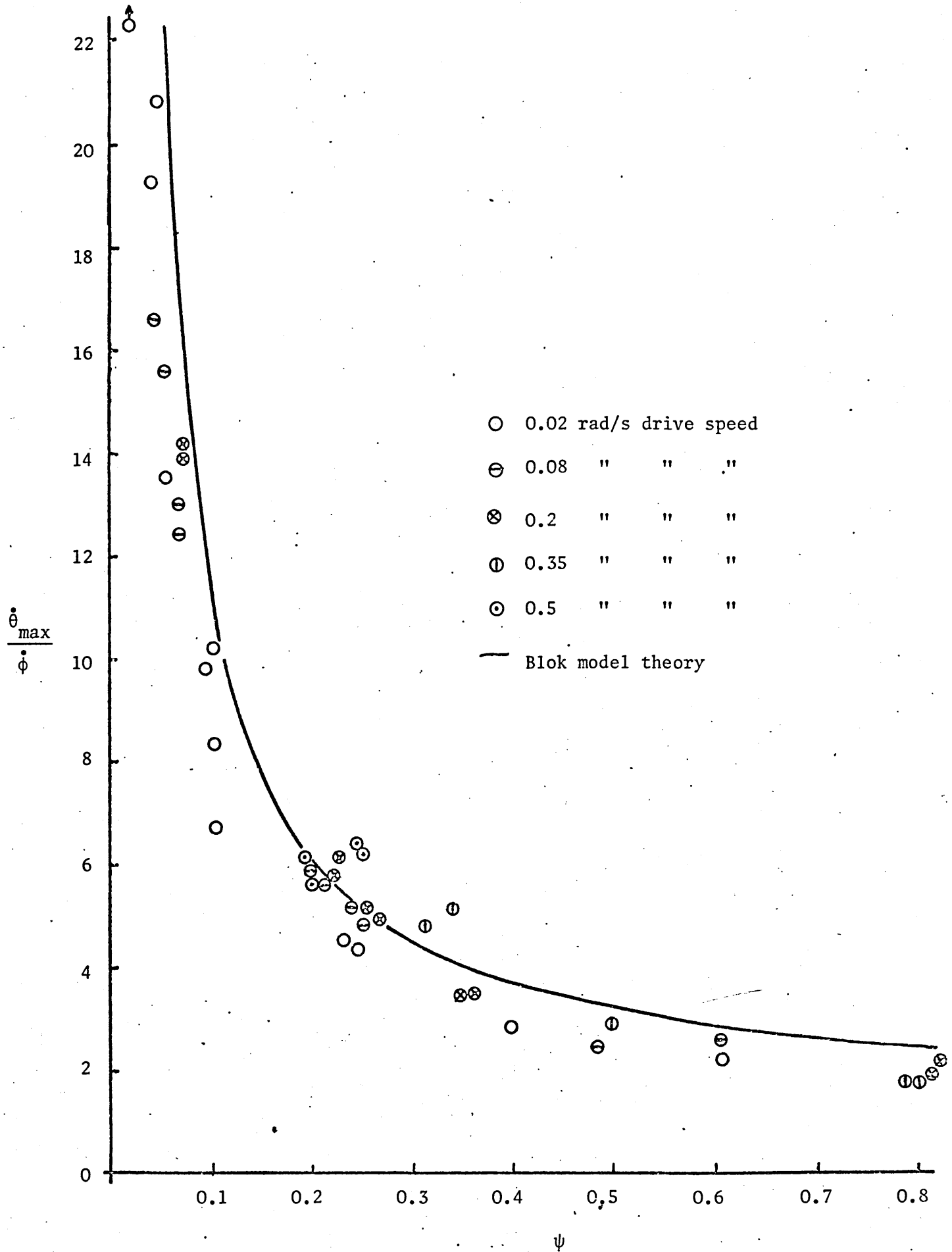


Fig. 4.18 Comparison of experimental  $\frac{\dot{\theta}_{\max}}{\dot{\phi}}$  with Blok model theory, cast iron



for variations in normal load, surface finish, system frequency and drive speed, cast iron

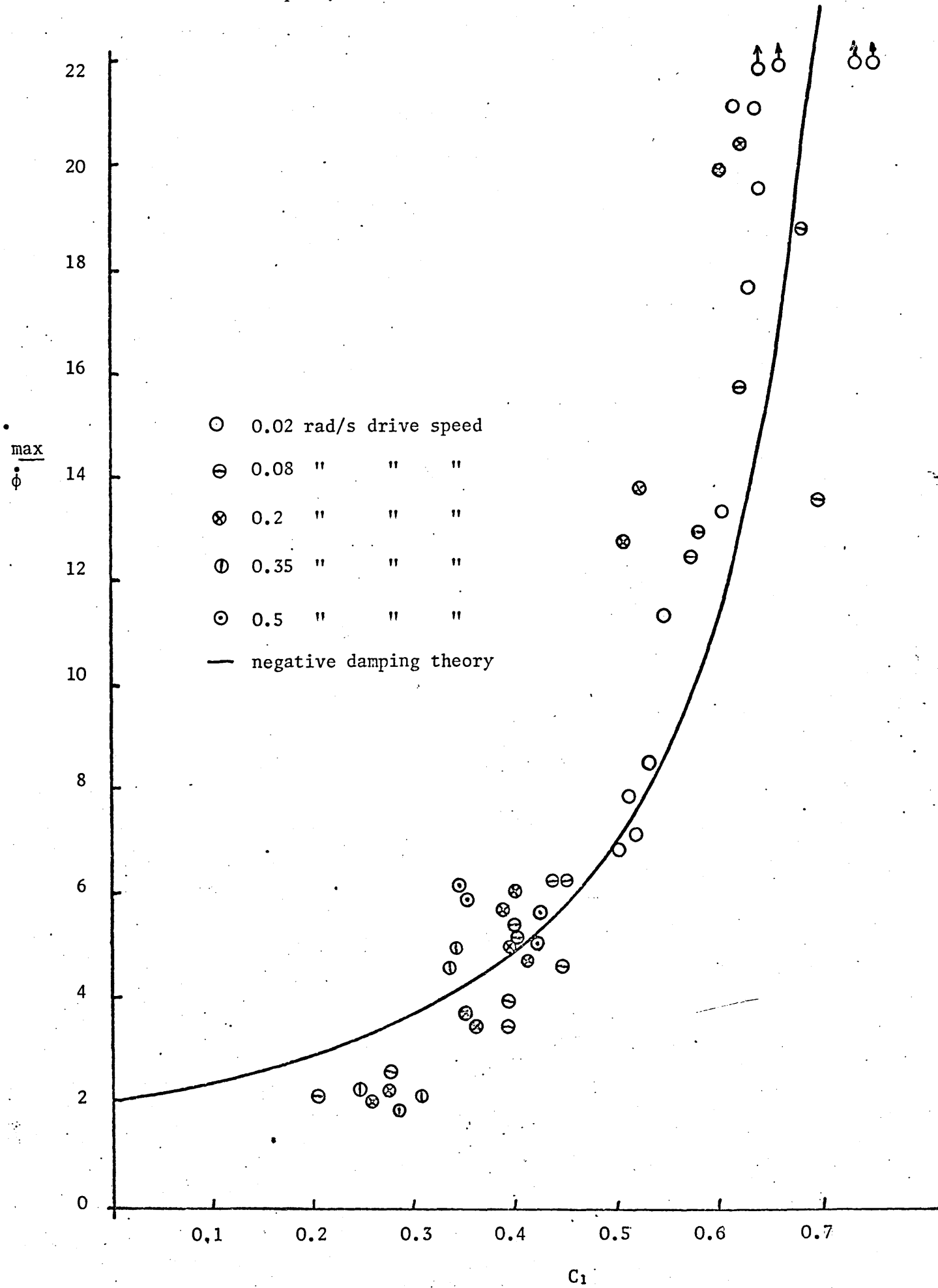
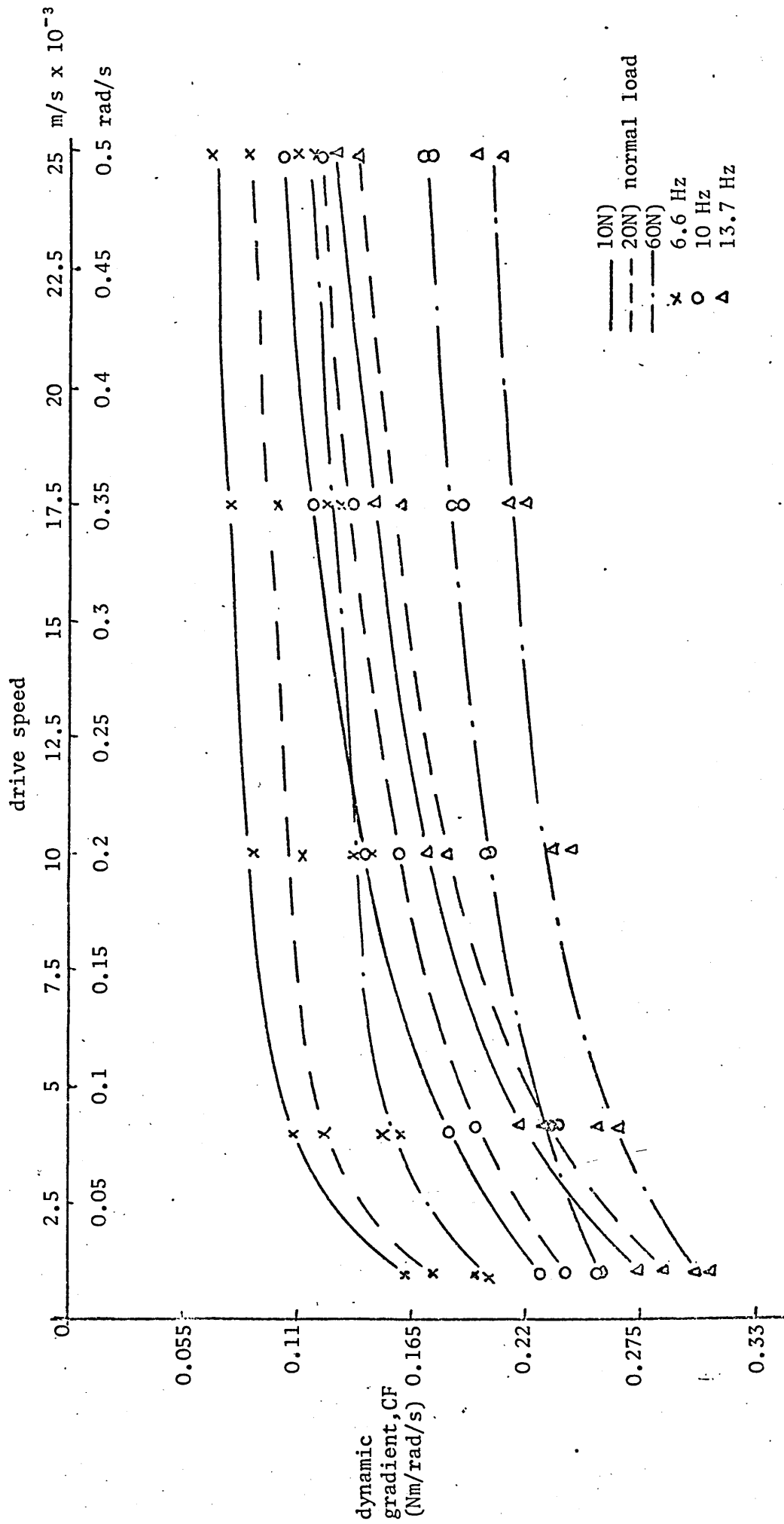


Fig. 4.20 Dynamic gradient as a function of drive speed for variations in normal load and system frequency, cast iron



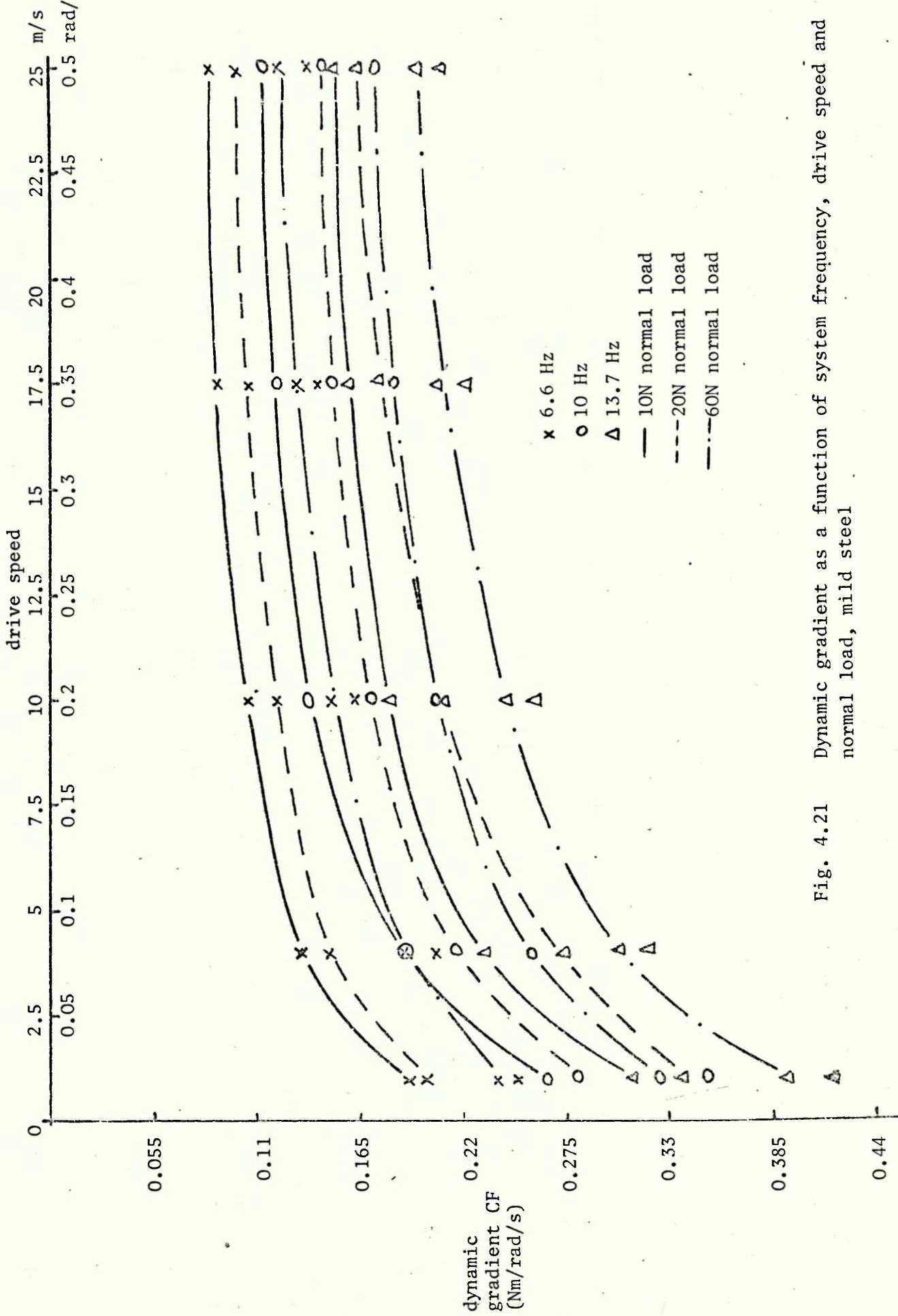


Fig. 4.21 Dynamic gradient as a function of system frequency, drive speed and normal load, mild steel

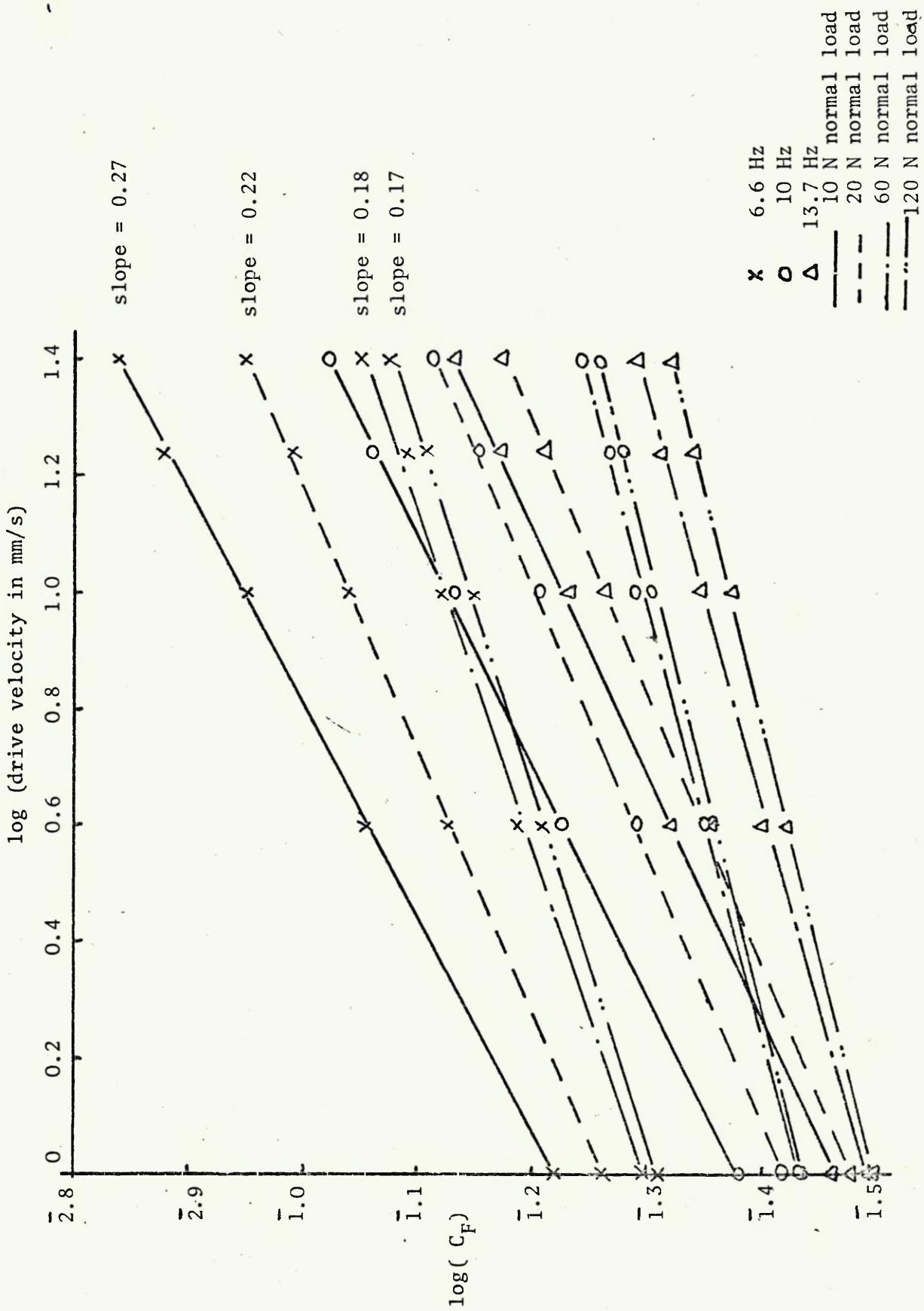


Fig 4.22 Dynamic gradient ( $C_F$ ) as a function of drive speed for variations in normal load and system frequency - cast iron (logarithmic plot)

Fig. 4.23 Dynamic gradient as a function of surface drive speed for variations in system frequency and normal load - steel (logarithmic plot)

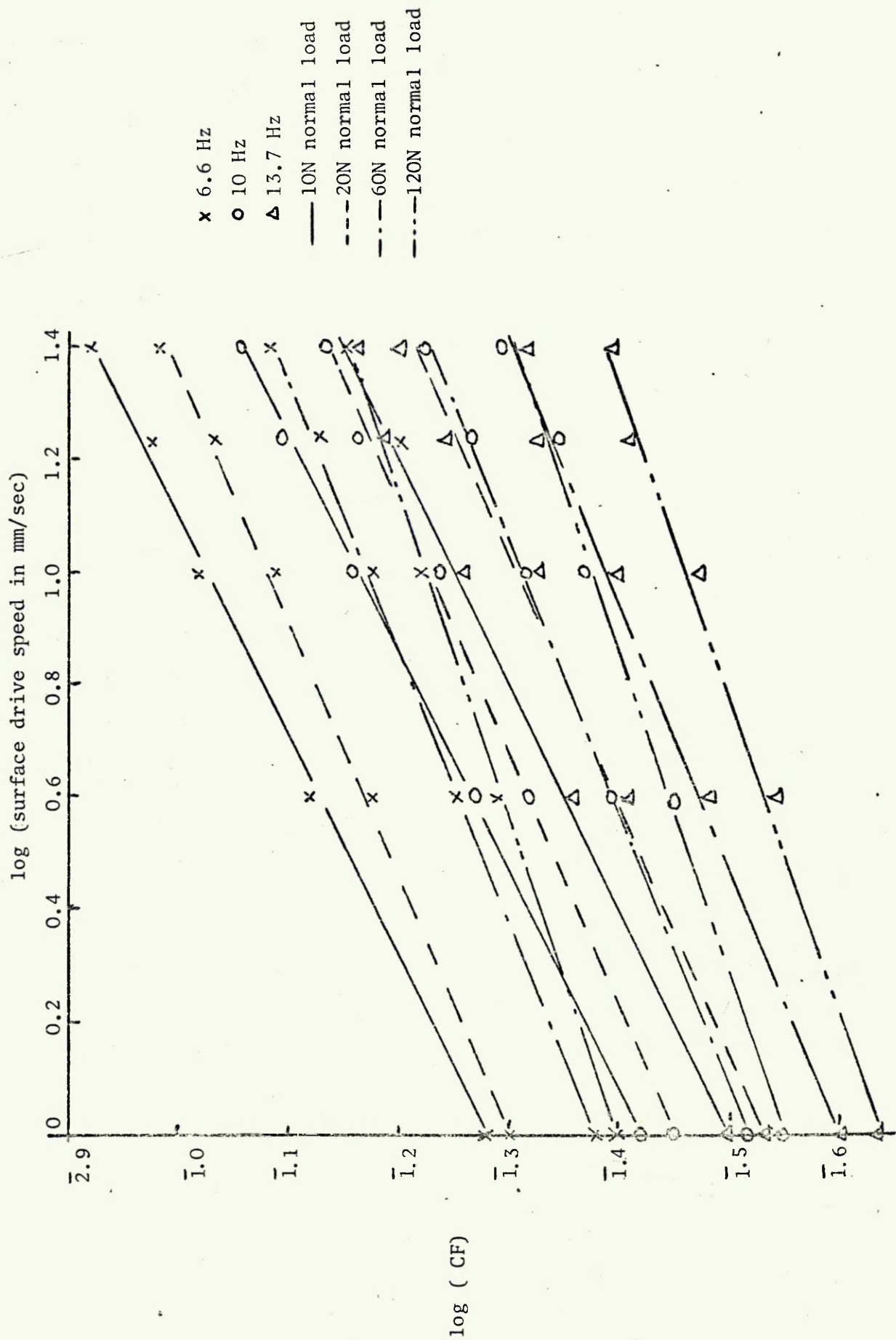


Fig. 4.24  $\log(\text{drive speed exponent 'x'})$  vs  $\log(\text{normal load (N)})$ , cast iron on cast iron

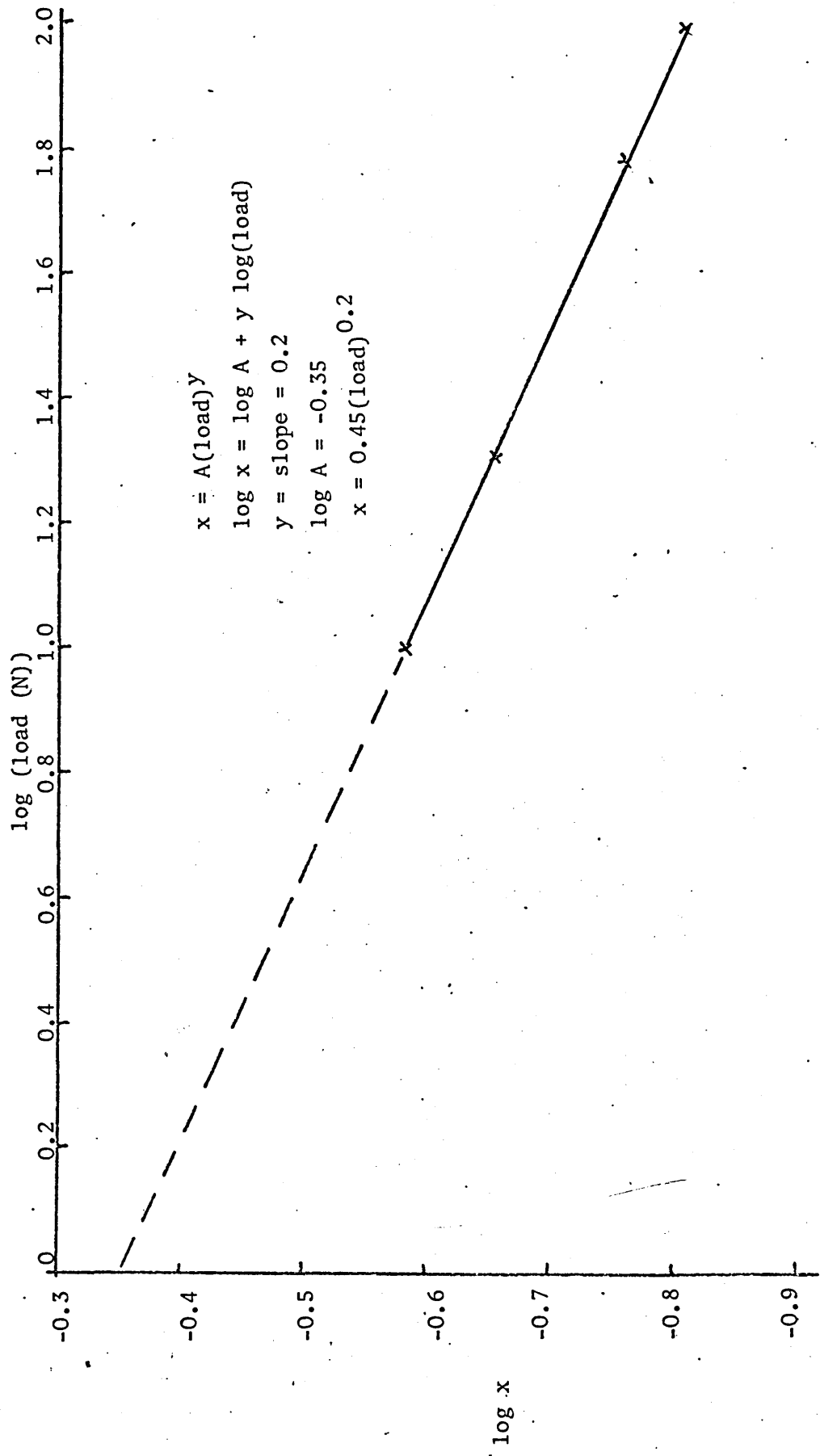




Fig. 4.26 Log (normal load (N)) vs log (C<sub>F</sub>) for cast iron on cast iron (drive speed = 0.02 rad/s)

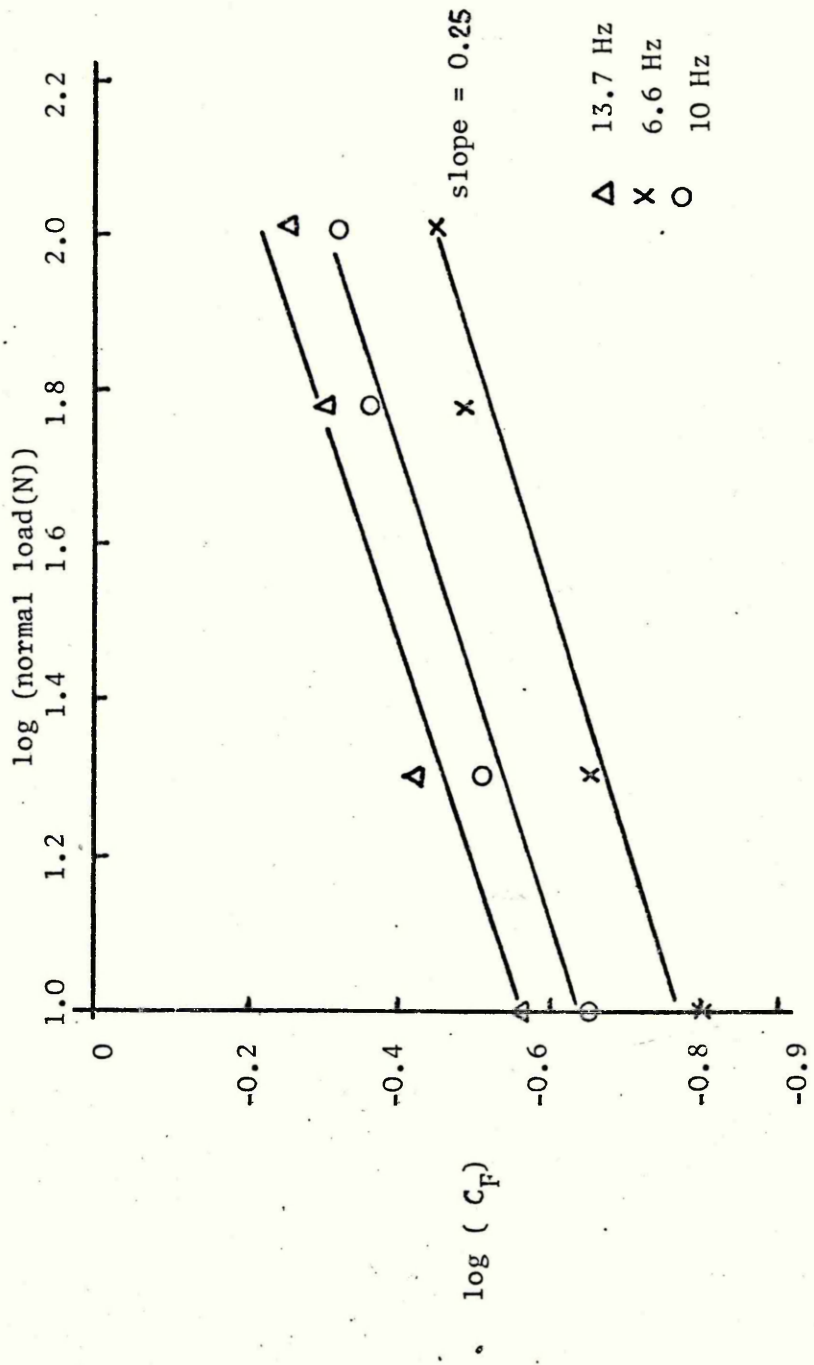


Fig. 4.27 Variation of negative damping coefficient with system frequency, Cast iron

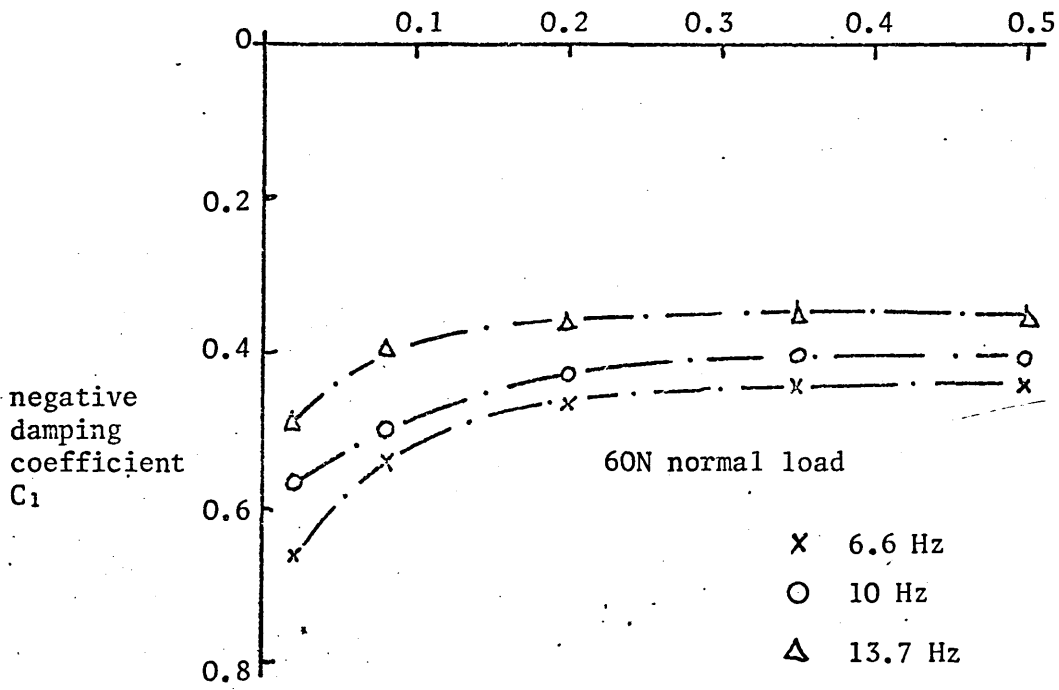
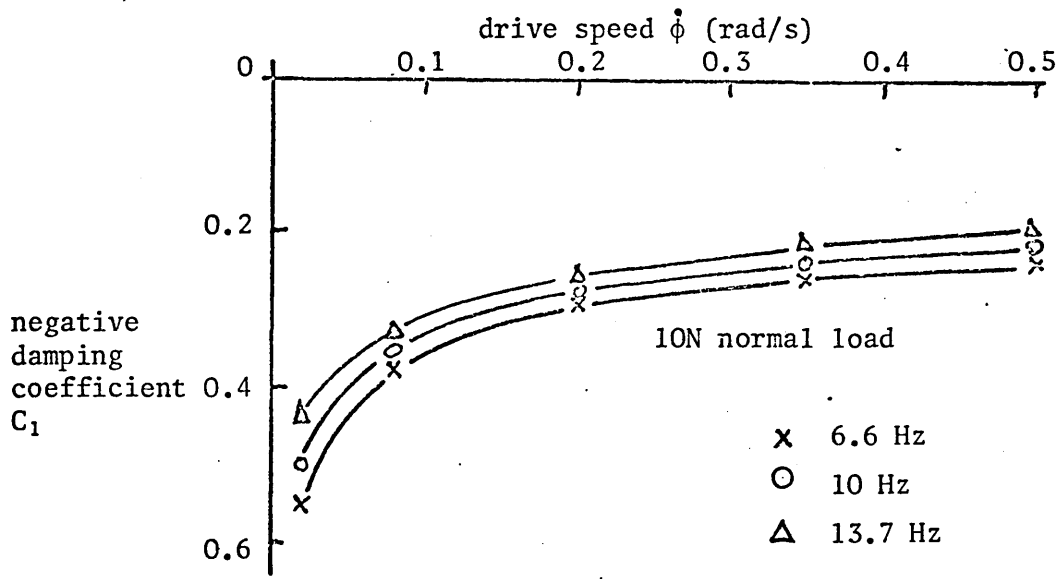
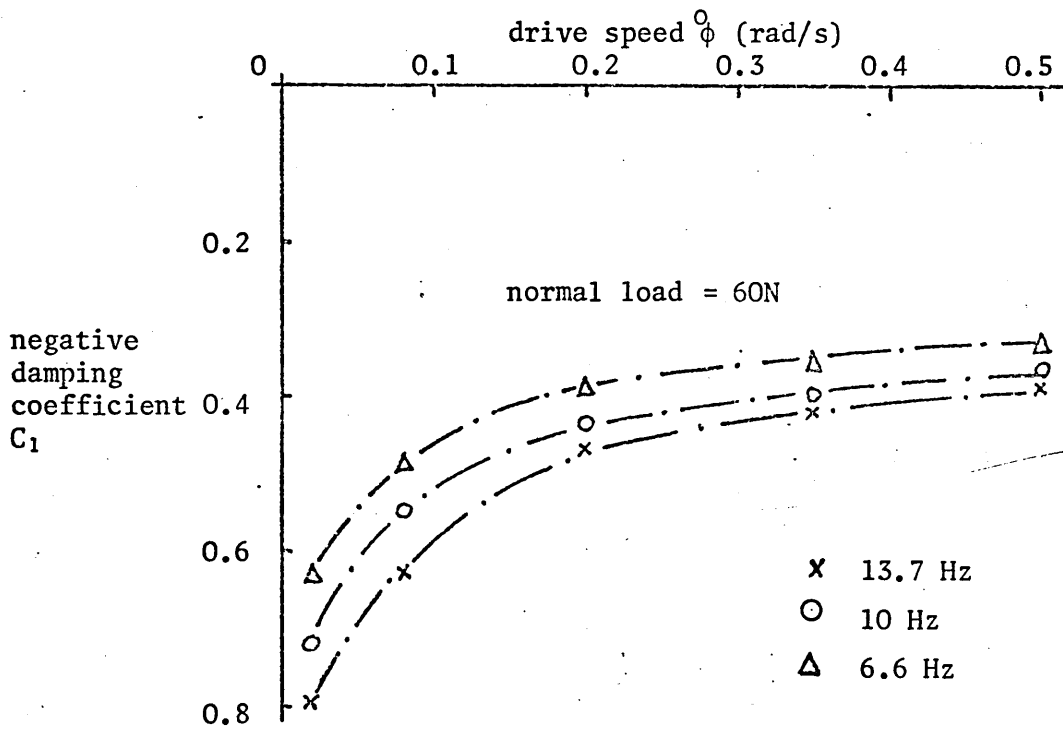
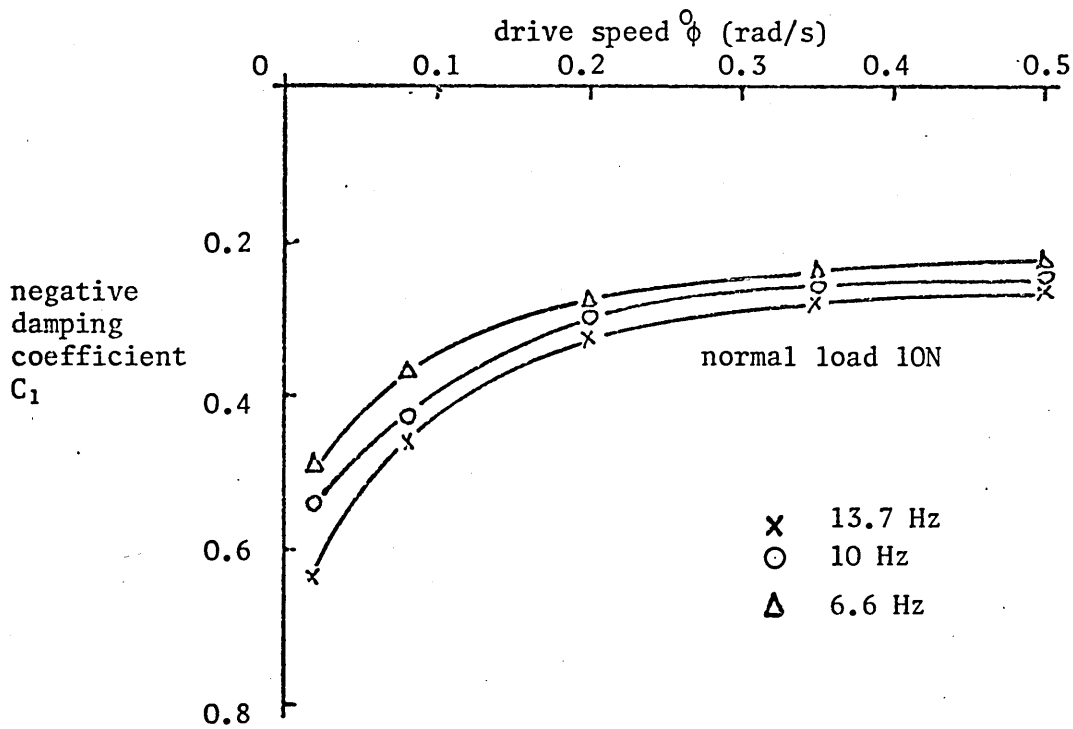


Fig. 4.28 Variation of dry negative damping coefficient with drive speed and system frequency for steel



### 5.1 Introduction

Tests were performed to establish the conditions under which stick slip vibrations are eliminated by the transfer lubricating technique. Transfer lubrication was achieved by allowing one metal piston of the experimental apparatus to be radially loaded on to the disc together with a diametrically opposed transfer lubricant component also loaded radially on to the disc. Motion of the disc brought about wear in the lubricant and caused it to be transferred to the metal interface with consequent modification to the frictional properties of the arrangement. Typical u.v. recorder traces demonstrating the reduction in vibration amplitude due to transfer lubrication techniques are shown in fig. 5.1.

The tests were performed for variations in system frequency, normal load, drive speed, surface finish and metal/lubricant combinations. Figs. 5.2, 3 and 4 illustrate in tabular form those combinations successful in causing the elimination of stick-slip vibrations or the minimum vibration amplitude obtained, expressed as a fraction of the maximum amplitude in any test.

Measurements were also taken of metal and lubricant dynamic friction characteristics, time taken to eliminate vibration and in selected cases the volumetric wear of the transfer lubricant compacts.

Prior to commencement of the tests both pistons were run-in on a dummy disc, providing a metal piston area of  $35 \times 10^{-6} \text{m}^2$  and a lubricant piston area of  $55 \times 10^{-6} \text{m}^2$ .

## 5.2 Dynamic Friction Characteristics

To examine the mechanism of transfer lubrication in terms of the theory suggested in chapter 2 it was necessary to have a measure of the metal to metal dynamic friction characteristic being continuously modified by the transferred lubricant, together with the viscous damping action of the transfer lubricant on the disc. This was achieved by periodically removing the transfer lubricant and measuring the metal to metal dynamic friction characteristic as originally outlined for dry stick slip (chapter 4). Oscilloscope photographs of such characteristics are shown in fig. 5.5 confirming the shape of the characteristic to be similar to that for dry sliding. Thus the proposed mechanism of negative damping metal to metal characteristic modified by transferred lubricant is seen to be acceptable. Although modified dynamic friction metal to metal characteristics were obtained simultaneously with the transfer lubricant dynamic characteristics, the latter will be presented and discussed separately.

## 5.3 Friction Components of Transfer Lubricants

### 5.3.1 Introduction

At the same time as the modified 'metal to metal' characteristic was obtained, it was also necessary to acquire the dynamic

characteristic of the transfer lubricant acting on the disc. An attempt was made to do this by measuring dynamic friction force with the transfer lubricant piston only, acting on the moving disc. U.v. traces indicated no reduction from static friction level to a lower kinetic friction level. Hence a dynamic friction model for the dry lubricant made up of coulomb and positive viscous components of frictional resistance is seen to be reasonable, but the assessment of lubricant dynamic friction characteristic is impossible using this technique. Using the method suggested by Kennedy (20) and outlined in section 2.5 the friction components were obtained by subjecting the system to an initial displacement and measuring the amplitudes of free vibrations of the disc under the influence of the transfer lubricant. By applying the procedures outlined in chapter 2 the coulomb and viscous values of friction were then determined. U.v. traces shown typically in fig. 5.6 and 7 were used to obtain the amplitude response curves required to calculate friction components.

Fig. 5.8 shows two such amplitude response curves plotted in log-linear form for graphite on cast iron(S.F.II) for system frequency of 10Hz, and normal loads of 20N and 36N. Constant values are added to each successive amplitude until a straight line is obtained on the graph. The coulomb and viscous friction components are then calculated as shown in fig. 5.9. Results obtained from direct measurements as described above provide a check on the coulomb friction levels. The above procedures were repeated at the same time as the metal to metal tests during

the transition phase from vibratory to smooth sliding. Little evidence of variation in the lubricant friction components with time was observed throughout the duration of the tests. Tables of typical results are given in appendix II.

### 5.3.2 Variation of Transfer Lubricant Friction Components with System Parameters

Using the above techniques, values of coulomb and viscous frictional resistance were obtained for a selection of lubricants and various system parameters. Since no variation in lubricant friction was observed with time then the results are given as a function of system frequency, normal load and material combinations. Initially surface finish II was used for all metal and lubricant combinations. For those combinations successful in eliminating stick-slip (steel/ptfe and graphite/C1) tests were extended to include surface finishes I and III; for those un-successful (steel/graphite and C1/ptfe) only surface finish II was utilised. From the results shown in figs.5.10 to 17, it can be seen that for all cases, both viscous and coulomb friction torques increase with increasing normal load. The maximum value of normal load for which experimental results could be obtained was that which would allow free vibrations and hence amplitude measurements. In addition, it can be seen that in all cases surface finish II produces the highest value of viscous resistance. Viscous damping coefficient can be seen to be reasonably independent of system frequency for the three frequencies used, as is the coulomb damping level.

It was felt desirable to perform some comparative check on these results although precise data was not found in a literature search. The coulomb friction torque values for ptfе/steel were converted to friction coefficients and plotted against normal pressure to allow direct comparison with results by O'Rourke (28) for the variation of steady state static coefficient of friction with normal pressure. No precise details of surface finish were given by O'Rourke except that the surface was highly polished. It can be seen that the shapes of all the curves are comparable, with a reduction of coefficient of friction from 0.3 at 0.05 MN/m<sup>2</sup> to a reasonably constant value at 0.2 MN/m<sup>2</sup> (fig. 5.18). O'Rourke's results suggest this value to be 0.09 to 0.1 compared with 0.1 to 0.13 for surface finishes I, II and III respectively, obtained by the author. The reduction of coulomb friction with increasing normal pressure for ptfе acting on cast iron is seen to be much less pronounced than for ptfе on steel.

Approximate comparisons can be made between dynamic characteristics and steady state data given by Hemingray (17) and Lewis (25) indicating the variation of coefficient of friction with sliding speed for ptfе acting on steel. Fig.5.19 shows details of these comparisons for a range of speeds relevant to stick slip vibrations, and nominal normal pressure of 0.8 MN/m<sup>2</sup>.

Therefore, the coulomb plus viscous damping model suggested for the dynamic friction characteristic of ptfе on steel compares favourably with the steady state results obtained by Hemingray and Lewis.

Although comparisons are unavailable, results for graphite rubbing on cast iron are presented in a similar form as above (figs. 5.20 and 21). These results indicate a similar trend to those of ptfе on steel, the coefficient of friction reducing with increasing pressure and increasing with increasing sliding speed.

## 5.4 Comparison of Experimental Results with Stability Theories

### 5.4.1 Introduction

By inspection of the theoretical graphs of chapter 2 it can be seen that the influence of viscous damping on the unlubricated friction characteristic has little significance in modifying the frequency of vibrations. In the case of the negative damping coefficient, for high friction gradient values an increase in slip frequency is predicted, for low friction gradient values a reduction in slip frequency is anticipated. For values of  $C_1$  around 0.4 to 0.5 little or no variation in slip frequency can be expected. Since these values of  $C_1$  occur regularly in the experimental apparatus then slip frequency is not a satisfactory parameter to confirm the damping action of the transfer lubricant in the elimination of stick slip motion.

Transfer lubricated stick slip results are thus presented on the basis of the stability relationships developed in chapter 2 utilising the viscous damping values presented in section 5.3. Tables of results are given in Appendix III.

#### 5.4.2 Stability Relationships

Combinations of metal to metal dynamic friction characteristics continuously modified by the transferred lubricant, together with the corresponding external viscous damping coefficient supplied by the transfer lubricant are presented on stability graphs, figs. 5.22 to 33. Results which induced stability and those which did not are presented and the identification of each type is available from the tables in figs. 5.2, 3 and 4.

As mentioned previously, the viscous damping action of the dry lubricant remained reasonably constant during each test for a particular set of system parameters. Hence the accuracy of the theoretical relationships developed is demonstrated by the proximity to the stability line of those metal to metal characteristics measured immediately prior to the occurrence of smooth sliding

The theoretical relationship developed from the Blok dynamic friction model shows poor correlation with experimental results for all combinations of dry lubricant and metal junctions where stability occurred. In addition, using this method of presentation it is difficult to distinguish between those results successful in eliminating stick slip and those not. This is not true for the negative damping dynamic friction model stability relationship. Results obtained from conditions where smooth sliding occurred compare favourably with the theoretical stability line whilst

those where instability persisted are evidently farther away from the stability line..

For the Blok model relationship, the degree of correlation between theory and experimental results varies considerably depending upon the system parameters. Stability results obtained with high drive velocities have high values of Blok parameter (see fig. 5.22 graphite on cast iron, SF II, 48N normal load, 0.2 rad/s drive speed) and hence show reasonable correlation with theory. However stability conditions for low drive velocity situations (fig. 5.22, graphite on cast iron, SF II, 48 N normal load, 0.08 rad/s drive speed) show large discrepancies between theoretical and experimental values.

This contrasts with the consistency of correlation obtained by plotting the same results in Fig. 5.23 using the negative damping dynamic friction model relationship. The fact that this method of presentation of the results also distinguishes between stable and unstable conditions is demonstrated specifically in figs. 5.22 and 5.23, the ptfе on cast iron results being farther away from the theoretical stability line.

These observations apply generally for the complete series of results shown in fig. 5.22 to 33.

## 5.5 Stick-Slip Elimination Distances and Transfer Lubricant Wear Rates

Measurements were taken to examine the stick-slip elimination point for variations in normal pressure and drive speed. The measurements were taken for graphite on cast iron and ptfе on steel. Results from these tests are shown in figs. 5.34 and 35. plotting normal load against sliding ratio, which is defined as the ratio of total sliding distance to disc circumference. System frequency for the measurements was confined to 6.6Hz and surface finish was varied through 3 values. The results are presented for two drive speeds, in the region where the dynamic gradient was approximately constant i.e. 0.2 rad/s and 0.4 rad/s.

Three significant points emerge from the graphs. Firstly, the elimination of stick slip is a function of sliding distance for those conditions where dynamic gradient is independent of drive speed. Secondly the level of damping exhibited by a material and surface finish combination directly influences stick slip elimination, i.e. the lower the damping level, the longer elimination takes. Thirdly, with increasing normal load the distance required to eliminate stick slip increases. In the case of surface finish I, ptfе on steel, stick slip elimination ceases to occur after 90N normal load ( $2.57 \text{ MN/m}^2$  normal pressure).

Since it was felt that volumetric wear of transferred lubricant would influence the modification of the dry dynamic characteristics, measurements of volumetric wear were taken concurrently with the above measurements for selected tests.

The wear measurements were also extended for a considerable period of time after smooth sliding had been achieved. Obviously the number of tests had to be restricted and surface finish II only was used. Results are shown in figs. 5.36 and 37. As would be anticipated volume wear is independent of drive speed and is directly proportional to normal load. These observations are compatible with the first two observations made previously in connection with the stick slip elimination distance but at first sight do not confirm the third point. Since the metal to metal dynamic gradient increases slightly with increasing normal load then the volume of transferred lubricant necessary to modify the dynamic gradient would be expected to be larger. But transferred lubricant volume wear is directly proportional to normal load and transfer lubricant damping has been shown to increase with normal load. This suggests that stick slip elimination point could reasonably be expected to reduce with increasing normal load. This is not borne out by the experimental results shown in figs. 5.34 and 35 which shows the sliding ratio continuously increasing with normal pressure. One explanation for this effect is the possibility of a limiting normal pressure being reached due to plastic deformation of the surface asperities at the metal interface. This then effectively denies access of the transferred lubricant to the dry friction junction and increases the stick slip elimination point.

Tests were also conducted for a differential loading situation, and the results are shown in figs. 5.38 and 5.39. The ratio of metal to lubricant normal load is plotted against

the inverse of sliding ratio as an indication of the limiting load levels which might exist. For both ptfе on steel and cast iron on graphite the loading ratio increases with decreasing normal load levels. Definite limits of stick slip elimination are seen to exist for both material combinations, the graphite on cast iron providing the highest value of 1.75 compared with 1.5 for ptfе on steel. Expressing these conditions in terms of nominal pressures gives limiting pressure levels of  $2.75 \text{ MN/m}^2$  and  $2.48 \text{ MN/m}^2$  for the cast iron and steel junctions respectively.

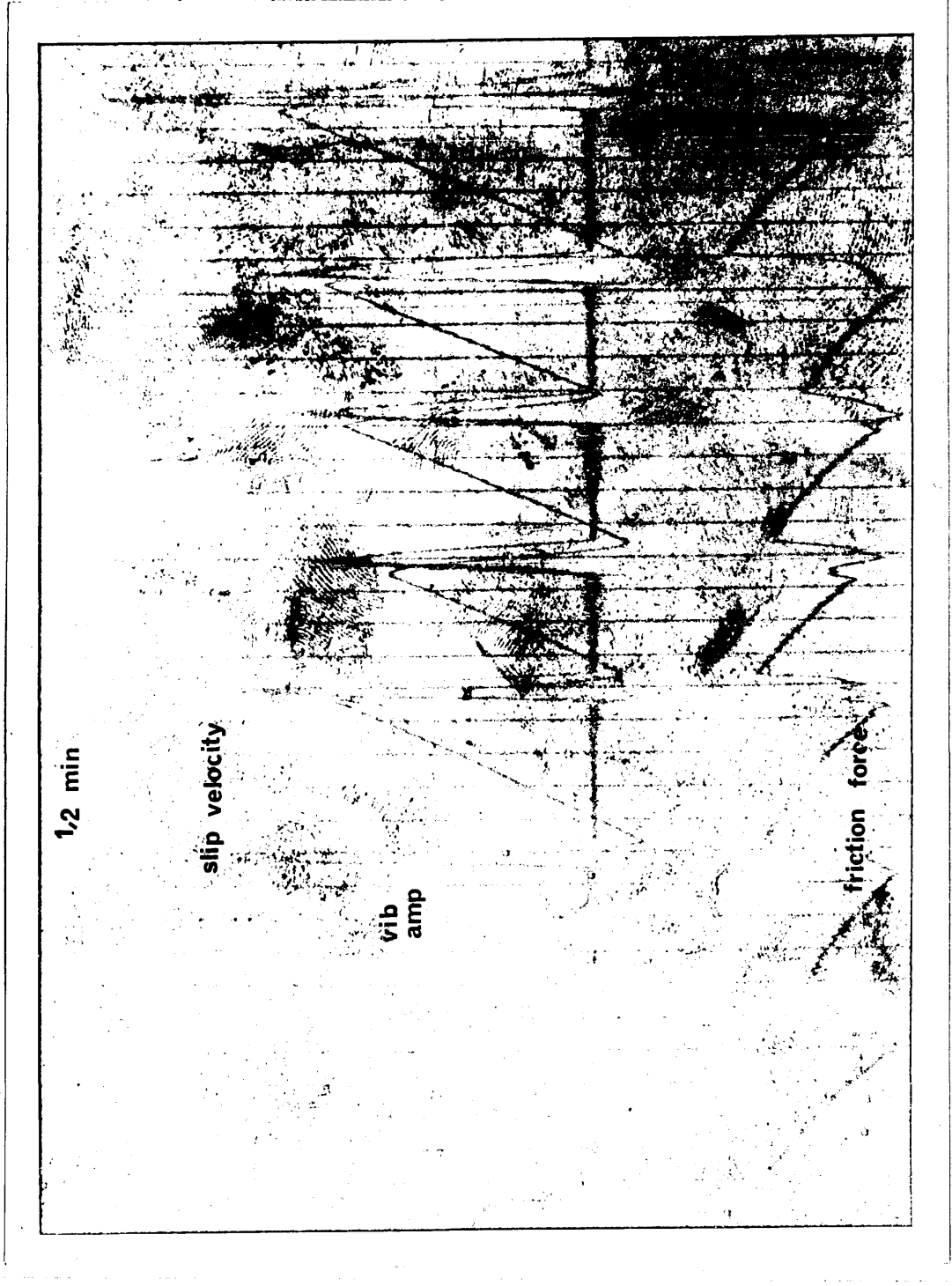
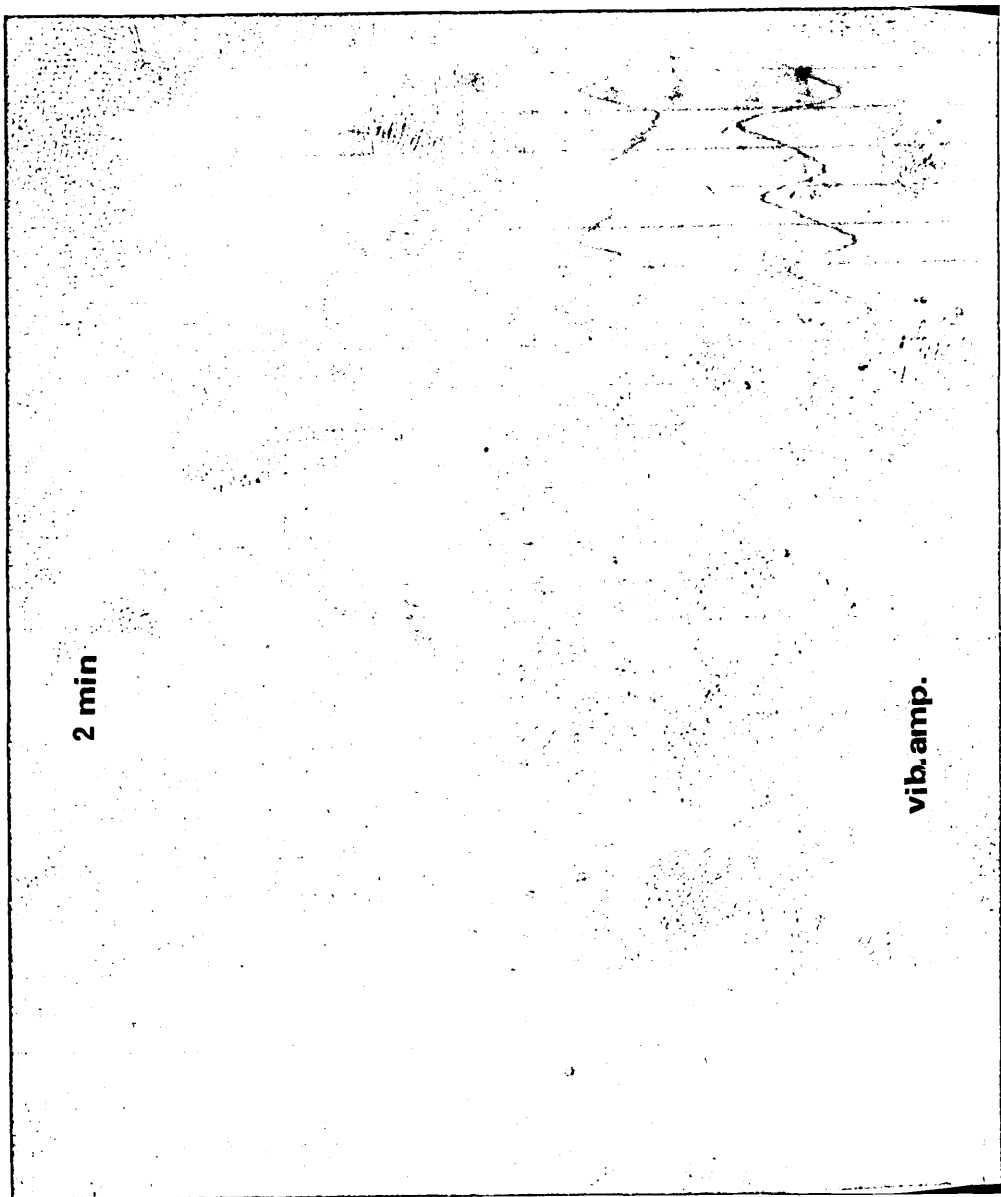
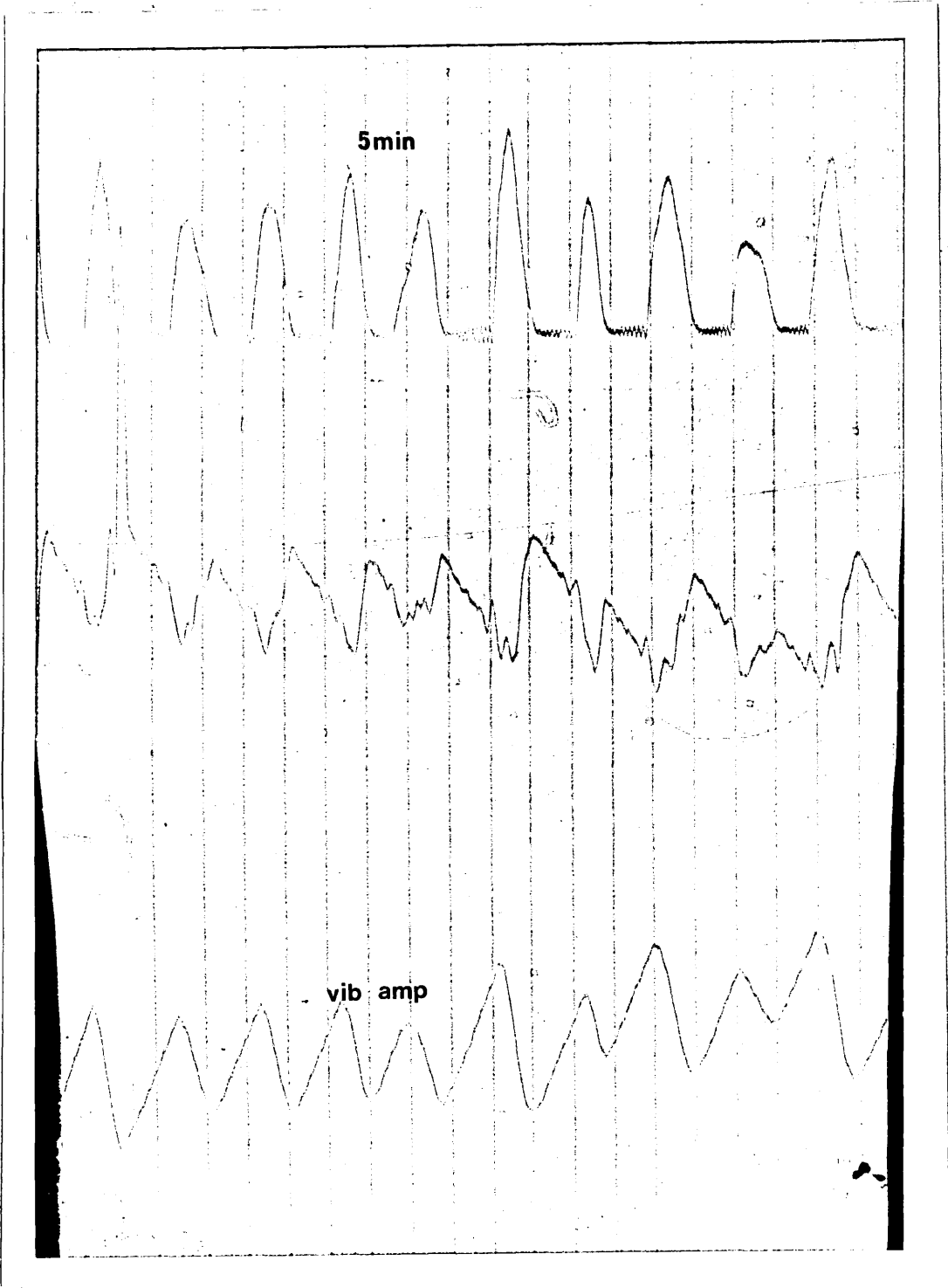


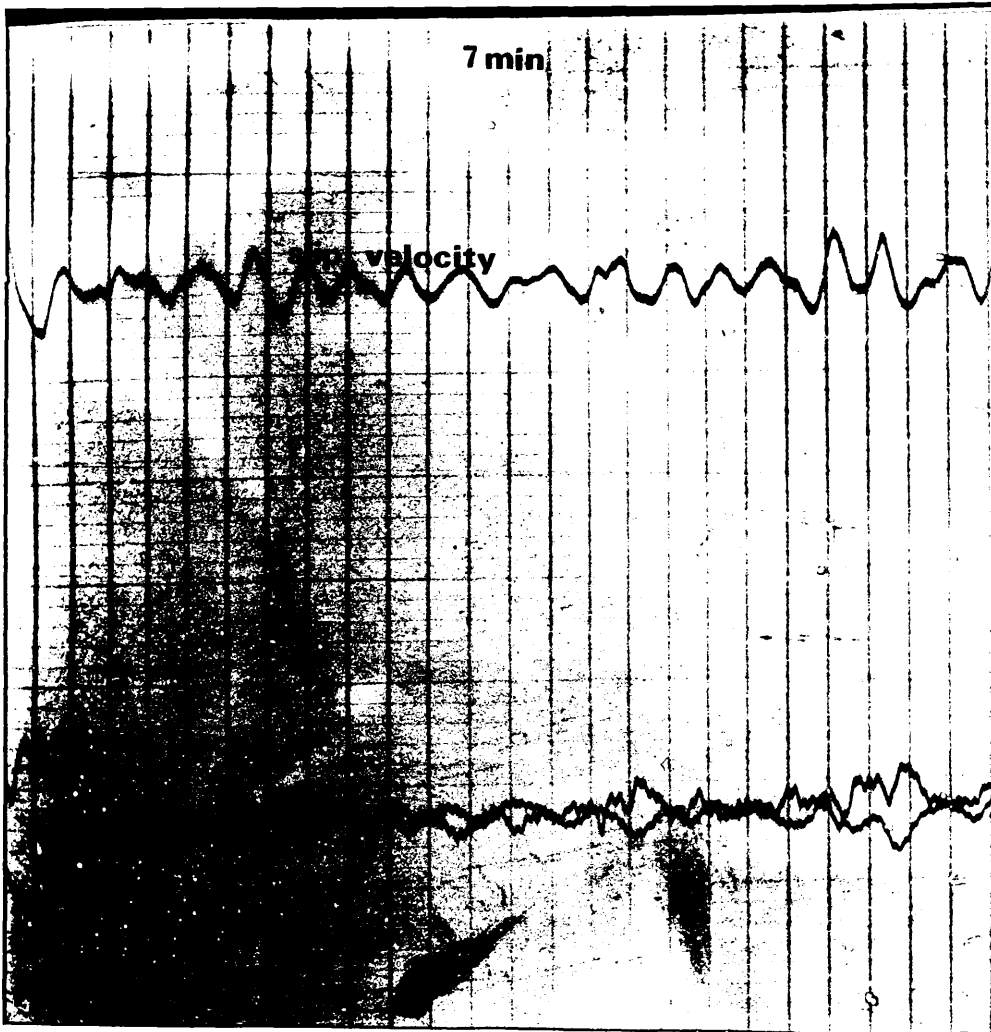
Fig.5.1. Reduction of stick slip due to transfer lubrication ptfe on steel 150N normal load SF II 0.08 rad/s drive speed



2 min

vib. amp.







SYSTEM FREQUENCY	SURFACE FINISH	6N			16N			24N			36N			48N			56N			90N			120N			150N														
		A	B	C	A	B	C	A	B	C	A	B	C	A	B	C	A	B	C	A	B	C	A	B	C															
		NORMAL LOAD			NORMAL LOAD			NORMAL LOAD			NORMAL LOAD			NORMAL LOAD			NORMAL LOAD			NORMAL LOAD			NORMAL LOAD			NORMAL LOAD														
6.6 Hz	I	X			X			X			X			X			X			X			X			X			0.33											
	II	X			X			X			X			X			X			X			X			X			X											
	III	X			X			X			X			X			X			X			X			X			X											
10 Hz	I	X			X			X			X			X			X			X			X			X			0.44			0.52			0.68					
	II	X			X			X			X			X			X			X			X			X			X			X								
	III	X			X			X			X			X			X			X			X			X			X			X								
13.7 Hz	I	X			X			X			X			X			X			X			X			X			X			0.45			0.54			0.63		
	II	X			X			X			X			X			X			X			X			X			X			X			X					
	III	X			X			X			X			X			X			X			X			X			X			X			X					

Fig. 5.3 Transfer lubricated tabular results for ptfе on steel

A = 0.08 rad/s drive speed  
 B = 0.2 rad/s drive speed  
 C = 0.4 rad/s drive speed

X = elimination of stick  
 numbers indicate ratio of minimum to maximum stick slip amplitude during tests

GRAPHITE ON STEEL

SYSTEM FREQUENCY	SURFACE FINISH	10N			24N			32N			40N			48N			120N			150N		
		A	B	C	A	B	C	A	B	C	A	B	C	A	B	C	A	B	C	A	B	C
6.6	II	X	0.68	0.57	0.72			0.68			0.48			X	0.33					0.38		
10		X	0.74		0.54		0.57	X	0.59	0.53					0.28					0.42		
13.7		X	0.53		0.48	X	0.52		0.66						0.22					0.31		

PTFE ON CAST IRON

SYSTEM FREQUENCY	SURFACE FINISH	10N			24N			32N			40N			48N			52N			120N			150N		
		A	B	C	A	B	C	A	B	C	A	B	C	A	B	C	A	B	C	A	B	C			
6.6	II	X	0.75		0.81		0.65			0.47	X			0.62					0.43						
10		X	0.83	X	0.8		0.6		0.54	X	0.64				0.48				0.35						
13.7		X	0.81	X	0.75		0.54		0.71		0.61				0.62				0.33						

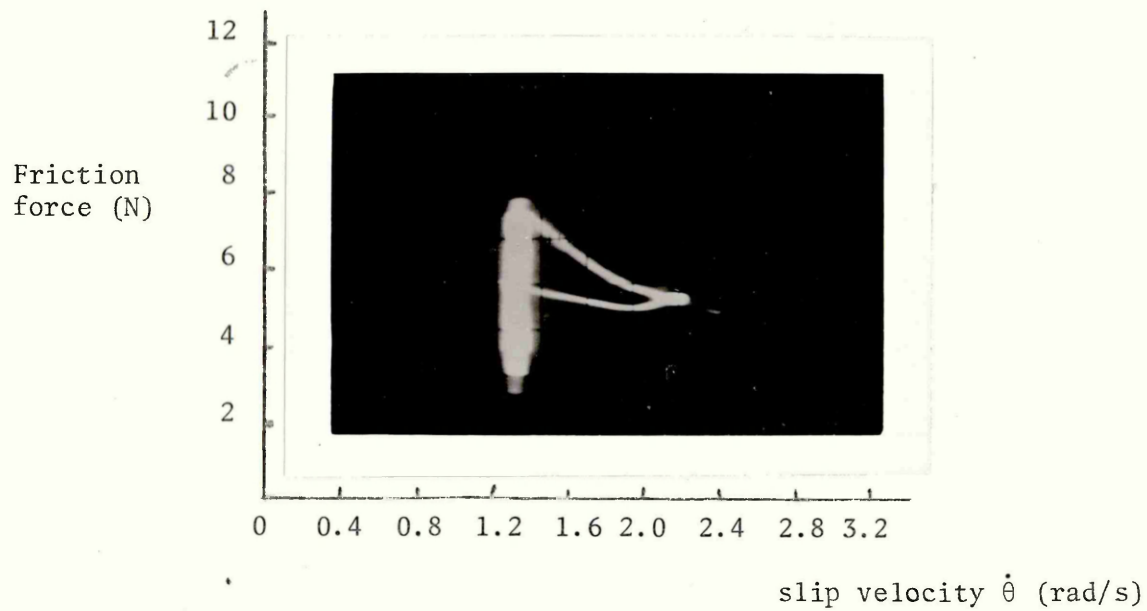
Fig. 5.4 Transfer lubricated tabular results for ptfе on cast iron and graphite on steel

X = elimination of stick slip

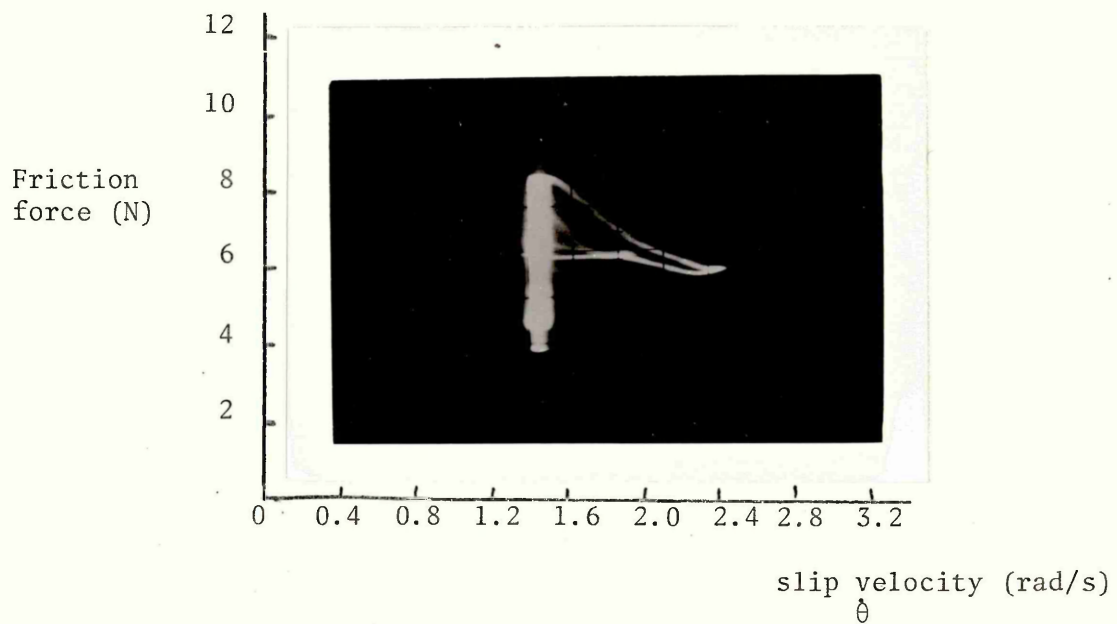
number refers to ratio of minimum to maximum stick slip amplitude during test

A = 0.08 rad/s drive speed  
 B = 0.2 rad/s drive speed  
 C = 0.4 rad/s drive speed

Fig 5.5 (a) Typical dynamic friction characteristics for transfer lubricated stick slip.

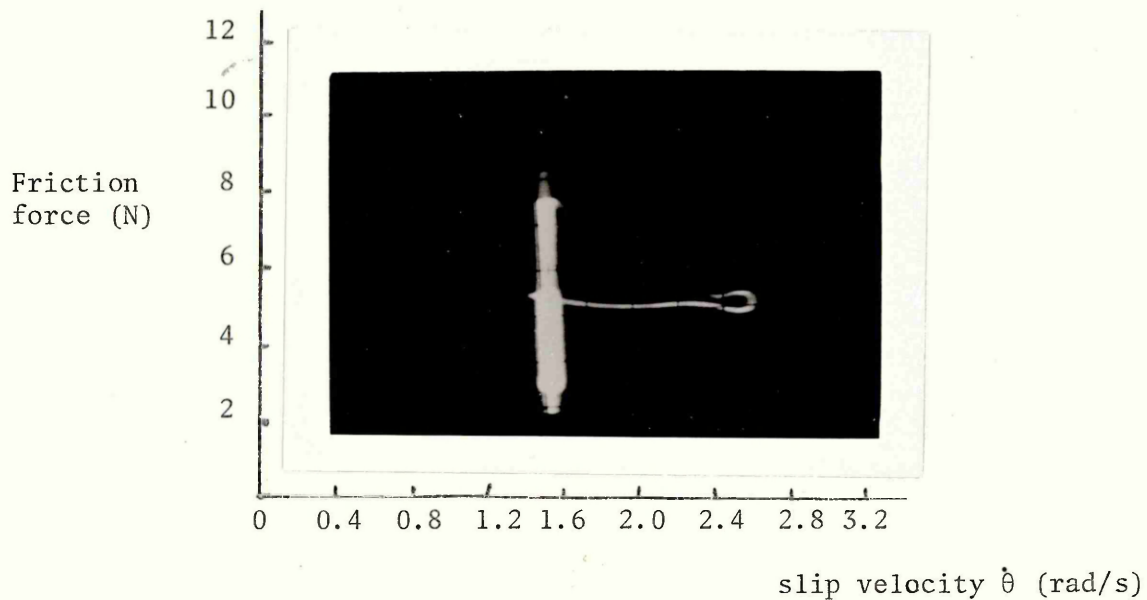


(i) Graphite on cast iron, 48N normal load, 13.7 Hz frequency, 0.08 rad/s drive speed, SF II.

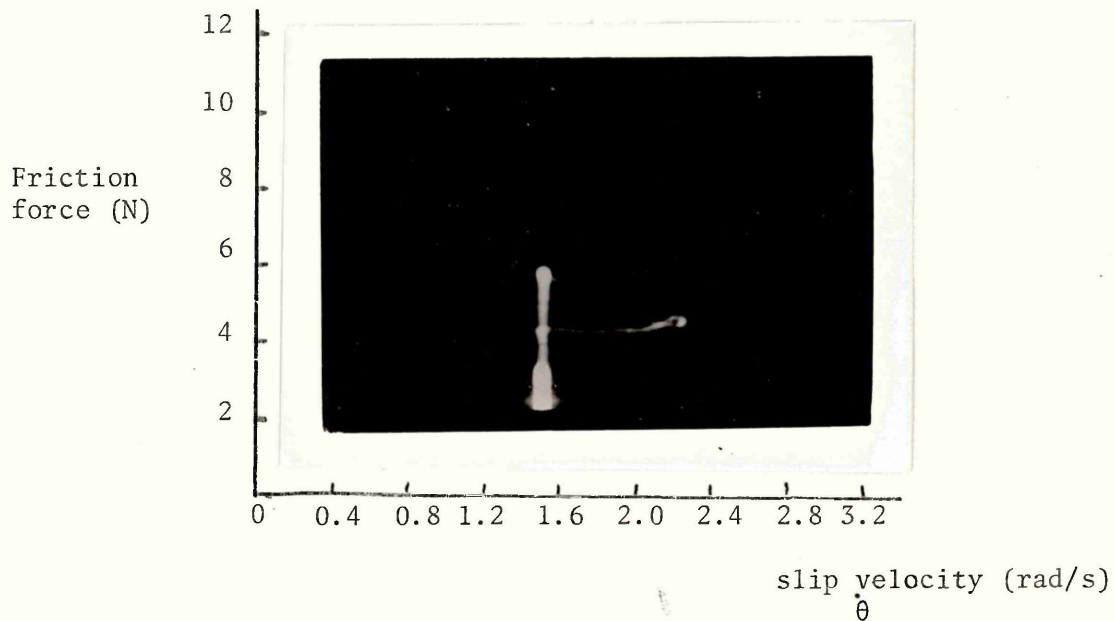


(ii) Graphite on cast iron, 48N normal load, 6.6 Hz frequency, 0.2 rad/s drive speed, SF I.

Fig 5.5 (b) Typical dynamic friction characteristics for transfer lubricated stick slip.



(i) PTFE on steel, 56N normal load, 13.7 Hz frequency, 0.08 rad/s drive speed, SF II.



(ii) PTFE on steel, 36N normal load, 0.2 rad/s drive speed, 10 Hz frequency, SF III.

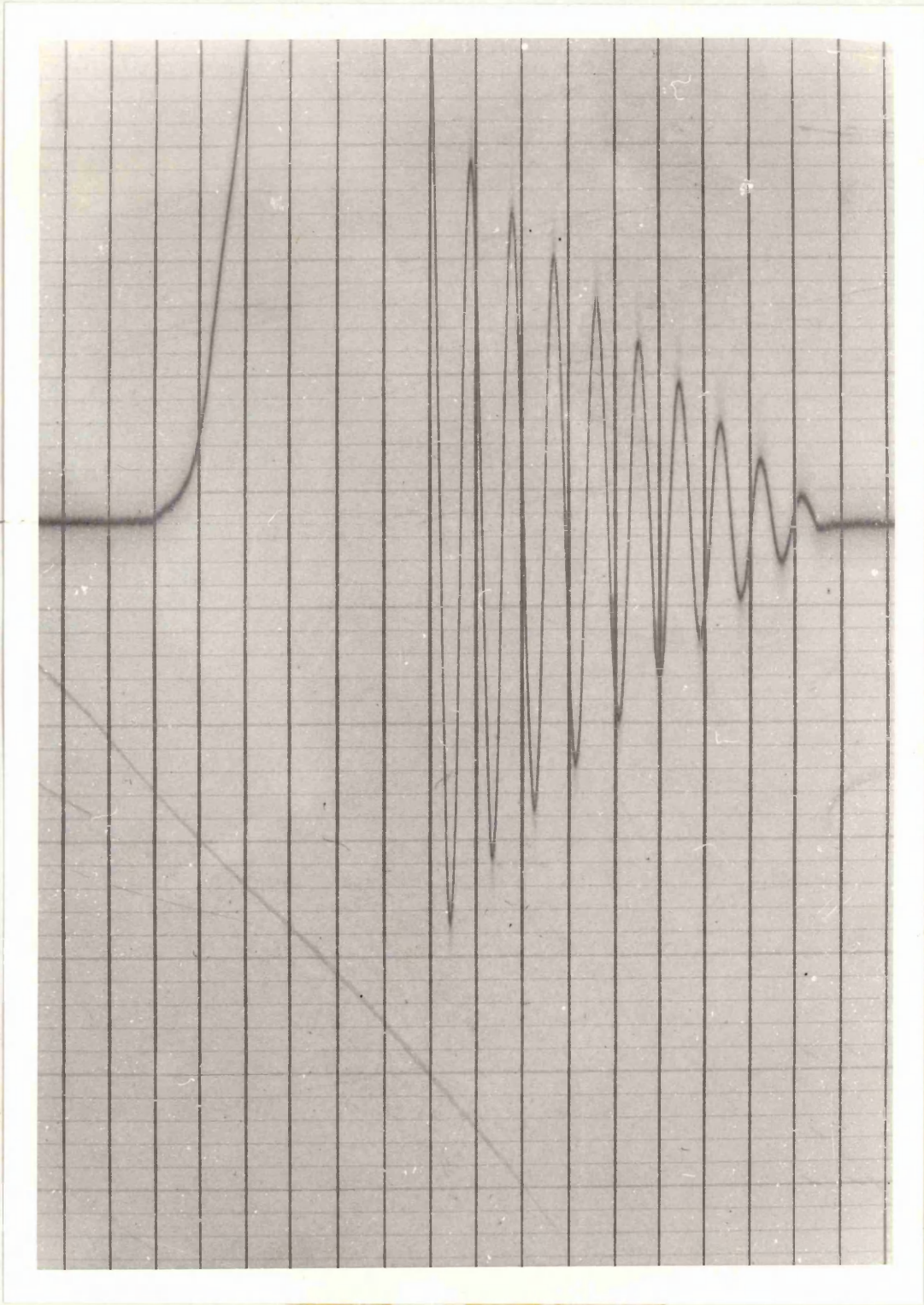


Fig. 5.6 Amplitude response trace for graphite on cast iron 8N normal load, frequency 10 Hz surface finish II

AF5

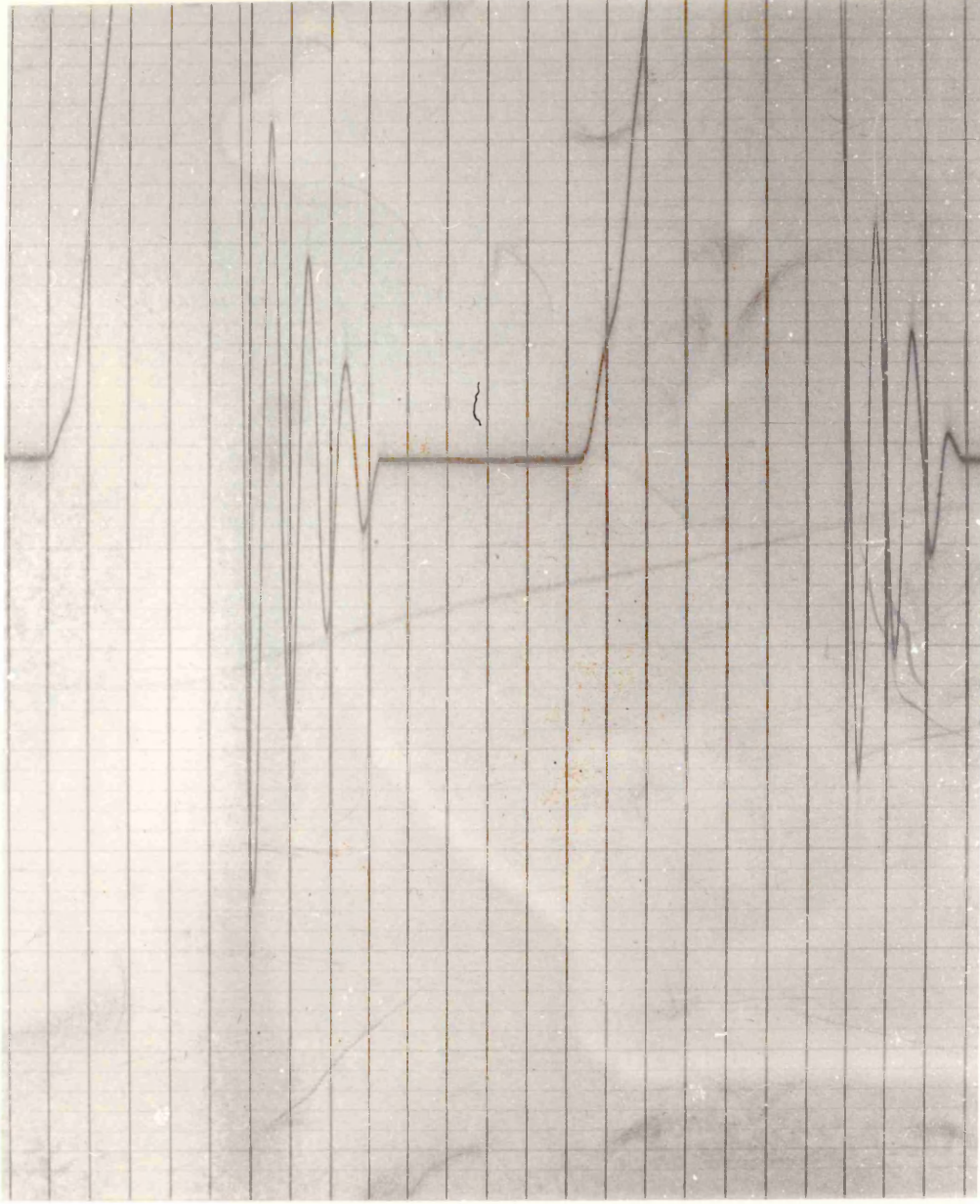


Fig. 5.7 Amplitude response trace for ptfе on steel 16N normal load, 6.6.Hz frequency surface finish II

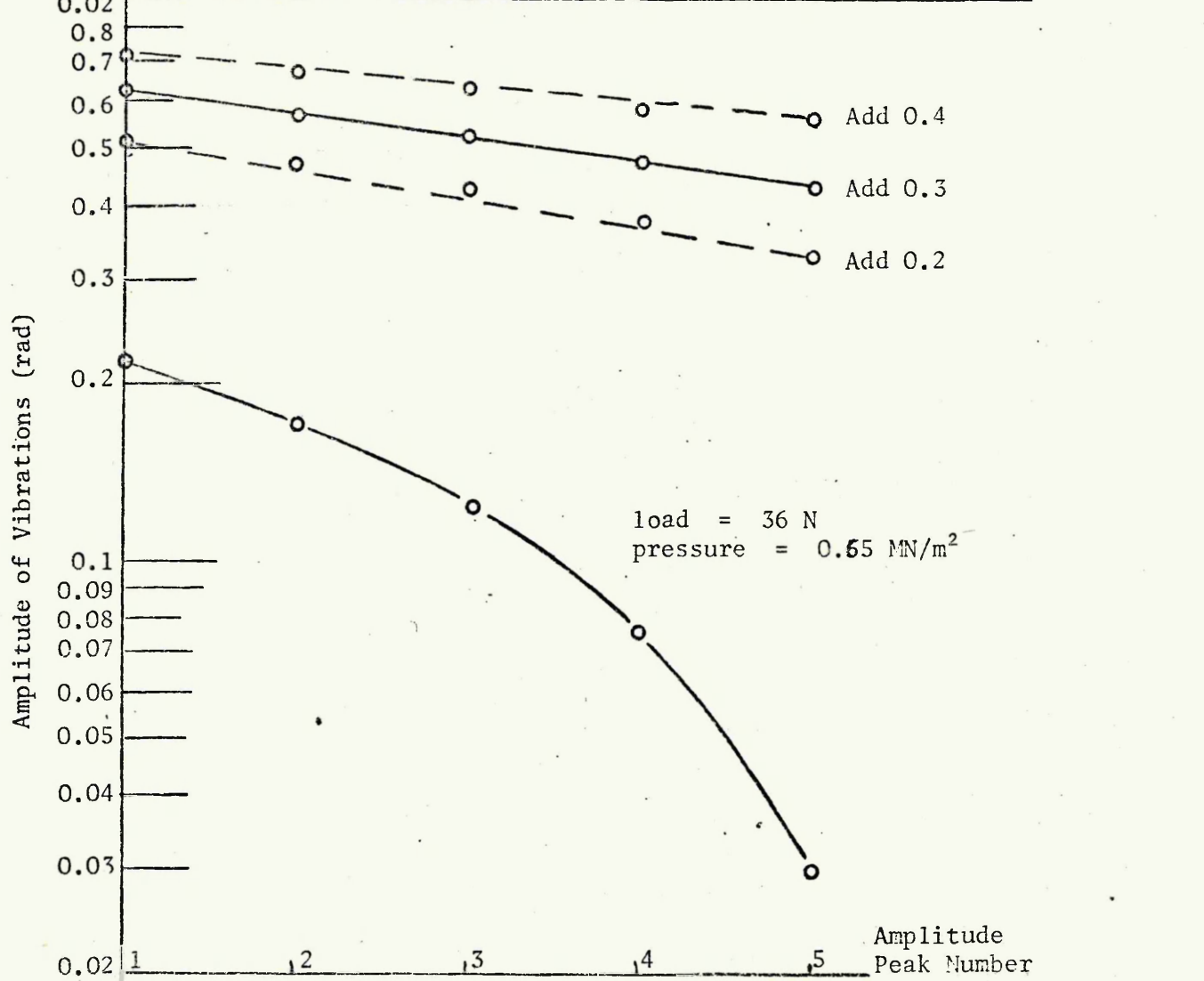
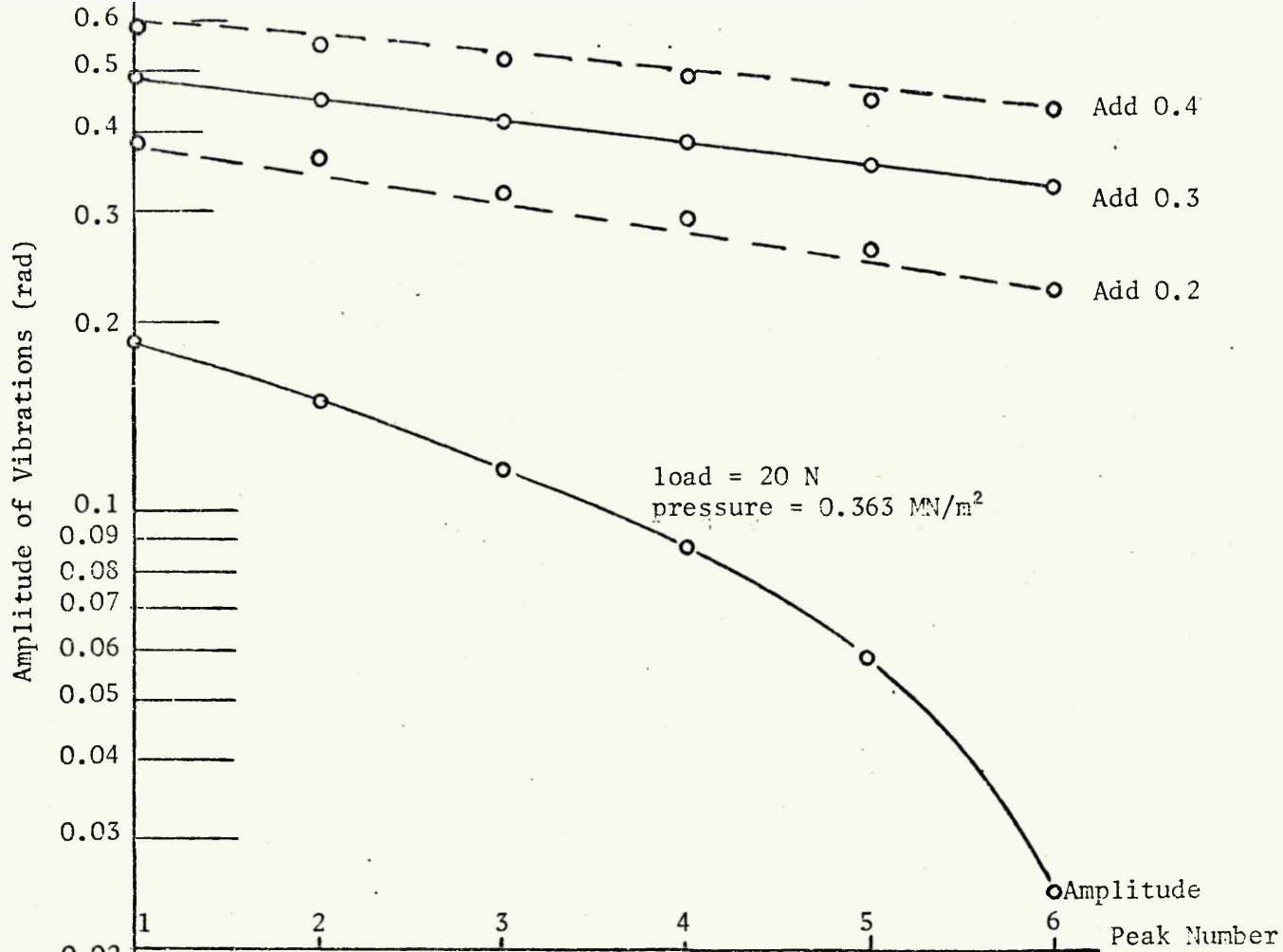


Fig. 5.9 Typical Calculations for Components of Friction of Transfer Lubricant

Graphite on cast iron surface finish II, 16.3 Nm spring stiffness, 0.004 Kgm<sup>2</sup> inertia

Normal Load		Peak Number					
		1	2	3	4	5	6
Actual Amplitude (rad)	20N	0.182	0.144	0.116	0.085	0.059	0.025
Modified Amplitude (rad)		0.482	0.444	0.316	0.385	0.359	0.325
Actual Amplitude (rad)	36N	0.212	0.165	0.121	0.077	0.03	
Modified Amplitude (rad)		0.512	0.465	0.421	0.377	0.33	

20N Load Case

From equation (12) Chapter 3

$$\frac{\theta_1}{\theta_n} = e^{(n-1)\frac{\mu\pi}{w}} = \frac{0.482}{0.325} = 1.483$$

$$\therefore \text{viscous damping component, } C = \frac{0.392 \times 4 \times 10.3 \times 0.004}{5} = \underline{0.011\text{Nm/rad/s}}$$

Also

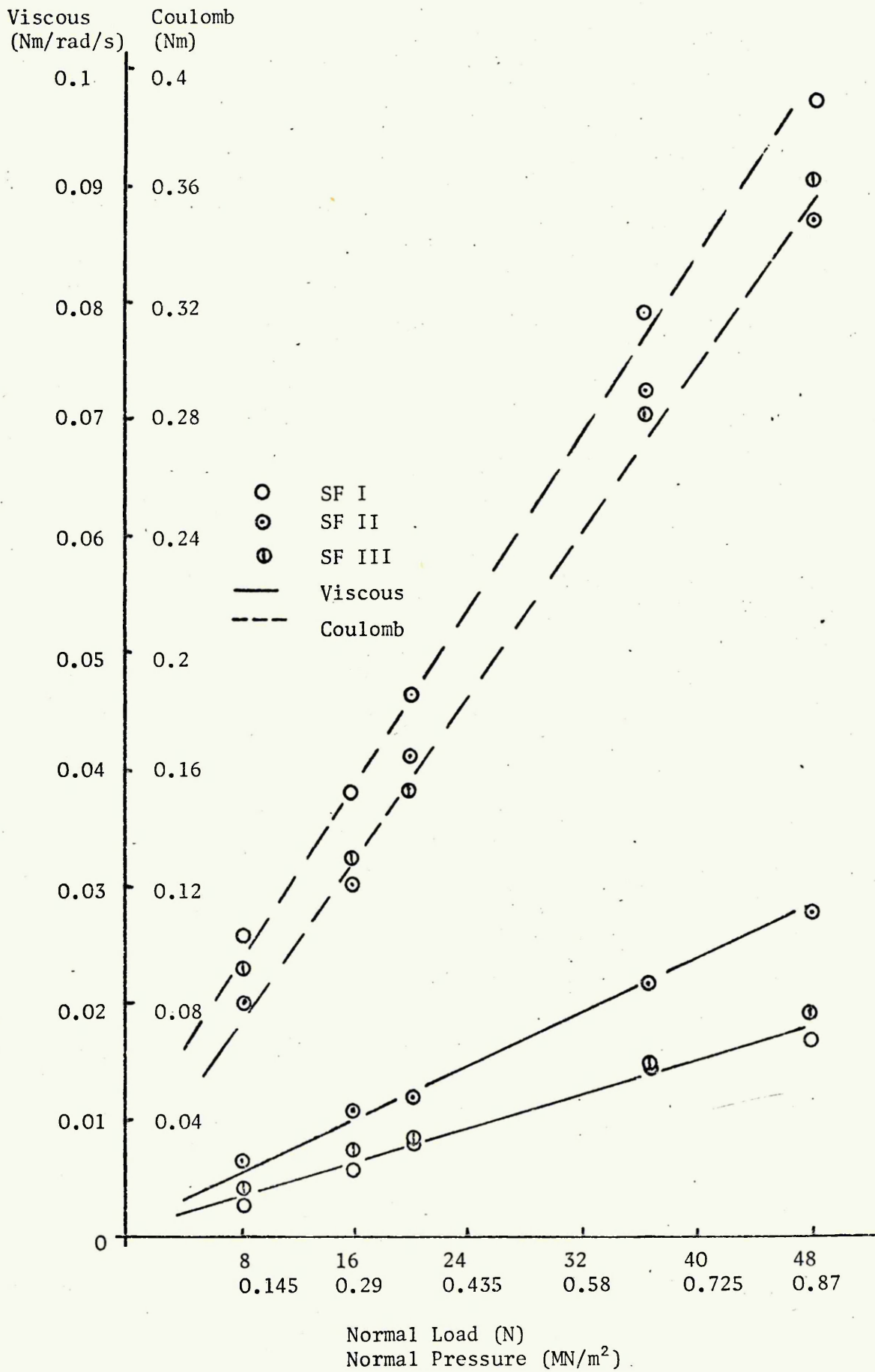
$$\frac{T}{K} \left[ \frac{1 + e^{-\frac{\mu\pi}{w}}}{1 + e^{\frac{\mu\pi}{w}}} \right] = 0.3$$

$$\therefore T = \frac{0.3 \times 16.3 \times 0.075}{1.925} = \underline{0.19\text{Nm}}$$

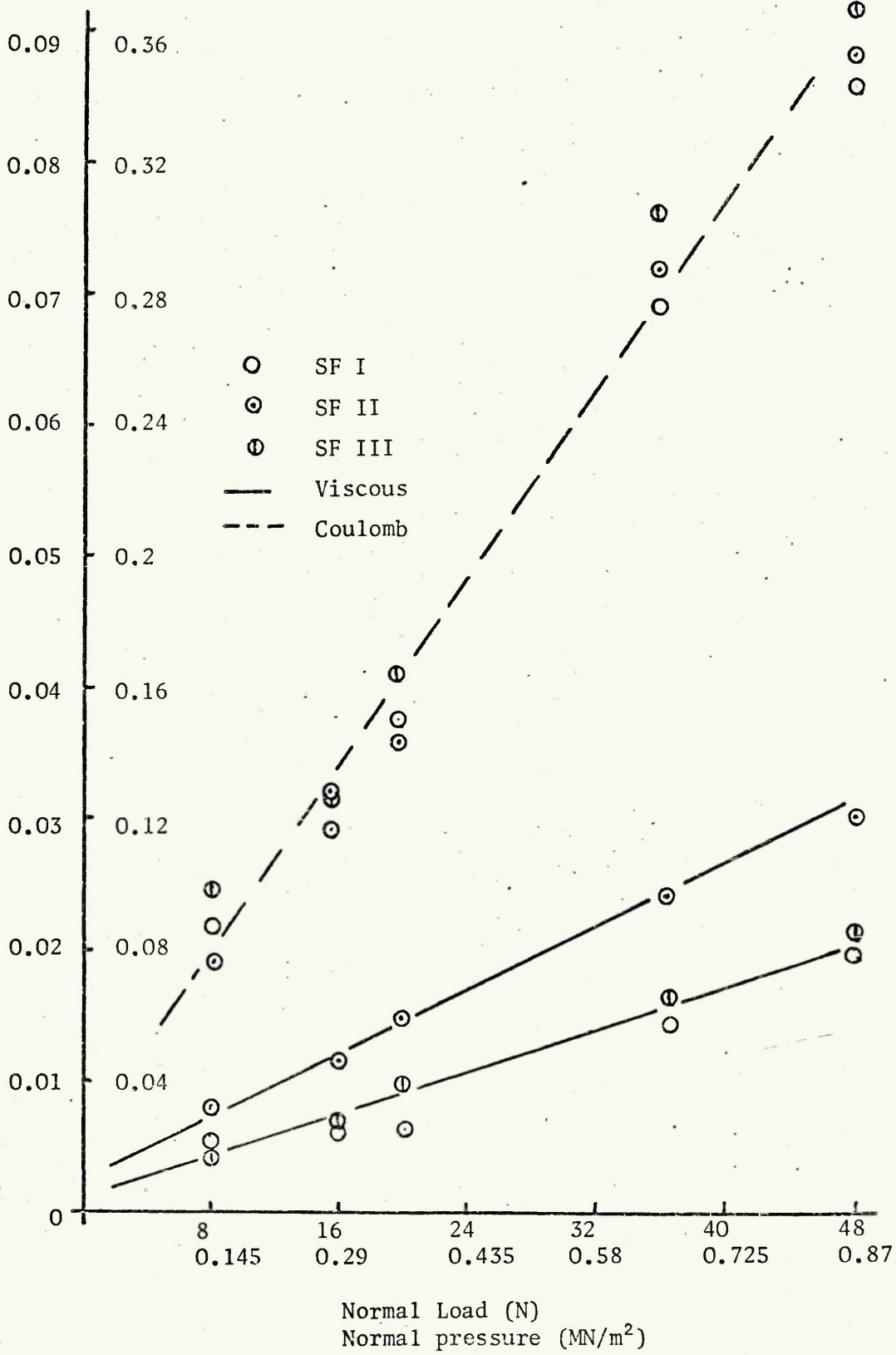
Applying similar procedures for 36N load case -  $C = \underline{0.013\text{Nm/rad/s}}$

$$T = \underline{0.25\text{Nm}}$$

Dynamic friction characteristics of graphite on cast iron - system  
frequency 6.6 Hz



Viscous (Nm/rad/s)      Coulomb (Nm)



Viscous  
(Nm/rad/s)

Coulomb  
(Nm)

0.09

0.36

0.08

0.32

0.07

0.28

0.06

0.24

0.05

0.20

0.04

0.16

0.03

0.12

0.02

0.08

0.01

0.04

0

8

0.145

16

0.29

24

0.435

32

0.58

40

0.725

48

0.87

- SF I
- ⊙ SF II
- ⊖ SF III
- Viscous
- - - Coulomb

Normal Load (N)  
Normal Pressure (MN/m<sup>2</sup>)

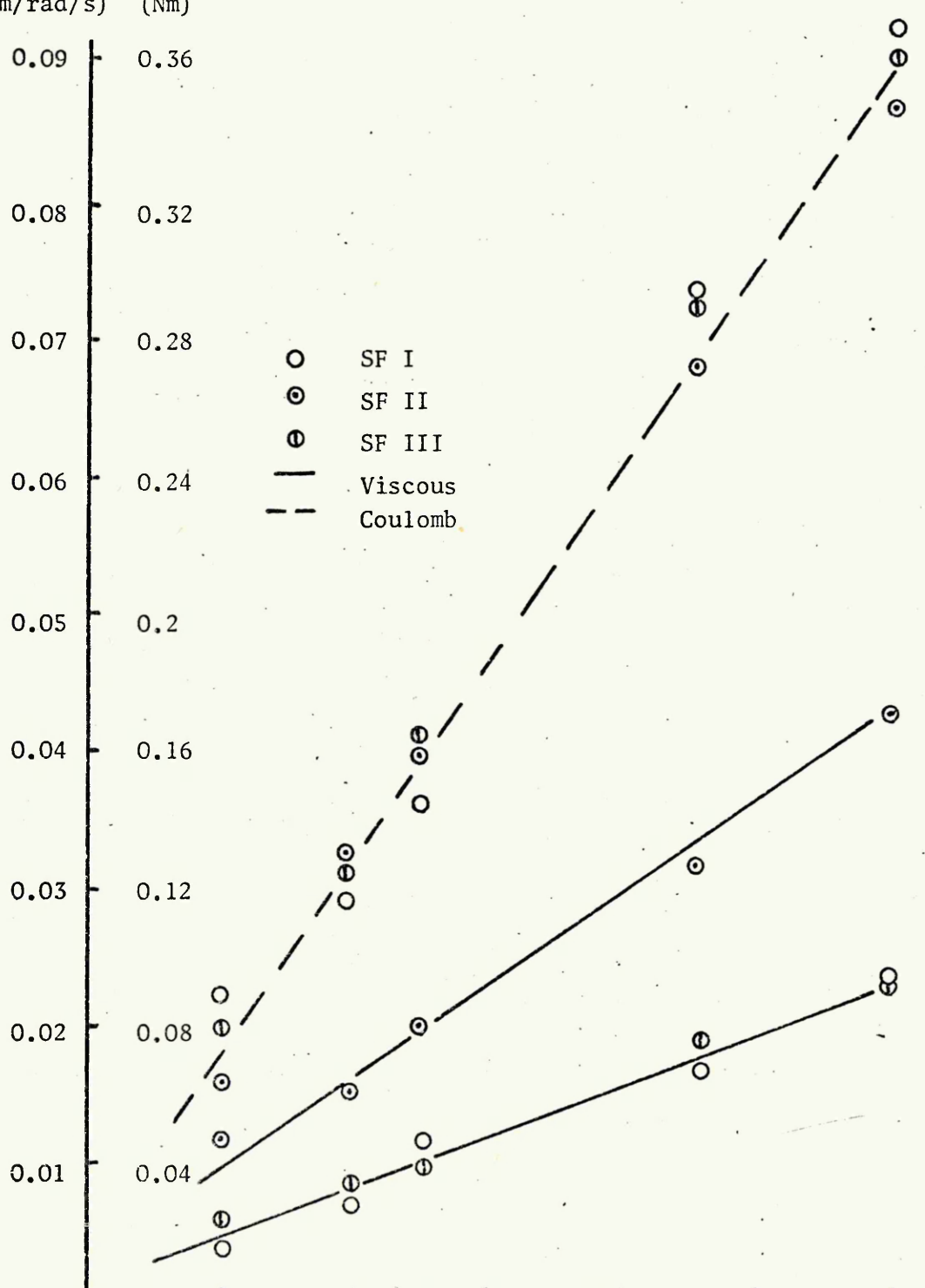
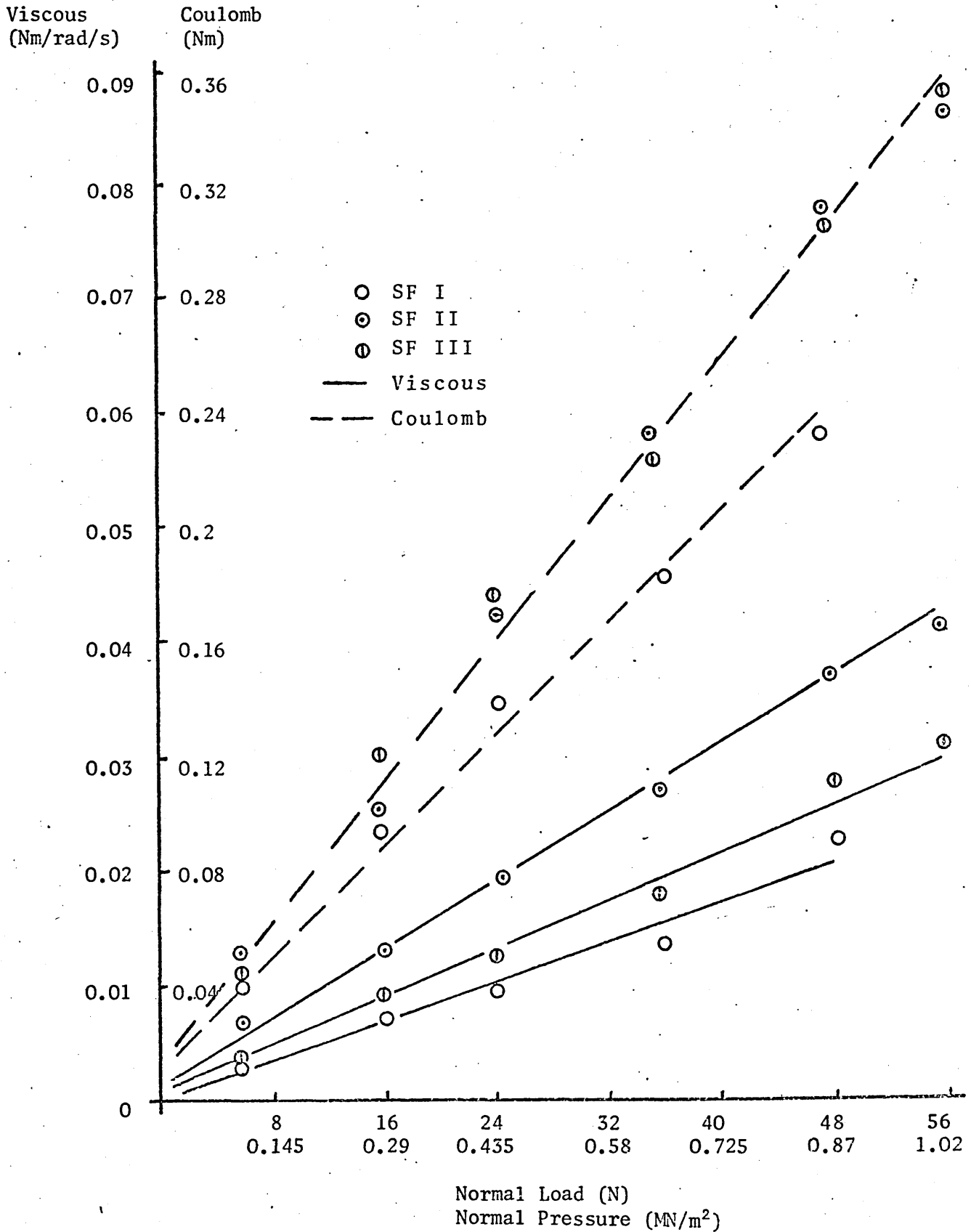
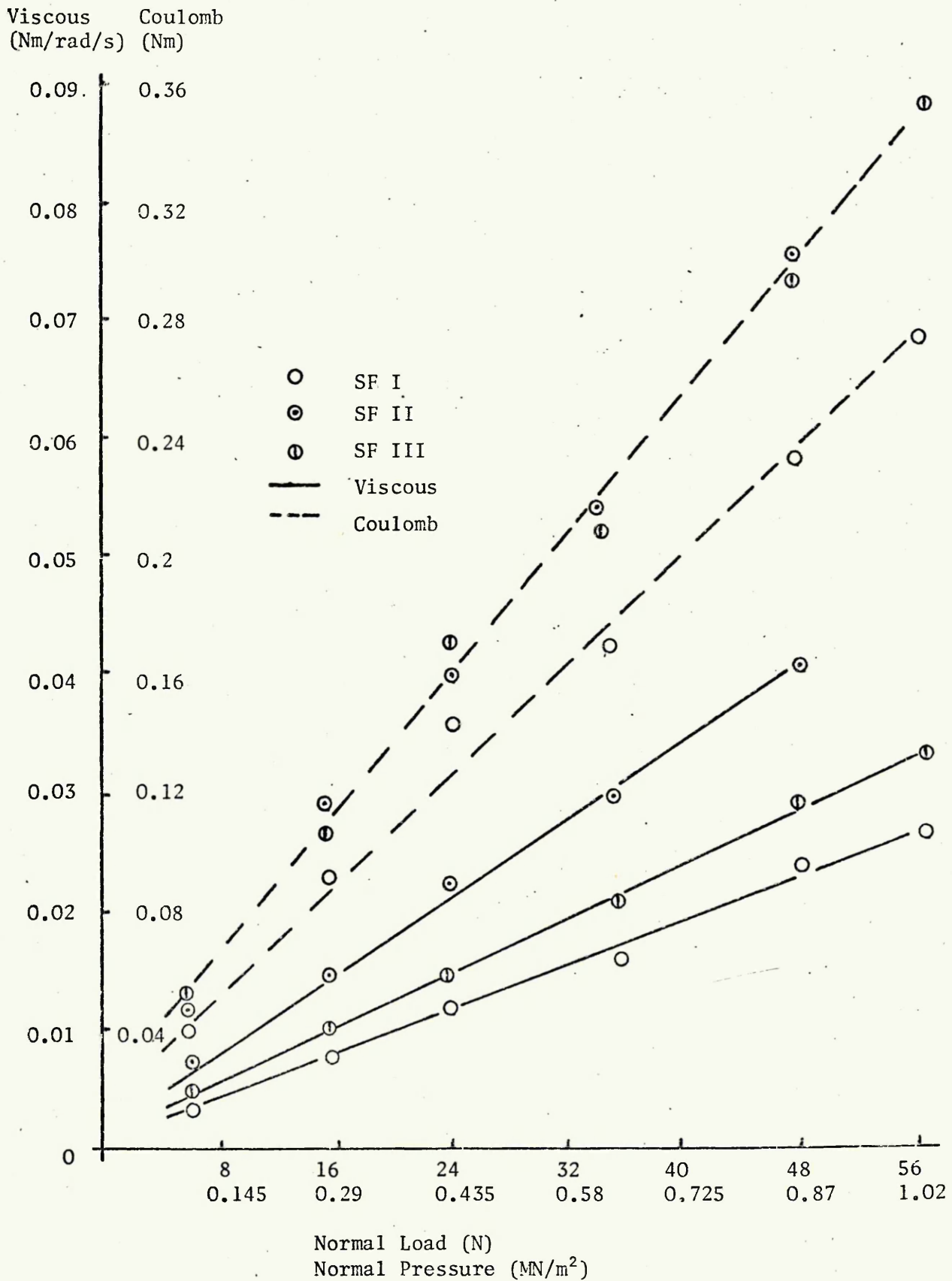


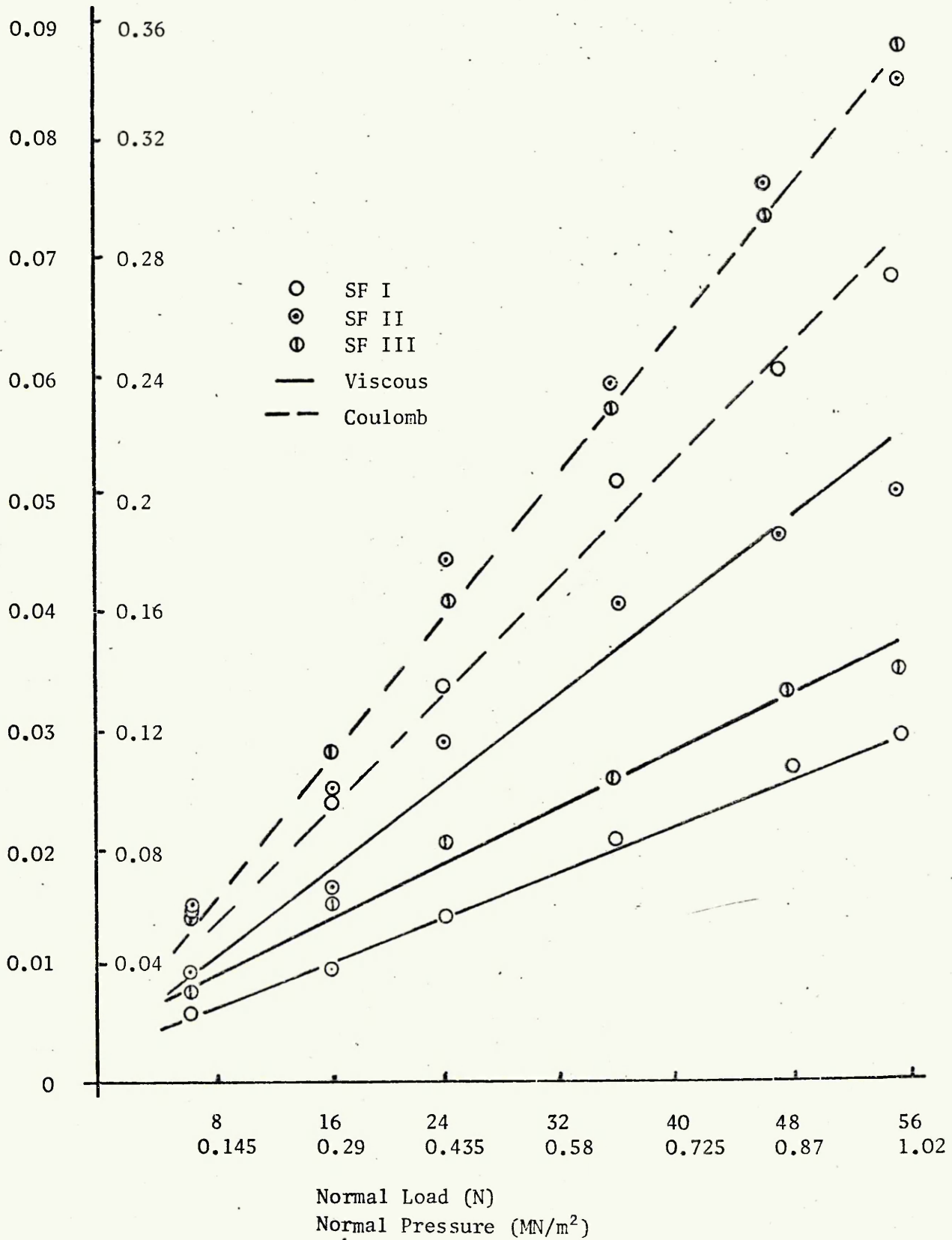
Fig. 5.13

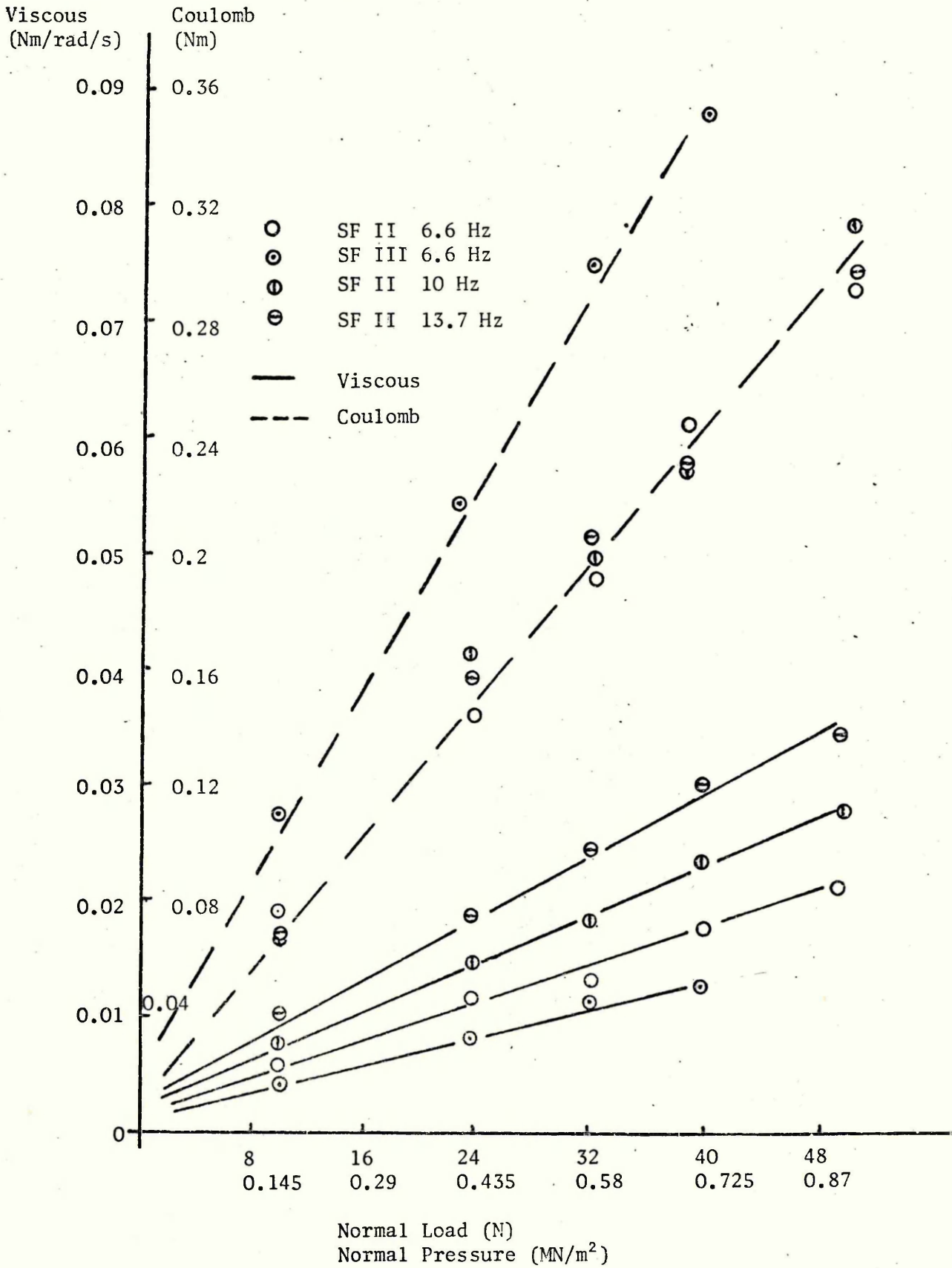
Dynamic Characteristics of PTFE on mild steel - system frequency 6.6 Hz





Viscous (Nm/rad/s)      Coulomb (Nm)





Dynamic Characteristics of PTFE on cast iron for all system frequencies

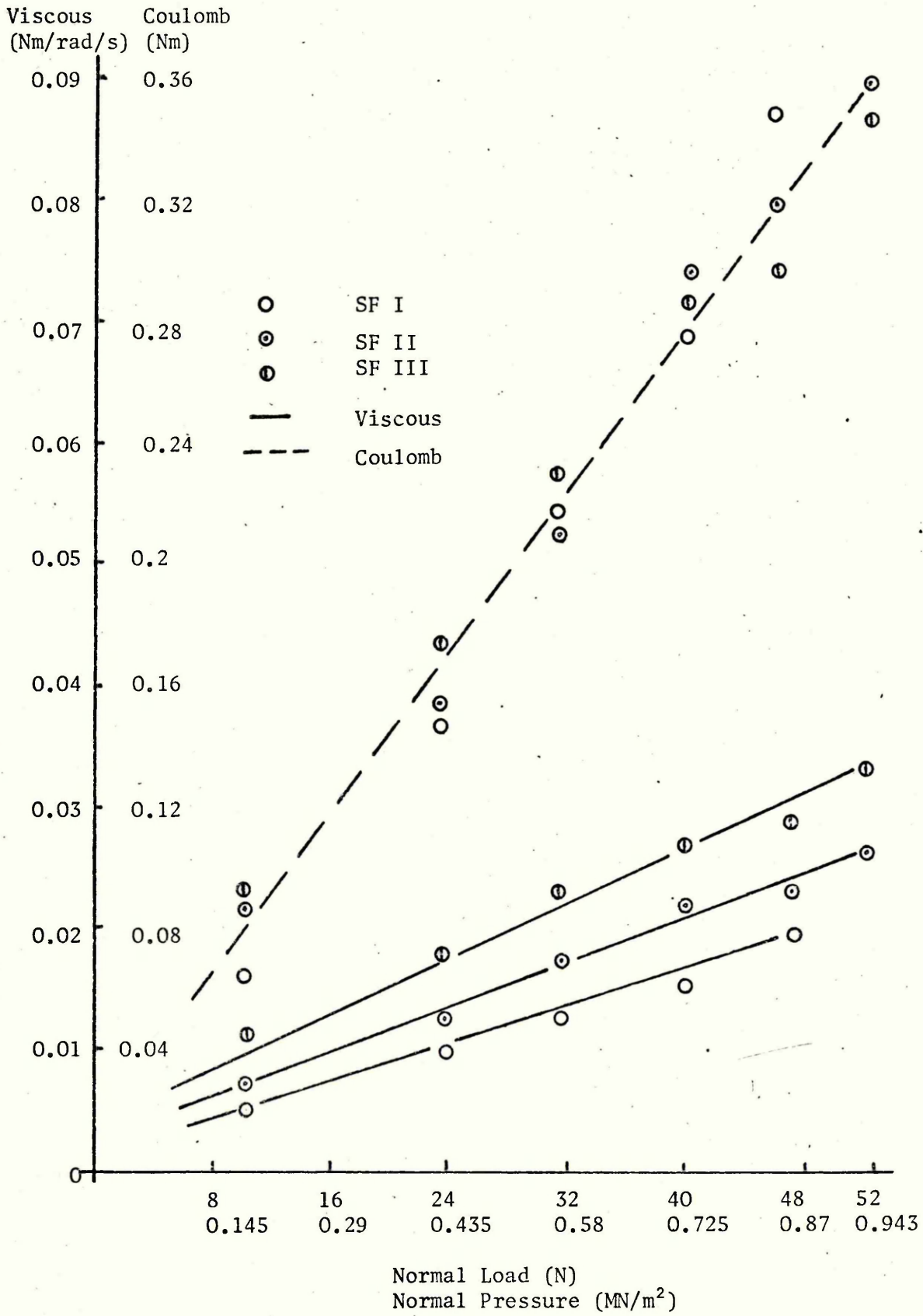


Fig. 5.18 Variation with normal pressure of dynamic friction coefficient at zero velocity for PTFE, 6.6 Hz.

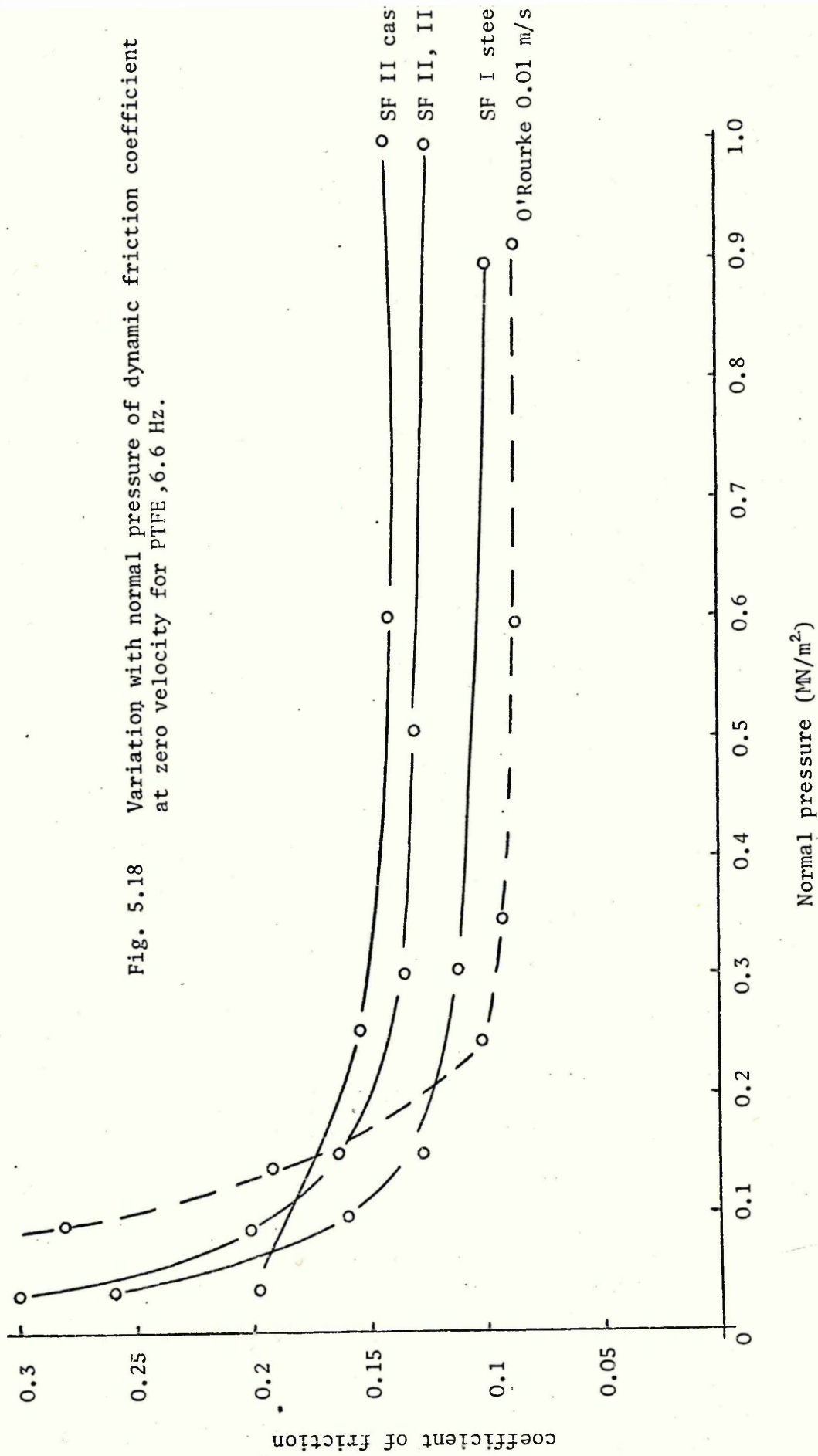


Fig. 5.19 Variation of dynamic coefficient of friction with sliding velocity for PTFE on steel 0.8MN/m<sup>2</sup> normal pressure system frequency 6.6Hz.

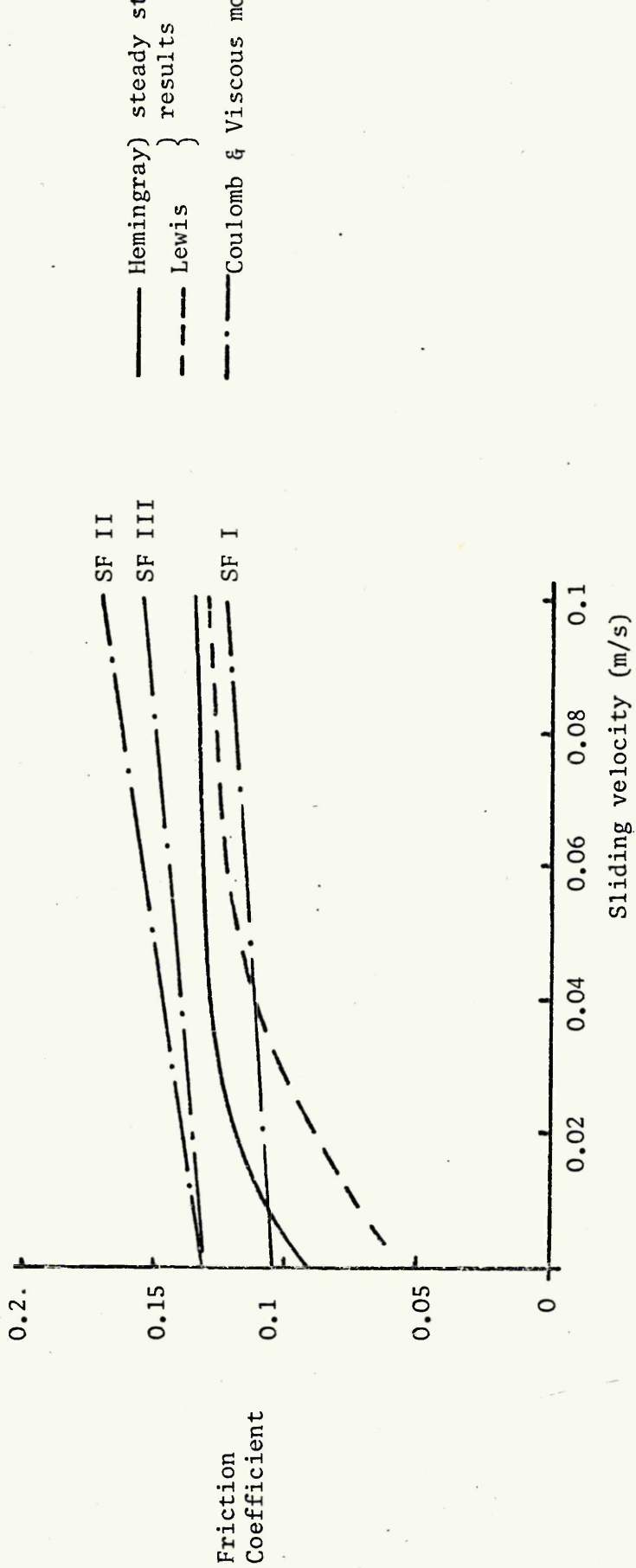


Fig. 5.20 Variation of dynamic friction coefficient with normal pressure for graphite, at zero sliding velocity, 6.6 Hz frequency.

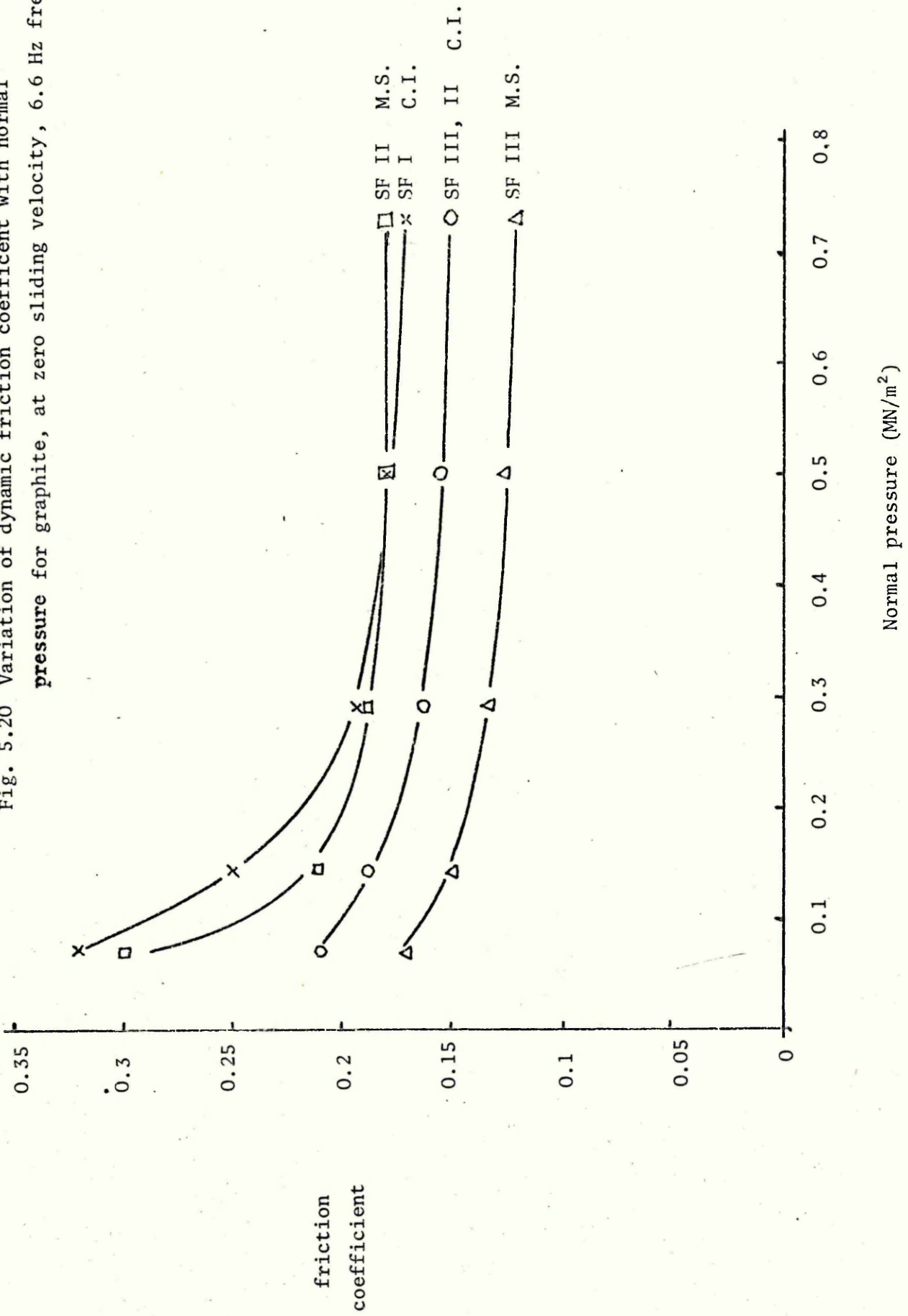
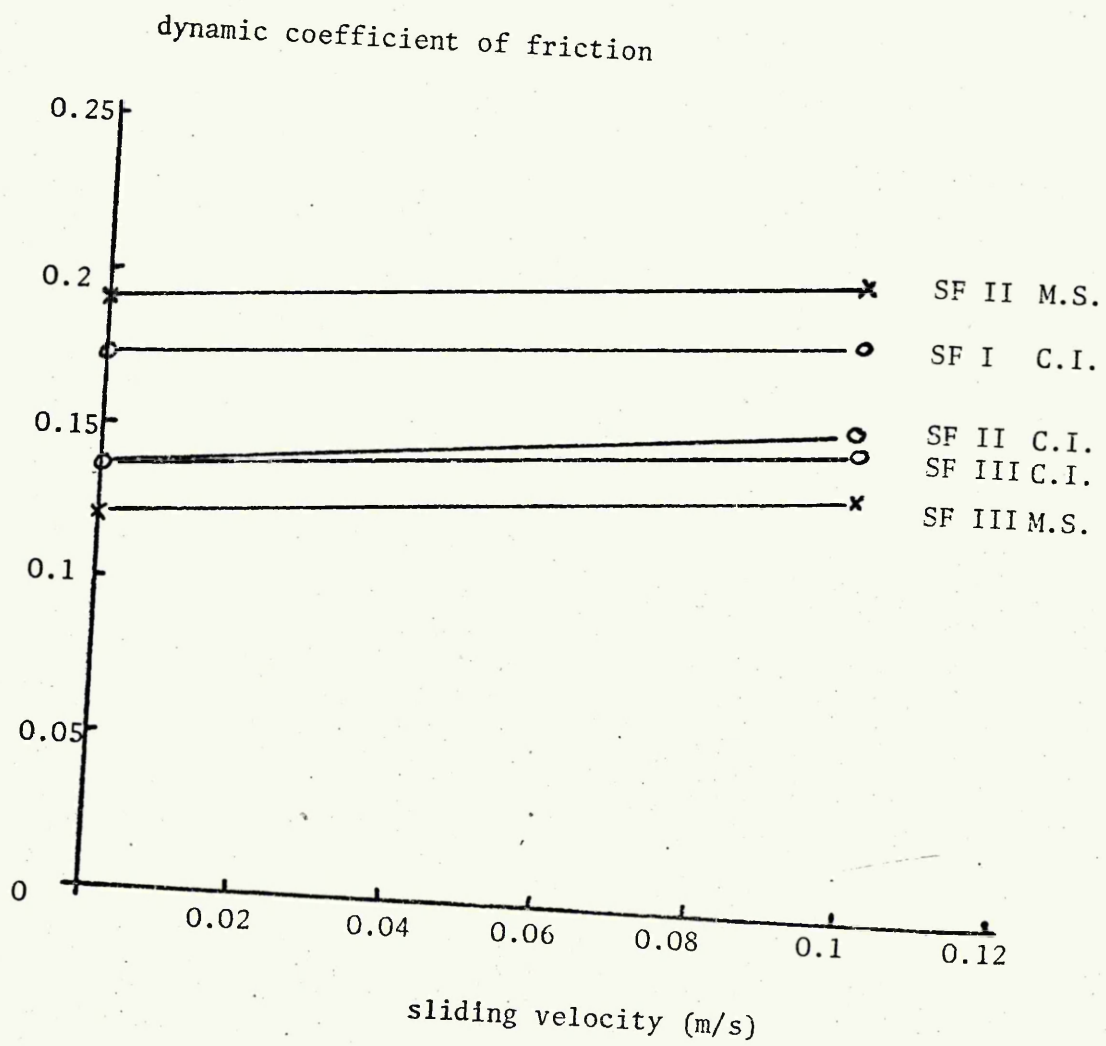
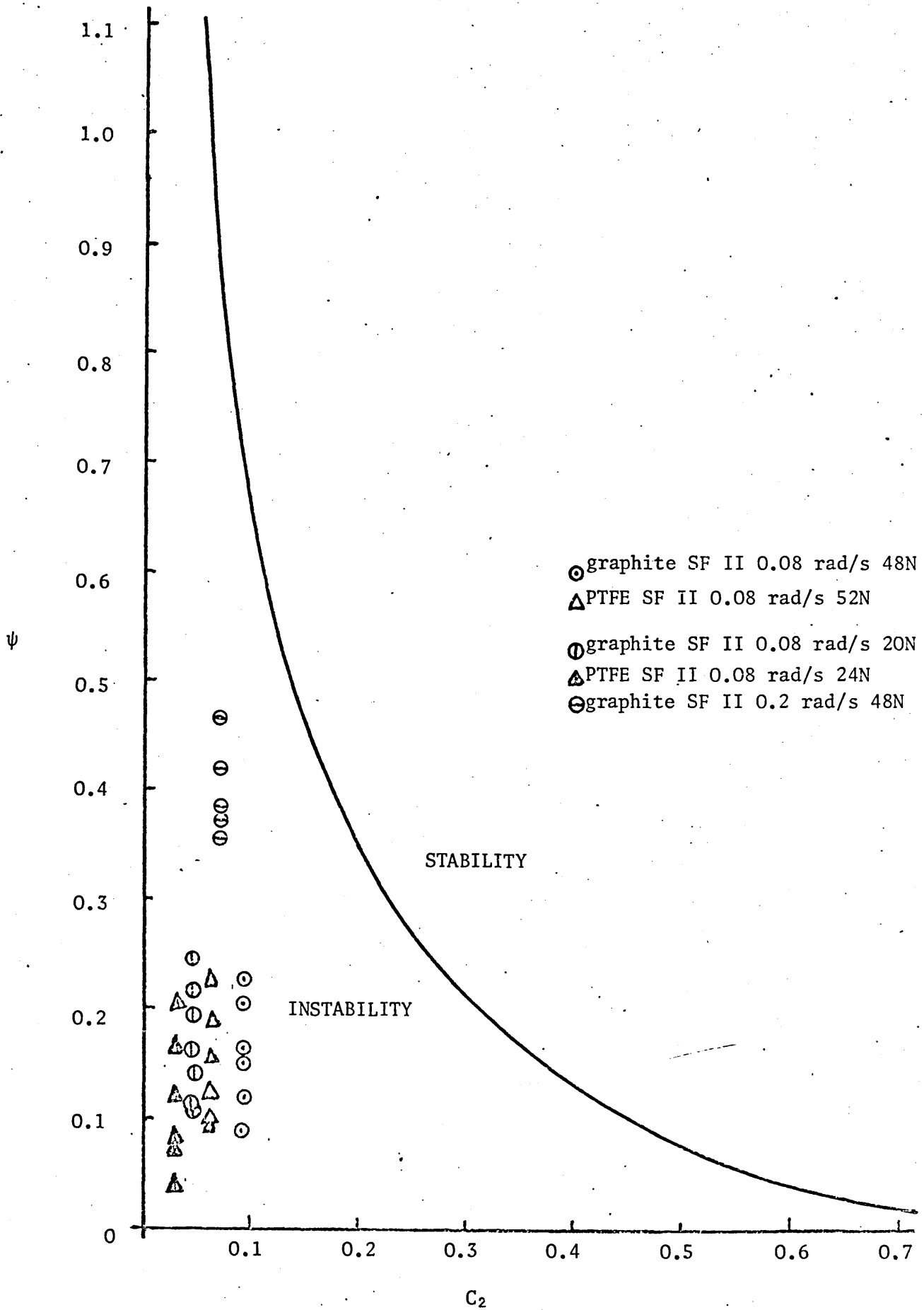
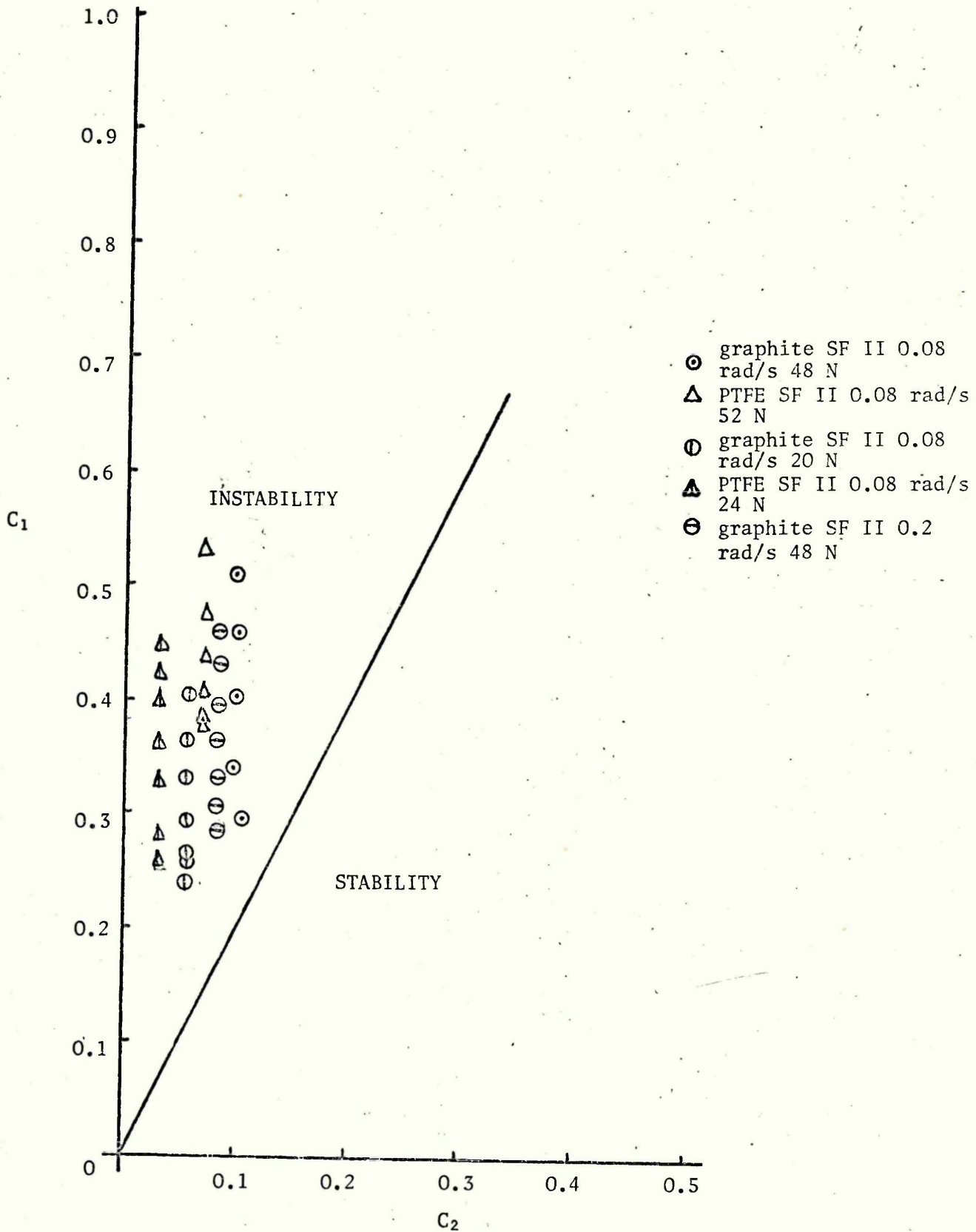


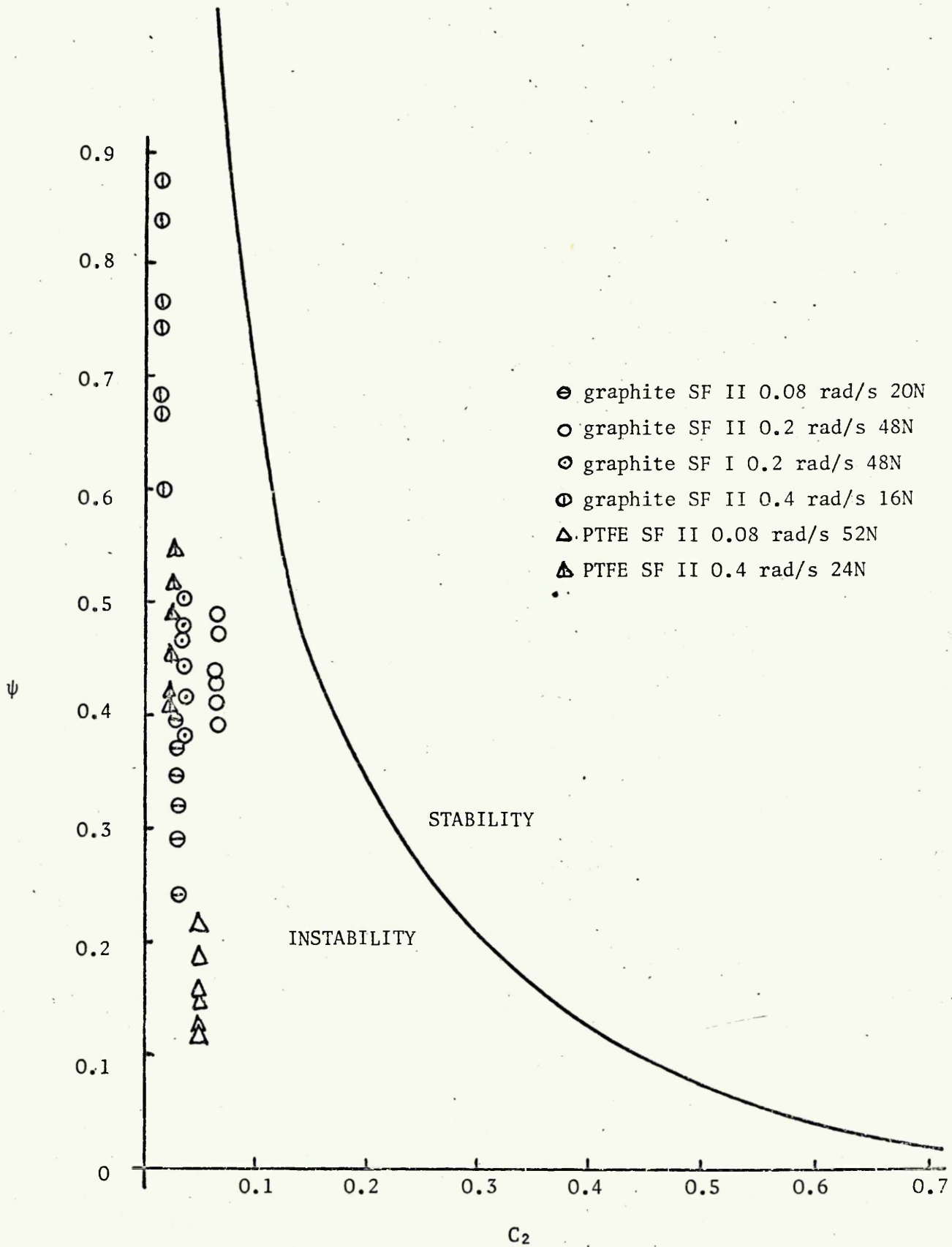
Fig. 5.21 Variation of dynamic coefficient of friction with sliding velocity for graphite, 0.8 MN/m<sup>2</sup> pressure 6.6 Hz frequency



Stability relationships - Blok model-cast iron - frequency 6.6 Hz







Stability relationship - negative damping model cast iron, 10 Hz frequency

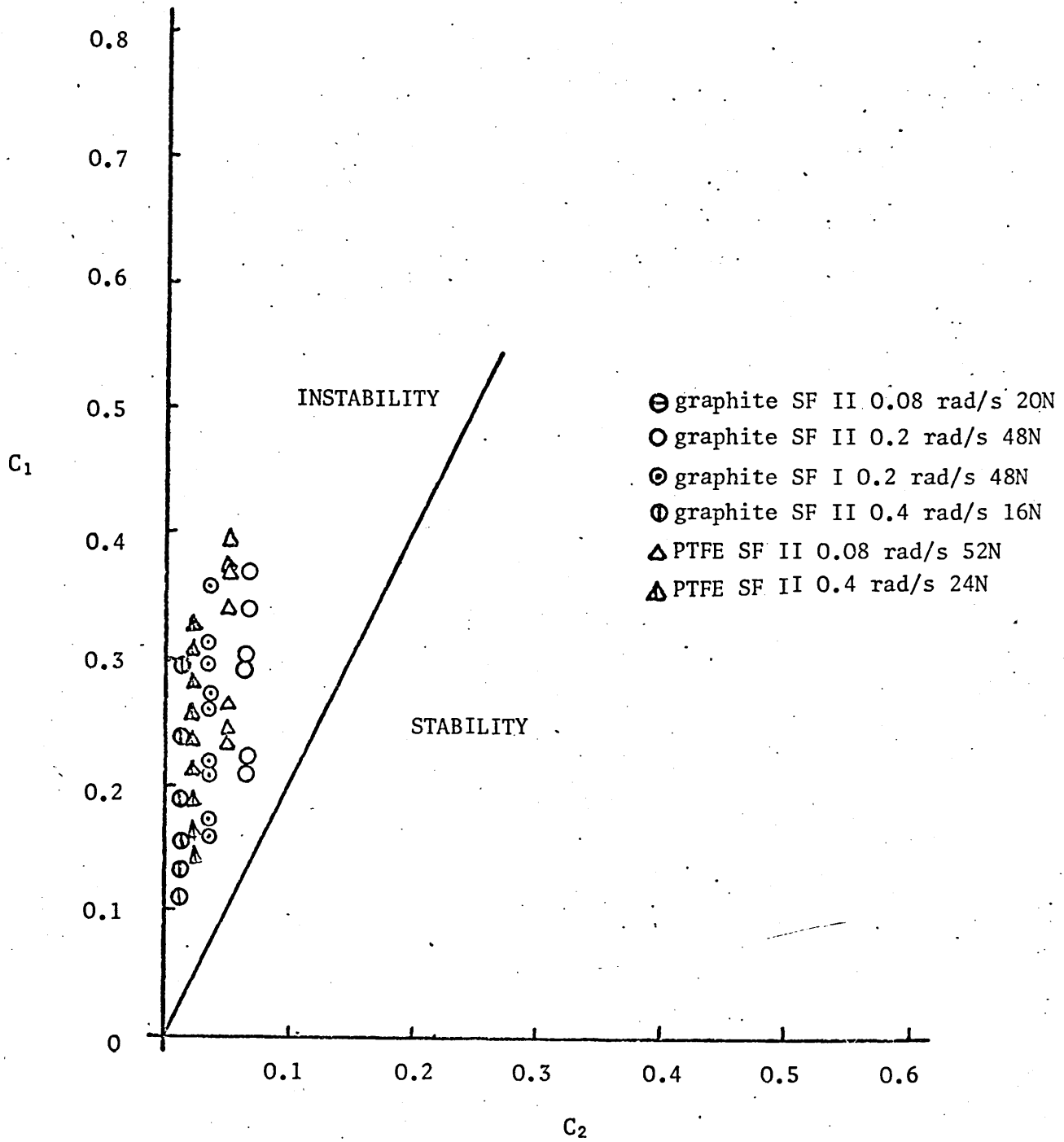


Fig. 5.26

Stability relationship - Blok model cast iron, 13.7 Hz frequency

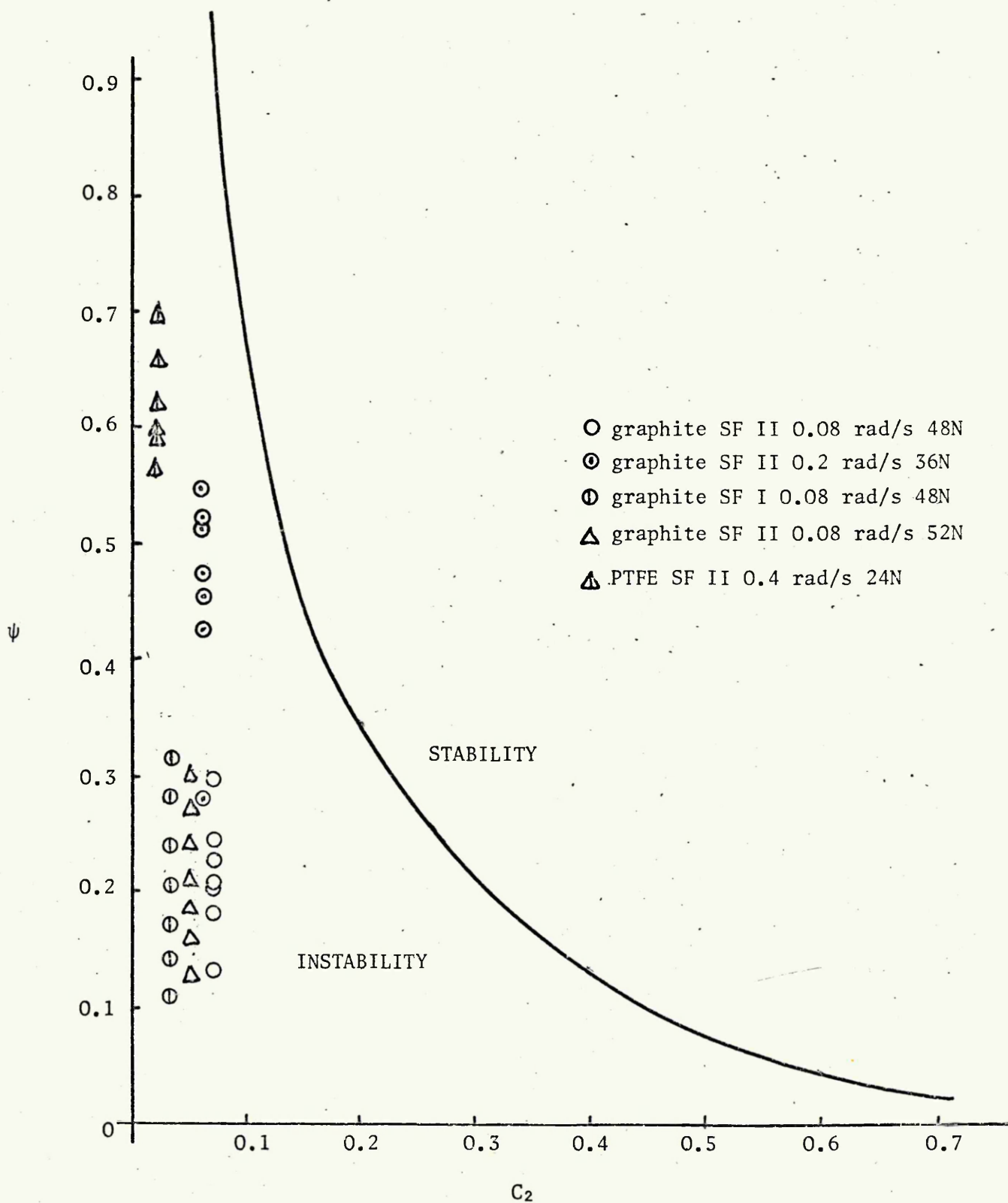
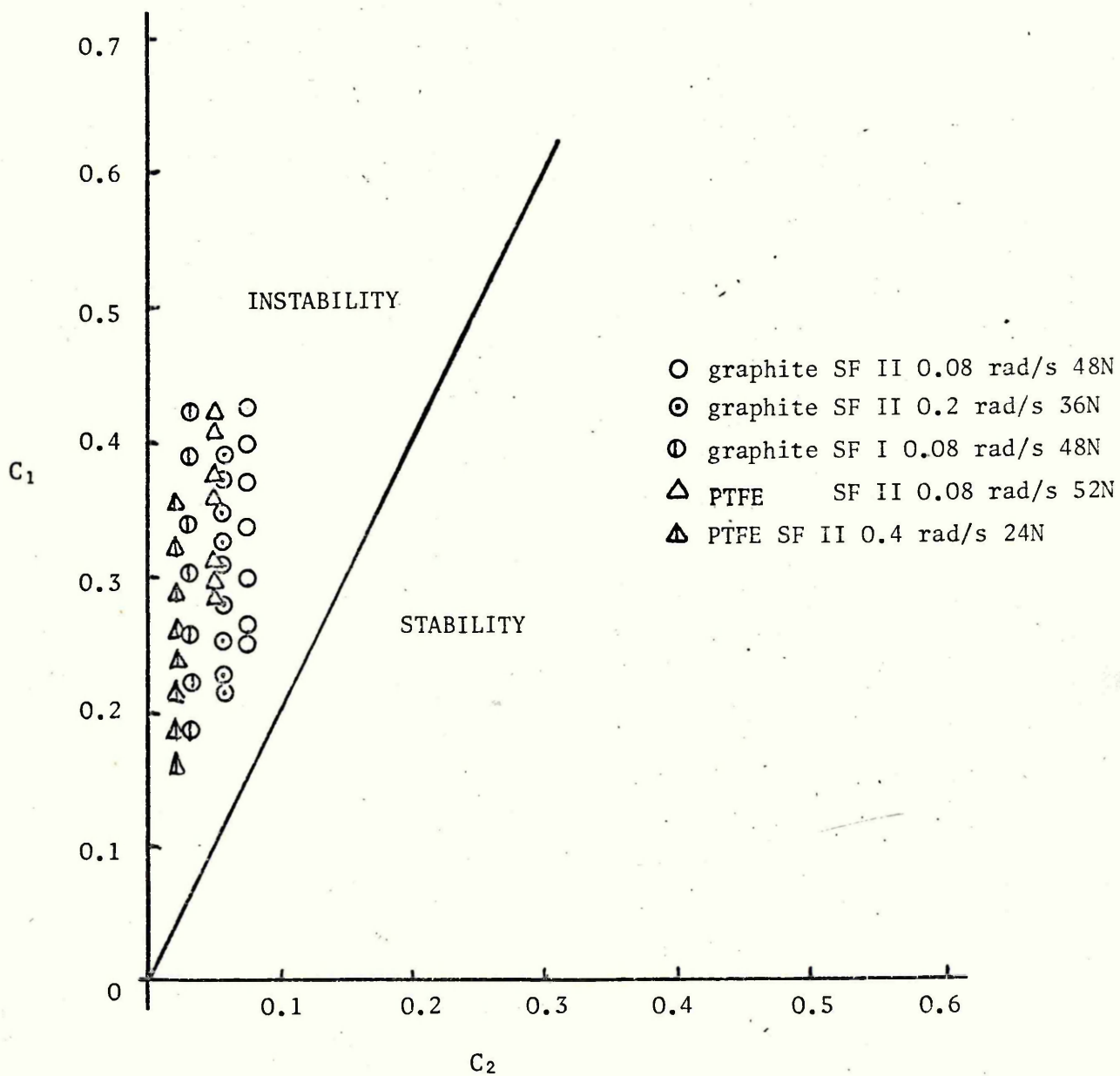


Fig. 5.27

Stability relationship, negative damping model cast iron,

frequency = 13.7 Hz



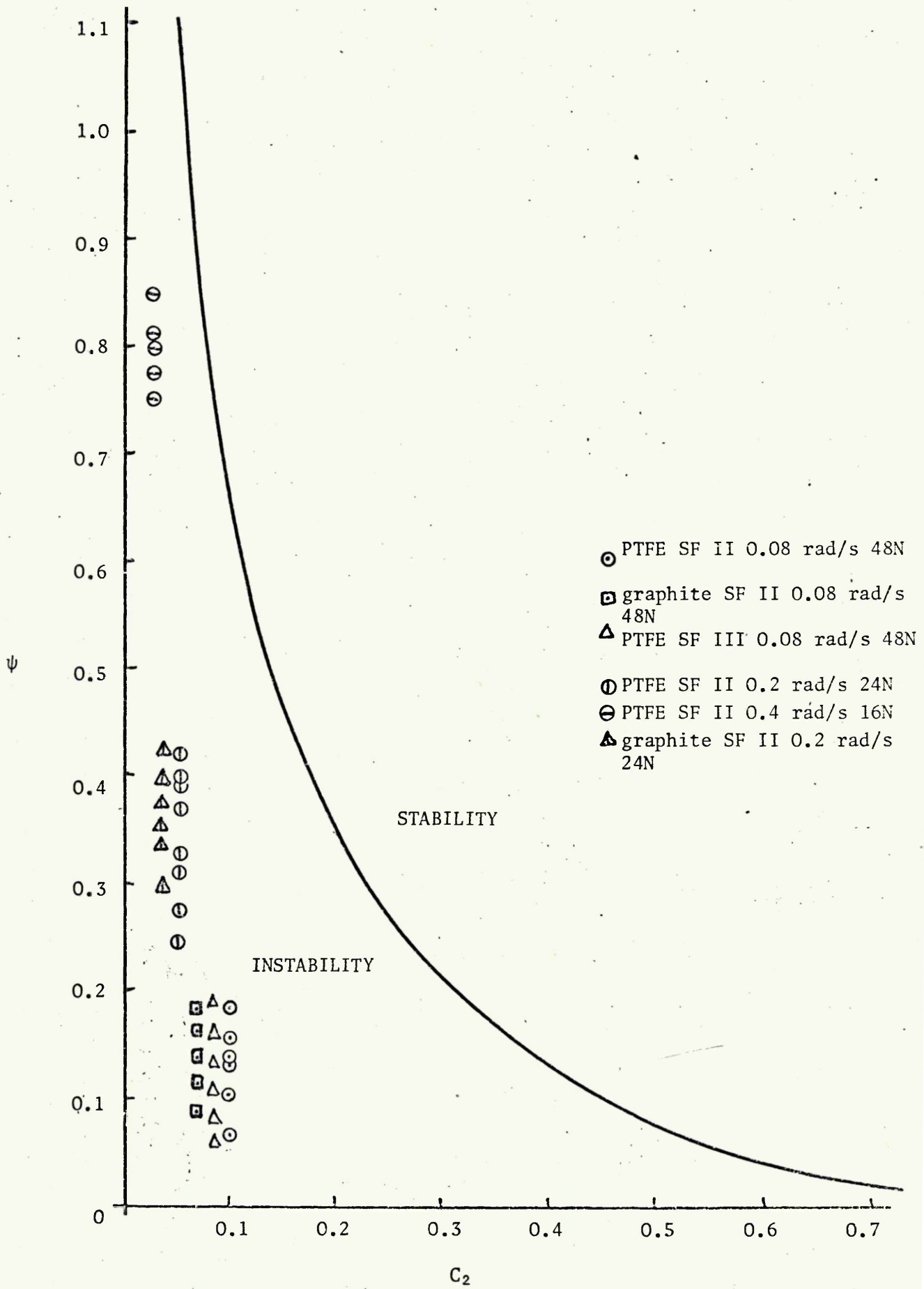
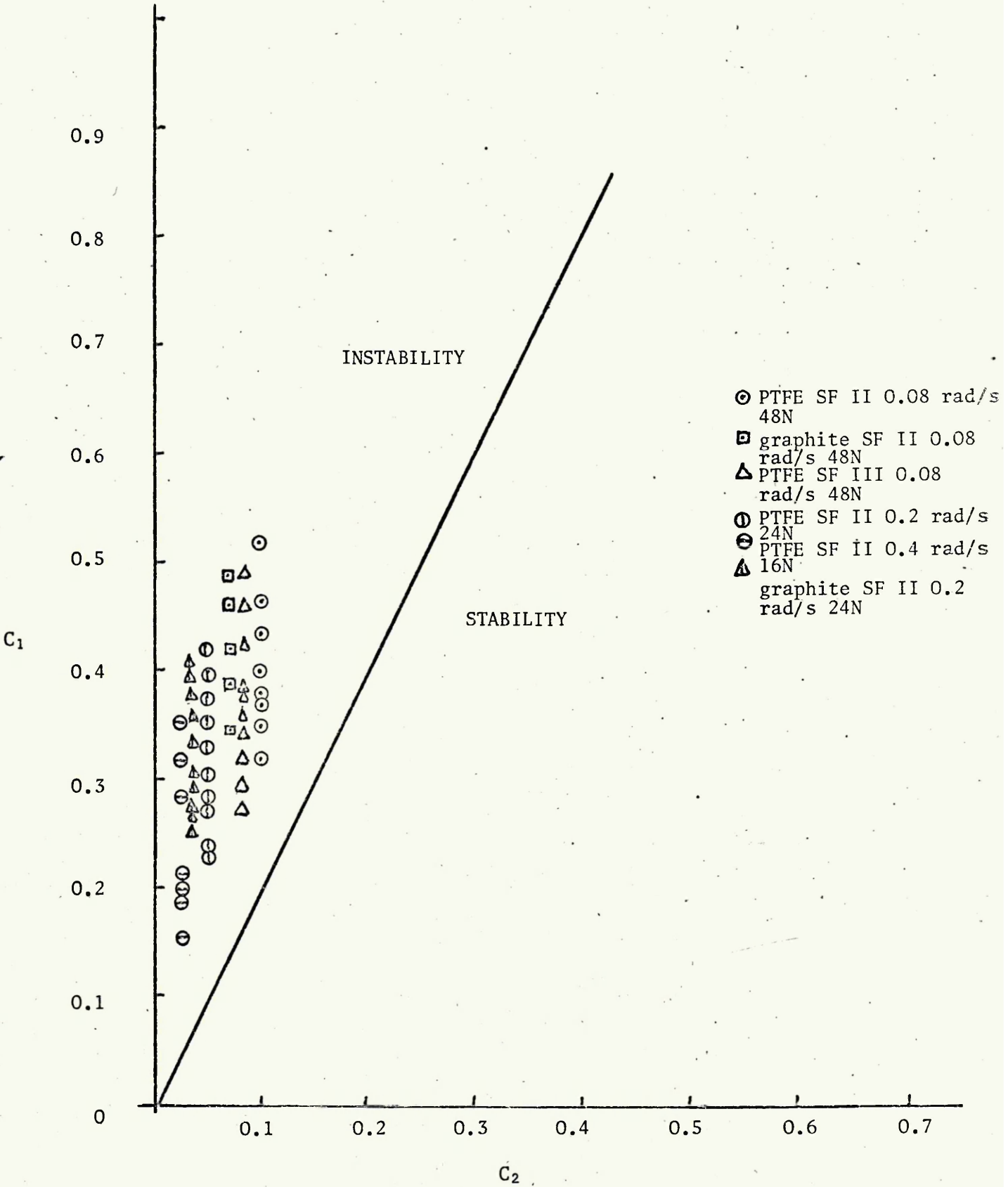


Fig. 5.29

Stability relationships - negative damping model mild steel, 6.6 Hz frequency





Stability relationship - negative damping model mild steel,

10 Hz frequency

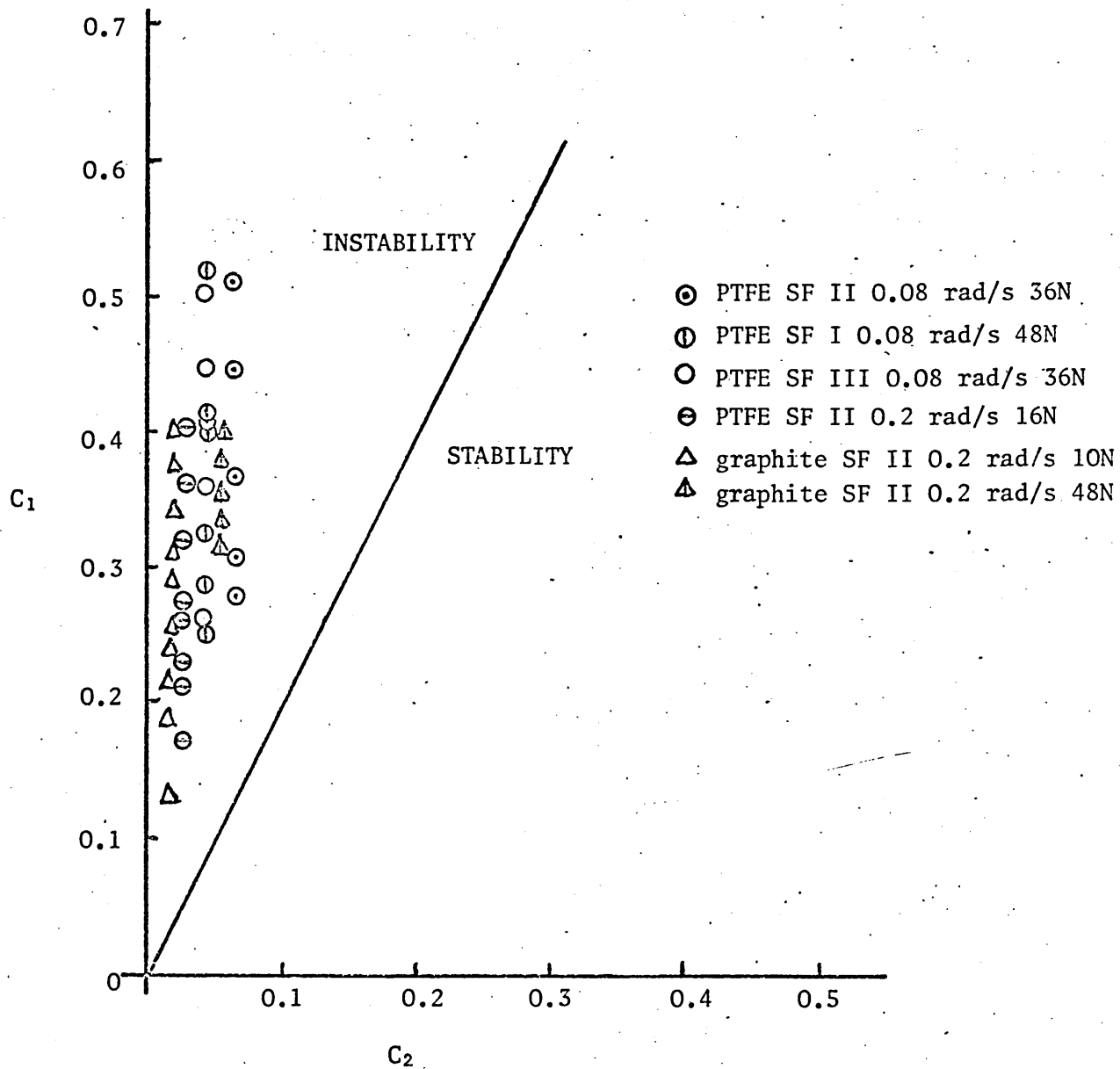


Fig. 5.32

Stability relationship - Blok model mild steel, 13.7 Hz frequency

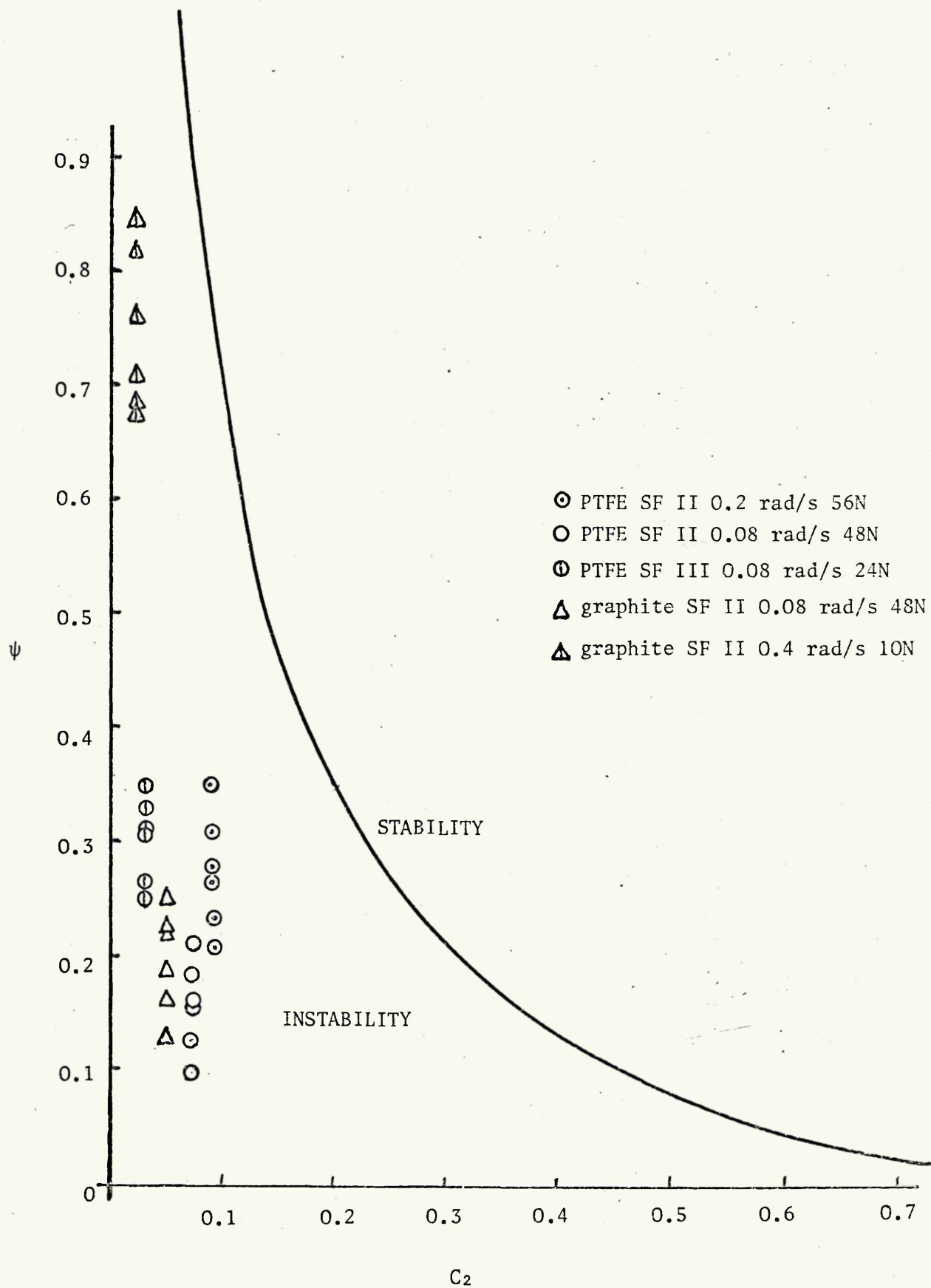


Fig. 5.33

Stability relationship - negative damping model mild steel, 13.7 Hz frequency

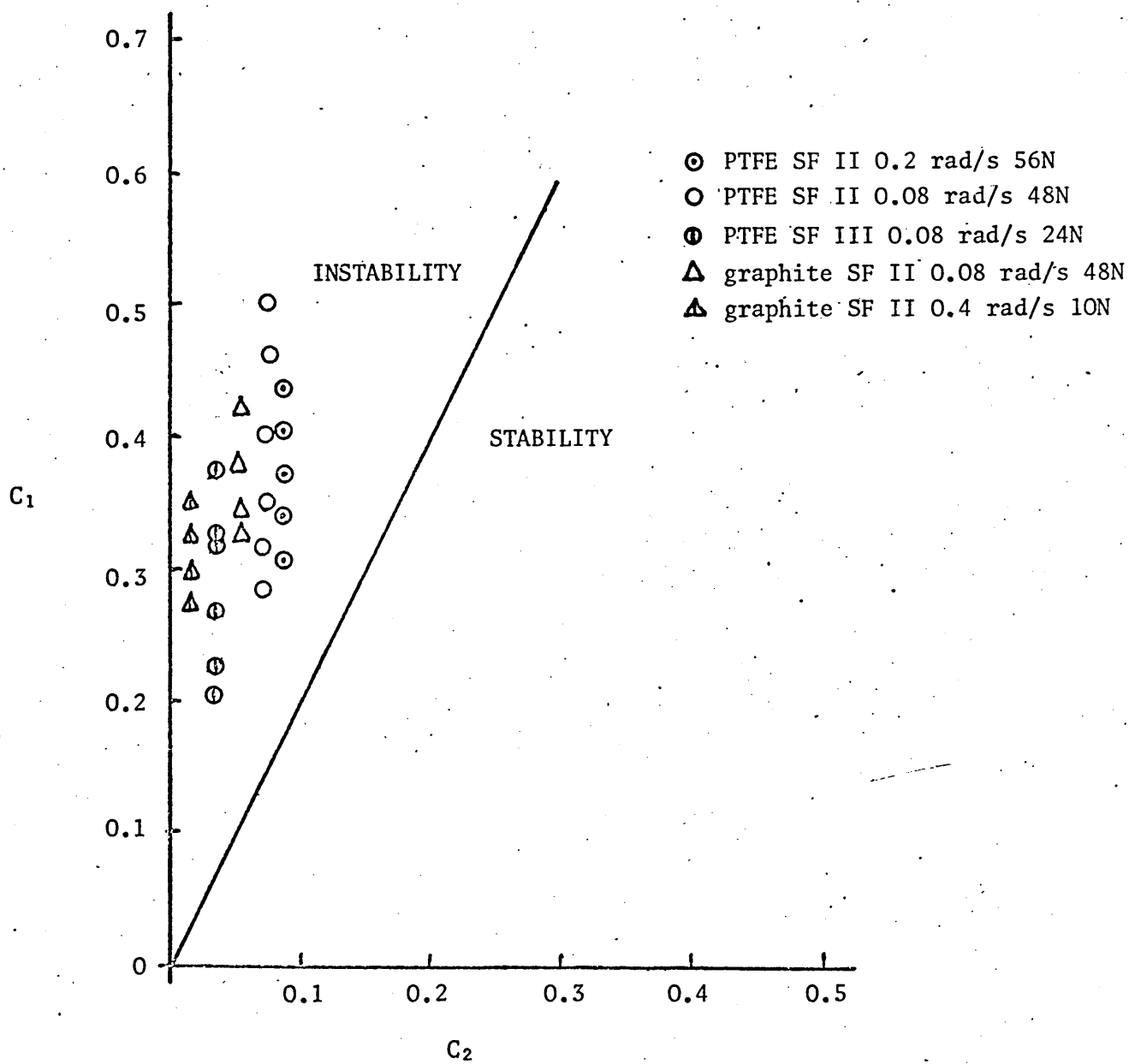


Fig. 5.34 The sliding ratio required to eliminate stick slip, graphite on cast iron frequency 6.6 Hz, variations in normal load, surface finish and drive speed

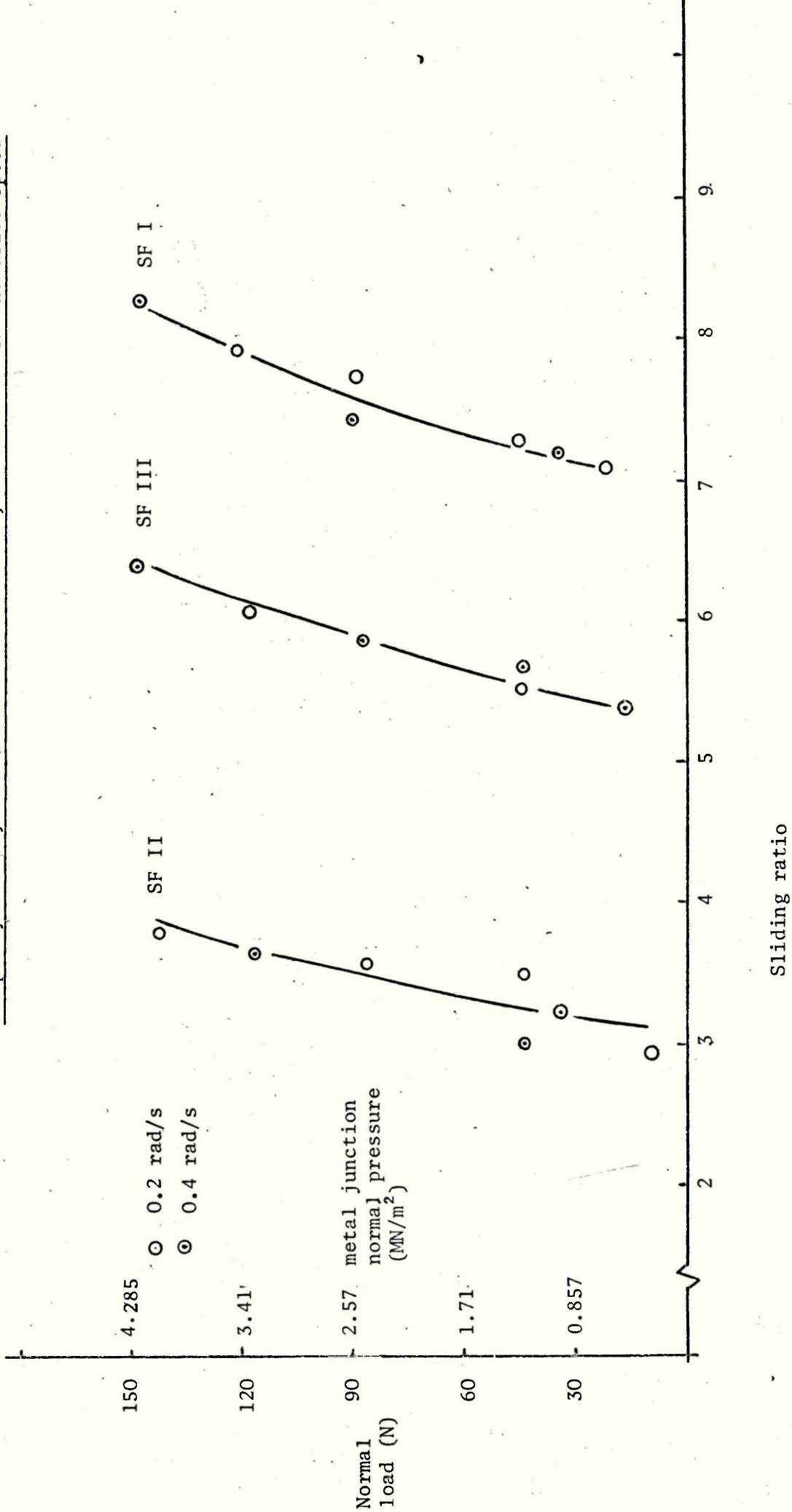


Fig. 5.35 The sliding ratio required to eliminate stick slip, ptfе on steel frequency 6.6 Hz, variations in normal load, surface finish and drive speed

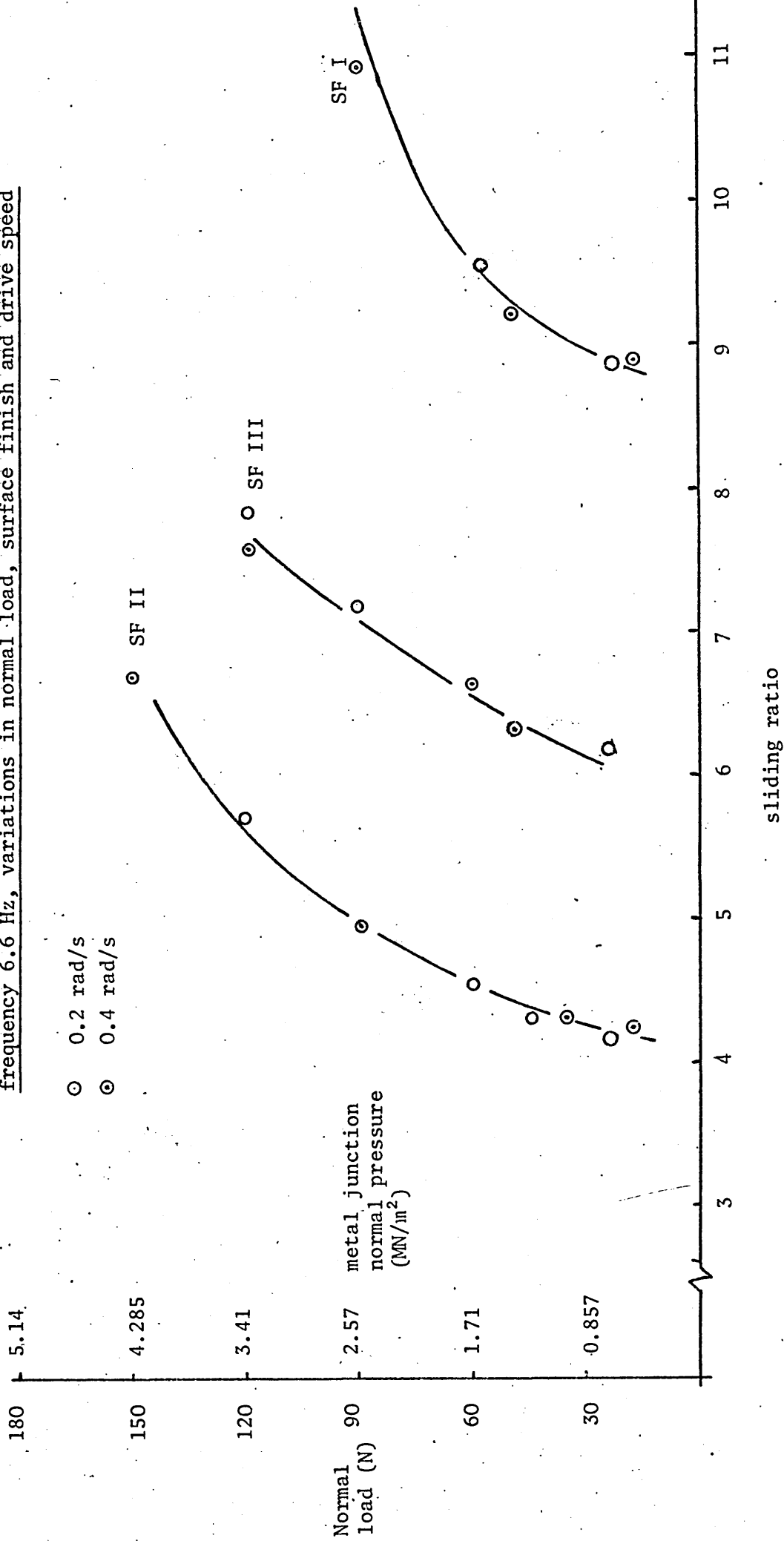


Fig 5.36 Wear volume against sliding ratio, graphite on cast iron  
 6.6 Hz frequency, variations in drive speed and normal load

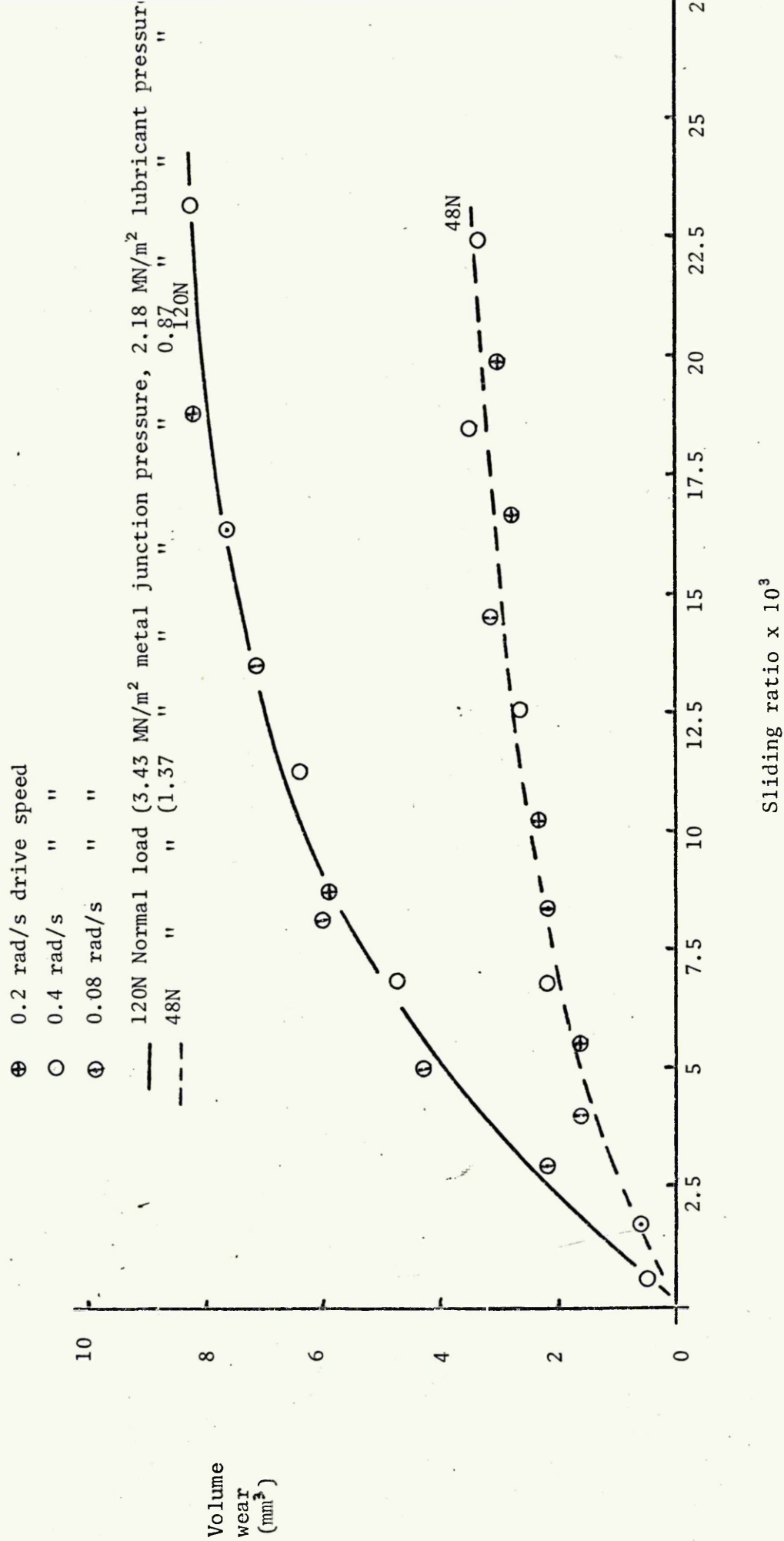


Fig 5.37 Wear volume against sliding ratio for ptfe on steel  
 6.6 Hz frequency, variations in normal load and drive speed

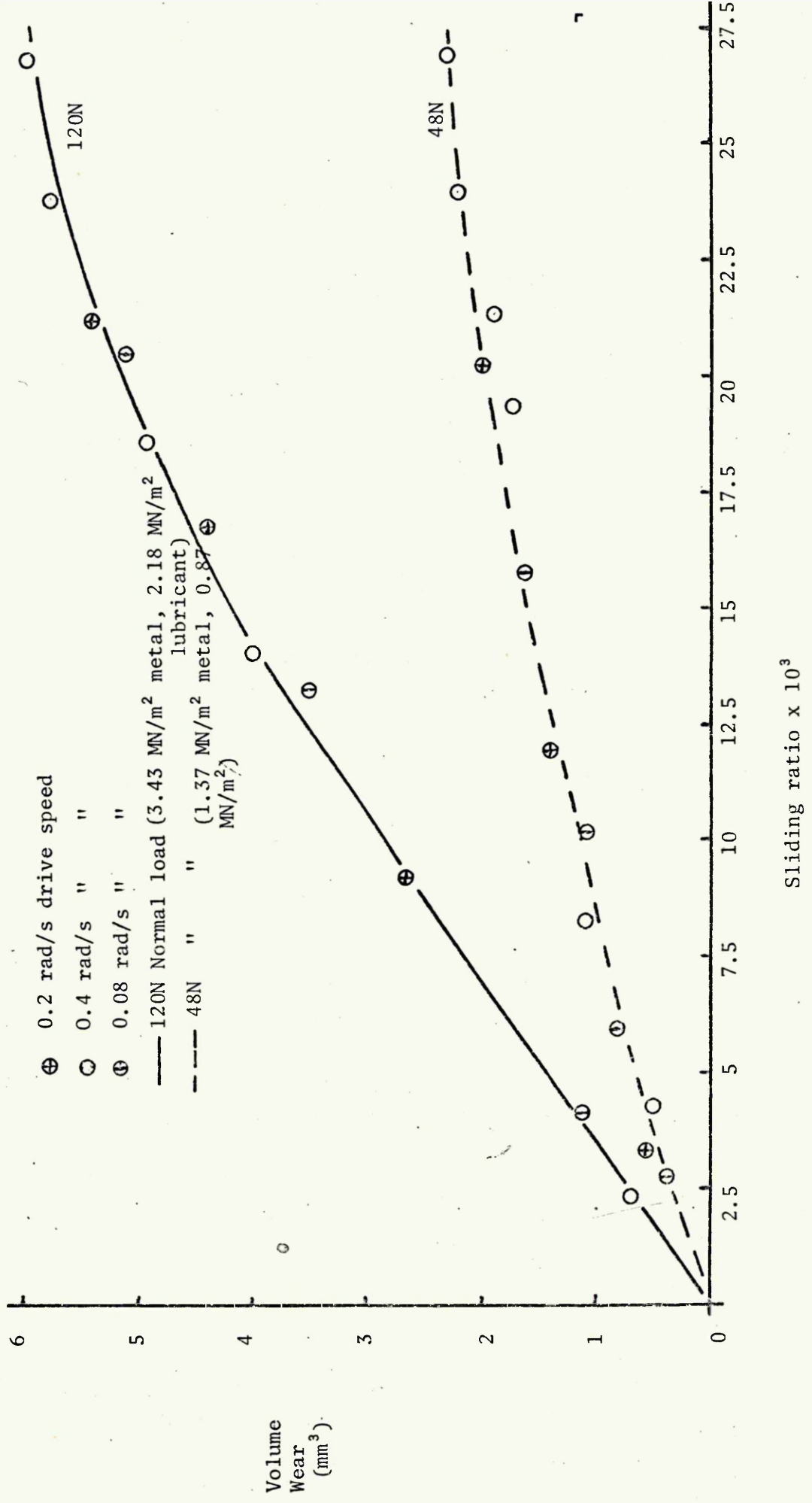


Fig 5.38 Reciprocal of sliding ratio at which stick-slip is eliminated against load ratio, for various loads; system frequency 6.6 Hz, SF II 0.08 rad/s drive speed. Graphite on cast iron

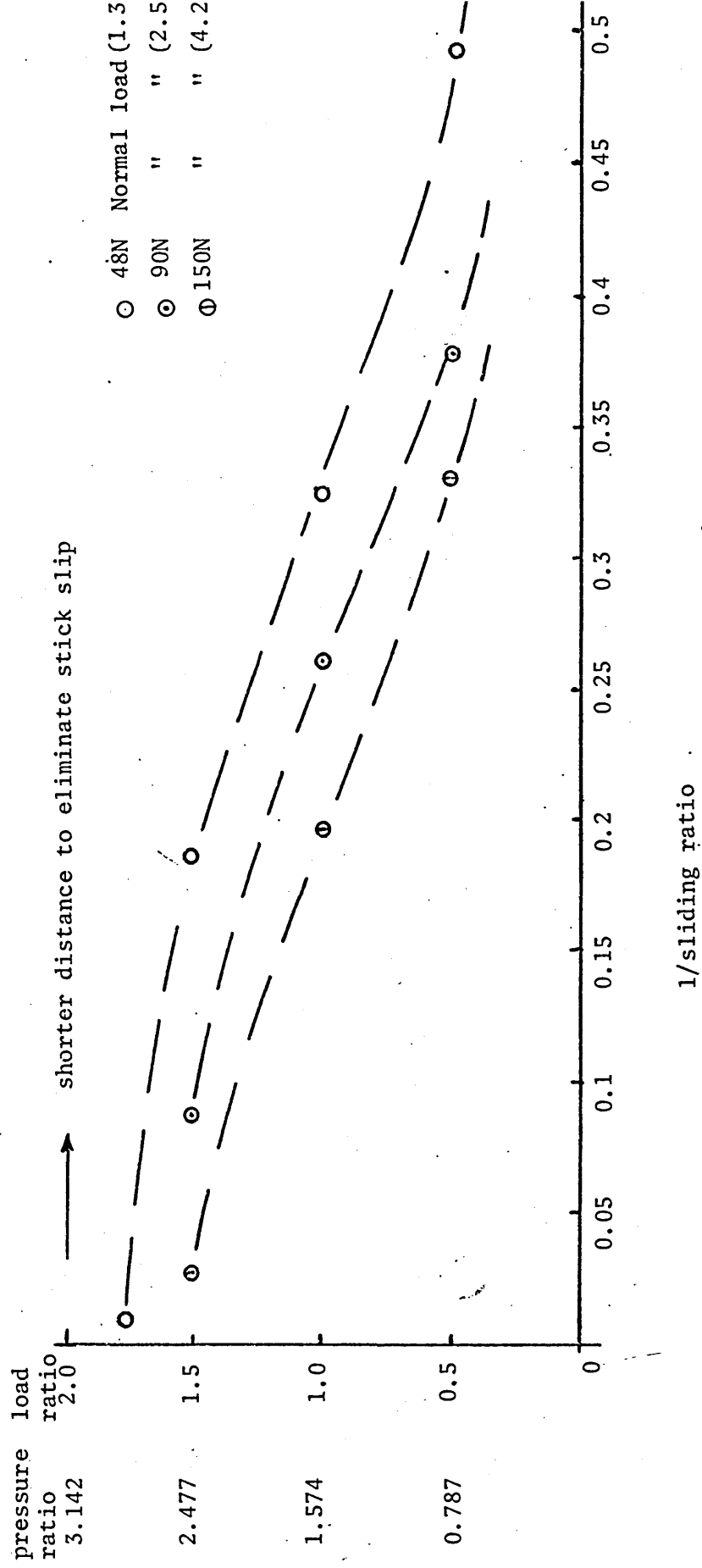
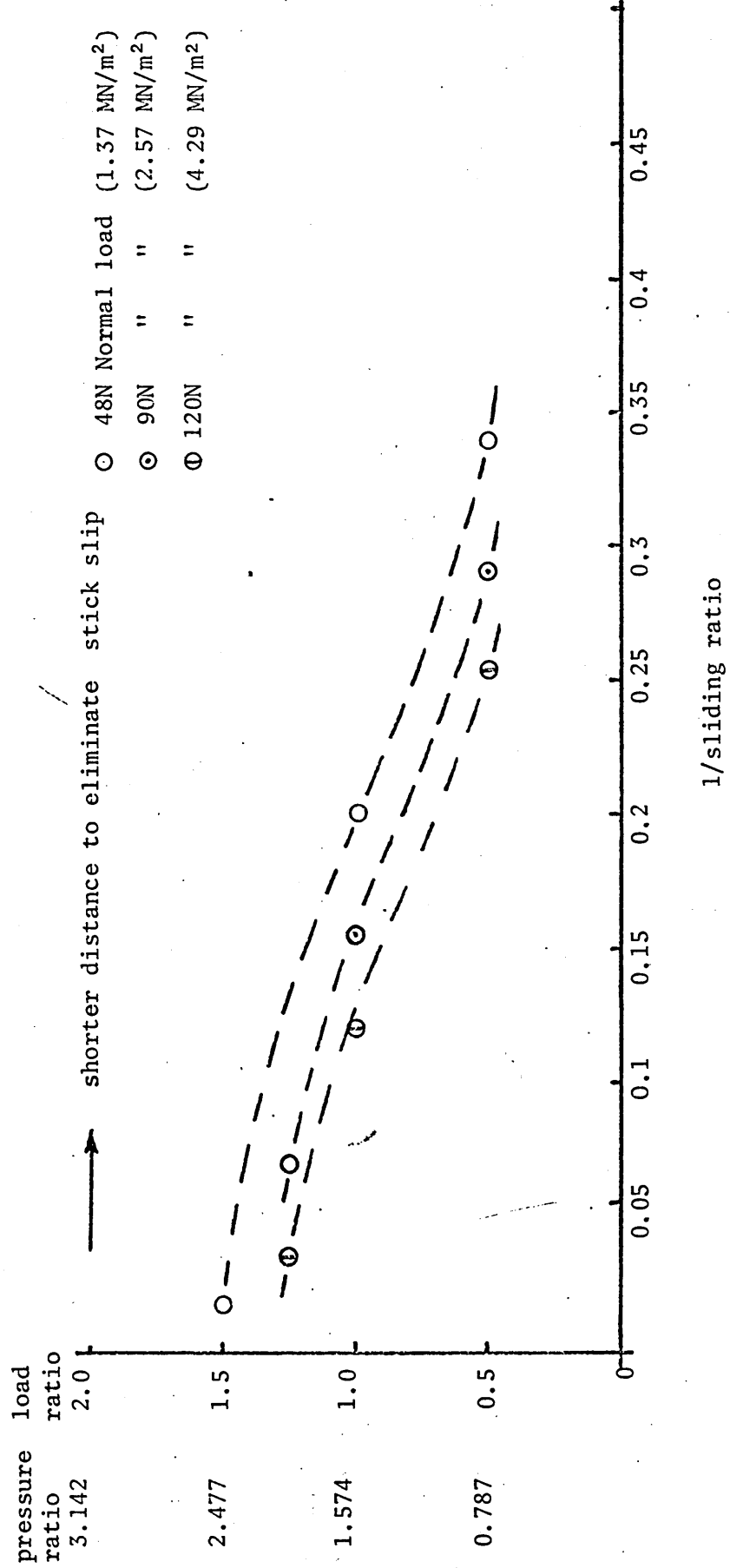


Fig 5.39 Reciprocal of sliding ratio at which stick-slip is eliminated against load ratio, for various loads; system frequency 6.6 Hz; SF II, drive speed 0.08 rad/s, ptfe on steel



### 6.1 Introduction

Having demonstrated the viability of transfer lubrication techniques in stick-slip elimination under chemically clean conditions it was decided to examine the effect upon the technique of oil contamination, which might be experienced in some engineering environments. A typical light machine oil, Shell Tellus 33 (kinematic viscosity of 66cSt at 37.8°C) was smeared upon the metal disc producing boundary lubrication conditions at the metal piston and disc interface with the dry lubricant compact acting diametrically opposite as previously. The stick slip machine was then run and the effects upon the transfer lubrication observed. Tests were confined to those metal and lubricant combinations which had shown most success in the uncontaminated tests.

### 6.2 Graphite on Cast Iron Results

Fig. 7.1 shows the amplitude against time relationship for graphite on cast iron, surface finish II, 0.08 rad/s drive speed, 6.6Hz frequency, 24, 48 and 120N normal load. It can be seen that elimination of the stick slip vibrations does occur and the oil contaminant has little or no effect. The transferred lubricant itself was seen to mix with the oil in forming a compound which still transferred adequately to the metal interface causing elimination of the stick slip vibrations.

### 6.3 PTFE on Steel Results

The above tests were repeated with a mild steel disc and piston

and ptfе as a dry lubricant. The graph of fig. 6.2 indicates a deterioration in the efficiency of stick slip elimination compared to the uncontaminated situation. In all load cases stick-slip vibrations still occurred considerably after they had been eliminated in the uncontaminated tests.

In order to ascertain the reason for this failure to eliminate the stick slip vibrations, measurements were taken of 'metal to metal' friction characteristic, dry lubricant coulomb and viscous friction components and dry lubricant volume wear.

The coulomb and viscous components of friction are shown in fig. 6.3 and are used in conjunction with the steel on steel negative damping coefficient values to produce the stability graph of fig. 6.4. Comparing the viscous damping values obtained with those shown in fig. 5.13 indicates little variation in this property due to the boundary lubrication effects of the oil. The stability graph however shows considerable discrepancy with that which might have been expected based on the results of chapter 5. This indicates the contaminant oil to be adversely affecting the transfer of dry lubricant and hence the modification of the 'metal to metal' characteristic. Further confirmation of this is given by the volumetric wear of the contaminated ptfе (fig. 6.5) compared to the uncontaminated wear shown in fig. 5.37. It can be concluded therefore that the failure of the ptfе to eliminate steel on steel stick slip vibrations is due to the effect of the oil in reducing the transfer of lubricant to the metal interface.

#### 6.4 Vespel on Steel Results

A composite dry lubricant, manufactured by Du Pont de Nemeurs and having the trade name 'Vespel SP211'\* was obtained to test the performance under oil contaminated stick slip conditions.

The graphs of figs. 6.6, 7 and 8 show this material to be satisfactory in eliminating the stick slip vibrations in circumstances where the ptfе had failed to do so.

\* A polyimide resin containing 15% graphite and 10% ptfе by weight - available from Messrs Du Pont de Nemours, Switzerland.

Fig 6.1 Stick slip amplitude vs. time of test for graphite on cast iron surface finish II, 0.08 rad/s drive speed, 6.6 Hz frequency, oil contaminated.

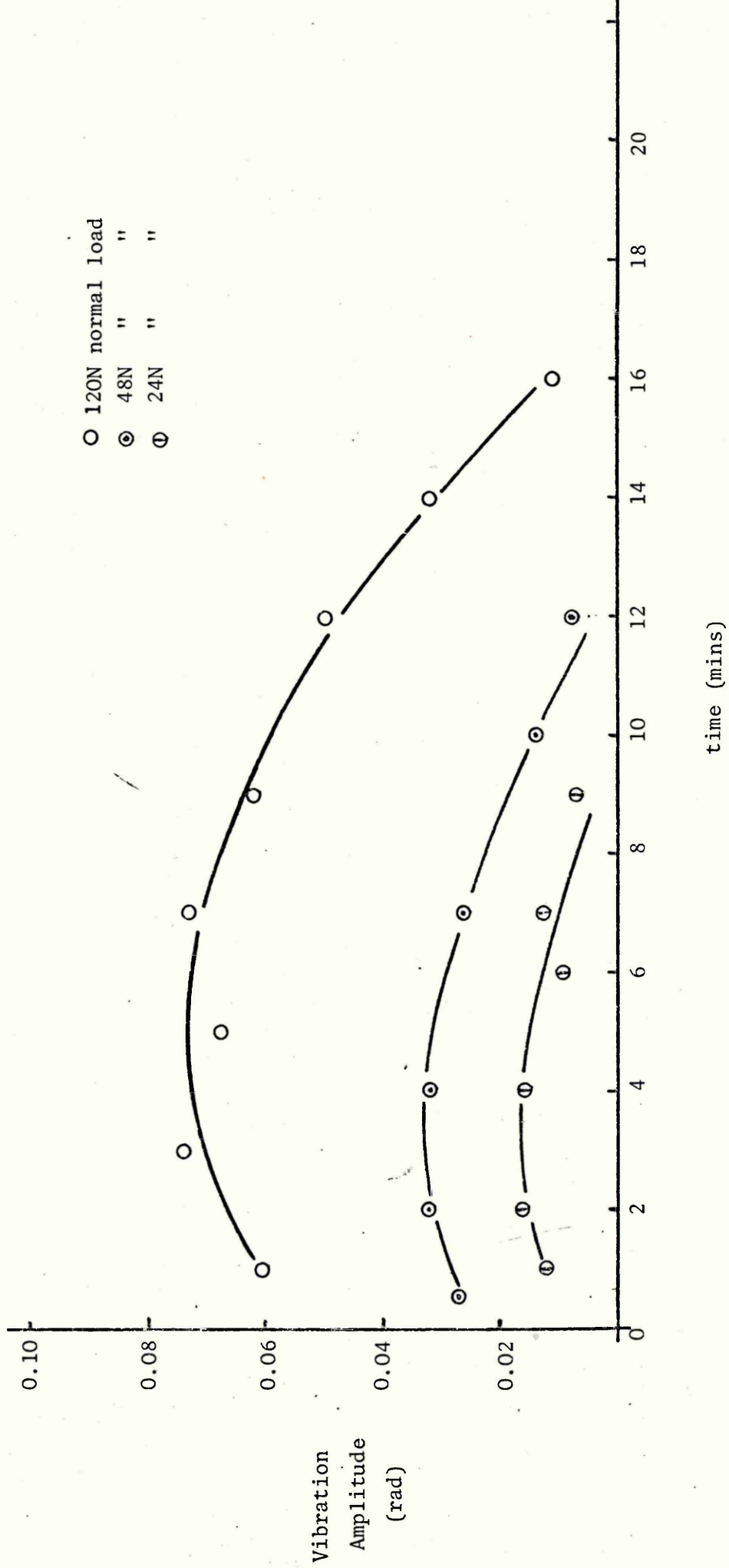


Fig 6.2 stick slip amplitude vs. time of test for ptfe on steel, oil contaminated surface finish II, 0.08 rad/s drive speed, 6.6 Hz frequency

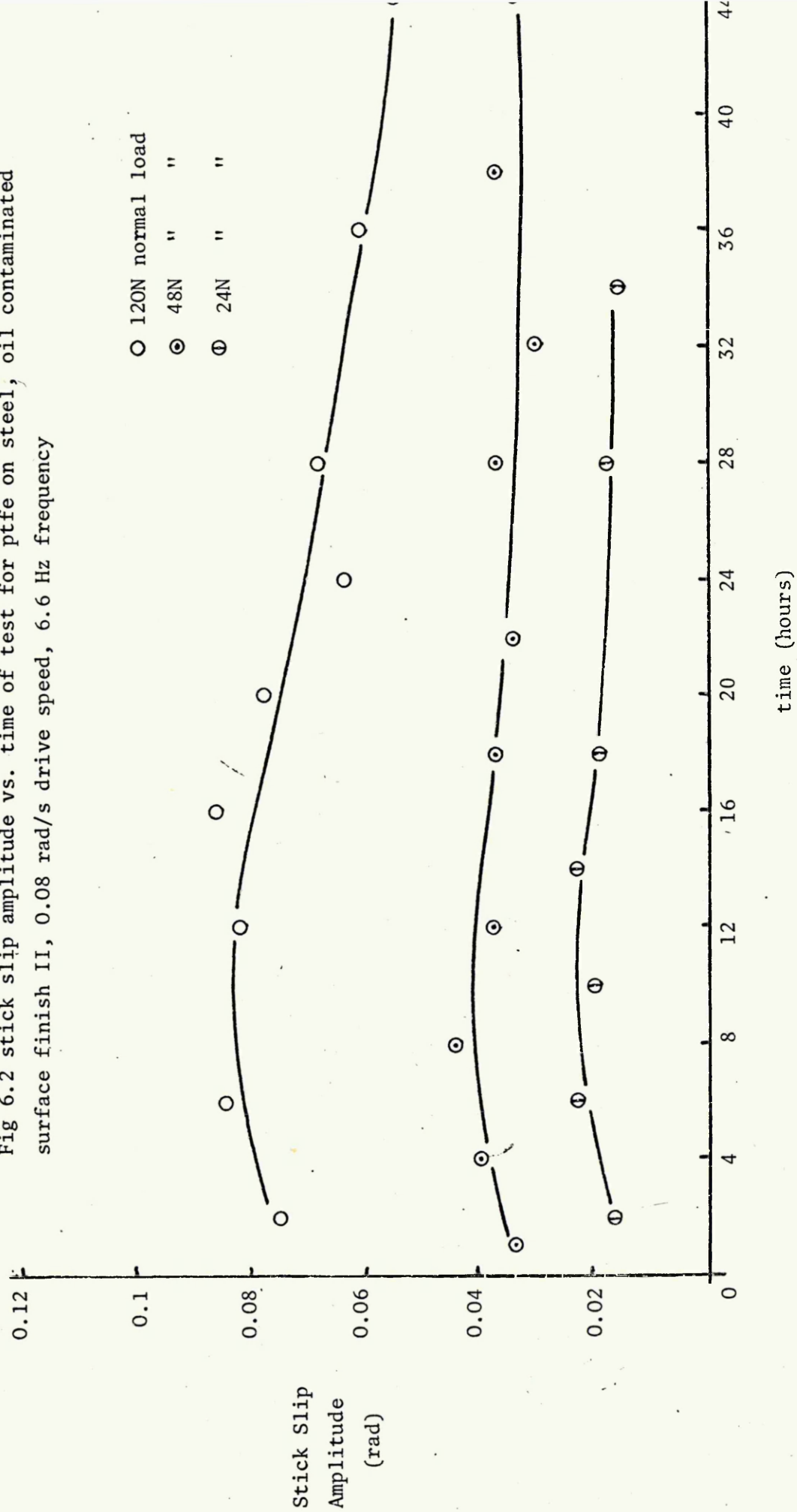


Fig 6.3 Components of friction, ptfе on steel  
Tellus 33 oil contamination, 6.6 Hz frequency

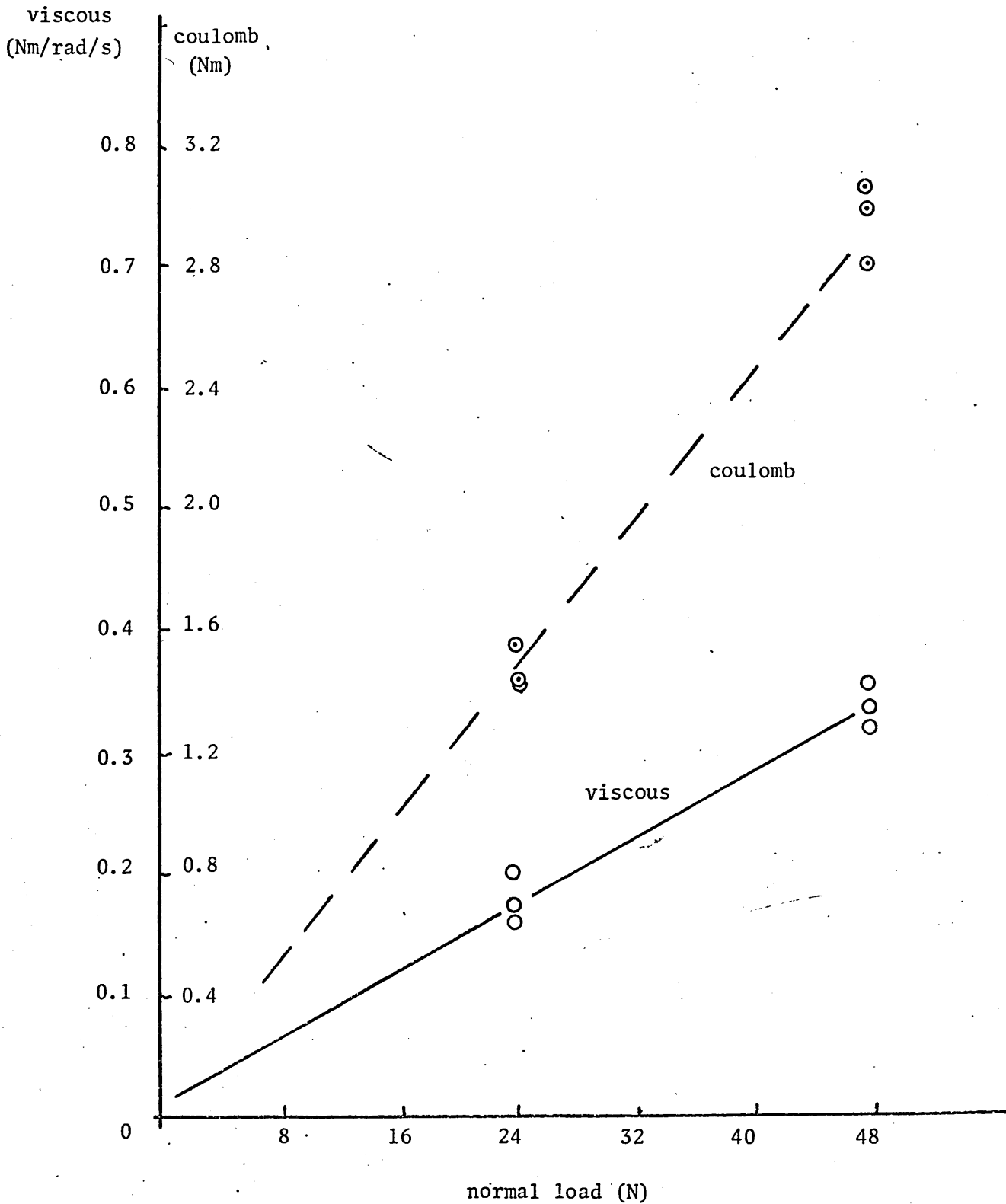


Fig 6.4 Stability relationship ptfе on mild steel  
oil contaminated, 6.6 Hz frequency, SF II, 0.08 rad/s  
drive speed

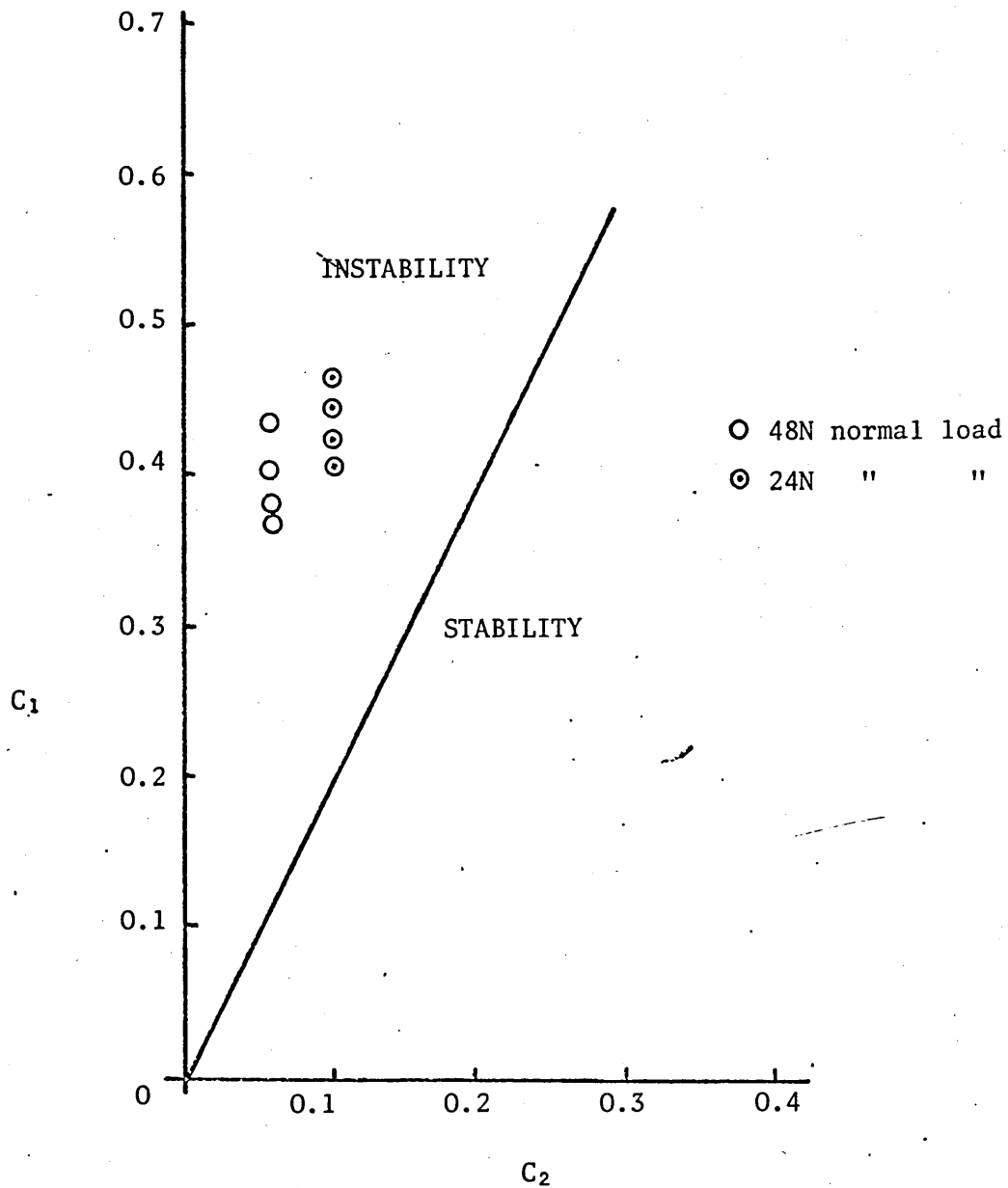


Fig 6.5 Volumetric wear of ptfe on steel, oil contaminated  
6.6Hz, SF II, 0.08 rad/s drive speed.

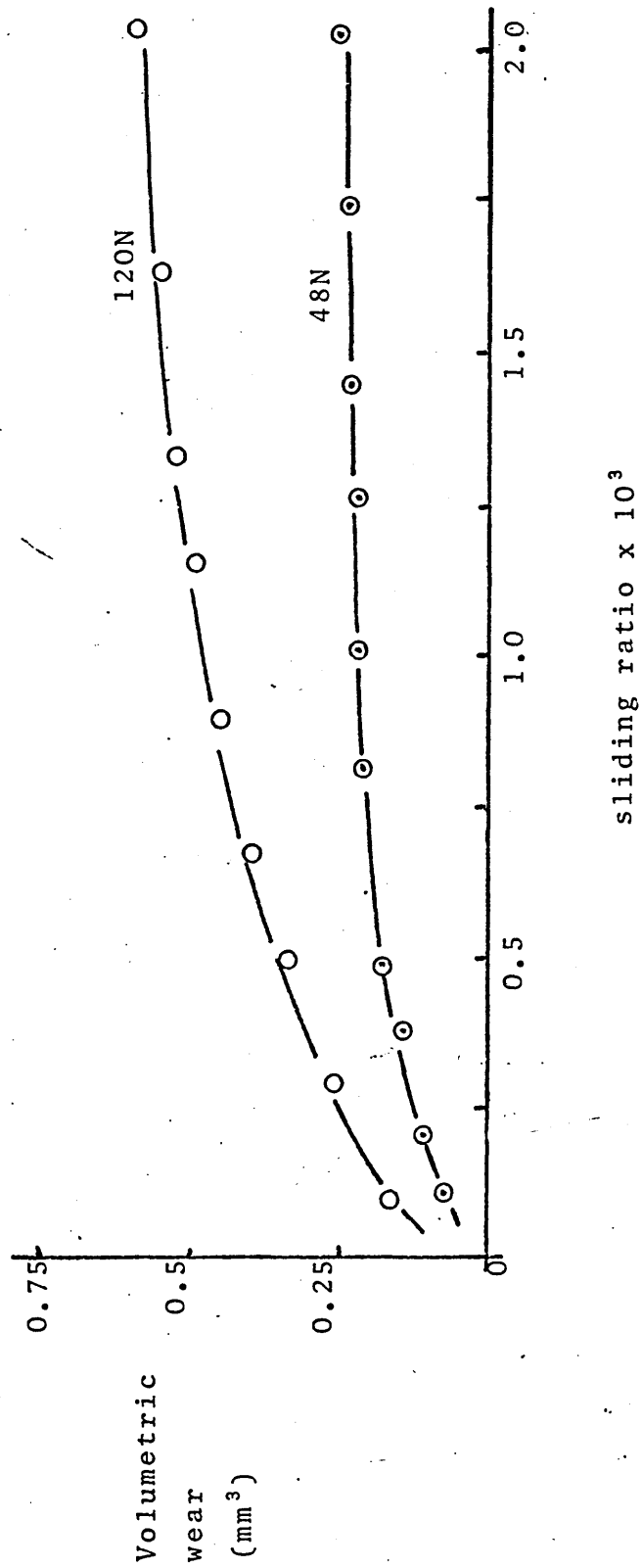


Fig 6.6 components of friction, vespel on mild steel,  
SF II 6.6 Hz frequency, oil contaminated.

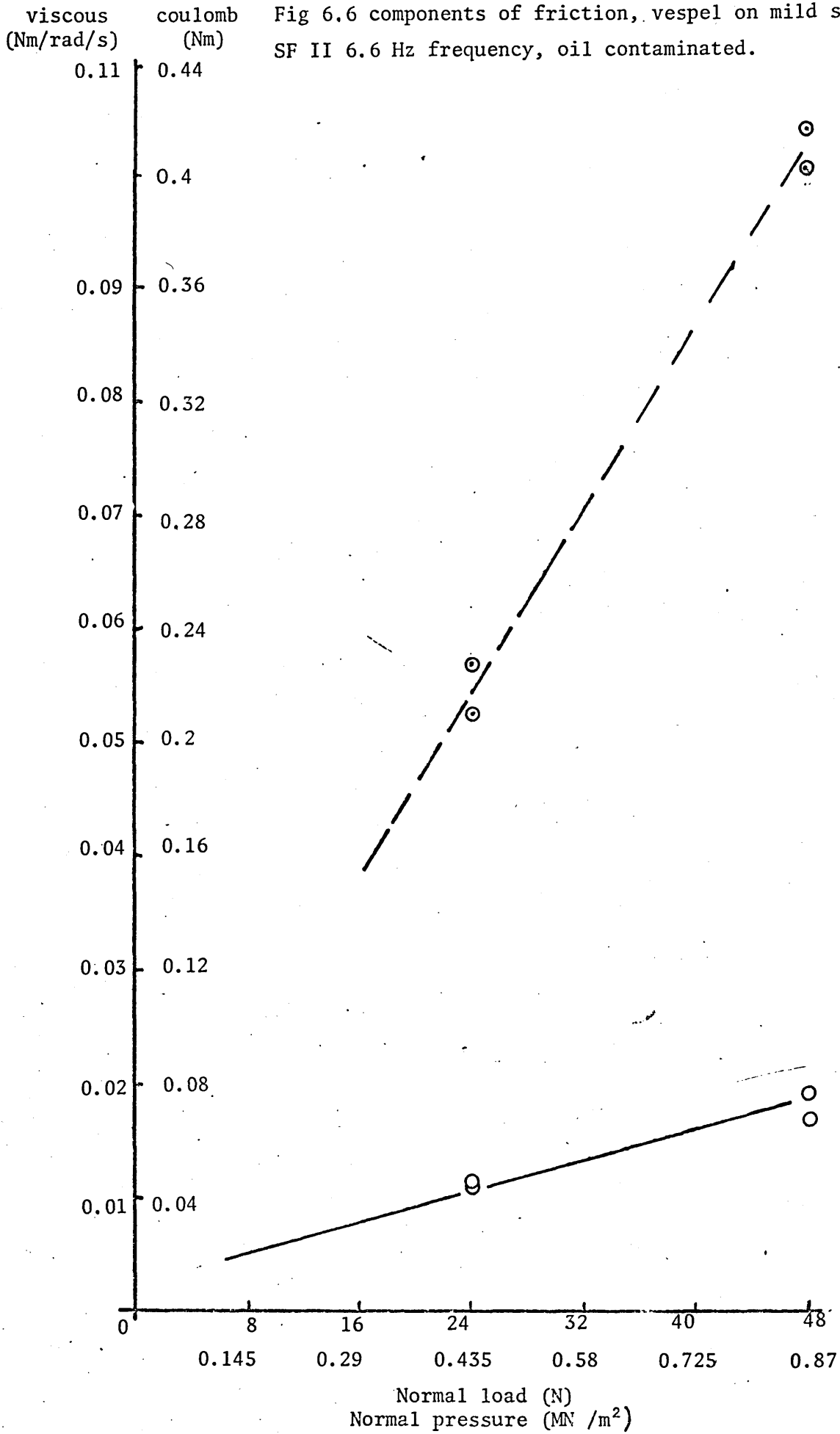


Fig 6.7 Stability relationship, vespel on steel, oil contaminated, SF II, drive speed = 0.08 rad/s  
negative damping theory

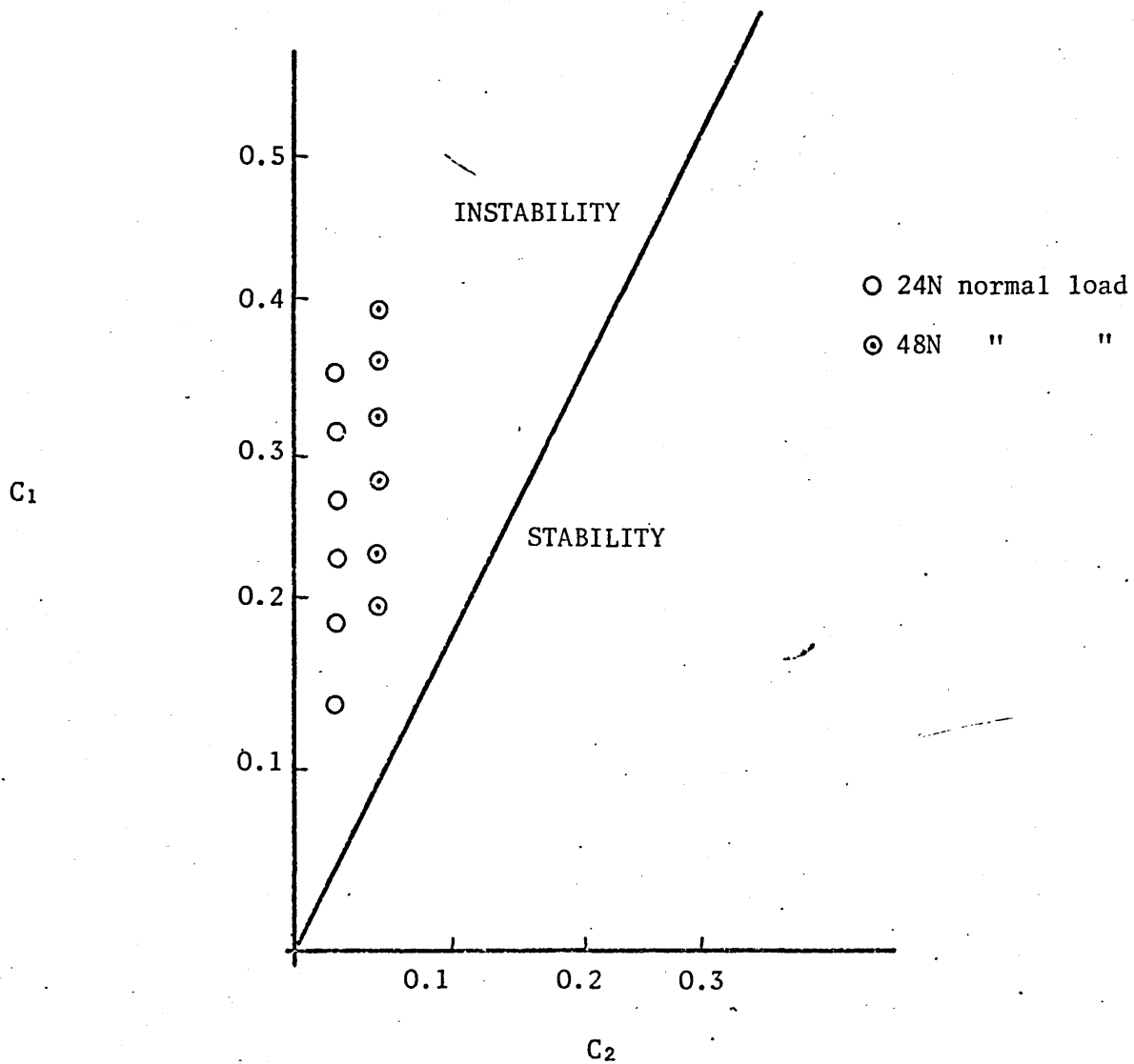
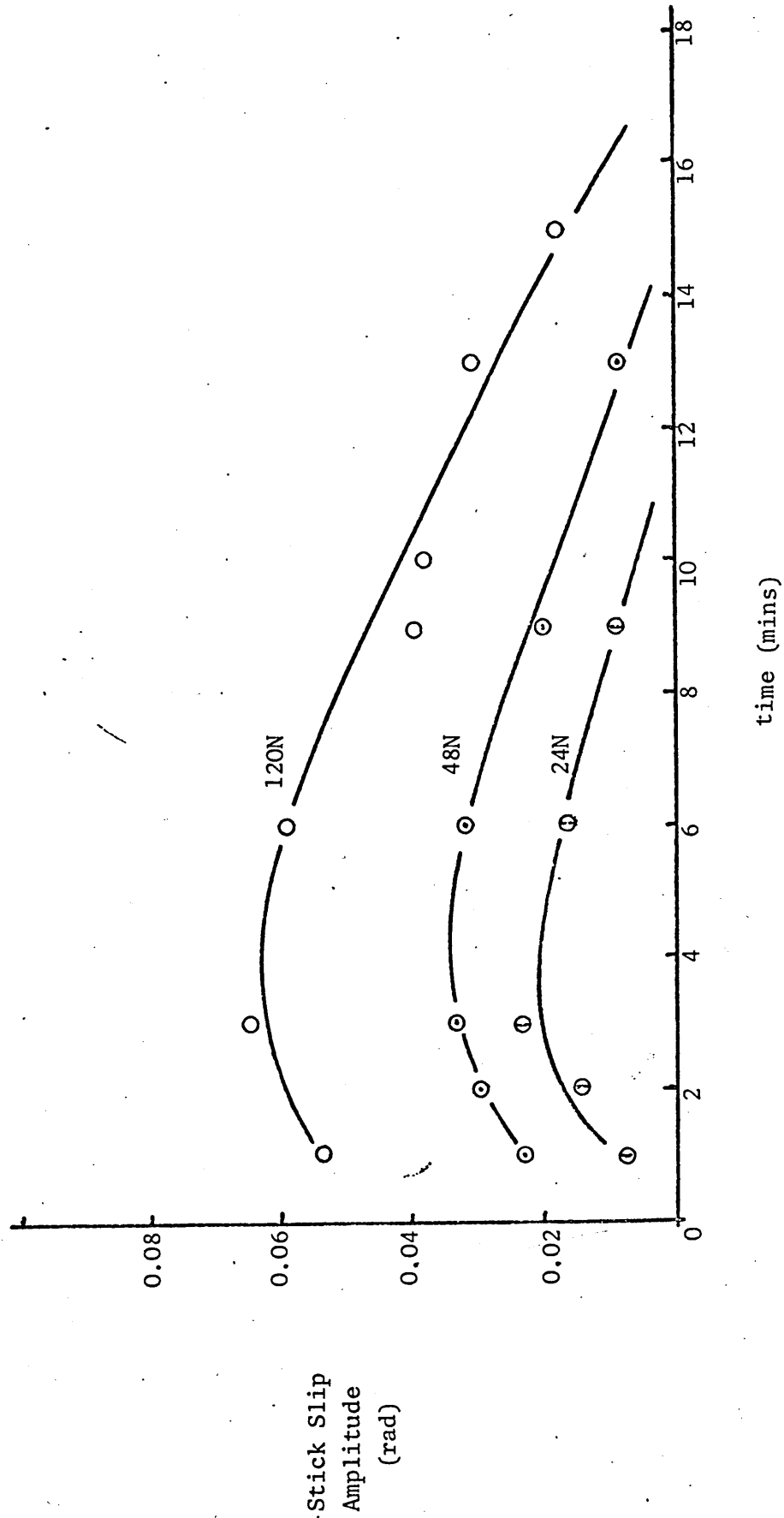


Fig 6.8 Amplitude of vibrations vs. time vespel on steel, oil contaminated, 6.6 Hz, 0.08 rad/s drive speed, SF II



### 7.1 Unlubricated Stick Slip

The original objective of this project was to produce a simple relationship concerning the stability of stick slip motion due to the viscous damping found in transfer lubrication. It follows then that any dynamic friction model needed to be simple and amenable to analysis. Two linearised models were therefore considered, a lower bound one suggested by Blok (6) and a discontinuous negative damping concept postulated by Bell and Burdekin (11). Corresponding stability relationships based upon the introduction of a viscous damper were thus developed.

Prior to the experimental programme to examine the effects of transfer lubrication upon stick slip, therefore, it was necessary to ascertain which of the two linearised models more closely represented the dynamic friction characteristic of unlubricated cast iron and mild steel.

All of the friction force slip velocity oscilloscope photographs in chapter 4 indicate the two materials utilised to have dynamic friction characteristics some way between the two models used and this is borne out by the various properties of stick slip used for comparison.

Figs. 4.4, 5, 12 and 13 show experimental and theoretical comparisons of the acceleration period, which is the critical property since both models utilise a constant deceleration force. The experimental values of acceleration period ( $w_1 t_2$ ) for steel on

for steel on steel (fig. 4.4 and 4.5) are seen to lie between dimensionless values of 2.4 and 2.9 whereas the upper bound (negative damping) model predicts values in excess of 3.142 and the lower bound (Blok) model predicts values in excess of 1.57. The range of error for the predictions of the negative damping model theory is +27.5% to +12%, and for the Blok model -70% to -17% deviation between predicted and experimental values is seen.

Similarly for the cast iron results, the upper bound theory predicts  $w_1 t_2$  values between 12% and 35% greater than experiment, and the lower bound theory predicts  $w_1 t_2$  values 7% to 40% less than found experimentally (see figs 4.12 and 13).

For the deceleration time period ( $w_1 t_3$ ) the negative damping model theory shows good agreement with experimental results for both materials used (figs. 4.7 and 15). This is not so for the Blok model theory (figs. 4.6 and 14) where the experimental results show positive and negative error compared to theory.

These two properties combined produce the normalised slip frequency relationships of figs. 4.8, 9, 16 and 17. As would be expected from the foregoing results the experimental slip frequencies lie between the theoretical predictions of the two theories for both materials used.

For steel on steel the negative damping theory predicts slip frequencies between 4% and 17% less than practical results, the Blok theory overpredicting by 7% to 40% (figs. 4.8 and 4.9).

Similarly, figs. 4.16 and 17 indicate a prediction between 2% and 20% less than experimental results for negative damping model, cast iron on cast iron and an 8% to 45% overprediction for the Blok model theory.

More significant perhaps is the general distribution of the experimental points rather than their percentage error from theory. In all cases, for the negative damping model theory, although deviation from theory undoubtedly exists, the distribution of the experimental results follows generally the shape of the theoretical line. In the case of the Blok model however the correlation between theory and experiment deviates considerably from point to point.

Considering now the maximum slip velocity as a function of drive velocity as shown in fig. 4.10, 11, 18 and 19. For the steel on steel results (figs. 5.10 and 11) the Blok model theoretical predictions show close agreement with experimental values compared with the negative damping model theory. Reasonable agreement occurs between the latter theory and experimental results at values of  $C_1$  less than 0.4 but deviation occurs for values of  $C_1$  greater than 0.4. The experimental slip velocities in this region are generally greater than those predicted by the negative damping theory.

For the cast iron results however (figs. 4.18 and 19) neither theory suggests itself as the more accurate in predicting maximum slip velocities. Isolated deviations from theory for

both models can be observed in the graphs but the main body of the results conforms reasonably to the theoretical predictions of both theories.

Therefore, the negative damping model is seen to be more accurate than the Blok model in representing the dynamic friction characteristic of mild steel and cast iron. Further exploration of this property, i.e. the dynamic gradient, was then undertaken by plotting experimental results in such a way as to examine the variation of dynamic gradient with system parameters. The tabular results of appendix I indicate little effect on dynamic gradient, of surface finish of the disc, and figs. 4.20 and 21 show the effect of normal load, system frequency and drive speed for surface finish values I, II and III. The first significant point to emerge from these results is the general constancy of the dynamic gradient values for drive speeds in excess of 0.1 rad/s (5 mm/s). For drive speeds slower than this, the dynamic gradient increases significantly for both cast iron and steel junctions. This coincides with results obtained by Burdekin and Bell (15) on a cast iron machine tool table, the increase in dynamic gradient occurring at speeds below 0.2 in/sec drive velocity.

The graphs of figs. 4.22 to 26 were constructed to enable the development of an empirical relationship between dynamic gradient and system parameters. The expressions serve to indicate the trend of dynamic gradient for variations in system parameters. Although the numerical values of dynamic gradient

for cast iron are lower than those of steel (hence making cast iron a better proposition for non-stick slip applications), the variation with system parameters is very similar for both materials. Both materials exhibit a dynamic gradient directly proportional to  $(KJ)^{0.4}$ , although since spring stiffness only was varied then this is the real relationship. Also proportionality to drive speed of the form

$$\frac{A}{(\text{normal load})^B}$$

(drive speed)

exists where  $A = 0.45$  for cast iron and  $0.35$  for steel;  $B = 0.2$  for cast iron and  $0.16$  for steel. This relationship is close enough to be considered the same for both materials.

The deviation between the two relationships lies in the proportionality of dynamic gradient to  $(\text{normal load})^C$ . For cast iron the value of  $C$  is  $0.25$ , for mild steel  $C$  is  $0.2$ . From these relationships, therefore, an indication of the variation dynamic  $C$  gradient is possible. Increase in dynamic gradient will ensue from an increase in normal load or spring stiffness or a decrease in drive velocity.

## 7.2 Transfer Lubricant Results

The theoretical stability relationships developed in section 2 suggest the mechanism of transfer lubrication to be two-fold. Dry lubricant, transferred to the metal friction junction, modifies that junction dynamic friction characteristic, whilst the dry lubricant compact, by contact with the metal disc, provides a viscous action, further contributing to the stick slip amplitude reduction. Whichever of the two linearised dynamic friction models is representative of the metal junction,

the positive viscous damping effect is theoretically indispensable in the process of stick slip elimination. Therefore, it was necessary to have a measure of the dry lubricant dynamic characteristic throughout the transfer lubricant tests. Literature survey and preliminary measurements indicated a kinetic friction force higher than static and increasing with sliding velocity, making the determination of lubricant dynamic friction characteristics impossible using the same technique as that to obtain the metal dynamic friction characteristics. Based upon the steady state measurements by Hemingray (17) and Lewis (25) a coulomb plus positive viscous damping model was suggested for the dry lubricant dynamic friction characteristics.

Amplitude response traces for an initial displacement of the disc subjected to dry lubricant loading enabled the components to be separated as shown in figs. 5.6 to 9. Dry lubricant measurements taken concurrently with modified metal junction characteristic measurements are presented in total, as a guide to the variation of dry lubricant properties with system parameters. Figs. 5.10 to 5.17 show both viscous and coulomb damping values to increase directly with normal load for all metal and lubricant combinations. It is impossible to distinguish the variation of coulomb damping due to surface finish, but the viscous component follows a definite trend. For both ptfе on steel and graphite on cast iron, surface finish II provides the highest viscous damping levels, with the ptfе on steel values the higher of the two.

In order to assess the validity of the dry lubricant properties some comparison with previously published data is desirable.

Thus the results of fig. 5.13 and 5.17 were converted to dynamic friction coefficients for comparison with the steady state results of refs. 17, 25 and 28. The coulomb damping components of figs. 5.13 and 17 are compared with steady state friction coefficients determined by O'Rourke for drive speeds of 0.01 m/s. Whilst exact correlation is not evident, nor would be anticipated, the general trend of the results is satisfactory. Similarly the variation of steady state friction coefficient with sliding velocity found by Hemingray and Lewis is compared with dynamic friction coefficients obtained from the coulomb and viscous damping results of fig. 5.13. This comparison shows the dynamic friction coefficients at zero velocity to be higher than those of the steady state results, the linearised slope of the dynamic model comparing favourably with steady state variations with sliding speed. Hence reasonable confirmation is provided for the coulomb and viscous components of dry lubricant dynamic damping determined in the circumstances of stick slip elimination.

The tables of fig. 5.2, 3 and 4 summarise the effectiveness of the transfer lubrication technique in eliminating stick slip vibrations. Generally, the graphite on cast iron and ptfе on steel combinations showed more success than graphite on steel and ptfе on cast iron. All the tests conducted with graphite on cast iron succeeded in eliminating the vibrations, those with ptfе on steel being also successful, apart from tests involving surface finish I at the higher normal loads (90N, 120N and 150N). Some success was found with graphite on steel and ptfе on cast iron, but mainly for high drive velocity and high system

frequency conditions. This would be anticipated, since these conditions tend to produce low amplitude vibrations in an unlubricated situation. For the low frequency low drive velocity conditions using ptfе on cast iron and graphite on steel no stick slip elimination was achieved.

Stability graphs representing modified metal dynamic friction characteristics against the positive viscous damping coefficient provided by the transfer lubricant are shown in figs. 5.22 to 33. Both theoretical relationships are used to assess the accuracy of each in predicting stability. Each graph contains results, both successful and unsuccessful in eliminating stick slip for normal loads up to 52N which was the limiting load of dry lubricant, viscous and coulomb damping determination.

From these graphs it can be seen that the negative damping model theory provides better stability predictions than the Blok model theory. The results plotted on the basis of the former theory also distinguish between successful and unsuccessful stick slip elimination, which is not so in the case of the latter theory. The negative damping theory does contain inaccuracies however, predicting damping values from 10% to 100% greater than those found necessary to eliminate vibrations experimentally. The accuracy of the Blok model theory is very limited and varies for different values of  $\psi$ . For high values of  $\psi$ , viscous damping predictions 100% greater than experimental are observed (e.g. graphite on cast iron, surface finish II, 0.2 rad/s drive speed, 36N normal load, fig. 5.25). At low values of  $\psi$  predictions of

7 times the actual viscous damping values found in practice can be seen (graphite on cast iron, surface finish I, 0.08 rad/s drive speed, 48N normal load, fig. 5.26).

A recent analog simulation by Cockerham and Cole (29) examined the stability relationship brought about by the action of viscous damping upon stick-slip vibrations induced by non-linear dynamic friction characteristics. Blok and negative damping linearised theories were used to present the results, which indicate three distinct stability conditions. The first condition is brought about by viscous damping sufficient to cause the slip velocity to continuously decay to the system drive velocity; the second occurs when additional damping produces one slip velocity oscillation reducing to drive velocity and the third condition is produced when the slip velocity immediately attains the drive velocity of the system. The experimental stability relationships of 5.22 to 33 show close proximity to the first condition of stability found in figs. 8 and 9 of the above paper.

The results of figs. 5.34 and 35 demonstrate the point at which stick slip elimination occurs, to be a function of distance rather than time. Results taken for drive speeds where the metal to metal dynamic gradient is constant indicate also that the lubricant and metal combination exhibiting the highest viscous damping eliminates stick slip in the shortest distance. Wear test results shown in figs. 5.36 and 37 indicate the volume wear of the dry lubricant to be a function of sliding distance and directly proportional to normal load. This suggests that the

reduction of the metal dynamic friction characteristic is dependent upon the volume of dry lubricant transferred to the metal junction. Further tests examining the effect of increasing the stick slip junction normal load relative to the dry lubricant normal load demonstrated the limiting load ratio at which stick slip elimination will not take place. This failure to eliminate vibrations is probably due to the metal friction normal pressure causing plastic deformation of the asperities at the stick slip junction, thus denying access of the transferred lubricant to that junction.

The effect of oil contamination upon the effectiveness of transfer lubrication is outlined in chapter 6. Tests performed with the same system parameters which had produced vibration elimination under chemically clean conditions, showed graphite upon cast iron to be effective in producing stability with Shell Tellus 33 oil contamination (fig. 6.1). This was not so for ptfе on steel however, which showed very little reduction in stick-slip amplitude (fig. 6.2). Of the two factors contributing to the mechanism of stick-slip elimination figs. 6.3 and 6.4 demonstrate the reduction of the metal friction characteristic as opposed to the viscous damping of the dry lubricant to be adversely affected by the oil contamination. This is confirmed by the volume wear tests of fig. 6.5 which show considerable reduction in wear of ptfе on steel with oil contamination compared with the non-contaminated tests of fig. 5.37. A transfer lubricant compact made from 'Vespel' proved to be an adequate substitute for the ptfе, causing stick slip stability in the oil contaminated steel tests as indicated in figs. 6.7 and 8.

## CONCLUSIONS

Transfer lubrication has been shown to be successful in eliminating stick slip vibrations, particularly for p.t.f.e. lubricating a steel junction and graphite transferred to a cast iron junction. However, for graphite on steel and p.t.f.e. on C.I. isolated successes were observed but, in general stick slip vibrations were not eliminated. For the combinations of lubricant and metal junction successful in producing stability a limiting ratio of stick slip junction normal load to dry lubricant normal load was definable. In the presence of oil as a contaminant, p.t.f.e. on steel failed to induce stability, but the action of graphite acting on cast iron was not unduly affected. The use of 'Vespel' as a lubricant acting on steel was found to be successful in eliminating stick slip vibrations.

Comparison of the experimental results with two theories based upon linearised unlubricated dynamic friction models showed a better correlation with the negative damping model theory than the Blok model theory. In addition the stability criterion based upon the metal to metal characteristic being modified by transferred lubricant together with the viscous damping effects of the transfer lubricant also proved more accurate using the negative damping dynamic friction model than the Blok model.

Dynamic viscous damping levels for p.t.f.e. on cast iron and

steel obtained from a coulomb plus viscous friction model compare favourably with steady state results obtained by Hemingray (17) and Lewis (25).

## REFERENCES

1. G.J. WOLF, 'Stick-Slip and Machine Tools', Jnl.American Soc.Lub.Engrs. Vol.21, No.7 (1965).
2. H. CATLING, 'Stick-Slip Friction as a Cause of Torsional Vibrations in Textile Drafting Rollers', Proc.Instn.Mech. Engrs., 174, 17 (1960).
3. G. HARRIS, 'Bearing Investigations in Wire Galvanising Tanks', Undergraduate Project, Sheffield Polytechnic (1975).
4. P.J. THOMPSON, 'The Hydrostatic Extrusion of Steel', UKAEA TRG 1664 (5) (1970).
5. S. THOMAS, Phil.Mag., Vol.9, p.329 (1930).
6. F.P. BOWDEN & L. LEBEN, 'The Nature of Sliding and the Analysis of Friction', Proc.Roy.Soc.A, 169 (1939).
7. F. MORGAN, M. MUSKAT & D.W. REED, 'Friction Phenomena and the Stick Slip Process', J.Appl.Phys., 12 (1941).
8. E. RABINOWICZ, 'The Intrinsic Variables Affecting the Stick Slip Process', Proc.Phys.Soc., 71, (1958).
9. I.V. KRAGELLSKII, 'Friction and Wear', Butterworths, published 1965.
10. H. BLOK, 'Fundamental Mechanical Aspects of Boundary Lubrication', Society of Automotive Engineers, New York (1940).
11. B.V. DERJAGUIN, V.E. PUSH & D.M. TOLSTOI, 'A Theory of Stick-Slip Sliding of Solids', Proc.Conf.Lubrication and Wear, I.Mech.E., B (1957).
12. C.A. BROCKLEY, R. CAMERON & A.F. POTTER, 'Friction Induced Vibration', Jnl.Lub.Tech. (April 1967).

13. A.K. BANNERJEE, 'Influence of Kinetic Friction on the Critical Velocity of Stick Slip Motion', Wear, 12 (1968).
14. G.R. SYMMONS, 'Dry Frictional Characteristics and Macroscopic Slip Motion during Stick Slip Oscillations', Ph.D. Thesis, University of Manchester (1969).
15. R. BELL & M. BURDEKIN, 'A Study of the Stick Slip Motion of Machine Tool Feed Drives', Proc.Instn.Mech.Engrs., Vol.184, Pt.1, No.30(1969-70).
16. R. BELL & M. BURDEKIN, 'Dynamic Behaviour of Plain Slideways', Proc.Instn.Mech.Engrs., Vol.181, Pt.1, No.8, (1966-67).
17. C.P. HEMINGRAY, 'The Friction and Wear of Plastics with Special Reference to Machine Tool Slideways', M.T.D.R. Conf., paper 23 (1970).
18. M. BURDEKIN, A. COWLEY & C.P. HEMINGRAY, 'Wear of Slideways', Tribology, (Feb 1971).
19. A.S. LAPIDUS, 'Wear of Plastics for Machine Tool Slideways', Machines and Tooling, Vol.32, No.12.
20. M.J. DEVINE, E.R. LAMSON & J.H. BOWER Jnr, 'Anti-Friction Bearing Design Considerations for Solid Lubrication', A.S.M.E. 63-M.D.-43 (May 1963).
21. A.C. WOOD, 'Bonding Methods for Dry Film Lubricants', Engg. Matls. and Design, (July 1971).
22. J.K. LANCASTER, 'Lubrication by Transferred Films of Solid Lubricants', A.S.L.E. trans.8, (1965).
23. J.K. LANCASTER, 'Composite Self Lubricating Bearing Materials', Proc.Instn.Mech.Engrs., Vol.182, Pt.1, No.2 (1967-8).

24. J.K. LANCASTER, 'Self-lubricating Composites for Bearings', C.M.E. (March 1968).
25. R.B. LEWIS, 'Predicting Bearing Performance of Filled Teflon T.F.E. Resin', Journal of Engineering for Industry (1967).
26. G. COCKERHAM & M. COLE, 'Analog Simulation of Mechanical Stick Slip', Int.Jnl. Math.Educ.Sci.Tech., Vol.5 (1974).
27. C. KENNEDY, 'Measuring the Coulomb and Viscous Components of Friction', Instruments, Vol.15, (Oct.1942).
28. J.T. O'ROURKE, 'Fundamentals of Friction, PV and Wear of Fluorocarbon Resins', Modern Plastics, Vol.43, No.1 (1965).
29. G. COCKERHAM & M. COLE, 'Stick Slip Stability by Analogue Simulation', Wear, Vol.36, No.2, pp.189-198. (1976)
30. A.B. CREASE, 'Design Data for the Wear Performance of Rubbing Bearing Surfaces', Tribology (1973).
31. R.C. BOWERS & W.A. ZISMAN, 'Frictional Properties of Polymers', Modern Plastic (Dec. 1963).

APPENDIX I : UNLUBRICATED STICK SLIP - TABLES OF RESULTS

Cast iron on cast iron

System frequency = 13.7 Hz normal load = 60N

Surface finish II drive speed = 0.35 rad/s

time	test number	TS(Nm)	TK(Nm)	$\dot{\theta}_{max}$ (r/s)	$C_F$ (Nm/rad/s)	$w_1 t_2$ (rad)	$w_1 t_3$ (rad)	Vibn. Amp. (rad)
1/2 min	1	0.91	0.76	0.61	0.245	2.6	1.95	0.01
	2	0.89	0.68	0.75	0.278	2.55	1.9	0.012
	3							
2 min	1	1.52	1.25	1.28	0.214	2.6	1.95	0.02
	2	1.11	0.76	1.15	0.216	2.65	1.9	0.019
	3							
4 min	1	1.12	0.80	1.42	0.217	2.65	1.95	0.021
	2	1.49	1.22	1.27	0.214	2.65	1.95	0.017
	3							
14 min	1	1.45	1.09	1.62	0.22	2.65	1.95	0.023
	2	1.43	1.11	1.53	0.21	2.6	1.95	0.021
	3							
	1							
	2							
	3							
	1							
	2							
	3							

Cast iron on cast iron

System frequency = 6.6Hz

Normal load = 20N

Surface finish II

Drive speed = 0.08rad/s

time	test number	TS(Nm)	TK(Nm)	$\dot{\theta}_{max}$ (r/s)	$C_F$ (Nm/rad /s)	$w_1 t_2$ (rad)	$w_1 t_3$ (rad)	Vibn. Amp. (rad)
1 min	1	0.304	0.233	0.42	0.17	2.8	1.95	0.017
	2	0.464	0.412	0.39	0.135	2.75	1.95	0.012
	3							
3 min	1	0.71	0.61	0.78	0.127	2.8	1.9	0.025
	2	0.68	0.59	0.765	0.122	2.75	1.95	0.022
	3							
5 min	1	0.63	0.53	0.8	0.126	2.75	1.95	0.024
	2	0.49	0.395	0.74	0.128	2.8	2.0	0.023
	3							
	1							
	2							
	3							
	1							
	2							
	3							
	1							
	2							
	3							

Handwritten text at the top of the page, possibly a title or header, which is mostly illegible due to fading and bleed-through.

The main body of the page contains a large grid of handwritten text, organized into columns and rows. The grid is formed by faint, dotted lines. The text within the grid is extremely faint and mostly illegible, appearing as light grey or black marks on the white background. It seems to be a ledger or account book with multiple columns for data entry.

Cast iron on cast iron

System frequency = 6.6Hz

normal load = 20N

Surface finish II

drive speed = 0.02rad/s

time	test number	TS(Nm)	TK(Nm)	$\dot{\theta}_{max}$ (r/s)	$C_F$ (Nm/rad /s)	$w_{1t_2}$ (rad)	$w_{1t_3}$ (rad)	Vibn. Amp. (rad)
½ min	1	0.304	0.236	0.36	0.19	2.75	1.85	0.015
	2	0.315	0.224	0.42	0.215	2.75	1.8	0.02
	3							
2 min	1	0.742	0.64	0.61	0.172	2.8	1.8	0.024
	2	0.784	0.68	0.586	0.178	2.75	1.85	0.028
	3							
	1							
	2							
	3							
6 min	1	0.8	0.69	0.6	0.176	2.75	1.85	0.028
	2	0.75	0.65	0.58	0.174	2.75	1.8	0.027
	3							
	1							
	2							
	3							
	1							
	2							
	3							



Cast iron on cast iron

System frequency = 6.6Hz

Normal Load = 20N

Surface Finish I

Drive speed = 0.02rad/s

time	test number	TS(Nm)	TK(Nm)	$\dot{\theta}_{max}$ (r/s)	$C_F$ (Nm/rad /s)	$w_{1t2}$ (rad)	$w_{1t3}$ (rad)	Vibn. Amp. (rad)
1 min	1	0.52	0.43	0.46	0.2	2.65	1.9	0.021
	2	0.37	0.29	0.43	0.19	2.65	1.95	0.019
	3							
2 min	1	0.73	0.62	0.625	0.177	2.6	1.9	0.027
	2	0.62	0.505	0.64	0.172	2.6	1.95	0.029
	3							
4 min	1	0.9	0.79	0.63	0.176	2.65	1.95	0.028
	2	1.0	0.89	0.65	0.175	2.6	1.95	0.028
	3							
	1							
	2							
	3							
	1							
	2							
	3							
	1							
	2							
	5							



Cast iron on cast iron

System frequency = 6.6Hz

Normal load = 10N

Surface finish I

Drive speed = 0.02rad/s

time	test number	TS(Nm)	TK(Nm)	$\dot{\theta}_{max}$ (r/s)	$C_F$ (Nm/rad/s)	$w_{12}$ (rad)	$w_{13}$ (rad)	Vibn. Amp. (rad)
½ min	1	0.21	0.16	0.24	0.21	2.7	1.9	0.012
	2	0.17	0.125	0.25	0.18	2.65	1.85	0.011
	3							
2 min	1	0.27	0.213	0.36	0.157	2.7	1.95	0.014
	2	0.295	0.240	0.34	0.164	2.65	1.9	0.013
	3							
4½ min	1	0.337	0.277	0.374	0.159	2.65	1.85	0.014
	2	0.312	0.256	0.35	0.161	2.6	1.9	0.014
	3							
	1							
	2							
	3							
	1							
	2							
	3							
	1							
	2							
	3							

steel on steel

system frequency 10Hz normal load 60N

surface finish, I drive speed 0.08 rad/s

time	test number	TS(Nm)	TK(Nm)	$\theta_{max}$ (r/s)	CF (Nm/rad/s)	$w_{1t2}$ (rad)	$w_{1t3}$ (rad)	Vibn. Amp. (rad)
0 min	1	2.15	1.87	0.98	0.285	2.55	1.95	0.034
	2	2.92	2.62	1.12	0.265	2.65	1.9	0.032
	3							
2 min	1	2.62	2.33	1.06	0.268	2.70	1.8	0.038
	2	2.32	2.04	1.02	0.272	2.65	1.85	0.035
	3							
3 min	1	2.55	2.27	1.04	0.27	2.65	1.9	0.056
	2	2.65	2.38	1.00	0.272	2.65	1.95	0.039
	3							
	1							
	2							
	3							
	1							
	2							
	3							
	1							
	2							
	3							

1041-100 (Rev. 10-1-80)

Form 1041-100 (Rev. 10-1-80)

1041-100 (Rev. 10-1-80)

Form 1041-100 (Rev. 10-1-80)

Line	Description	Amount
1		
2		
3		
4		
5		
6		
7		
8		
9		
10		
11		
12		
13		
14		
15		
16		
17		
18		
19		
20		
21		
22		
23		
24		
25		
26		
27		
28		
29		
30		
31		
32		
33		
34		
35		
36		
37		
38		
39		
40		
41		
42		
43		
44		
45		
46		
47		
48		
49		
50		
51		
52		
53		
54		
55		
56		
57		
58		
59		
60		
61		
62		
63		
64		
65		
66		
67		
68		
69		
70		
71		
72		
73		
74		
75		
76		
77		
78		
79		
80		
81		
82		
83		
84		
85		
86		
87		
88		
89		
90		
91		
92		
93		
94		
95		
96		
97		
98		
99		
100		

Cast iron on cast iron

System frequency = 6.6Hz

Normal load = 20N

Surface finish III

Drive speed = 0.02rad/s

time	test number	TS(Nm)	TK(Nm)	$\dot{\theta}_{max}$ (r/s)	$C_F$ (Nm/rad/s)	$w_{12}$ (rad)	$w_{13}$ (rad)	Vibn. Amp. (rad)
½ min	1	0.53	0.45	0.35	0.22	2.6	1.95	0.018
	2	0.54	0.48	0.295	0.205	2.6	1.9	0.014
	3							
2 min	1	0.88	0.77	0.63	0.175	2.65	1.9	0.026
	2	0.72	0.613	0.61	0.176	2.65	1.9	0.025
	3							
4 min	1	0.85	0.74	0.622	0.177	2.65	1.95	0.028
	2	0.78	0.67	0.619	0.174	2.65	1.9	0.026
	3							
	1							
	2							
	3							
	1							
	2							
	3							
	1							
	2							
	3							

Cast iron on cast iron

System frequency = 6.6Hz

Normal load = 120N

Surface finish 20CLA

Drive speed = 0.08rad/s

time	test number	TS(Nm)	TK(Nm)	$\dot{\theta}_{max}$ (r/s)	$C_f$ (Nm/rad/s)	$w_1 t_2$ (rad)	$w_1 t_3$ (rad)	Vibn. Amp. (rad)
1/2 min	1	3.22	2.67	2.62	0.21	2.7	1.9	0.12
	2	2.14	1.77	1.94	0.19	2.7	1.85	0.09
	3							
5 min	1	2.56	2.23	2.04	0.16	2.65	1.9	0.08
	2	2.84	2.5	2.1	0.162	2.7	1.9	0.094
	3							
10 min	1	2.90	2.56	2.16	0.16	2.6	1.95	0.085
	2	2.83	2.5	2.04	0.159	2.6	2.05	0.075
	3							
	1							
	2							
	3							
	1							
	2							
	3							
	1							
	2							
	3							



Cast iron on cast iron

System frequency = 13.7Hz

Normal load = 120N

Surface finish II

Drive speed = 0.5rad/s

time	test number	TS(Nm)	TK(Nm)	$\dot{\theta}_{max}$ (r/s)	$C_F$ (Nm/rad/s)	$w_{t2}$ (rad)	$w_{t3}$ (rad)	Vibn. Amp. (rad)
0 min	1	2.64	2.13	1.95	0.26	2.65	1.95	0.028
	2	2.46	2.05	1.74	0.235	2.6	1.95	0.021
	3							
1 min	1	3.05	2.52	2.4	0.22	2.6	2.05	0.032
	2	2.57	2.13	2.19	0.2	2.6	2.0	0.030
	3							
3 min	1	3.32	2.8	2.46	0.214	2.65	1.95	0.031
	2	2.88	2.4	2.32	0.207	2.65	2.0	0.029
	3							
	1							
	2							
	3							
	1							
	2							
	3							
	1							
	2							
	3							



Cast iron on cast iron

System frequency = 13.7Hz

Normal load = 10N

Surface finish I

Drive speed = 0.2rad/s

time	test number	TS(Nm)	TK(Nm)	$\dot{\theta}_{max}$ (r/s)	$C_F$ (Nm/rad/s)	$w_{1t2}$ (rad)	$w_{1t3}$ (rad)	Vibn. Amp. (rad)
½ min	1	0.32	0.24	0.40	0.20	2.65	1.85	0.006
	2	0.21	0.17	0.23	0.174	2.6	1.95	0.01
	3							
2 min	1	0.242	0.18	0.36	0.173	2.65	1.95	0.006
	2	0.216	0.158	0.324	0.177	2.75	1.95	0.008
	3							
5 min	1	0.305	0.244	0.35	0.172	2.75	1.95	0.01
	2	0.284	0.275	0.335	0.176	2.65	1.95	0.01
	3							
	1							
	2							
	3							
	1							
	2							
	3							
	1							
	2							
	3							



Cast iron on cast iron

System frequency = 6.6Hz

Normal load = 120N

Surface finish III

Drive speed = 0.02rad/s

time	test number	TS(Nm)	TK(Nm)	$\dot{\theta}_{max}$ (r/s)	$C_F$ (Nm/rad/s)	$w_{1t_2}$ (rad)	$w_{1t_3}$ (rad)	Vibn. Amp. (rad)
1 min	1	2.32	2.00	1.32	0.24	2.8	1.7	0.08
	2	2.84	2.52	1.36	0.235	2.85	1.7	0.08
	3							
2½ min	1	3.65	3.32	1.56	0.209	2.8	1.85	0.085
	2	3.73	3.45	1.48	0.202	2.85	1.75	0.07
	3							
4½ min	1	3.61	3.25	1.64	0.207	2.85	1.75	0.09
	2	3.27	2.97	1.42	0.205	2.85	1.8	0.08
	3							
	1							
	2							
	3							
	1							
	2							
	3							
	1							
	2							
	3							



Cast iron on cast iron

System frequency = 6.6Hz

Normal load = 60N

Surface finish II

Drive speed = 0.2rad/s

time	test number	TS(Nm)	TK(Nm)	$\dot{\theta}_{max}$ (r/s)	$C_F$ (Nm/rad/s)	$w_1 t_2$ (rad)	$w_1 t_3$ (rad)	Vibn. Amp. (rad)
½ min	1	1.11	0.96	0.88	0.17	2.6	1.95	0.055
	2	0.86	0.62	1.14	0.21	2.6	1.95	0.088
	3							
1 min	1	0.97	0.78	1.02	0.19	2.6	1.95	0.07
	2	0.92	0.68	1.5	0.16	2.55	1.95	0.088
	3							
2½ min	1	2.01	1.69	2.36	0.135	2.65	1.95	0.117
	2	1.71	1.40	2.21	0.139	2.65	1.95	0.118
	3							
6 min	1	2.02	1.69	2.38	0.138	2.9	1.9	0.128
	2	1.82	1.52	2.18	0.136	2.8	1.95	0.143
	3							
	1							
	2							
	3							
	1							
	2							
	3							



Cast iron on cast iron

System frequency = 10Hz

Normal load = 20N

Surface finish III

Drive speed = 0.08rad/s

time	test number	TS(Nm)	TK(Nm)	$\dot{\theta}_{max}$ (r/s)	$C_F$ (Nm/rad/s)	$w_1 t_2$ (rad)	$w_1 t_3$ (rad)	Vibn. Amp. (rad)
½ min	1	0.63	0.54	0.35	0.26	2.35	2.05	0.015
	2	0.52	0.44	0.33	0.24	2.65	1.95	0.01
	3							
3 min	1	0.82	0.72	0.52	0.195	2.6	1.95	0.013
	2	0.63	0.54	0.463	0.199	2.65	1.9	0.012
	3							
9 min	1	0.93	0.82	0.54	0.196	2.6	1.9	0.012
	2	0.71	0.61	0.49	0.199	2.65	1.9	0.011
	3							
	1							
	2							
	3							
	1							
	2							
	3							
	1							
	2							
	3							







Section 1: Introduction

This document is a preliminary report on the project.

Date	Time	Location	Activity	Remarks
10/01/2023	08:00	Site A	Initial Survey	Established base point.
10/02/2023	09:00	Site B	Topographic Survey	Completed contouring.
10/03/2023	07:30	Site A	Photogrammetry	Collected aerial photos.
10/04/2023	10:00	Site C	Ground Control Points	Marked and measured GCPs.
10/05/2023	08:30	Site A	Data Processing	Started software processing.
10/06/2023	09:30	Site B	Quality Check	Reviewed field notes.
10/07/2023	08:00	Site A	Report Writing	Drafting the final report.
10/08/2023	09:00	Site C	Final Review	Checked all data and maps.
10/09/2023	08:30	Site A	Project Closure	Finalized all documents.

Cast iron on cast iron

System frequency = 10Hz

Normal load = 10N

Surface finish I

Drive speed = 0.02rad/s

time	test number	TS(Nm)	TK(Nm)	$\dot{\theta}_{max}$ (r/s)	$C_F$ (Nm/rad/s)	$w_{1t_2}$ (rad)	$w_{1t_3}$ (rad)	Vibn. Amp. (rad)
1 min	1	0.216	0.17	0.15	0.31	3.0	1.9	0.006
	2	0.302	0.245	0.22	0.26	3.0	1.8	0.01
	3							
4 min	1	0.306	0.246	0.26	0.23	2.90	1.85	0.01
	2	0.306	0.256	0.23	0.22	2.90	1.9	0.01
	3							
10 min	1	0.317	0.263	0.24	0.225	2.95	1.85	0.01
	2	0.291	0.242	0.216	0.2285	2.9	1.9	0.006
	3							
	1							
	2							
	3							
	1							
	2							
	3							
	1							
	2							
	3							



Cast iron on cast iron

System frequency = 6.6Hz

Normal load = 60N

Surface finish II

Drive speed = 0.02rad/s

time	test number	TS(Nm)	TK(Nm)	$\dot{\theta}_{max}$ (r/s)	$C_F$ (Nm/rad/s)	$w_{1t_2}$ (rad)	$w_{1t_3}$ (rad)	Vibn. Amp. (rad)
½ min	1	1.32	1.12	0.71	0.28	2.65	1.75	0.07
	2	1.01	0.88	0.51	0.263	2.65	1.75	0.047
	3							
1½ min	1	1.21	1.02	0.73	0.26	2.65	1.7	0.07
	2	0.87	0.69	0.71	0.253	2.65	1.7	0.062
	3							
3 min	1	2.07	1.84	1.13	0.202	2.75	1.7	0.086
	2	1.77	1.57	0.99	0.199	2.65	1.75	0.078
	3							
6 min	1	2.18	1.94	1.19	0.2	2.65	1.75	0.088
	2	1.84	1.62	1.06	0.205	2.65	1.75	0.081
	3							
	1							
	2							
	3							
	1							
	2							
	3							

# Mathematical Analysis

Chapter 1: Introduction to Real Analysis

Section	Topic	Key Concepts
1.1	Real Numbers	Completeness, Archimedean Property
1.2	Set Theory	Countability, Cardinality
1.3	Topology	Open and Closed Sets, Compactness
1.4	Continuity	Intermediate Value Theorem, Uniform Continuity
1.5	Derivatives	Differentiability, Mean Value Theorem
1.6	Integration	Riemann Integration, Fundamental Theorem of Calculus
1.7	Series	Convergence, Power Series
1.8	Measure Theory	Lebesgue Measure, Integration
1.9	Advanced Topics	Fractal Dimension, Hausdorff Measure

Cast iron on cast iron

System frequency = 6.6Hz

Normal load = 60N

Surface finish III

Drive speed = 0.02rad/s

time	test number	TS(Nm)	TK(Nm)	$\dot{\theta}_{max}$ (r/s)	$C_F$ (Nm/rad/s)	$w_{1t_2}$ (rad)	$w_{1t_3}$ (rad)	Vibn. Amp. (rad)
½ min	1	1.01	0.82	0.77	0.27	2.75	1.75	0.03
	2	0.83	0.66	0.65	0.261	2.75	1.75	0.048
	3							
1½ min	1	1.33	1.11	0.92	0.24	2.75	1.75	0.08
	2	1.52	1.33	0.71	0.27	2.75	1.75	0.07
	3							
4½ min	1	2.02	1.68	1.67	0.202	2.75	1.75	0.121
	2	1.51	1.24	1.41	0.198	2.75	1.7	0.1
	3							
15 min	1	1.72	1.4	1.58	0.20	2.7	1.75	0.115
	2	1.55	1.25	1.51	0.199	2.75	1.75	0.11
	3							
	1							
	2							
	3							
	1							
	2							
	3							

1. Simplify the expression:  $2x^2 + 3x - 4x^2 + 5x - 6$

2. Solve the equation:  $3x + 7 = 2x - 5$

Problem	Solution
1. Simplify the expression: $2x^2 + 3x - 4x^2 + 5x - 6$	$-2x^2 + 8x - 6$
2. Solve the equation: $3x + 7 = 2x - 5$	$x = -12$
3. Simplify the expression: $5x^2 - 3x + 2x^2 - 4x + 1$	$7x^2 - 7x + 1$
4. Solve the equation: $4x - 9 = 3x + 2$	$x = 11$
5. Simplify the expression: $6x^2 - 2x + 3x^2 - 5x + 4$	$9x^2 - 7x + 4$
6. Solve the equation: $5x + 12 = 4x - 8$	$x = -20$
7. Simplify the expression: $8x^2 - 4x + 1x^2 - 6x + 3$	$9x^2 - 10x + 3$
8. Solve the equation: $6x - 15 = 5x - 3$	$x = 12$
9. Simplify the expression: $9x^2 - 5x + 2x^2 - 7x + 6$	$11x^2 - 12x + 6$
10. Solve the equation: $7x + 18 = 6x - 4$	$x = -22$
11. Simplify the expression: $10x^2 - 6x + 3x^2 - 8x + 5$	$13x^2 - 14x + 5$
12. Solve the equation: $8x - 21 = 7x - 9$	$x = 12$
13. Simplify the expression: $11x^2 - 7x + 4x^2 - 9x + 7$	$15x^2 - 16x + 7$
14. Solve the equation: $9x + 24 = 8x - 6$	$x = -30$
15. Simplify the expression: $12x^2 - 8x + 5x^2 - 10x + 8$	$17x^2 - 18x + 8$
16. Solve the equation: $10x - 27 = 9x - 11$	$x = 16$
17. Simplify the expression: $13x^2 - 9x + 6x^2 - 11x + 9$	$19x^2 - 20x + 9$
18. Solve the equation: $11x + 30 = 10x - 13$	$x = -43$
19. Simplify the expression: $14x^2 - 10x + 7x^2 - 12x + 10$	$21x^2 - 22x + 10$
20. Solve the equation: $12x - 33 = 11x - 17$	$x = 16$

Cast iron on cast iron

System frequency = 10Hz

Normal load = 60N

Surface finish II

Drive speed = 0.02rad/s

time	test number	TS(Nm)	TK(Nm)	$\theta_{max}$ (r/s)	$C_F$ (Nm/rad/s)	$w_{1t2}$ (rad)	$w_{1t3}$ (rad)	Vibn. Amp. (rad)
1 min	1	0.72	0.48	0.65	0.37	2.9	1.9	0.03
	2	0.58	0.39	0.61	0.31	2.95	1.9	0.025
	3							
4 min	1	2.16	1.81	1.35	0.252	2.8	1.8	0.043
	2	1.75	1.42	1.27	0.258	2.75	1.85	0.04
	3							
15 min	1	1.82	1.49	1.3	0.253	2.85	1.85	0.04
	2	1.72	1.4	1.26	0.256	2.8	1.85	0.04
	3							
	1							
	2							
	3							
	1							
	2							
	3							
	1							
	2							
	3							



Cast iron on cast iron

System frequency = 10Hz

Normal load = 20N

Surface finish II

Drive speed = 0.35 rad/s

time	test number	TS(Nm)	TK(Nm)	$\dot{\theta}_{max}$ (r/s)	$C_F$ (Nm/rad/s)	$w_{1t_2}$ (rad)	$w_{1t_3}$ (rad)	Vibn. Amp. (rad)
½ min	1	0.52	0.44	0.47	0.17	2.6	1.95	0.09
	2	0.46	0.37	0.58	0.154	2.65	1.95	0.01
	3							
1½ min	1	0.74	0.622	0.86	0.137	2.75	1.95	0.014
	2	0.63	0.528	0.78	0.139	2.7	2.0	0.011
	3							
6 min	1	0.78	0.65	0.92	0.136	2.7	1.95	0.014
	2	0.78	0.67	0.81	0.134	2.7	2.0	0.012
	3							
	1							
	2							
	3							
	1							
	2							
	3							
	1							
	2							
	3							



Cast iron on cast iron

System frequency = 6.6Hz

Normal load = 120N

Surface finish I

Drive speed = 0.02rad/s

time	test number	TS(Nm)	TK(Nm)	$\dot{\theta}_{max}$ (r/s)	$C_F$ (Nm/rad/s)	$w_{1t_2}$ (rad)	$w_{1t_3}$ (rad)	Vibn. Amp. (rad)
1/2 min	1	3.3	2.93	1.46	0.26	2.95	1.95	0.10
	2	1.73	1.35	2.0	0.185	2.9	1.95	0.09
	3							
3 min	1	3.02	2.67	1.77	0.2	2.95	1.9	0.083
	2	2.82	2.43	1.85	0.21	2.9	1.9	0.09
	3							
5 min	1	3.16	2.78	1.82	0.204	2.95	1.85	0.1
	2	3.62	2.63	1.87	0.206	2.9	1.9	0.075
	3							
	1							
	2							
	3							
	1							
	2							
	3							
	1							
	2							
	3							



steel on steel

system frequency = 6.6Hz normal load = 20N

surface finish II drive speed = 0.02 rad/s

time	test number	TS(Nm)	TK(Nm)	$\dot{\theta}_{max}$ (r/s)	CF (Nm/rad/s)	$w_{1t_2}$ (rad)	$w_{1t_3}$ (rad)	Vibn. Amp. (rad)
1/2 min	1	1.04	0.92	0.72	0.165	2.3	2.1	0.032
	2	0.73	0.60	0.645	0.195	2.3	2.05	0.028
	3							
2 min	1	0.825	0.69	0.66	0.205	2.35	2.05	0.03
	2	0.795	0.667	0.645	0.198	2.35	2.0	0.028
	3							
3 min	1	0.947	0.811	0.68	0.2	2.4	2.0	0.029
	2	0.916	0.78	0.655	0.206	2.45	2.0	0.035
	3							
	1							
	2							
	3							
	1							
	2							
	3							
	1							
	2							
	3							

Date	Description	Debit	Credit	Balance
1900				
1901				
1902				
1903				
1904				
1905				
1906				
1907				
1908				
1909				
1910				
1911				
1912				
1913				
1914				
1915				
1916				
1917				
1918				
1919				
1920				
1921				
1922				
1923				
1924				
1925				
1926				
1927				
1928				
1929				
1930				
1931				
1932				
1933				
1934				
1935				
1936				
1937				
1938				
1939				
1940				
1941				
1942				
1943				
1944				
1945				
1946				
1947				
1948				
1949				
1950				
1951				
1952				
1953				
1954				
1955				
1956				
1957				
1958				
1959				
1960				
1961				
1962				
1963				
1964				
1965				
1966				
1967				
1968				
1969				
1970				
1971				
1972				
1973				
1974				
1975				
1976				
1977				
1978				
1979				
1980				
1981				
1982				
1983				
1984				
1985				
1986				
1987				
1988				
1989				
1990				
1991				
1992				
1993				
1994				
1995				
1996				
1997				
1998				
1999				
2000				
2001				
2002				
2003				
2004				
2005				
2006				
2007				
2008				
2009				
2010				
2011				
2012				
2013				
2014				
2015				
2016				
2017				
2018				
2019				
2020				
2021				
2022				
2023				
2024				
2025				
2026				
2027				
2028				
2029				
2030				
2031				
2032				
2033				
2034				
2035				
2036				
2037				
2038				
2039				
2040				
2041				
2042				
2043				
2044				
2045				
2046				
2047				
2048				
2049				
2050				
2051				
2052				
2053				
2054				
2055				
2056				
2057				
2058				
2059				
2060				
2061				
2062				
2063				
2064				
2065				
2066				
2067				
2068				
2069				
2070				
2071				
2072				
2073				
2074				
2075				
2076				
2077				
2078				
2079				
2080				
2081				
2082				
2083				
2084				
2085				
2086				
2087				
2088				
2089				
2090				
2091				
2092				
2093				
2094				
2095				
2096				
2097				
2098				
2099				
2100				

steel on steel

system frequency = 6.6Hz normal load = 20N

surface finish. I drive speed = 0.2rad/s

time	test number	TS(Nm)	TK(Nm)	$\dot{\theta}_{max}$ (r/s)	CF (Nm/rad/s)	$w_1 t_2$ (rad)	$w_1 t_3$ (rad)	Vibn. Amp. (rad)
1/2 min	1	1.02	0.88	1.22	0.115	2.2	1.95	0.04
	2	0.75	0.622	0.94	0.136	2.3	1.9	0.036
	3							
3 min	1	0.933	0.805	0.98	0.13	2.3	1.95	0.042
	2	0.845	0.72	0.94	0.132	2.35	1.85	0.038
	3							
6 min	1	0.893	0.765	0.98	0.132	2.35	1.85	0.044
	2	0.933	0.80	1.04	0.128	2.4	1.85	0.04
	3							
	1							
	2							
	3							
	1							
	2							
	3							
	1							
	2							
	3							

THE UNIVERSITY OF CHICAGO  
DEPARTMENT OF CHEMISTRY

Run	Temp. (°C)	Time (min)	Pressure (mm Hg)	Flow Rate (ml/min)	Detector Response
1	100	10	100	1.0	0.1
2	100	20	100	1.0	0.2
3	100	30	100	1.0	0.3
4	100	40	100	1.0	0.4
5	100	50	100	1.0	0.5
6	100	60	100	1.0	0.6
7	100	70	100	1.0	0.7
8	100	80	100	1.0	0.8
9	100	90	100	1.0	0.9
10	100	100	100	1.0	1.0
11	100	110	100	1.0	0.9
12	100	120	100	1.0	0.8
13	100	130	100	1.0	0.7
14	100	140	100	1.0	0.6
15	100	150	100	1.0	0.5
16	100	160	100	1.0	0.4
17	100	170	100	1.0	0.3
18	100	180	100	1.0	0.2
19	100	190	100	1.0	0.1
20	100	200	100	1.0	0.0

steel on steel

system frequency = 6.6Hz normal load = 60N

surface finish II drive speed = 0.08rad/s

time	test number	TS(Nm)	TK(Nm)	$\dot{\theta}_{max}$ (r/s)	CF (Nm/rad/s)	$w_{1t_2}$ (rad)	$w_{1t_3}$ (rad)	Vibn. Amp. (rad)
1 min	1	2.16	1.87	1.74	0.165	2.25	2.0	0.08
	2	1.57	1.3	1.52	0.174	2.25	1.95	0.072
	3							
4 min	1	2.46	2.11	1.83	0.187	2.35	1.95	0.092
	2	2.63	2.2	2.21	0.192	2.35	1.90	0.096
	3							
8 min	1	2.25	1.94	1.66	0.189	2.3	1.95	0.085
	2	2.46	2.1	1.88	0.192	2.35	1.9	0.088
	3							
	1							
	2							
	3							
	1							
	2							
	3							
	1							
	2							
	3							



steel on steel

system frequency = 6.6Hz normal load = 60N

surface finish. I drive speed = 0.5rad/s

time	test number	TS(Nm)	TK(Nm)	$\dot{\theta}_{max}$ (r/s)	CF (Nm/rad/s)	$w_1 t_2$ (rad)	$w_1 t_3$ (rad)	Vibn. Amp. (rad)
1/2 min	1	1.73	1.34	2.45	0.16	2.2	2.1	0.095
	2	1.88	1.56	2.55	0.125	2.25	2.1	0.088
	3							
2 min	1	2.16	1.76	2.98	0.135	2.25	2.10	0.098
	2	2.63	2.24	2.83	0.138	2.25	1.95	0.102
	3							
5 min	1	2.33	1.92	2.99	0.137	2.2	2.1	0.095
	2	2.45	2.06	2.83	0.157	2.25	2.05	0.090
	3							
	1							
	2							
	3							
	1							
	2							
	3							
	1							
	2							
	3							

steel on steel

system frequency = 13.7Hz normal load = 10N

surface finish II drive speed = 0.2rad/s

time	test number	TS(Nm)	TK(Nm)	$\dot{\theta}_{max}$ (r/s)	CF (Nm/rad/s)	$w_1 t_2$ (rad)	$w_1 t_3$ (rad)	Vibn. Amp. (rad)
1 min	1	0.52	0.44	0.47	0.16	2.4	2.05	0.008
	2	0.38	0.314	0.36	0.184	2.45	2.0	0.008
	3							
3 min	1	0.46	0.382	0.42	0.185	2.4	2.05	0.010
	2	0.442	3.7	0.395	0.182	2.45	2.05	0.010
	3							
6 min	1	0.47	0.39	0.44	0.184	2.4	2.05	0.01
	2	0.455	0.38	0.415	0.186	2.5	2.0	0.011
	3							
	1							
	2							
	3							
	1							
	2							
	3							
	1							
	2							
	3							



steel on steel

system frequency = 10Hz normal load 10N

surface finish II dirve speed 0.08rad/s

time	test number	TS (Nm)	TK (Nm)	$\dot{\theta}_{max}$ (r/s)	CF (Nm/rad/s)	$w_{it_2}$ (rad)	$w_{it_3}$ (rad)	Vibn. Amp. (rad)
1 min	1	0.44	0.37	0.41	0.175	2.4	2.0	0.01
	2	0.325	0.255	0.385	0.18	2.45	2.0	0.008
	3							
3 min	1	0.465	0.38	0.43	0.192	2.45	2.0	0.012
	2	0.392	0.316	0.405	0.188	2.5	2.0	0.01
	3							
8 min	1	0.44	0.36	0.425	0.19	2.45	2.0	0.01
	2	0.465	0.38	0.45	0.188	2.45	2.0	0.01
	3							
	1							
	2							
	3							
	1							
	2							
	3							
	1							
	2							
	3							



steel on steel

system frequency 10Hz normal load = 20N

surface finish III drive speed 0.2rad/s

time	test number	TS(Nm)	TK(Nm)	$\dot{\theta}_{max}$ (r/s)	CF (Nm/rad/s)	$w_1 t_2$ (rad)	$w_1 t_3$ (rad)	Vibn. Amp. (rad)
1 min	1	0.63	0.565	0.475	0.135	2.6	1.9	0.01
	2	0.48	0.41	0.42	0.175	2.55	1.95	0.012
	3							
2½ min	1	0.94	0.81	0.73	0.178	2.55	1.95	0.014
	2	0.825	0.696	0.714	0.181	2.6	1.95	0.012
	3							
7 min	1	0.96	0.825	0.755	0.178	2.55	1.95	0.014
	2	0.865	0.735	0.72	0.18	2.6	1.9	0.012
	3							
	1							
	2							
	3							
	1							
	2							
	3							
	1							
	2							
	3							



steel on steel

system frequency 13.7Hz normal load 20N

surface finish II drive speed 0.35 rad/s

time	test number	TS(Nm)	TK(Nm)	$\dot{\theta}_{max}$ (r/s)	CF (Nm/rad/s)	$w_{1t2}$ (rad)	$w_{1t3}$ (rad)	Vibn. Amp. (rad)
1/2 min	1	0.99	0.86	0.715	0.175	2.65	2.1	0.008
	2	0.74	0.6	0.695	0.195	2.65	2.15	0.008
	3							
3 min	1	0.943	0.822	0.69	0.175	2.65	2.2	0.01
	2	0.965	0.836	0.715	0.18	2.7	2.15	0.01
	3							
5 min	1	0.875	0.75	0.695	0.177	2.65	2.15	0.01
	2	0.95	0.82	0.73	0.175	2.7	2.15	0.01
	3							
	1							
	2							
	3							
	1							
	2							
	3							
	1							
	2							
	3							

APPENDIX II : TRANSFER LUBRICANT DYNAMIC FRICTION  
COMPONENTS - TABLES OF RESULTS

Transfer lubricant characteristics

P.T.F.E. on mild steel

system frequency = 6.6 Hz normal load - 48N

surface finish I

Successive  
peak  
amplitudes  
(rad)

time (min)	$\frac{1}{2}$ min			7 min					
test number	1	2	3	1	2	3	1	2	3
1	0.362	0.346		0.383	0.371				
2	0.222	0.212		0.246	0.237				
3	0.114	0.108		0.136	0.129				
4	0.03	0.028		0.049	0.044				
5									
6									
7									
8									
9									
10									
D	0.25	0.25		0.3	0.3				
C (Nm/rad/s)	0.022	0.021		0.021	0.021				
T (Nm)	0.24	0.245		0.25	0.255				

Transfer lubricant characteristics

P.T.F.E. on mild steel

system frequency = 6.6 Hz normal load = 16N

surface finish III

time (min)	1 min			3 min			6 min		
	1	2	3	1	2	3	1	2	3
test number									
1	0.311	0.331		0.298	0.306		0.331	0.328	
2	0.243	0.262		0.24	0.247		0.26	0.258	
3	0.182	0.203		0.187	0.194		0.2	0.196	
4	0.128	0.149		0.14	0.146		0.145	0.141	
5	0.08	0.101		0.096	0.103		0.1	0.096	
6	0.038	0.058		0.056	0.064		0.056	0.051	
7		0.018		0.019	0.026		0.016	0.013	
8									
9									
10									
D	0.3	0.3		0.35	0.35		0.30	0.30	
C (Nm/rad/s)	0.01	0.012		0.008	0.008		0.01	0.011	
T (Nm)	0.12	0.122		0.10	0.108		0.121	0.12	

Successive  
peak  
amplitudes  
(rad)

Transfer lubricant characteristics

P.T.F.E. on mild steel

system frequency = 10 Hz normal load = 48N

surface Finish I

Successive  
peak  
amplitudes  
(rad)

time (min)	$\frac{1}{2}$ min			4 min					
test number	1	2	3	1	2	3	1	2	3
1	0.181	0.164		0.168	0.158				
2	0.123	0.106		0.11	0.102				
3	0.075	0.058		0.062	0.054				
4	0.033	0.017		0.021	0.016				
5									
6									
7									
8									
9									
10									
D	0.2	0.2		0.2	0.2				
C (Nm/rad/s)	0.21	0.02		0.022	0.021				
T (Nm)	0.24	0.23		0.25	0.23				

Transfer lubricant characteristics

P.T.F.E. on mild steel

system frequency = 10 Hz normal load = 24N

surface finish III

time (min)	1 min			7½ min					
	1	2	3	1	2	3	1	2	3
test number									
1	0.141	0.147		0.126	0.129				
2	0.111	0.116		0.097	0.101				
3	0.084	0.09		0.072	0.074				
4	0.059	0.065		0.049	0.053				
5	0.038	0.043		0.028	0.032				
6	0.018	0.023		0.01	0.013				
7									
8									
9									
10									
D	0.15	0.15		0.15	0.15				
C (Nm/rad/s)	0.014	0.015		0.015	0.014				
T (Nm)	0.165	0.17		0.16	0.17				

Transfer lubricant characteristics

P.T.F.E. on mild steel

system frequency = 13.7 Hz normal load = 8N

surface finish I

Successive  
peak  
amplitudes  
(rad)

time (min)	½ min			6 min					
test number	1	2	3	1	2	3	1	2	3
1	0.085	0.075		0.072	0.075				
2	0.079	0.069		0.064	0.066				
3	0.073	0.062		0.057	0.059				
4	0.067	0.056		0.05	0.052				
5	0.061	0.05		0.043	0.045				
6	0.056	0.049		0.037	0.039				
7	0.05	0.04		0.03	0.028				
8	0.045	0.034		0.024	0.022				
9	0.04	0.030		0.019	0.017				
10									
D	0.1	0.1		0.15	0.15				
C (Nm/rad/s)	0.006	0.007		0.008	0.006				
T (Nm)	0.06	0.065		0.07	0.06				

Transfer lubricant characteristics

P.T.F.E. on mild steel

system frequency = 13.7 Hz normal load = 52N

surface finish II

time (min)	1 min			10 min					
	1	2	3	1	2	3	1	2	3
Successive peak amplitudes (rad)	1	0.122	0.112		0.128	0.122			
	2	0.072	0.064		0.076	0.074			
	3	0.033	0.022		0.037	0.035			
	4	0.006			0.010	0.008			
	5								
	6								
	7								
	8								
	9								
	10								
D	0.1	0.1		0.1	0.1				
C (Nm/rad/s)	0.045	0.047		0.046	0.045				
T (Nm)	0.34	0.35		0.34	0.345				

Transfer lubricant characteristics

graphite on cast iron

system frequency = 13.7 Hz normal load = 20N

surface finish I

Successive  
peak  
amplitudes  
(rad)

time (min)	1 min			8 min					
test number	1	2	3	1	2	3	1	2	3
1	0.116	0.109		0.095	0.098				
2	0.101	0.095		0.079	0.081				
3	0.087	0.082		0.063	0.066				
4	0.074	0.069		0.048	0.049				
5	0.061	0.055		0.035	0.038				
6	0.049	0.045		0.021	0.024				
7	0.039	0.034							
8									
9									
10									
D	0.15	0.15		0.2	0.2				
C (Nm/rad/s)	0.01	0.012		0.011	0.01				
T (Nm)	0.14	0.145		0.14	0.151				

Transfer lubricant characteristics

graphite on cast iron

system frequency = 13.7 Hz normal load = 8N

surface finish II

time (min)	$\frac{1}{2}$ min			5 min			9 min		
	1	2	3	1	2	3	1	2	3
test number									
1	0.151	0.121		0.11	0.118		0.102	0.104	
2	0.119	0.108		0.094	0.098		0.089	0.089	
3	0.108	0.099		0.08	0.086		0.076	0.077	
4	0.097	0.087		0.067	0.073		0.065	0.066	
5	0.087	0.077		0.054	0.061		0.054	0.055	
6	0.078	0.069		0.043	0.05		0.044	0.044	
7	0.069	0.059		0.032	0.039		0.035	0.035	
8	0.062	0.053							
9									
10									
D	0.05	0.05		0.1	0.1		0.05	0.05	
C (Nm/rad/s)	0.012	0.013		0.013	0.013		0.012	0.013	
T (Nm)	0.06	0.065		0.058	0.06		0.06	0.065	

Successive  
peak  
amplitudes  
(rad)

Transfer lubricant characteristics

graphite on cast iron

system frequency = 6.6 Hz normal load = 48N

surface finish I

Successive  
peak  
amplitudes  
(rad)

time (min)	1 min			5½ min					
test number	1	2	3	1	2	3	1	2	3
1	0.463	0.481		0.549	0.531		0.483	0.488	
2	0.282	0.297		0.365	0.348		0.301	0.305	
3	0.131	0.149		0.217	0.202		0.151	0.158	
4	0.006	0.026		0.091	0.073		0.03	0.036	
5									
6									
7									
8									
9									
10									
D	0.65	0.65		0.65	0.65		0.6	0.6	
C (Nm/rad/s)	0.015	0.014		0.015	0.016		0.015	0.016	
T (Nm)	0.38	0.37		0.37	0.37		0.375	0.385	



Transfer lubricant characteristics

graphite on cast iron

system frequency = 6.6 Hz normal load = 16N

surface finish III

time (min)	$\frac{1}{2}$ min			7 min			$14\frac{1}{2}$ min		
test number	1	2	3	1	2	3	1	2	3
1	0.421	0.387		0.377	0.365		0.388		
2	0.354	0.322		0.314	0.303		0.322		
3	0.292	0.262		0.251	0.239		0.259		
4	0.234	0.206		0.196	0.185		0.204		
5	0.18	0.153		0.144	0.134		0.149		
6	0.13	0.104		0.095	0.084		0.101		
7	0.083	0.058		0.047	0.036		0.056		
8	0.039	0.015							
9									
10									
D	0.55	0.6		0.6	0.6		0.6		
C (Nm/rad/s)	0.006	0.006		0.0064	0.0064		0.006		
T (Nm)	0.13	0.133		0.132	0.13		0.13		

Successive  
peak  
amplitudes  
(rad)

Transfer lubricant characteristics

graphite on cast iron

system frequency = 6.6 Hz normal load = 48N

surface finish II

Successive  
peak  
amplitudes  
(rad)

time (min)	0 min			5½ min			9 min		
test number	1	2	3	1	2	3	1	2	3
1	0.431	0.443		0.507	0.499		0.489	0.501	
2	0.211	0.234		0.279	0.276		0.274	0.277	
3	0.057	0.089		0.12	0.121		0.119	0.118	
4				0.009	0.011		0.01	0.009	
5									
6									
7									
8									
9									
10									
D	0.3	0.25		0.25	0.25		0.25	0.25	
C (Nm/rad/s)	0.028	0.029		0.028	0.0285		0.029	0.028	
T (Nm)	0.36	0.37		0.37	0.365		0.37	0.37	

Transfer lubricant characteristics

graphite on cast iron

system frequency = 6.6 Hz normal load = 16N

surface finish II

time (min)	½ min			6 min			10 min		
	1	2	3	1	2	3	1	2	3
test number									
1	0.411	0.323		0.313	0.32		0.41	0.59	
2	0.371	0.290		0.281	0.287		0.369	0.348	
3	0.333	0.259		0.249	0.254		0.33	0.311	
4	0.299	0.23		0.221	0.225		0.295	0.276	
5	0.267	0.204		0.20	0.199		0.263	0.244	
6	0.238	0.18		0.172	0.177		0.234	0.215	
7	0.211	0.158		0.148	0.145		0.209	0.188	
8	0.186	0.137		0.127	0.125		0.184	0.165	
9	0.164	0.119		0.11	0.107				
10									
D	0.1	0.1		0.1	0.1		0.1	0.1	
C (Nm/rad/s)	0.007	0.007		0.007	0.007		0.0068	0.007	
T (Nm)	0.08	0.081		0.082	0.081		0.08	0.083	

Successive  
peak  
amplitudes  
(rad)

Transfer lubricant characteristics

graphite on mild steel

system frequency = 13.7 Hz normal load = 32N

surface finish II

time (min)	1 min			5 min					
	1	2	3	1	2	3	1	2	3
test number									
1	0.131	0.22		0.141	0.136				
2	0.058	0.114		0.067	0.063				
3	0.015	.048		0.024	0.020				
4		0.009							
5									
6									
7									
8									
9									
10									
D	0.05	0.05		0.05	0.05				
C (Nm/rad/s)	0.09	0.095		0.09	0.09				
T (Nm)	0.2	0.21		0.21	0.22				

Successive  
peak  
amplitudes  
(rad)

Transfer lubricant characteristics

graphite on mild steel

system frequency = 6.6 Hz normal load = 40N

surface finish I

Successive  
peak  
amplitudes  
(rad)

time (min)	1 min			5½ min			12 min		
test number	1	2	3	1	2	3	1	2	3
1	0.291	0.288		0.328	0.321		0.29	0.295	
2	0.181	0.180		0.204	0.2		0.18	0.183	
3	0.08	0.079		0.099	0.096		0.078	0.081	
4	0.010	0.009		0.012	0.01		0.009	0.012	
5									
6									
7									
8									
9									
10									
D	0.4	0.4		0.45	0.45		0.4	0.4	
C (Nm/rad/s)	0.015	0.015		0.016	0.155		0.015	0.016	
T (Nm)	0.24	0.255		0.245	0.265		0.245	0.24	



Transfer lubricant characteristics

P.T.F.E. on cast iron

system frequency (Hz) = 10 normal load (N) = 40

surface finish II

Successive  
peak  
amplitudes  
(rad)

time (min)	1 min			5 min			13 min		
test number	1	2	3	1	2	3	1	2	3
1	0.274	0.211		0.278	0.301				
2	0.198	0.147		0.194	0.199				
3	0.133	0.092		0.131	0.141				
4	0.078	0.045		0.072	0.078				
5	0.032			0.035	0.039				
6									
7									
8									
9									
10									
D	0.25	0.25		0.25	0.25				
C (Nm/rad/s)	0.02	0.021		0.021	0.022				
T (Nm)	0.29	0.3		0.294	0.287				

Transfer lubricant characteristics

P.T.F.E. on cast iron

system frequency = 13.7 Hz normal load = 40N

surface finish II

time (min)		$\frac{1}{2}$ min			6 min			14 min		
test number		1	2	3	1	2	3	1	2	3
Successive peak amplitudes (rad)	1	0.11	0.122		0.116	0.11		0.122		
	2	0.074	0.095		0.081	0.076		0.096		
	3	0.044	0.061		0.052	0.048		0.059		
	4	0.005	0.010		0.009	0.006		0.010		
	5									
	6									
	7									
	8									
	9									
	10									
	D	0.15	0.15		0.15	0.15		0.15		
	C (Nm/rad/s)	0.026	0.027		0.027	0.026		0.026		
	T (Nm)	0.28	0.285		0.28	0.28		0.285		

Transfer lubricant characteristics

graphite on cast iron

system frequency 10 Hz normal load = 48N

surface finish II

time (min)		1 min			4 min			9 min		
test number		1	2	3	1	2	3	1	2	3
Successive peak amplitudes (rad)	1	0.211	0.173		0.22	0.226		0.211	0.216	
	2	0.125	0.106		0.128	0.131		0.128	0.131	
	3	0.057	0.052		0.063	0.065		0.065	0.065	
	4	0.005	.010		0.009	0.008		0.008	0.008	
	5									
	6									
	7									
	8									
	9									
	10									
	D	0.2	0.15		0.21	0.2		0.2	0.2	
	C (Nm/rad/s)	0.03	0.029		0.032	0.031		0.032	0.031	
	T (Nm)	0.36	0.034		0.371	0.368		0.36	0.365	

Transfer lubricant characteristics

P.T.F.E. on cast iron

system frequency (Hz) = 6.6 normal load = 24N

surface finish II

time (min)	0 min			5 min			13 min		
test number	1	2	3	1	2	3	1	2	3
1	0.323	0.298	0.302	0.314	0.321		0.311	0.321	
2	0.244	0.221	0.231	0.233	0.239		0.236	0.251	
3	0.182	0.169	0.173	0.178	0.182		0.173	0.181	
4	0.113	0.102	0.110	0.105	0.111		0.115	0.119	
5	0.061	0.054	0.057	0.055	0.060		0.056	0.061	
6									
7									
8									
9									
10									
D	0.4	0.4	0.4	0.4	0.45		0.4	0.4	
C (Nm/rad/s)	0.0097	0.0093	0.0095	0.0095	0.087		0.0094	0.0096	
T (Nm)	0.144	0.138	0.14	0.146	0.152		0.146	0.146	

Successive  
peak  
amplitudes  
(rad)

Transfer lubricant characteristics

graphite on cast iron

system frequency (Hz) = 10 normal load = 20N

surface finish II

time (min)	0 min			6 min			12 min		
test number	1	2	3	1	2	3	1	2	3
1	0.182	0.191		0.217	0.226				
2	0.144	0.149		0.173	0.183				
3	0.116	0.122		0.140	0.142				
4	0.085	0.091		0.106	0.111				
5	0.059	0.055		0.077	0.08				
6	0.025	0.024		0.048	0.049				
7				0.023	0.024				
8									
9									
10									
D	0.3	0.3		0.25	0.25				
C (Nm/rad/s)	0.0114	0.012		0.013	0.012				
T (Nm)	0.161	0.155		0.159	0.161				

Successive  
peak  
amplitudes  
(rad)

P.T.F.E. on mild steel

system frequency = 6.6 Hz normal load = 16N

surface finish II

Successive  
peak  
amplitudes  
(rad)

time (min)	0 min			6 min			15 min		
test number	1	2	3	1	2	3	1	2	3
1	0.357	0.361	0.388	0.464	0.434		0.382	0.391	
2	0.274	0.283	0.292	0.341	0.351		0.29	0.299	
3	0.20	0.211	0.213	0.252	0.242		0.221	0.231	
4	0.14	0.143	0.148	0.178	0.172		0.141	0.144	
5	0.087	0.084	0.089	0.117	0.102		0.083	0.085	
6	0.037	0.041	0.045	0.065	0.061		0.041	0.043	
7				.022	0.23				
8									
9									
10									
D	0.2	0.2	0.22	0.22	0.25		0.2	0.21	
C (Nm/rad/s)	0.0148	0.015	0.016	0.0143	0.014		0.0146	0.141	
T (Nm)	0.117	0.122	0.130	.119	0.121		0.127	0.116	

Transfer lubricant characteristics

Graphite on mild steel

System frequency = 6.6 Hz Normal load = 32N

Surface finish III

time (min)	0 min			5 min			12 min			
test number	1	2	3	1	2	3	1	2	3	
Successive peak amplitudes (rad)	1	0.663	0.67		0.682	0.66		0.655	0.66	
	2	0.40	0.42		0.43	0.40		0.377	0.38	
	3	0.234	0.241		0.24	0.23		0.25	0.261	
	4	0.065	0.073		0.71	0.61		0.047	0.053	
	5									
	6									
	7									
	8									
	9									
	10									
D	0.4	0.4		0.38	0.4		0.4	0.4		
C (Nm/rad/s)	0.01	0.011		0.09	0.01		0.098	0.096		
T (Nm)	0.28	0.029		0.28	0.272		0.275	0.28		



Transfer lubricant characteristics

P.T.F.E. on cast iron

system frequency (Hz) = 10 normal load (N) = 8

surface finish II

time (min)	$\frac{1}{2}$ min			6 min			11 min		
test number	1	2	3	1	2	3	1	2	3
Successive peak amplitudes (rad)	1	0.182	0.172	0.175	0.177		0.185		
	2	0.164	0.154	0.155	0.159		0.165		
	3	0.147	0.136	0.138	0.139		0.149		
	4	0.132	0.12	0.118	0.128		0.135		
	5	0.117	0.105	0.101	0.111		0.119		
	6	0.103	0.091	0.09	0.095		0.106		
	7	0.089	0.077	0.075	0.081		0.091		
	8	0.077	0.064	0.060	0.069		0.076		
	9		0.052	0.050					
	10								
D	0.15	0.15	0.15	0.15			0.15		
C (Nm/rad/s)	0.007	0.0075	0.0072	0.0071			0.0073		
T (Nm)	0.06	0.061	0.06	0.062			0.06		

Transfer lubricant characteristics

P.T.F.E. on mild steel

system frequency = 13.7 Hz normal load = 24N

surface finish III

time (min)	1 min			4 min					
	1	2	3	1	2	3	1	2	3
Successive peak amplitudes (rad)	1	0.114	0.09		0.106	0.11			
	2	0.096	0.075		0.084	0.086			
	3	0.081	0.061		0.064	0.067			
	4	0.066	0.049		0.046	0.049			
	5	0.054	0.039		0.03	0.034			
	6	0.043	0.029		0.016	0.019			
	7	0.033							
	8								
	9								
	10								
D	0.05	0.05		0.1	0.1				
C (Nm/rad/s)	0.02	0.021		0.021	0.022				
T (Nm)	0.16	0.155		0.16	0.15				

Transfer lubricant characteristics

P.T.F.E. on cast iron

system frequency (Hz) = 6.6 normal load (N) = 8

surface finish II

time (min)	$\frac{1}{2}$ min			5 min			15 min		
	1	2	3	1	2	3	1	2	3
test number									
Successive peak amplitudes (rad)	1	0.125	0.178		0.143	0.128		0.126	0.161
	2	0.11	0.154		0.12	0.117		0.113	0.151
	3	0.092	0.139		0.102	0.099		0.091	0.134
	4	0.076	0.115		0.083	0.079		0.075	0.109
	5	0.058	0.104		0.067	0.062		0.059	0.091
	6	0.044	0.081		0.053	0.048		0.040	0.074
	7	0.032	0.070		0.037	0.037		0.032	0.065
	8	0.02	0.054		0.028	0.023		0.019	0.047
	9		0.039						0.029
	10								
D	0.2	0.2		0.2	0.2		0.2	0.2	
C (Nm/rad/s)	0.0045	0.0047		0.0043	0.0043		0.0044	0.0045	
T (Nm)	0.036	0.036		0.0351	0.0371		0.0345	0.036	

CONFIDENTIAL - SECURITY INFORMATION

CONFIDENTIAL - SECURITY INFORMATION

CONFIDENTIAL - SECURITY INFORMATION

Item	Description	Quantity	Unit	Value	Remarks
1	...	...	...	...	...
2	...	...	...	...	...
3	...	...	...	...	...
4	...	...	...	...	...
5	...	...	...	...	...
6	...	...	...	...	...
7	...	...	...	...	...
8	...	...	...	...	...
9	...	...	...	...	...
10	...	...	...	...	...
11	...	...	...	...	...
12	...	...	...	...	...
13	...	...	...	...	...
14	...	...	...	...	...
15	...	...	...	...	...
16	...	...	...	...	...
17	...	...	...	...	...
18	...	...	...	...	...
19	...	...	...	...	...
20	...	...	...	...	...
21	...	...	...	...	...
22	...	...	...	...	...
23	...	...	...	...	...
24	...	...	...	...	...
25	...	...	...	...	...
26	...	...	...	...	...
27	...	...	...	...	...
28	...	...	...	...	...
29	...	...	...	...	...
30	...	...	...	...	...
31	...	...	...	...	...
32	...	...	...	...	...
33	...	...	...	...	...
34	...	...	...	...	...
35	...	...	...	...	...
36	...	...	...	...	...
37	...	...	...	...	...
38	...	...	...	...	...
39	...	...	...	...	...
40	...	...	...	...	...
41	...	...	...	...	...
42	...	...	...	...	...
43	...	...	...	...	...
44	...	...	...	...	...
45	...	...	...	...	...
46	...	...	...	...	...
47	...	...	...	...	...
48	...	...	...	...	...
49	...	...	...	...	...
50	...	...	...	...	...
51	...	...	...	...	...
52	...	...	...	...	...
53	...	...	...	...	...
54	...	...	...	...	...
55	...	...	...	...	...
56	...	...	...	...	...
57	...	...	...	...	...
58	...	...	...	...	...
59	...	...	...	...	...
60	...	...	...	...	...
61	...	...	...	...	...
62	...	...	...	...	...
63	...	...	...	...	...
64	...	...	...	...	...
65	...	...	...	...	...
66	...	...	...	...	...
67	...	...	...	...	...
68	...	...	...	...	...
69	...	...	...	...	...
70	...	...	...	...	...
71	...	...	...	...	...
72	...	...	...	...	...
73	...	...	...	...	...
74	...	...	...	...	...
75	...	...	...	...	...
76	...	...	...	...	...
77	...	...	...	...	...
78	...	...	...	...	...
79	...	...	...	...	...
80	...	...	...	...	...
81	...	...	...	...	...
82	...	...	...	...	...
83	...	...	...	...	...
84	...	...	...	...	...
85	...	...	...	...	...
86	...	...	...	...	...
87	...	...	...	...	...
88	...	...	...	...	...
89	...	...	...	...	...
90	...	...	...	...	...
91	...	...	...	...	...
92	...	...	...	...	...
93	...	...	...	...	...
94	...	...	...	...	...
95	...	...	...	...	...
96	...	...	...	...	...
97	...	...	...	...	...
98	...	...	...	...	...
99	...	...	...	...	...
100	...	...	...	...	...

CONFIDENTIAL - SECURITY INFORMATION

Transfer lubricant characteristics

graphite on cast iron

system frequency = 13.7 Hz normal load = 36N

surface finish III

time (min)	$\frac{1}{2}$ min			4 min			10 min		
test number	1	2	3	1	2	3	1	2	3
1	0.121	0.13		0.101	0.106		0.119	0.122	
2	0.088	0.09		0.069	0.076		0.085	0.086	
3	0.059	0.069		0.039	0.045		0.056	0.055	
4	0.033	0.044		0.024	0.029		0.031	0.034	
5	0.011	0.02					0.01	0.011	
6									
7									
8									
9									
10									
D	0.15	0.15		0.15	0.15		0.15	0.15	
C (Nm/rad/s)	0.019	0.018		0.018	0.018		0.019	0.0185	
T (Nm)	0.29	0.29		0.28	0.291		0.28	0.028	

Successive  
peak  
amplitudes  
(rad)



Transfer lubricant characteristics

P.T.F.E. on mild steel

system frequency = 10 Hz normal load = 36N

surface finish II

time (min)	$\frac{1}{2}$ min			5 min					
	1	2	3	1	2	3	1	2	3
test number									
1	0.182	0.165		0.168	0.171				
2	0.117	0.103		0.115	0.118				
3	0.065	0.051		0.073	0.076				
4	0.022	0.010		0.039	0.044				
5				0.012	0.015				
6									
7									
8									
9									
10									
D	0.15	0.15		0.1	0.1				
C (Nm/rad/s)	0.028	0.029		0.027	0.028				
T (Nm)	0.22	0.235		0.22	0.23				

Successive  
peak  
amplitudes  
(rad)

Transfer lubricant characteristics

graphite on cast iron

system frequency (Hz) = 10 normal load (N) = 36

surface finish III

time (min)	1 min			5 min					
	1	2	3	1	2	3	1	2	3
test number									
1	0.173	0.180		0.18	0.171				
2	0.119	0.122		0.124	0.118				
3	0.069	0.072		0.074	0.067				
4	0.026	0.029		0.029	0.027				
5									
6									
7									
8									
9									
10									
D	0.35	0.35		0.35	0.35				
C (Nm/rad/s)	0.014	0.013		0.013	0.014				
T (Nm)	0.28	0.281		0.281	0.28				

Successive  
peak  
amplitudes  
(rad)

Transfer lubricant characteristics

graphite on mild steel

system frequency = 6.6 Hz normal load = 10N

surface finish II

time (min)	$\frac{1}{2}$ min			3 min			9 min		
	1	2	3	1	2	3	1	2	3
test number									
1	0.212	0.231		0.216	0.216		0.221	0.212	
2	0.171	0.194		0.175	0.171		0.175	0.169	
3	0.132	0.157		0.154	0.132		0.134	0.13	
4	0.096	0.122		0.099	0.099		0.096	0.096	
5	0.062	0.089		0.064	0.063		0.065	0.062	
6	0.029	0.058		0.031	0.031		0.031	0.028	
7		0.029							
8									
9									
10									
D	0.5	0.45		0.5	0.5		0.5	0.5	
C (Nm/rad/s)	0.005	0.006		0.005	0.005		0.0055	0.005	
T (Nm)	0.08	0.081		0.083	0.083		0.081	0.081	

Successive  
peak  
amplitudes  
(rad)

Transfer lubricant characteristics

Graphite on mild steel

system frequency = 6.6 Hz Normal load = 10N

surface finish III

Successive  
peak  
amplitudes  
(rad)

time (min)	0.5 min			4 min			12 min		
test number	1	2	3	1	2	3	1	2	3
1	0.466	0.553		0.481	0.499		0.46	0.48	
2	0.370	0.349		0.385	0.381		0.338	0.345	
3	0.32	0.25		0.36	0.34		0.25	0.28	
4	0.244	0.209		0.256	0.251		0.204	0.23	
5	0.198	0.128		0.203	0.20		0.122	0.154	
6	0.122	0.087		0.14	0.13		0.076	0.093	
7	0.069	0.025		0.075	0.71		0.02	0.032	
8	0.017			0.021	0.191				
9									
10									
D	0.65	0.5		0.6	0.55		0.3	0.35	
C (Nm/rad/s)	0.0046	0.005		0.0045	0.0052		0.006	0.0059	
T (Nm)	0.114	.116		0.12	0.13		0.13	0.112	

Transfer lubricant characteristics

P.T.F.E. on mild steel

system frequency = 6.6 Hz normal load = 48N

surface finish II

time (min)	1 min			5 min			12 min		
	1	2	3	1	2	3	1	2	3
test number									
1	0.845	0.79		0.83	0.838		0.881	0.841	
2	0.516	0.48		0.52	0.528		0.541	0.526	
3	0.386	0.362		0.36	0.381		0.398	0.371	
4	0.125	0.107		0.113	0.121		0.131	0.119	
5	0.012	0.008		0.010	0.008		0.141	0.011	
6									
7									
8									
9									
10									
D	0.25	0.3		0.25	0.25		0.23	0.25	
C (Nm/rad/s)	0.032	0.030		0.03	0.031		0.029	0.031	
T (Nm)	0.27	0.299		0.25	0.253		0.243	0.272	

Successive  
peak  
amplitudes  
(rad)

Transfer lubricant characteristics

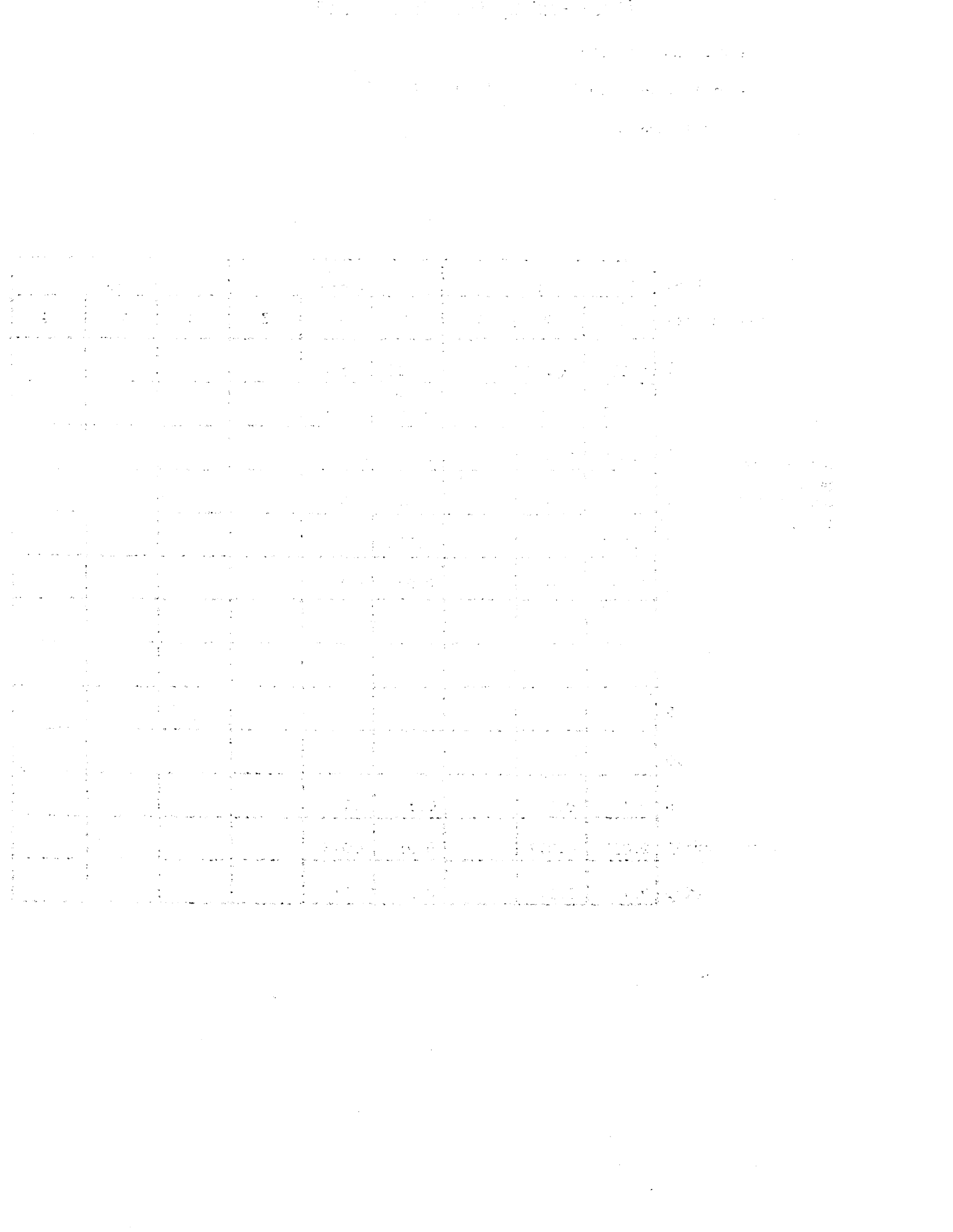
P.T.F.E. on cast iron

system frequency (Hz) = 6.6 normal load = 48N

surface finish II

time (min)	1 min			4 min			12 min		
	1	2	3	1	2	3	1	2	3
test number	1	2	3	1	2	3	1	2	3
1	0.481	0.491	0.488	0.541	0.552		0.521	0.531	
2	0.299	0.501	0.291	0.324	0.331		0.316	0.321	
3	0.156	0.162	0.152	0.155	0.159		0.154	0.155	
4	0.045	0.046	0.046	0.023	0.031		0.023	0.026	
5									
6									
7									
8									
9									
10									
D	0.35	0.35	0.4	0.45	0.45		0.4	0.45	
C (Nm/rad/s)	0.018	0.017	0.019	0.02	0.02		0.021	0.02	
T (Nm)	0.31	0.314	0.311	0.349	0.338		0.341	0.351	

Successive  
peak  
amplitudes  
(rad)



P.T.F.E. on cast iron

system frequency (Hz) = 13.7 normal load (N) = 8

surface finish II

Successive  
peak  
amplitudes  
(rad)

time (min)	1 min			4 min			10 min		
test number	1	2	3	1	2	3	1	2	3
1	0.121	0.112		0.116	0.121				
2	0.103	0.099		0.101	0.099				
3	0.086	0.081		0.086	0.86				
4	0.071	0.069		0.071	0.073				
5	0.057	0.054		0.055	0.055				
6	0.044	0.041		0.045	0.045				
7									
8									
9									
10									
D	0.1	0.1		0.1	0.1				
C (Nm/rad/s)	0.011	0.012		0.01	0.013				
T (Nm)	0.1	0.11		0.11	0.11				

Transfer lubricant characteristics

graphite on mild steel

system frequency = 13.7 Hz normal load = 8N

surface finish II

Successive  
peak  
amplitudes  
(rad)

time (min)	1/2 min			5 min			13 min		
test number	1	2	3	1	2	3	1	2	3
1	0.101	0.114		0.095	0.097		0.104	0.108	
2	0.09	0.102		0.086	0.087		0.093	0.097	
3	0.079	0.09		0.078	0.078		0.081	0.083	
4	0.069	0.079		0.07	0.069		0.071	0.073	
5	0.060	0.07		0.063	0.062		0.061	0.063	
6	0.051	0.06		0.056	0.054		0.052	0.054	
7	0.043	0.051		0.049	0.048		0.044	0.046	
8	0.035	0.042		0.043	0.042		0.033	0.036	
9		0.034							
10									
D	0.1	0.1		0.05	0.05		0.1	0.1	
C (Nm/rad/s)	0.01	0.095		0.011	0.12		0.011	0.012	
T (Nm)	0.06	0.065		0.054	0.058		0.06	0.063	

Transfer lubricant characteristics

graphite on cast iron

system frequency (Hz) = 10 normal load (N) = 8

surface finish I

	time (min)	1 min			6 min					
		1	2	3	1	2	3	1	2	3
Successive peak amplitudes (rad)	test number									
	1	0.16	0.154		0.188	0.181				
	2	0.141	0.139		0.168	0.162				
	3	0.123	0.121		0.149	0.145				
	4	0.106	0.104		0.119	0.118				
	5	0.09	0.096		0.102	0.1				
	6	0.074	0.071		0.086	0.086				
	7	0.06	0.057		0.07	0.068				
	8									
	9									
	10									
	D	0.25	0.25		0.25	0.25				
	C (Nm/rad/s)	0.006	0.006		0.0058	0.0059				
	T (Nm)	0.09	.091		0.091	0.089				

APPENDIX III : TRANSFER LUBRICATED STICK SLIP

- TABLES OF RESULTS

Transfer lubricant results

ptfe on cast iron

system frequency = 13,7 Hz normal load = 48N

surface finish II drive speed = 0,08 rad/s

time	test number	$T_s - T_k$ (Nm)	$\theta_{max}$ (rad/s)	$C_1$	$C_2$	$\psi$	Vibn. Amp. (rad)
1/2 min		0,133	0,45	0,44	0,045	0,19	0,01
		0,182	0,65	0,42		0,18	0,012
2 min		0,145	0,51	0,425		0,19	0,012
		0,13	0,47	0,415		0,195	0,014
5 min		0,136	0,47	0,435		0,195	0,012
		0,119	0,43	0,418		0,21	0,012
15 min				0,443			
		0,125	0,5	0,375		0,2	0,012
		0,115	0,49	0,355		0,21	0,01
25 min		0,119	0,495	0,364		0,21	0,012
		0,112	0,59	0,287		0,21	0,01
		0,119	0,65	0,274		0,2	0,01
65 min		0,108	0,55	0,295		0,21	0,01
		0,104	0,55	0,282		0,215	0,012





Transfer lubricant results

graphite on cast iron

system frequency = 10 Hz normal load = 20N

surface finish I drive speed 0,4 rad/s

time	test number	Ts-Tk (Nm)	$\vartheta_{max}$ (rad/s)	C <sub>1</sub>	C <sub>2</sub>	$\psi$	Vibn. Amp. (rad)
1/2 min		0,11	0,72	0,32	0,015	0,87	0,014
		0,125	0,77	0,34		0,77	0,018
		0,135	0,82	0,345		0,71	0,019
1 1/2 min		0,09	1,0	0,18		1,0	0,012
		0,1	1,1	0,194		0,96	0,011
		0,095	1,05	0,186		0,99	0,011
2 min		0,085	1,2	0,145		1,05	0,008
		0,093	1,4	0,138		0,99	0,008
		0,088	1,56	0,135		1,04	0,008
3 min			eliminated				















Transfer lubricant results

ptfe on steel

system frequency 6.6 Hz normal load = 48N

surface finish III drive speed = 0.4 rad/s

time	test number	Ts-Tk (Nm)	θmax (rad/s)	C <sub>1</sub>	C <sub>2</sub>	ψ	Vibn. Amp. (rad)
0 min	1	0.132	1.28	0.32	0.08	0.485	0.036
	2	0.11	1.12	0.205		0.581	0.031
	3	0.115	1.14	0.315		0.557	0.032
½ min		0.125	1.08	0.36		0.512	0.029
		0.11	1.0	0.345		0.581	0.027
1 min		0.095	1.2	0.245		0.674	0.019
		0.105	1.43	0.22		0.64	0.014
		0.098	1.3	0.235		0.653	0.012
1½ min							
			eliminated				







Transfer lubricant results

ptfe on steel

system frequency = 13.7 Hz normal load = 36N

surface finish II drive speed = 0.2 rad/s

time	test number	$T_s - T_{k\theta max}$ (Nm)	$\theta_{max}$ (rad/s)	$C_1$	$C_2$	$\psi$	Vibn. Amp. (rad)
0 min		0.142	0.62	0.38	0.06	0.46	0.012
		0.173	0.71	0.37		0.38	0.014
		0.112	0.478	0.355		0.59	0.012
1/2 min		0.142	0.66	0.324		0.46	0.012
		0.185	0.53	0.346		0.36	0.016
1 1/2 min		0.195	0.84	0.35		0.34	0.014
		0.183	0.56	0.34		0.36	0.012
		0.174	0.76	0.345		0.38	0.012
2 1/2 min		0.156	0.78	0.3		0.42	0.008
		0.136	0.78	0.26		0.485	0.008
		0.143	0.88	0.245		0.46	0.008
3 1/2 min		0.105	0.74	0.21		0.63	0.006
		0.117	0.82	0.215		0.56	0.008
		0.121	0.81	0.225		0.54	0.006
4 1/2 min							
			eliminated				





Transfer lubricant results

ptfe on steel

system frequency = 13,7 Hz normal load = 48N

surface finish II drive speed = 0,08 rad/s

time	test number	$T_s - T_k$ (Nm)	$\theta_{max}$ (rad/s)	$C_1$	$C_2$	$\psi$	Vibn. Amp. (rad)
0 min	1	0.22	0,81	0.42	0,07	0.135	0.015
	2	0.27	0.83	0.49	"	0.1	0.017
	3	0,14	0.49	0.43	"	0,18	0.1
1 min	1	0.26	0.94	0.42		0,1	0,018
	2	0.27	0.96	0.425		0.1	0,02
	3	0.23	0,83	0.42		0,11	0,017
2 min	1	0,195	0.82	0.36		,142	0,014
	2	0,205	0.9	0.343		,140	0,014
	3	0,178	0.76	0.34		,148	0,012
4 min	1	0.14	0.78	0.27		,188	0,008
	2	0,126	0.68	0.282		,21	0,01
	3	0,154	0.82	0.285		,174	0.006
4½ min							
			eliminated				





Transfer lubricant results

graphite on cast iron

system frequency = 10 Hz normal load = 48N

surface finish II drive speed = 0.2 rad/s

time	test number	$T_s - T_k$ (Nm)	$\theta_{max}$ (rad/s)	$C_1$	$C_2$	$\psi$	Vibn. Amp. (rad)
0 min		0.112	0.68	0.34	0.07	0.42	0.016
		0.145	0.82	0.365		0.33	0.022
1/2 min		0.115	0.64	0.37		0.42	0.016
		0.122	0.71	0.355		0.41	0.018
		0.115	0.68	0.348		0.42	0.022
1 min		0.115	1.08	0.22		0.42	0.010
		0.108	1.07	0.205		0.46	0.012
3 min			eliminated				

Transfer lubricant results

ptfe on steel

system frequency = 13,7 Hz normal load = 48N

surface finish I drive speed 0,08 rad/s

time	test number	T <sub>s</sub> -T <sub>k</sub> (Nm)	θ <sub>max</sub> (rad/s)C <sub>1</sub>	C <sub>2</sub>	ψ	Vibn. Amp. (rad)	
0 min	1	0,28	0,90	0,47	0,05	0,094	0,018
	2	0,29	1,05	0,41		0,091	0,02
	3	0,21	0,82	0,39		0,125	0,018
1½ min		0,185	0,75	0,4		0,14	
		0,195	0,77	0,385		0,135	
3 min		0,22	0,82	0,41		0,12	0,018
		0,19	0,67	0,43		0,14	0,013
		0,243	0,87	0,425		0,11	0,014
4 min		0,184	0,96	0,29		0,143	0,010
		0,175	0,88	0,305		0,15	0,010
5 min		0,113	0,71	0,24		0,23	0,008
		0,126	0,83	0,23		0,21	0,007
		0,095	0,58	0,245		0,27	0,006
6 min			gone				



Transfer lubricant results

ptfe on steel

system frequency 6.6 Hz normal load = 24N

surface finish I drive speed = 0.2 rad/s

time	test number	T <sub>s</sub> -T <sub>k</sub> (Nm)	θ <sub>max</sub> (rad/s)	C <sub>1</sub>	C <sub>2</sub>	ψ	Vibn. Amp. (rad)
1/2 min		0,145	1,38	0,325	0.030	0,220	0,04
		0,115	1,14	0,315		0,278	0,034
		0,175	1,52	0,36		0,18	0,042
1 min		0,122	1,07	0,355		0,26	0,036
		0,115	0,96	0,364		0,278	0,032
2 min		0,120	1,53	0,245		0,25	0,026
		0,113	1,24	0,285		0,266	0,021
3 min		0,11	1,43	0,24		0,274	0,015
		0,106	1,43	0,225		0,284	0,011
4 1/2 min			eliminated				





APPENDIX IV

STATEMENT OF ADVANCED STUDIES UNDERTAKEN BY CANDIDATE DURING  
PERIOD OF RESEARCH

1. Non-Linear Vibrations, by G R Symmons  
Short Course of 8 hours duration at Sheffield Polytechnic  
1971.
2. Selected Lectures from MSc Course in Tribology  
at Leeds University March 1971, 15 hours duration